Development of plant-produced African horse sickness virus vaccines

By

Susan Jennifer Dennis

Thesis presented for the degree of

DOCTOR OF PHILOSOPHY

In the Department of Molecular and Cell Biology,

Faculty of Science, University of Cape Town

January 2019

Declaration

The work presented in this thesis was conducted at the Biopharming Research Unit in the Department of Molecular and Cell Biology at the University of Cape Town. The research was conducted under the supervision of Professor Ed Rybicki and co-supervision of Associate Professor Inga Hitzeroth and Dr Ann Meyers.

I, Susan Jennifer Dennis, hereby declare that the work included in this thesis is my own original research (except where acknowledged otherwise) and that neither the whole work, nor any part of it has been or is being submitted for another degree at this or any other university. All assistance provided by other people has been acknowledged. All citations in this manuscript are reflected using the CSIRO reference style as the convention. Furthermore, I authorize the university to reproduce for the purpose of research either the whole or any portion of the contents in any form whatsoever.

Signed by candidate

Signature

To my father, Robert Bruce Hall, who believed in me from the start……

Acknowledgements

I wish to express my sincere appreciation to the many people who supported me during the course of my research and the writing of this thesis:

My supervisor, Prof Ed Rybicki, who made it all possible. Ed, I will always be enormously grateful for that chance meeting in a supermarket and the fact that in spite of all the intervening years, you were gracious, willing and brave enough to take me on as a student again. Never in my wildest dreams did I imagine getting to this point…… Thank you for inspiring me to adventure into the world of biopharming and for all I have learnt from you along the way. I could not have wished for a kinder, more knowledgeable, supportive and committed supervisor.

My co-supervisors, Assoc. Prof Inga Hitzeroth and Dr Ann Meyers, for their tireless enthusiasm and invaluable mentorship. Thank you for always having an open door and for being willing to constructively engage and advise, even at the times when you were busy with so much else. Inga, thank you for empowering me to believe that I could succeed and for challenging me to extend myself beyond where I would naturally have gone. Ann, your commitment and effort and the lengths to which you have gone to support and assist me have been extraordinary. From endlessly reviewing and wisely and constructively criticizing reports, ethics applications, journal submissions and this thesis, to driving around the countryside collecting blood samples when I couldn't, nothing was ever too much for you and I am deeply grateful. Thank you both so much for your warm friendship too – it has meant a lot to me.

My colleagues and fellow members of the Biopharming Research Unit. I have so enjoyed getting to know all of you and I am especially grateful for the warm and friendly way in which you welcomed me back into the lab. In particular, I would like to thank, Dr Alta van Zyl, my office mate and good friend. Alta, your careful and patient listening and extremely constructive and practical research advice, has been invaluable. I owe so much of what I have learnt to you. Thank you for always being willing to stop whatever you were doing at short notice and uncomplainingly look at a gel, solve an Excel dilemma or locate a much-needed piece of equipment or reagent. You have also provided very valuable emotional support, for which I am truly grateful.

Dr Sandiswa Mbewana, for insightful advice and many happy and engaging conversations, including being my travel companion to Singapore! Dr Aleyo Chebada, for your enthusiasm and encouragement and for giving me such a warm welcome right from the start, Dr Megan Hendrikse my tireless and very supportive centrifuge buddy, Dr Guy Regnard for your patient IT assistance, Dr Bruna Galvao, for your genuine kindness and warm-hearted friendship, Maureen Baloyi for smilingly and patiently teaching me how to vacuum infiltrate plants, Shelley Fearon, my project co-

worker and friend, for helpful AHSV conversations and for making Hannah's beautiful matric dance dress, and my fellow PhD students Mélie Buyse and Jenni Wayland for sharing this journey with me and for all the encouragement along the way.

I would like to say a very special thank you to Mohamed Jaffer at the Electron Microscopy Unit. Mo, your expert and patient assistance in viewing endless EM grids and your willingness to accommodate me at odd times, often at the spur of the moment, is deeply appreciated. Thank you too for always being so interested in my work and for helpful suggestions and insightful advice during the course of the project. Thank you very much to Dr Brandon Weber at the EM unit too for helpful discussion and assistance with regard to the purification of VLPs.

There are many unsung heroes who ensure the smooth running of the department. I would like to thank all the departmental assistants and administrative and other support staff, both past and present, especially Uli Mutzeck, Neil Bredenkamp, Derrick September, Madhu Chauhan, Yolande Burrows, Glynnis Spannenberg Cheryl Saunders, Ghakiema Salie, Fazeela Felton, Pey-Yin Liebrich, Shaheeda Johnson, Mlungisi Sisusa, Mario Paulse, Maureen Adams, Unis Verdier, Michael Gcwabe, Jenny Swarts, Priscilla Adonis, Blommie Filmer and Peter Louw.

Rodney Lucas, the animal technician at the UCT Animal Unit, for your kind and patient handling of the guinea pigs and for your assistance in drafting the ethics applications.

Dr Koos Neuland and Dr Charon de Villiers, at the Medical Research Council facility at Driftsands, for being willing to allow me to use your horses in the safety study and for assistance with the horse immunizations and care of the animals.

Carina Lourens from the University of Pretoria for so proficiently conducting the virus neutralization tests.

Dr Maretha O'Kennedy, Dr Daria Rutkowska and Dr Tsepo Tsekoa from the Council for Scientific and Industrial Research, for skillful preparation of the filtered vaccine samples.

Chris Janitzek and Dr Susan Thrane, at the Centre for Medical Parasitology in Copenhagen, Denmark, for very helpful assistance and advice with the SpyTag/SpyCatcher coupling technology and for providing the AP205 antiserum and *E. coli* ST and SC recombinant clones.

Dr Peter Coetzee at the Equine Research Institute, for the generous gift of AHSV dsRNA.

Prof Alan Guthrie at the Equine Research Institute, for the invitation to attend the Viruses without Borders workshop in Pretoria and for helpful insight and conversation with regard to AHS and AHSV.

Dr Christiaan Potgieter from Deltamune, for informative advice and the gift of AHSV antisera.

Dr Alison Lubisi at the Onderstepoort Veterinary Institute for conducting the iELISA tests.

Prof George Lomonossoff from the John Innes Institute, UK, for the gift of the pEAQ cloning vector.

Elizabeth Waldron at the Centre for Proteomic and Genomic Research for conducting LC-MS on the plant-produced AHSV capsid proteins.

I gratefully acknowledge financial and conference travel assistance from the Technology and Innovation Agency, the Council for Scientific and Industrial Research, the Poliomyelitis Research Foundation, the National Research Foundation and WhiteSci during the course of my PhD.

This research would never have been possible without the enduring love and support of my family and friends.

My dear friends Tessa Ferrandi, LeeAnne Hyslop and Belinda Russell. Thank you for standing by me and supporting me in this wild venture. For patiently enduring the absence of coffee dates, but always being there at the end of the phone when I needed a listening ear or an encouraging voice. You are the best! And to all my Book Club friends, thank you so much for your loving and interested support and for tolerating my lack of non-science reading! And a very special thank you to Lynn Benjamin for unwavering administrative help and support and to Iris Jack for your invaluable assistance in helping me look after our home.

My dearest Mom and Dad – I am who I am today because of you. Thank you so much for all the opportunities you have given me, for all the sacrifices you have made and for your love and guidance through the years. I have been blessed beyond words to have had you as parents and I am deeply grateful to both of you. Wendy, Clive and Louise, Graham, Brian and Lou, Jen and Simon, Lucy, Tom and Alex, Paul and Jess and your families, thank you for encouraging me and putting up with my general unavailability and long periods between visits and phone calls. Your quiet support and confidence in me have meant so much.

My children of whom I am so proud: Matt and Tory, your quiet, caring and loving support and genuine interest in my work during this very busy, exciting and sometimes challenging time of your own lives, encouraged me to believe I could do this. Thank you for your strength and example and for the great joy you have given us. Tim, my stalwart and trusted advisor, not only in all thing's science but in life in general. Your wise words have directed my thoughts and actions more than once and I have been so grateful to have had you at home during my PhD journey. Thank you for all the meals you cooked and the school lifts you did when I stayed late in the lab. Thank you

especially for not baulking at the thought of being in the same department as your mom, but instead embracing the change and cheering me on. I will be forever grateful to you…. Simon, kind, gentle and undemanding soul, you patiently and uncomplainingly listened to my scientific ramblings, even though the vocabulary was far removed from your type of science! Thank you too for your loving support and for always being happy to step in and assist your barely computer-literate mother with all thing's software and IT related. You are a star! And my lovely Hannah, thank you for happily accepting my return to the lab and for being so undemanding as you took all the adjustments in your stride, even when things were not always that easy. Thank you for the coffee dates and holiday adventures and above all, for the close relationship we share. Thank you all from the bottom of my heart for believing in me, supporting and encouraging me and making so many sacrifices to enable me to see this journey through. You mean the world to me. How blessed I am to be your Mom!

And last, but by no means least, to my best friend and loving husband, Dave. Thank you for allowing me the freedom to follow my dreams, for your overwhelming encouragement, prayerful support and passionate interest in my work. Thank you for accompanying me on late night visits to the lab and never complaining when meals were late, and things fell apart at home. Thank you for embracing this unexpected turn in our life journey together and above all, for walking with me every step of the way. I love you very much….

The earth is the Lord's, and everything in it…… Ps 24 v 1

Table of Contents

Development of plant-produced African horse sickness vaccines

By

Susan Jennifer Dennis

Biopharming Research Unit

Department of Molecular and Cell Biology, Faculty of Science,

University of Cape Town, South Africa

Abstract

African horse sickness is a devastating disease that causes great suffering and many fatalities amongst horses in sub-Saharan Africa. It is caused by nine different serotypes of the orbivirus African horse sickness virus (AHSV) and it is spread by *Culicoid* midges. The disease has significant economic consequences for the equine industry both in southern Africa and increasingly further afield as the geographic distribution of the midge vector broadens with global warming and climate change. Live attenuated vaccines (LAV) have been used with relative success for many decades, but carry the risk of reversion to virulence and/or genetic re-assortment between outbreak and vaccine strains. Furthermore, the vaccines lack DIVA capacity, the ability to distinguish between vaccine-induced immunity and that induced by natural infection. These concerns have motivated interest in the development of new, more favourable recombinant vaccines, initially focusing on the use of insect and mammalian cell expression systems. More recently, several studies have demonstrated the potential for using plant expression systems for the production of virus-like particles (VLPs), which are excellent vaccine candidates, as they do not contain virus genetic material and are DIVA compliant.

A vaccine alternative to the currently used live vaccine necessarily needs to provide protection against all nine serotypes of the virus. Cross-protection has been shown to exist between certain serotypes of the virus and as capsid protein VP2 is the protein responsible for AHSV serotype specificity, the idea of a plant-produced VLP vaccine containing a representative VP2 protein from each of the different serotype groups, was conceived. Such a vaccine would potentially

provide protection against all 9 serotypes of the virus and would have DIVA capability. Furthermore, it would address local concerns regarding the use of a live vaccine and would serve as a potentially acceptable prophylactic or rapid response antidote in the wider international context. This work describes two approaches in the development of VLP vaccines in plants.

In the first part of this study, the ability of 2 different serotypes of plant-produced AHSV VLPs to safely stimulate an immune response in horses, was investigated. Co-infiltration of *Nicotiana benthamiana* plants with *Agrobacterium* constructs encoding the four AHSV serotype 5 structural proteins VP2, VP3, VP5 and VP7, was shown to result in assembly of complete VLPs. Furthermore, co-infiltration with the constructs, encoding VP3 and VP7, together with constructs encoding the two outer capsid proteins VP2 and VP5 of a second serotype, AHSV 4, resulted in assembly of complete AHSV 4 VLPs. Horses vaccinated with plant-produced AHSV 4 and 5 VLPs, all seroconverted after two doses of the vaccine and the virus neutralization titres indicated that the plant-produced VLP vaccines are likely to be at least as effective as the current LAV in protecting against AHSV 4 or AHSV 5. However, they have the added advantage of being free from any of the associated risks of a live vaccine, such as reversion to virulence or genetic re-assortment with field or vaccine strains.

In the second part of the study, the use of the so-called SpyTag/SpyCatcher or bacterial "superglue" technology was investigated. This technology is based on the peptide SpyTag irreversibly coupling to the SpyCatcher protein, forming an isopeptide bond when the two are mixed together. The plant-based expression system was used to produce Spy VLPs consisting of either *Acinetobacter* phage (AP205) VLPs or tobacco mosaic virus (TMV) VLPs displaying a SpyTag or SpyCatcher peptide. In addition, AHSV 5 VP2 displaying SpyTag was expressed in plants and several coupling strategies were tested to determine whether AP205 particles displaying AHSV 5 VP2 could be formed as a result of binding between the SpyTag/SpyCatcher moieties of the recombinant proteins. Although it was not proven that coupling occurred, this research will pave the way towards developing a multivalent vaccine platform whereby VP2 of different AHSV serotypes can be displayed on the Spy VLP surface to allow optimal presentation of these proteins to the animal's immune system.

Together, the results obtained in this study show that there is great potential for the production of novel, diverse, efficacious and economically viable AHSV VLP vaccines in plants.

List of Symbols and Abbreviations

A	adenosine
Ab	antibody
AHS	African horse sickness
AHSV	African horse sickness virus
Ala	alanine
AP205	*Acinetobacter* phage AP205
Arg	arginine
BeYDV	bean yellow dwarf mastrevirus
bp	base pair(s)
BPV	bovine papilloma virus
BSA	bovine serum albumin
BTV	bluetongue virus
CaMV	cauliflower mosaic virus
cDNA	complementary deoxyribonucleic acid
CEF	cytopathic effect
CLP(s)	core-like particle(s)
CP	coat protein
CPE	cytopathic effect
CPMV	cowpea mosaic virus
CVA	chorioallantosis vaccinia virus Ankara
dATP(s)	deoxy-adenosine triphosphate(s)
DIVA	Distinguish Vaccinated from Infected Animals
DISA	Disabled Infectious Single Animal vaccine
DISC	Disabled Infectious Single Cycle vaccine
DNA	deoxyribonucleic acid
dNTPs	deoxy-ribonucleoside triphosphates
dpi	days post infiltration
dsRNA	double-stranded ribonucleic acid
ECRA	Entry Competent Replication Abortive vaccine
EEV	equine encephalosis virus
EVA	equine viral arteritis
EtBr	ethidium bromide

FMDV	foot-and-mouth disease virus
g	gram
G	guanine
Gly	glycine
goi	gene of interest
GRAS	generally regarded as safe
HBVcAg	Hepatitis B virus core antigen
HBVsAg	Hepatitis B virus surface antigen
His	histidine
hr(s)	hour(s)
iELISA	indirect enzyme-linked immunosorbent assay
IFNAR	Interferon-alpha/beta receptor
Ile	isoleucine
IPTG	Isopropyl β-D-1-thiogalactopyranoside
kb	kilobase(s)
kDa	kilodalton(s)
kg(s)	kilogram(s)
kPa	kiloPascal(s)
l	litre
LAV	live attenuated vaccine
LB	Luria Bertani
LBB	Luria Bertani-based Broth
M	molar
MAbs	monoclonal antibodies
MEM	minimal essential medium
MES	morpholinoethane sulfonic acid
Met	methionine
mg	miligram(s)
min(s)	minute(s)
mL	mililitre(s)
mM	milimolar

mRNA	messenger RNA
MVA	modified vaccinia Ankara
ng	nanogram(s)
nm	nanometre(s)
NOS	nopaline synthase
NS	
O/N	overnight
OD_{600}	optical density at 600 nanometer wavelength light
OIE	Office International des Epizooties
OOA	origin of assembly
PAGE	polyacrylamide gel electrophoresis
PBMC	peripheral blood mononuclear cells
PBS	phosphate-buffered saline
PCR	polymerase chain reaction
PI	protease inhibitor
PP	percentage positive
PTGS	post-transcriptional gene silencing
PVX	potato virus X
rpm	revolutions per minute
RTqPCR	reverse transcription qualitative PCR
RVFV	Rift Valley fever virus
s	second(s)
SA	sialic acid
SC	SpyCatcher
SDS	sodium dodecyl
Ser	serine
ssRNA	single-stranded ribonucleic acid
ST	SpyTag
TBE	Tris-borate-EDTA buffer
TBSV	tomato bushy stunt virus
TC	transription complex
TFF	tangential flow filtration

TEM	transmission electron microscopy
Thr	threonine
TMV	tobacco mosaic virus
TS	type-specific
TSP	total soluble protein
TVCV	Turnip vein clearing virus
ug	microgram(s)
UTR	untranslated region
UV	ultraviolet
VIB(s)	viral inclusion bodies
VLP(s)	virus-like particle(s)
VNAb	virus neutralizing antibody
vnt(s)	virus neutralization titre(s)
VP	viral protein
WNV	West Nile virus
wt	wildtype
X-gal	5-bromo-4-chloro-3-indolyl-β-D-galactopyranoside
µg	microgram(s)
µl	microlitre(s)
µM	micromolar

C H A P T E R O N E

LITERATURE REVIEW

1.1 Introduction

For several centuries, the devastating African horse sickness (AHS) has been a cruel scourge to horse owners in South Africa. The disease is infectious but non-contagious, and is endemic to sub-Saharan Africa, causing high fatality rates in susceptible hosts. It is listed as a notifiable viral disease by the World Organization for Animal Health (OIE) because of its severity and the potential risk it poses for rapid global spread (Mellor and Hamblin 2004). AHS remains the most economically significant equine disease worldwide.

The first known historical reference to AHS is recorded in an Arabian document entitled “Le Kitab El-Akoual El-Kafiah Wa El Chafiah,” which apparently relates to an epidemic that occurred in the Yemen in 1327 (Henning 1956). However, the virus is believed to have originated in Africa, with the first record of the disease on the continent being made by Father Monclaro in his account of the journey of Francisco Barreto to East Africa in 1569 (Mellor and Hamblin 2004). Unlike zebra, which are endemic to the region, horses are not native to southern Africa and reference to AHS in South Africa was first made about fifty years after the introduction of horses and donkeys to the Cape of Good Hope by the early Dutch Settlers in 1657. A major outbreak occurred in 1719 when almost 1700 animals are reported to have succumbed to the dreaded “perreziekte” or “pardeziekte” (Henning 1956). Prior to 1953, periodic outbreaks seemed to occur at roughly 20 - 30 year intervals, the most severe being the outbreak in South Africa in 1854 – 1855 which claimed the lives of nearly 70 000 horses, more than 40 percent of the entire horse population of the Cape at the time (Coetzer and Guthrie 2004).

The disease occurs regularly in southern African countries, but the virus has also occasionally escaped its geographical limitations and extended further afield to countries in North Africa, the Middle East, the Arabian Peninsula and the Mediterranean region (Mirchamsy and Hazrati 1973; Lubroth 1988; Mellor 1993). Global climate change is thought to be contributing to the gradual northward migration of the midge vector, which has led to a sobering international awareness that AHS-free countries with milder climate conditions are possibly increasingly at risk for outbreaks of the disease or even the establishment of endemicity (Herholz *et al.* 2008; de Vos *et al.* 2012; Hopley and Toth 2013). The emergence of the generically related bluetongue virus (BTV) in north-

western Europe in 2006 (Darpel *et al.* 2007), as well as the extended AHS outbreak that occurred in western Mediterranean countries between 1987 and 1991 (Rodriguez *et al.* 1992), have only served to reinforce these concerns.

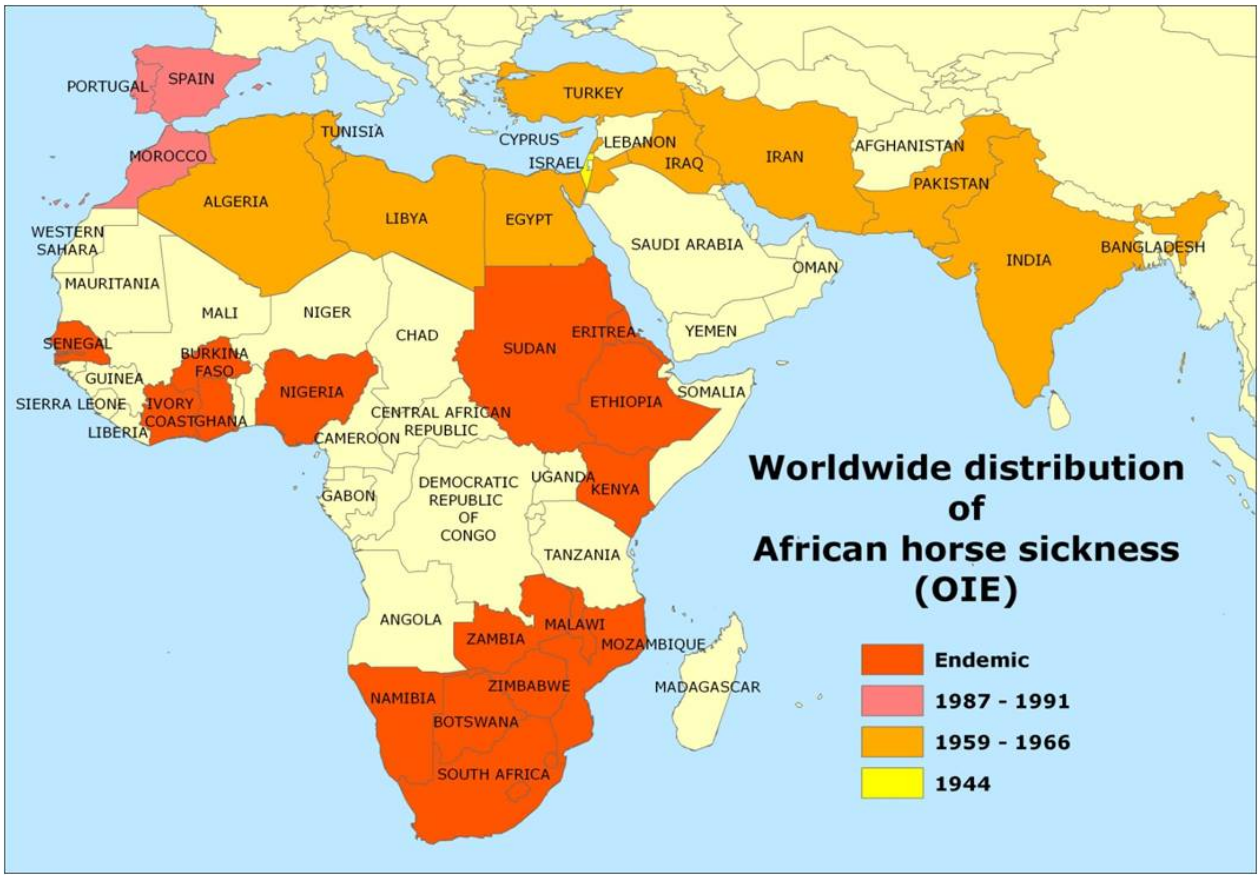

Figure 1.1: Worldwide distribution of African horse sickness. *Image was retrieved from* http://www.afrivip.org/sites/default/files/african_horse_sickness_2_epidemiology.pdf *under the Creative Commons Attribution (CC-BY) license.*

As is presently the case in South and southern Africa, AHS outbreaks in Europe would result in substantial economic losses to the equine industry and would have a significant emotional impact on owners and lovers of horses. There is thus a pressing need to develop new, safe, efficacious and cost-effective vaccines which would additionally allow differentiation between vaccinated and infected animals (DIVA). Such vaccines would not only address the concerns of the South African equestrian community, but would also serve as acceptable prophylactic or rapid response vaccines in the European and other emerging outbreak contexts. An investigation into the potential of using a plant-based expression system to produce vaccines of this nature, is the main goal underlying the work presented in this thesis.

1.2 African horse sickness virus

1.2.1 Aetiology

The first sign that the causative agent of AHS may be a virus was provided by M'Fadyean (1900), who demonstrated the filterability of the infectious organism by successfully transmitting the disease using a bacteria-free blood filtrate from an infected horse. This finding was later confirmed by Theiler and Nocard, who concluded that the disease was caused by a virus (Henning 1956). Further work done by Theiler led to the suggestion that more than one strain of the virus may exist, and that acquired immunity against one strain would not necessarily afford protection against a different heterologous strain (Coetzer and Guthrie 2004).

It is now known that the disease is caused by nine distinct serotypes of African horse sickness virus (AHSV) (McIntosh 1958; Howell 1962), a virus with a multicomponent linear double stranded RNA (dsRNA) genome belonging to the *Orbivirus* genus of the family *Reoviridae* (Calisher and Mertens 1998; Mellor and Hamblin 2004). The idea that AHSV may possibly be transmitted by hematophagous arthropods of the *Culicoides* genus was first suggested by Pitchford and Theiler in 1903 (Coetzer and Guthrie 2004). Du Toit (1944) subsequently demonstrated that mixed pools of wild-caught *Culicoides* species were infected with AHSV. This was confirmed by Mellor *et al.* (1975) and Boorman *et al.* (1975), who demonstrated the occurrence of AHSV replication within a *Culicoides* species after oral ingestion. Field and laboratory-based trials have implicated *C. imicola* and, to a lesser extent, *C. bolitinos* as the primary vectors of AHSV, although some evidence does exist for possible AHSV transmission by other arthropod vectors (Carpenter *et al.* 2017). The ability of AHSV to propagate in both arthropod and mammalian cells is a notable feature shared with all orbiviruses, and one which distinguishes them from some other members of the family *Reoviridae* (Roy 2004).

Figure 1.2: Photograph of a female *Culicoides imicola* midge – the primary AHSV transmission vector (photo retrieved from http://v3.boldsystems.org/index.php/Taxbrowser_Taxonpage?taxid=27425).

Zebra are generally resistant to AHS and have been identified as asymptomatic maintenance hosts of AHSV, while mules and donkeys are much less susceptible than horses to the disease (Barnard 1998). Dogs are the only non-equine animal species that have been shown to contract AHS, with the route of infection believed to be via the ingestion of infected meat (Theiler 1910; McIntosh 1955). However, dogs do not appear to be important hosts for AHSV, most likely due to the fact that they are not preferential feeding targets of the midge vector.

1.2.2 Structure and Assembly

1.2.2.1 Morphology

The African horse sickness virion is a structurally complex and highly organized non-enveloped isometric particle with a diameter of ± 80 nm (Oellermann *et al.* 1970; Coetzer and Erasmus 1994). Like the genus prototype bluetongue virus (BTV), with which it is morphologically almost identical, the non-enveloped virion is quasi-icosahedrally symmetrical and is composed of three concentric protein layers (Bremer 1976; Bremer *et al.* 1990; Grubman and Lewis 1992). The innermost layer encloses the AHSV genome, which consists of 10 segments of linear dsRNA, encoding 7 structural (four major and three minor) and 5 non-structural proteins (Roy *et al.* 1994b). Two of the major structural proteins, VP5 and VP2, make up the outer capsid layer, while the other two major structural proteins VP3 and VP7, and the three minor structural proteins, VP1, VP4 and VP6, make up the AHSV core particle (Figure 1.3).

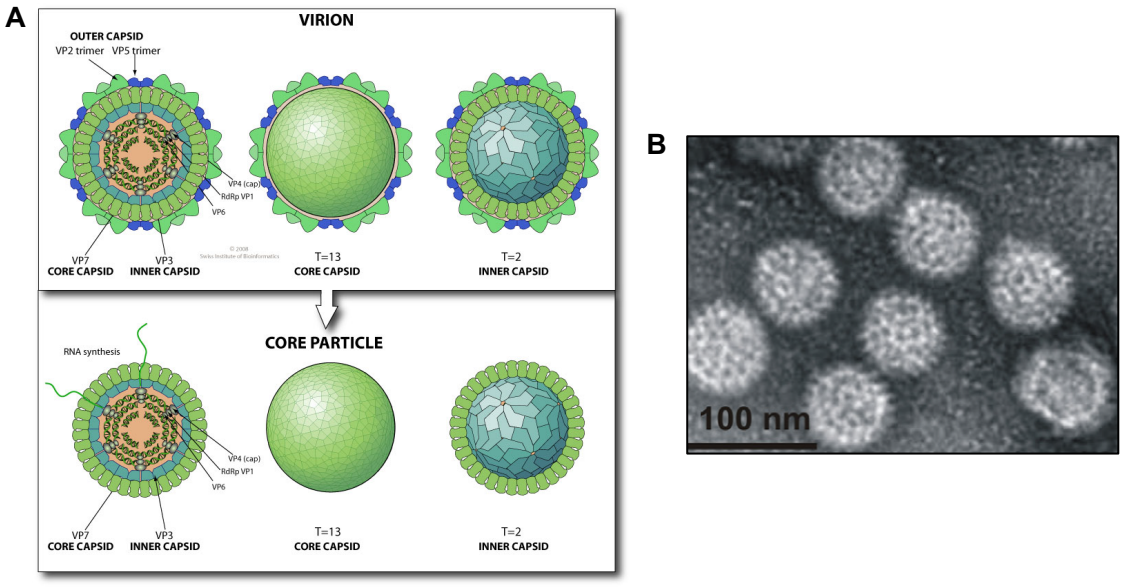

Figure 1.3: AHSV particle structure. (A) Schematic of the morphologically identical BTV particle showing the organisation of the 7 BTV structural proteins and the dsRNA genome (Photo retrieved from https://viralzone.expasy.org/106?outline=complete_by_species). (B) Transmission electron micrograph of authentic AHSV cores purified from virions. Image adapted from Maree *et al.* (2016). *Image used with permission from the publisher.*

In recent years, considerable advances have been made in determining the BTV atomic structure and mechanism of assembly as well as the functions of the individual protein components of the viral particles (Grimes *et al.* 1998; Nason *et al.* 2004; Roy 2004; Zhang *et al.* 2010; Zhang *et al.* 2016). This has recently been clearly and concisely reviewed elsewhere (Roy 2017). Less extensive studies have been conducted on the molecular biology of AHSV, but the morphological and biochemical similarity between BTV and AHSV is indicative of a similar mode of replication and assembly for both viruses.

1.2.2.2 Inner Core

The inner core layer of AHSV is composed of 60 asymmetric dimers of protein VP3 (103 kD), the most conserved protein among the different serotypes (Iwata *et al.* 1992). Each dimer consists of two VP3 isoforms comparable to the A and B conformations of BTV VP3 (Grimes *et al.* 1998) and the inner core is thus completed by the assembly of 12 decamers, each of which consists of five copies of the VP3 (A) molecule with five VP3 (B) molecules in between (Figure 1.4). This architecture is not in agreement with the hypothesis for icosahedral symmetry proposed by Caspar and Klug (1962), but a model of geometrical quasi-equivalence has been proposed whereby the symmetry of the VP3 layer is T=2 rather than T=1 (Grimes *et al.* 1998). The thin VP3 shell thus defines the overall shape and size of the viral particle and provides a scaffold for the deposition of the outer core and capsid protein layers (Stuart *et al.* 1998).

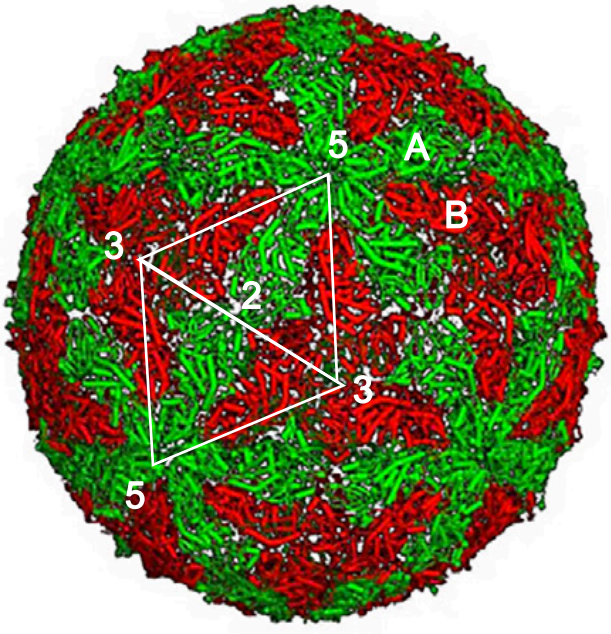

Figure 1.4: The BTV/AHSV VP3 (T=2) scaffold. The icosahedrally unique molecules A and B are coloured in green and red, respectively and the 2 -, 3 - and 5 - fold axes are indicated. Adapted from Grimes *et al.* (1998). *Image used with permission from the publisher.*

In both BTV and AHSV, the minor structural proteins VP1 (RNA-dependent RNA polymerase, 150kD), VP4 (capping enzyme, 78kD) and VP6 (helicase and ATPase, 36kD) form 12 flower-shaped transcription complexes (TC) attached to the VP3 layer directly under each of the fivefold vertices (Grimes *et al.* 1998; Nason *et al.* 2004; Manole *et al.* 2012). Internal concentric layers of RNA comprising the full dsRNA genome are situated around these transcription complexes in shallow grooves in the inner VP3 surface (Stuart *et al.* 1998; Gouet *et al.* 1999) (Figure 1.5).

BTV contains pores in the VP3 layer at the fivefold axes which are lined with four arginine (Arg) residues that are conserved across all the serotypes, and which are believed to play a role in electrostatic steering of RNA entering or leaving the sub-core (Grimes *et al.* 1998). In the 3D image construction of AHSV these pores were closed (Manole *et al.* 2012), but the same 4 Arg residues are strictly conserved across all 9 AHSV serotypes. It is possible that, as has been shown to be the case for BTV (Stuart and Grimes 2006), these pores may be enlarged by activation of VP1 during transcription permitting the exit of nascent mRNA.

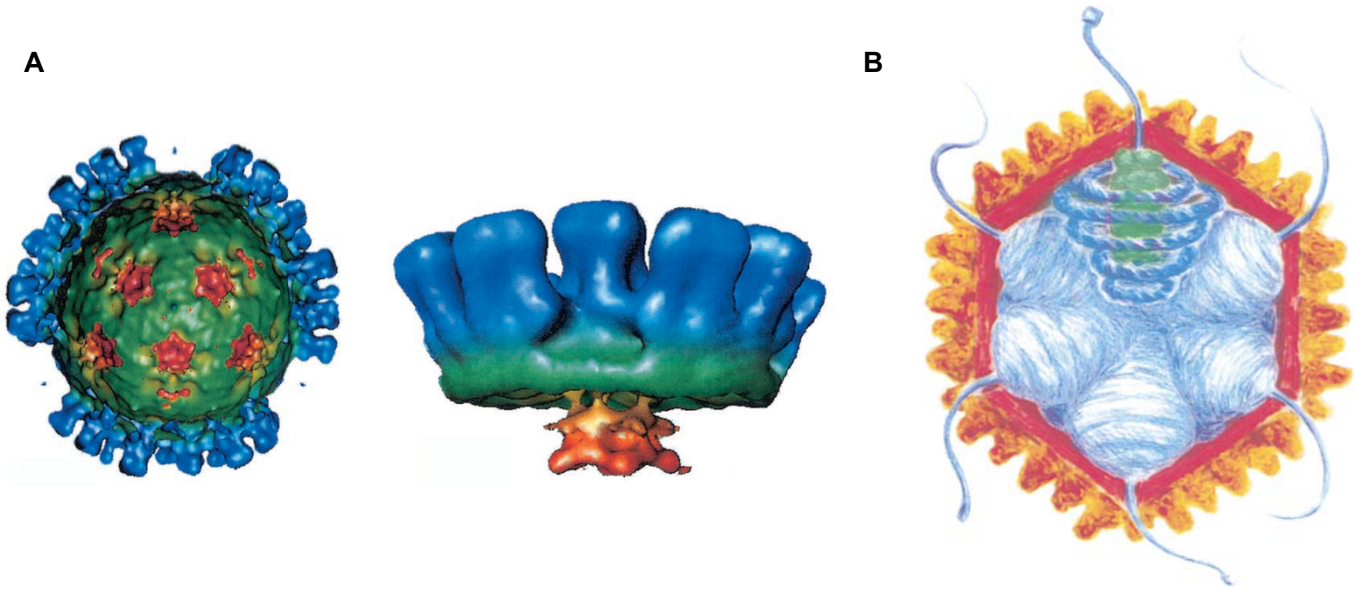

Figure 1.5: Molecular arrangement of the BTV/AHSV inner core. (A) Inside view and conical cutaway of a BTV CLP reconstruction showing the flower-shaped transcription complex (TC), containing VP1, VP4 and VP6 (red) attached to the inside surface of VP3 (green) at all the fivefold axes. Image adapted from Nason *et al.* (2004) *Image used with permission from the publisher.* (B) Cartoon depicting the deposition of the dsRNA gene segments (blue) coiled around the TC (green) at the 5-fold vertices. Image adapted from Gouet *et al.* (1999). *Image used with permission from the publisher.*

1.2.2.3 Outer Core

The AHSV core is made rigid by the addition of 780 monomers of protein VP7 (38 kD) which is highly conserved across the serotypes and is the group-specific antigen currently used in AHSV ELISA-based diagnostic tests (Chuma *et al.* 1992) . The atomic structure of BTV VP7 has been determined by x-ray crystallography (Grimes *et al.* 1995), but only the upper domain of AHSV VP7 has been crystallized (Basak *et al.* 1996), as the protein was unfortunately cleaved in half during the crystallization process. The VP7 monomers contain a helical lower domain and an upper anti-parallel-ß-sandwich domain (Grimes *et al.* 1997): these trimerize in solution by twisting around each other so that the top domain of one monomer rests on the lower domain of the adjacent VP7 subunit (Figure 1.6).

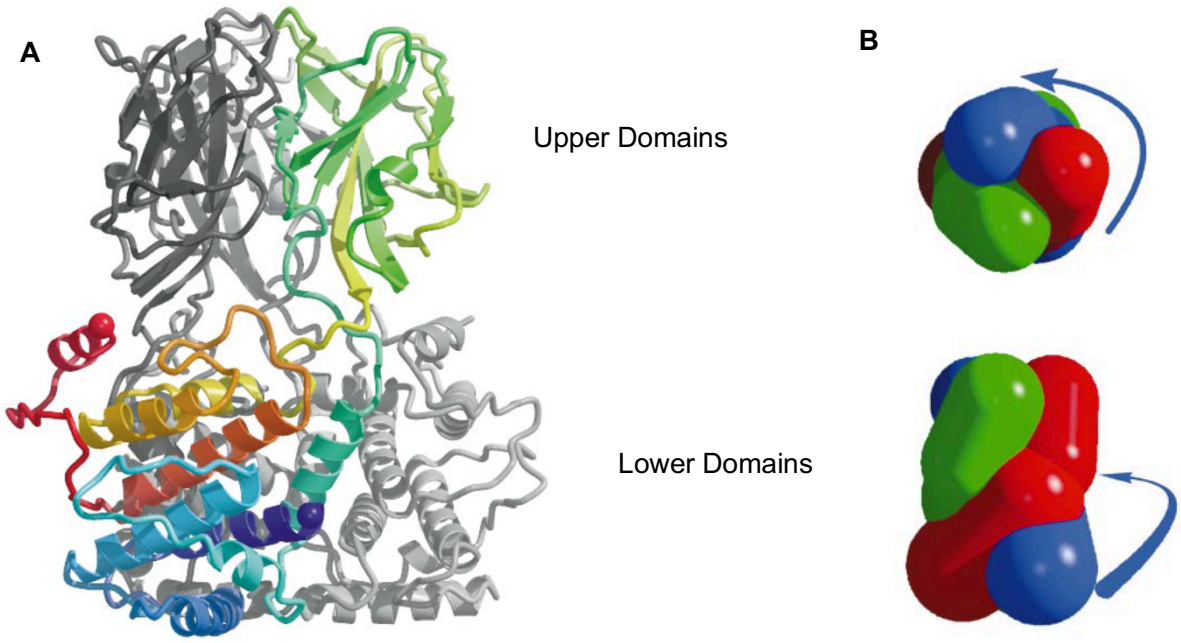

Figure 1.6: Trimerization of the BTV/AHSV VP7 monomers. (A) One monomer of the trimer is shown in colour, while the other two monomers are depicted in grey. (B) Cartoon demonstrating the movement of the lower domains of 3 VP7 monomers (shown in red, blue and green) around the threefold axis of the molecule, while the top domain is kept fixed. The top image shows the view from above, while the lower image shows the corresponding side view. Image adapted from Basak *et al.* (1997) *Images used with permission from the publisher*

These 260 VP7 trimers conform to the principle of quasi-equivalence as, although they are chemically identical, five different trimer types can be identified based on slightly different side chain arrangements. These are named P, Q, R, S and T denoting their position with regard to the five-fold vertices. They crystallize perpendicularly onto the VP3 sub-core making thirteen unique contacts so that each icosahedral subunit contains a P, Q, R and S trimer and one monomer of a shared T trimer located on the adjacent three-fold axis (Grimes *et al.* 1998; Roy and Noad 2006).

The trimers are robust building blocks which also make extensive connections between each other (Grimes *et al.* 1995). They are arranged as either six-member rings, or five-member rings at the fivefold vertices, thus forming 132 channels over the core particle surface. Symmetries between the inner and outer core layers are best matched at the three-fold axes and, as the T trimers situated here also seem to be the most tightly attached, it has been suggested that these are probably the first set of trimers to attach to the VP3 layer while the P trimers, which are more loosely attached, assemble last (Limn *et al.* 2000) (Figure 1.7).

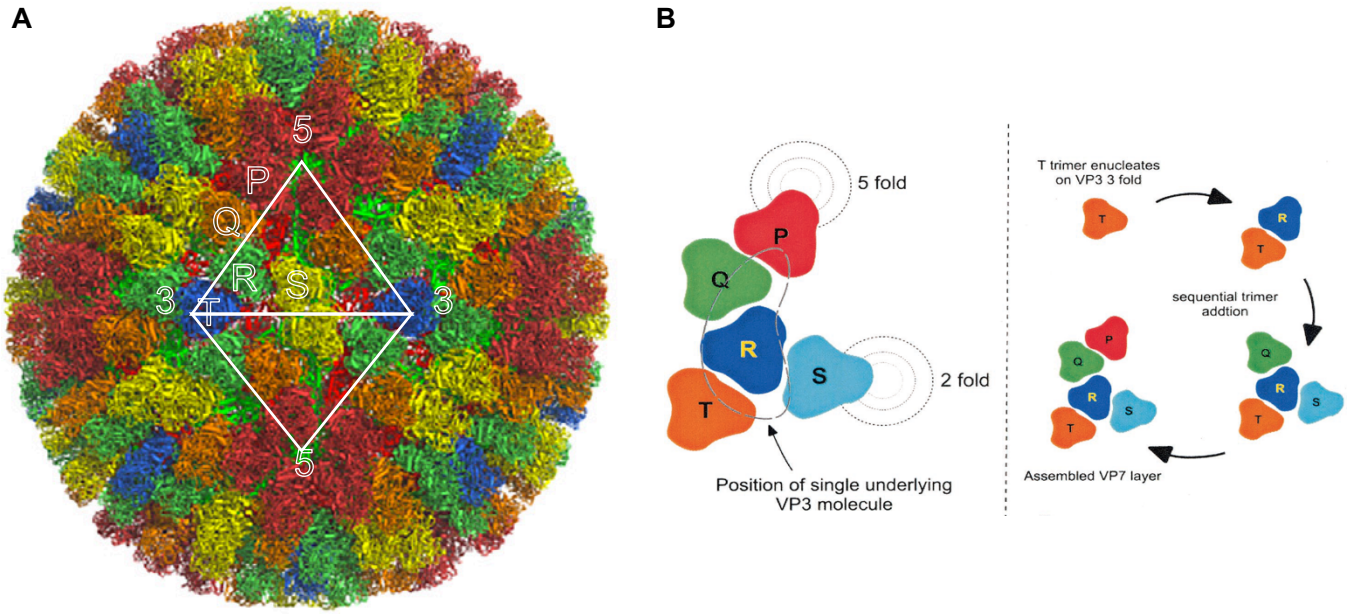

Figure 1.7: Architecture of the BTV/AHSV outer core particle. (A) The icosahedral asymmetric unit is depicted as a triangular area marked by the symmetry axes of the icosahedron and contains 13 copies of VP7 (T=13) arranged as 5 trimers, P, Q, R, S and T, coloured red, orange, green, yellow and blue, respectively. Trimer T sits on the icosahedral three-fold axis and contributes a monomer to each icosahedron. Image adapted from Grimes *et al.* (1998) *Image used with permission from the publisher.* (B) Proposed model for the juxtaposition and assembly pathway of the VP7 trimers in relation to VP3. The T trimers (orange) are believed to be attached first, followed by the R (blue), Q (green), S (turquoise) and lastly the P trimers (red), which are located on the fivefold axes and provide the centre of each icosahedral unit. Image adapted from Limn and Roy (2003). *Image used with permission from the publisher.*

An interesting phenomenon which distinguishes AHSV VP7 from BTV VP7 is the fact that, despite the 70% amino acid sequence homology (Roy *et al.* 1991), BTV VP7 is soluble while AHSV VP7 is not. AHSV VP7 is in fact highly hydrophobic, and the VP7 trimers have been shown to aggregate into flat hexagonal crystals up to 250 um in length and up to 25 um wide, both when expressed in insect cells via baculovirus-mediated expression and in naturally infected mammalian cells (Chuma *et al.* 1992; Burroughs *et al.* 1994).

1.2.2.4 Outer Capsid

The viral particle is completed by the addition of 120 globular trimers of VP5 (57 kD) and 60 triskelion-like VP2 (123 kD) spikes which together form the outer capsid layer. VP2 is the most variable protein among the serotypes and contains the antigenic determinants which elicit serotype-specific neutralizing antibodies (Burrage *et al.* 1993). The viral particles contain 180 monomers of VP2, each of which contains a hub, body, hairpin and tip domain, the latter containing the neutralizing antibody binding sites (Manole *et al.* 2012; Zhang *et al.* 2016). Cryo-EM and 3D reconstruction have revealed that the VP2 spikes are formed by trimerization of the hub domains of three VP2 monomers. The base of each VP2 spike interacts with a Q type VP7 trimer, while the body domains of the three VP2 monomers connect with a P, R and S - type VP7 trimer respectively. Furthermore, for BTV, Zhang *et al.* (2010) identified a zinc finger motif and a putative sialic acid (SA) binding domain in the VP2 trimer hub (Figure 1.8).

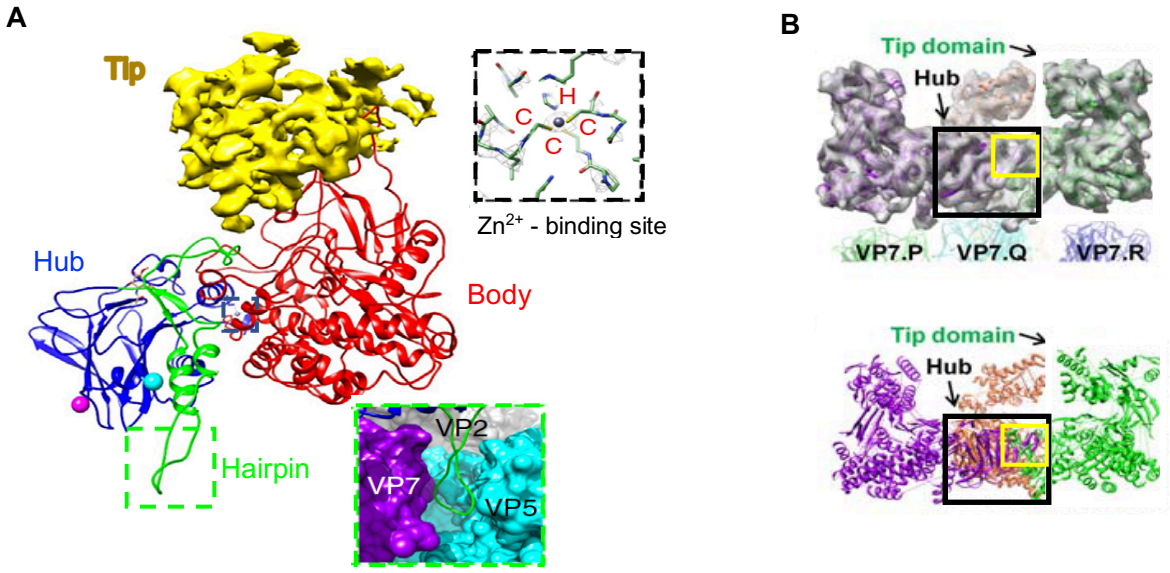

Figure 1.8: The BTV/AHSV outer capsid protein VP2. (A) Ribbon model of the VP2 monomer showing the different domains colour-coded. The dashed inserts show a putative Zn^{2+} motif (black) and the hairpin loop region interacting with VP7 and VP5 (green). (B) The VP2 triskelion shape is formed by trimerization of three VP2 hub domains (black box), the base of which interacts with a Q VP7 trimer. The VP2 SA binding site is indicated by the yellow box. Image adapted from Zhang *et al.* (2010), Zhang *et al.* (2016) and Roy (2017). *Images used with permission from the publishers.*

The VP5 trimers exist as two quasi-equivalent conformers and are positioned between the propeller-like arms of the VP2 triskelions, bridging the 120 channels formed by the six-member VP7 trimer rings. The viral outer shell therefore covers nearly all of the inner shell, but significantly, leaves the 20 VP7 T trimer spikes on the icosahedral three-fold axes accessible to possible antibody binding (Hewat *et al.* 1992) (Figure 1.9).

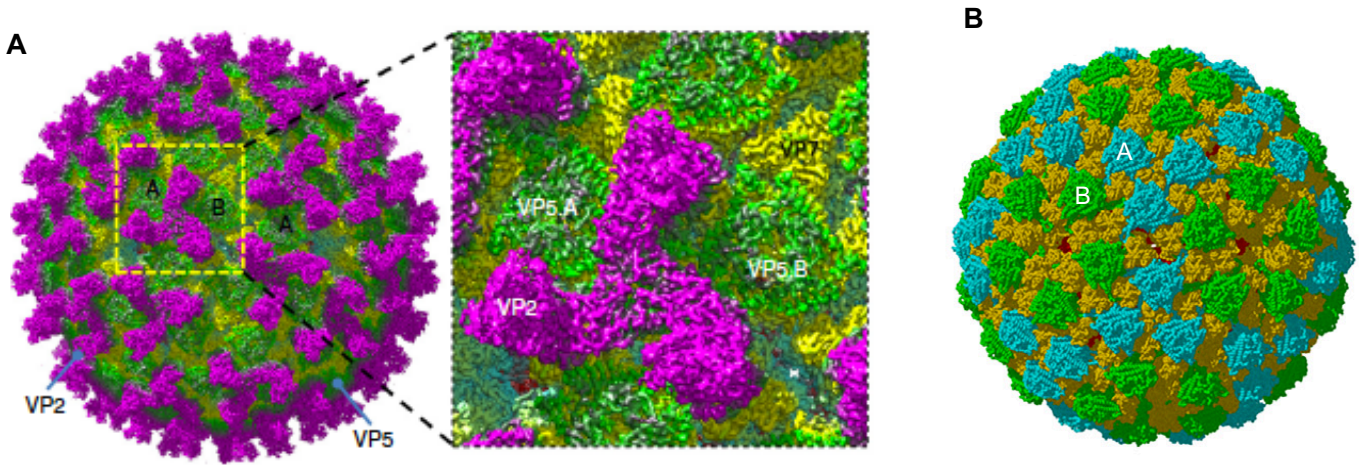

Figure 1.9: Molecular reconstruction of the BTV/AHSV virion showing the arrangement of the outer capsid layer. (A) The outer core contains 60 VP2 trimers (purple) with 120 VP5 trimers (green) positioned between the arms of the VP2 triskelions. The boxed inset shows a close-up view of an icosahedral subunit. (B) The two trimer conformers (A and B) which make up the VP5 layer, are depicted in green and cyan and the 260 VP7 trimers are shown in yellow. The 120 VP3 monomers, which make up the inner core (red), are almost completely occluded by the VP7 layer. Image adapted from Zhang *et al.* (2016) and Roy (2017). *Images used with permission from the publishers.*

1.2.2.5 Non-Structural Proteins

In addition to the seven structural proteins that make up the viral particles, five non-structural proteins, NS1, NS2, NS3, NS3a (lacking 13 N-terminal amino acids) and NS4, are also synthesized in infected cells. These are involved in virus replication, assembly and transport from infected cells (Roy *et al.* 1994b). The tubular structures commonly observed in the cytoplasm of infected cells are composed of NS1, which has been shown to play a role in the preferential up-regulation of viral protein synthesis (Boyce *et al.* 2012). The single-stranded RNA (ssRNA)-binding protein NS2 forms viral inclusion bodies (VIBs), which recruit viral ssRNA and form a scaffold for viral replication and core assembly (Van Staden *et al.* 1991; Patel and Roy 2014). Viral particle release is mediated by NS3/NS3a, the only AHSV glycosylated membrane protein. This, unlike BTV NS3/NS3a which is highly conserved, is the second most variable protein across the different serotypes. Once the outer capsid proteins VP2 and VP5 have been acquired by the newly formed cores, NS3 facilitates egress of fully

formed viral particles from infected cells (Quan *et al.* 2008; Celma and Roy 2011). The most recently identified non-structural protein, NS4, is thought to play a role in modulating host innate immunity by counteracting the interferon response in infected cells (Ratinier *et al.* 2011; Zwart *et al.* 2015).

1.2.3 Viral Infection and Replication

AHSV host infection is believed to be initiated by the outer capsid protein VP2, the host cellular surface receptor and capsid protein VP5, which contains a characteristic coiled-coil motif typical of membrane fusion proteins (Hassan *et al.* 2001; Zhang *et al.* 2010). Due to the location of the putative sialic acid (SA) binding domain in the VP2 trimer hub, Zhang *et al.* (2010) have postulated that the VP2 trimers may attach to the surface of cells through two different interactions. First, the antigenic tip domains bind to certain surface cell receptors which have not yet been identified. These bonds are then stabilised by a second connection between the SA-binding domain and a surface glycoprotein. The sensitivity of VP2 to serum proteases has been established (Burroughs *et al.* 1994; Marchi *et al.* 1995), and it has been suggested (Manole *et al.* 2012) that a central domain at the top of the AHSV VP2 triskelion hub, which is absent in BTV VP2 trimers, could be the target site for such a horse serum protease. This domain is situated directly above the BTV putative SA-binding site and cleavage of AHSV VP2 in this region would thus increase accessibility to this potential binding site (Figure 1.10).

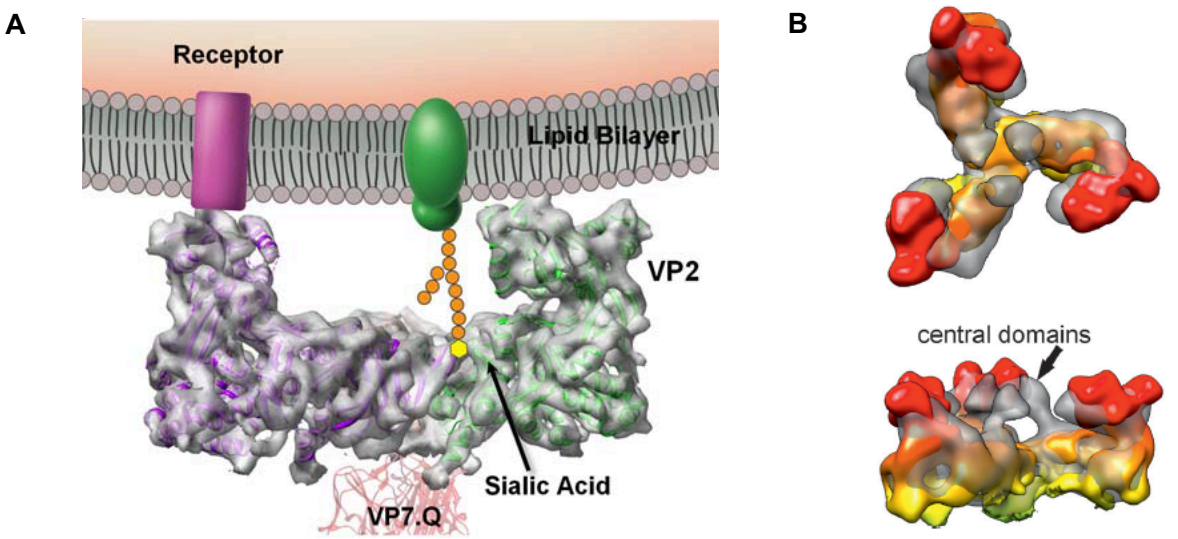

Figure 1.10: Schematic illustration of BTV/AHSV VP2 attachment to the host cell membrane. (A) BTV/AHSV VP2 trimers are thought to attach via their tip domains to cell surface receptors and by the SA-binding domain to a cell surface glycoprotein. Image adapted from Zhang *et al.* (2010). (B) Superposition of AHSV (grey) and BTV (colour) VP2 proteins from above (top) and from the side (below), demonstrating the presence of the additional central domain in the center of the triskelion on top of the hub, which is believed to be the target site for the horse serum protease. Image adapted from Manole *et al.* (2012) *Image used with permission from the publisher.*

Due to the structural similarity between the two viruses, a model for the entry of AHSV into the host cell can be derived from the current understanding of BTV infection. The process is believed to be initiated by proteolytic cleavage of VP2 either in infected insect saliva or in the host serum, after which the virion attaches to the host cell membrane and undergoes clathrin-mediated endocytosis (Forzan *et al.* 2007). Within the early endosome the low pH (6.5 - 6.0) disturbs the interactions between VP2 and VP7, facilitating detachment of the VP2 trimers and disrupting the zinc finger motif situated at the interface between the VP2 hub and body domains, which is believed to play a role in controlling conformational changes (Zhang *et al.* 2016). Together with a further lowering of the pH (~ 5.0) in the late endosome, the removal of VP2 causes a re-folding of VP5, which in turn leads to the outward protrusion of barb-like structures from the particle surface with the VP5 protein trimers remaining tethered to the particle by their anchoring domains (Forzan *et al.* 2004; Zhang *et al.* 2010). These barb-like fusion peptides insert themselves into the endosomal membrane causing release of the viral core particle into the cytoplasm (Figure 1.11).

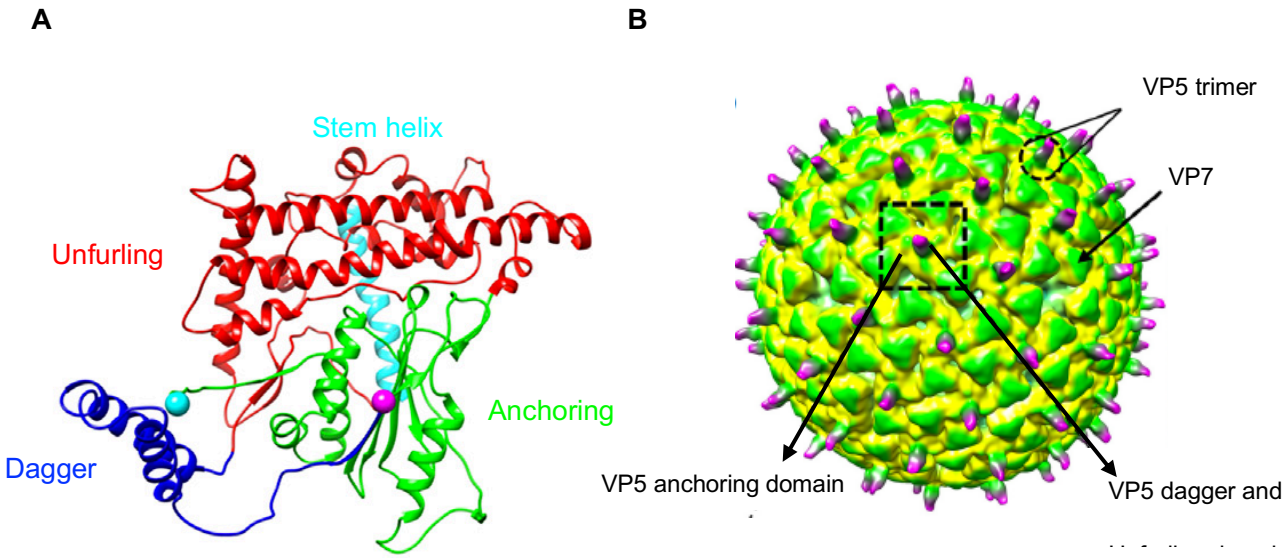

Figure 1.11: Molecular re-arrangement of BTV/AHSV VP5 at low pH. (A) Ribbon model of the VP5 monomer showing the different domains colour-coded, with the stem helix of the unfurling domain shown in turquoise and the N and C termini indicated as purple and turquoise balls respectively. Image adapted from Roy (2017). (B) CryoEM re-construction of the BTV virion at acidic pH showing that VP2 is detached and VP5 has undergone a conformational change leading to the outward protrusion of the dagger and unfurling domains (purple), while the trimer remains tethered to the particle by the anchoring domain (yellow). Image adapted from Zhang *et al.* (2016). *Images used with permission from the publishers.*

The removal of the outer capsid proteins, and release of viral cores into the cellular environment containing the necessary host substrates and transcription factors, causes the core to become

transcriptionally active. Each of the gene segments is then simultaneously and repeatedly transcribed by VP1 to produce ssRNAs (Boyce *et al.* 2004; Zhang *et al.* 2016), which are modified by the capping and methylation activity of enzyme VP4 within the core before being released into the cytoplasm (Ramadevi *et al.* 1998). The viral dsRNA is thus kept within the core particle protected from detection by components of the host cell innate immunity. The nascent ssRNAs act as mRNAs for the synthesis of viral proteins using the host cell machinery and later, in the newly-formed cores, as templates for dsRNA gene synthesis. The VIBs act as the sites of viral assembly and protein NS2 plays a role in directly and specifically sequestering the 10 ssRNAs, together with the three enzymatic proteins VP1, VP4 and VP6 and inner core protein VP3, for encapsidation and the formation of new sub-core particles (Kar *et al.* 2007; Patel and Roy 2014).

The deposition of VP7 trimers serves to stabilize the particles, and phosphorylation of NS2 then regulates their exit from the VIBs in order to acquire the 2 outer capsid proteins VP5 and VP2 for the formation of mature progeny virions (Modrof *et al.* 2005; Mohl and Roy 2016). Although the release of these virions from infected mammalian cells is predominantly effected by cell lysis accompanied by significant cytopathic effects, the viruses have also been shown to use a budding mechanism for viral egress earlier on in the infection cycle. The latter is mediated by utilising the host exocytosis pathway and the membrane destabilising action of non-structural glycoprotein NS3, which functions as a viroporin and also interacts with calpactin to function as a bridging molecule between the new virions and the host cell export machinery (Beaton *et al.* 2002; Celma and Roy 2009). In the insect vector, where the establishment of a persistent viral infection is important, there is no observable cytopathic effect and viral release is mediated exclusively via vesicle formation at the cytoplasmic membrane (Patel and Roy 2014) (Figure 1.12). It is interesting to note that the more variable AHSV NS3 causes a much greater cytopathic effect (CPE) earlier on in the infection cycle than BTV NS3, possibly indicating that AHSV NS3 is expressed at a higher level or is more toxic than BTV NS3 (Venter *et al.* 2014).

Although the primary route of BTV and AHSV host infection is believed to be initiated by the outer capsid proteins, there is evidence to suggest that BTV core-like particles (CLPs), ie. particles that have lost the outer capsid proteins, are also able to infect both insect and, to a lesser extent, mammalian cells (Mertens *et al.* 1996). Interesting in this regard, is the fact that the upper domains of both BTV and AHSV VP7 trimers have characteristic Arg-Gly-Asp (RGD) motifs, albeit in slightly different locations (Basak *et al.* 1996). RGD domains in biological systems are associated with integrin-ligand recognition and fusion of molecules to cell membranes (Ruoslahti 1996). The fact that there are holes in the surface of the outer capsid layer of both BTV and AHSV particles, makes it tempting to speculate that these RGD sites on VP7 may play a role in the ability of viral CLPs to infect cells.

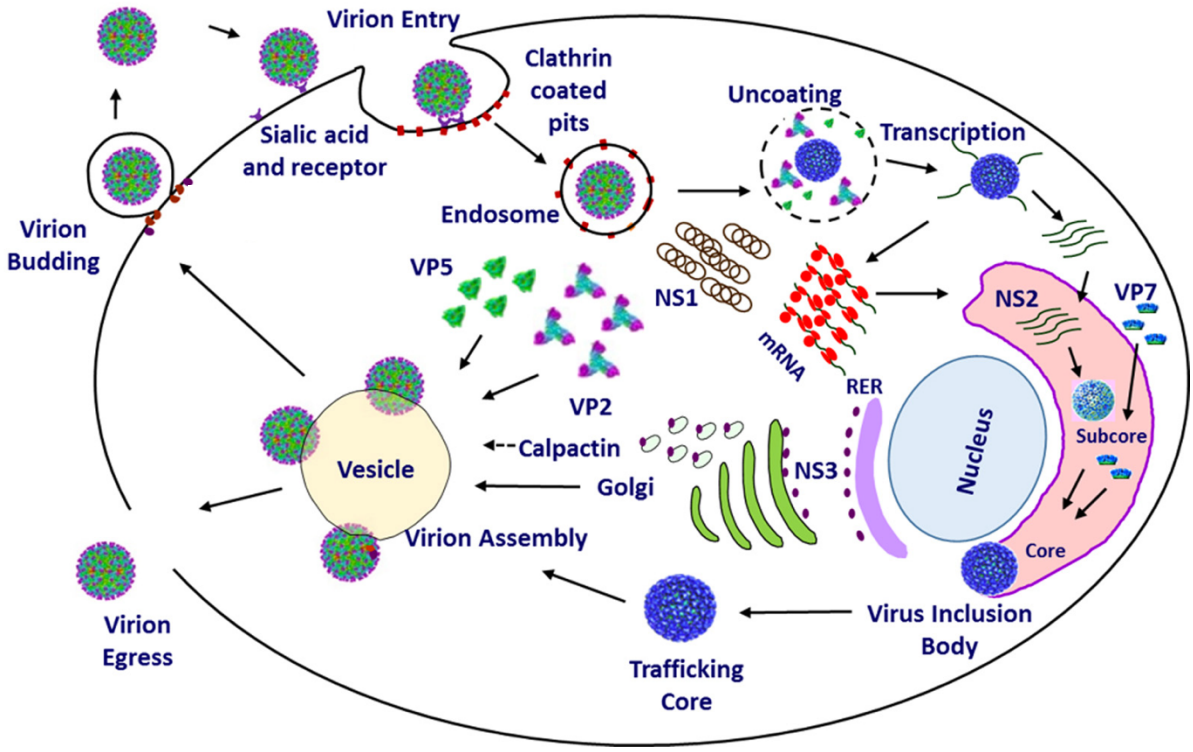

Figure 1.12: Diagrammatic representation of the replication cycle of BTV/AHSV. The virus enters the cell by the attachment of VP2 to sialic acid receptors and clathrin-mediated endocytosis. The acidic pH in the endosome causes loss of VP2 and mediates VP5 membrane permeabilization which results in uncoating of the virion and release of the transcriptionally active core particle into the host cell cytoplasm. Transcription and translation of viral proteins occurs utilizing the host cell machinery and the VIBs act as sites of assembly for the progeny virions. Assembled core particles are then trafficked from the VIB on exocytotic vesicles by NS3 interaction with calpactin. The outer capsid proteins VP5 and VP2 are acquired during this process to produce mature virions. Particles are released from the cell via budding mediated by NS3 or via host cell lysis. Image adapted from Patel and Roy (2014). *Image used with permission from the publisher.*

1.3 African horse sickness disease

1.3.1 Clinical symptoms

Three distinct forms as well as a mixed form of AHS have been described (Figure 1.13). However, it is possible that these represent points on a continuum of virulence as some disease outbreaks are characterized by only one form of the disease, while during other outbreaks, multiple forms occur (Burrage and Laegreid 1994). The most severe form of AHS, with mortality rates exceeding 95%, is the pulmonary form or “dunkop” (thin head). This is an acute febrile disease accompanied by mild depression, sweating, spasmodic coughing, anorexia and respiratory distress, with a possible frothy nasal discharge in the terminal stages (Coetzer and Guthrie 2004; Mellor and Hamblin 2004). The cardiac form or “dikkop” (thick head), with a mortality of about 50%, is characterized by fever, swelling of the head, neck and supraorbital fossae and sometimes petechial hemorrhages in the eyes. The mildest form of AHS is generally not fatal and is accompanied by a low-grade fever, often more pronounced in the afternoon, anorexia, depression and congestion of the mucous membranes. The most common form, with a 70% mortality rate, is a mix of the pulmonary and cardiac forms.

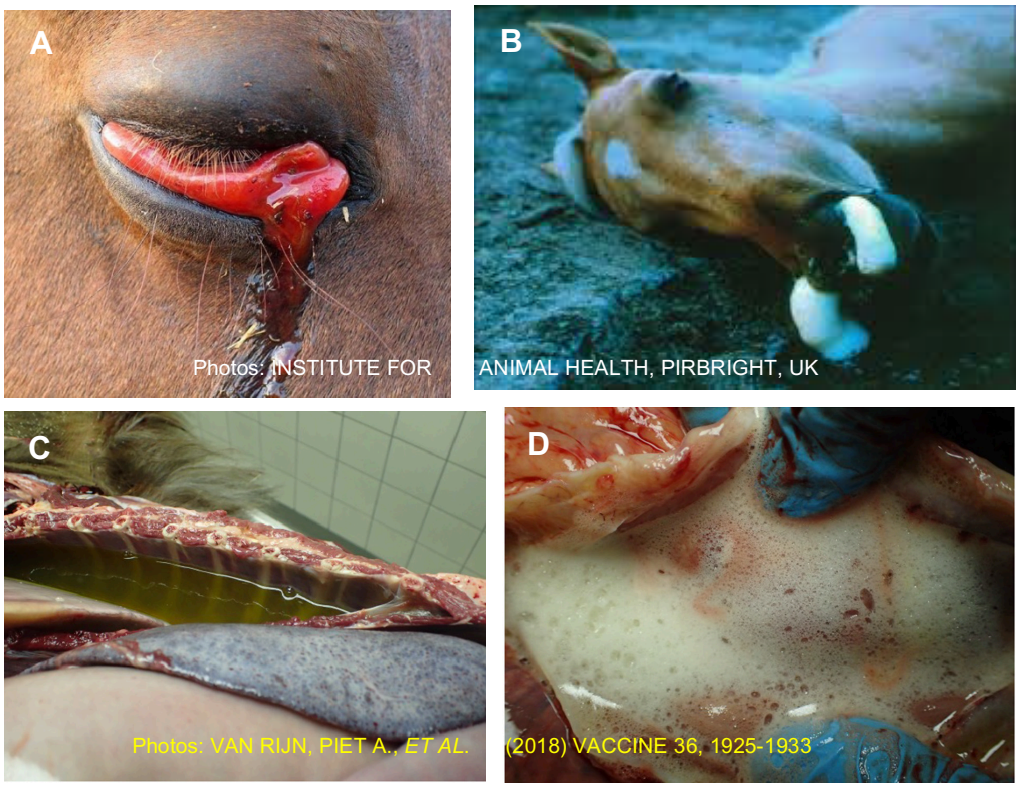

Figure 1.13: Clinical symptoms of AHS. (A) Petechial hemorrhages associated with the cardiac form or “dikkop” (thick head) (Thompson et al. 2012). (B) Frothy nasal discharge sometimes observed during the terminal stages of the pulmonary form or “dunkop” (thin head) (Thompson et al. 2012). Post mortem signs of (C) hydrothorax and (D) foam in the windpipe and bronchia following AHSV infection (van Rijn et al. 2018). *Images under the Creative Commons Attribution (CC-BY) license or used with permission from the publisher.*

1.3.2 Pathogenesis

The bite of an infected *Culicoides* midge signals the potential initiation of infection in a susceptible host, after which initial AHSV replication occurs in the regional lymph nodes. This primary viraemia is responsible for disseminating the virus to all parts of the body (Mellor and Hamblin 2004). Viral particles are known to associate with erythrocytes and monocytes, and are transported in the bloodstream to the endothelial cells of the lungs, spleen and other lymphoid tissue, which are the main sites of secondary replication (Burrage and Laegreid 1994; Wohlsein *et al.* 1997). Although the level of replication is relatively low in these organs, the virus causes severe injury to the endothelial cells, and the symptoms of oedema and pleural effusion which characterize the severe form of AHS are believed to be the result of increased vascular permeability and the impairment of circulatory and respiratory systems.

The primary factors which influence the severity and duration of the disease in horses are related to the virulence of the virus and the immune status and susceptibility of the animal. Host genetics must play a role, as is evidenced by the susceptibility of both horses and zebra to AHSV, yet only horses contract AHS disease. An animal which has recovered from a prior infection is fully protected by re-infection with the same serotype, and may well only contract a fever or the cardiac form of AHS upon exposure to a heterotypic viral strain. However, Erasmus (1978) has noted that excessive vaccine administration may lead to an immunological unresponsiveness or even hypersensitivity.

Virulence is related to tissue tropism, and it would seem that the virus itself is the primary determinant of the resultant form of disease (Erasmus 1974). AHSV field isolates are believed to be composed of a mixed virus population with regard to the host tissue target, and the virulence of the particular isolate will be determined by the percentage of particles affecting vital organs such as the lungs, for example. In this sense, Erasmus (1974) suggests that viral attenuation may be the result of specific selection of viruses which do not have affinity for the tissues of vital organs.

Alexander (1935) was the first to demonstrate the humoral nature of the AHSV immune response when he utilized a mouse neutralization test to indicate a strong association between the production of neutralizing antibodies and protective immunity. The antigenic determinants responsible for this neutralising antibody response are located on capsid protein VP2: several studies have suggested putative sites for these epitopes, mainly in the 5' terminal half of the protein (Burrage *et al.* 1993; Bentley *et al.* 2000; Venter *et al.* 2000; Martinez-Torrecuadrada *et al.* 2001; Manole *et al.* 2012; Mathebula *et al.* 2017). However, the probable contribution of cell-mediated immunity cannot be ignored - at least three $CD8^{+}$ receptors have been identified on VP2 or NS1 (de la Poza *et al.* 2015) and others have reported the stimulation of IFN-y responses in vaccinated

animals (El Garch *et al.* 2012; Pretorius *et al.* 2012). The degree to which the presence of neutralizing antibodies may be regarded as an adequate correlate of protection therefore remains to be established.

1.3.3 Surveillance and Diagnosis

African Horse Sickness is on the OIE list of notifiable viral diseases, which means that it is compulsory for member states like South Africa to inform the organization of any change of disease status. In South Africa, the Western Cape Province has historically been relatively free of AHS; in order to maintain the country's horse export status, an AHS controlled area - to and from which the movement of all horses is strictly monitored - was established in 1997 (Weyer *et al.* 2016). The area consists of an AHS-free zone, which is the small Cape Metropolis where no cases of AHS have ever been recorded, a surrounding surveillance zone and beyond that, a zone of protection (Figure 1.14). Whenever a new outbreak occurs in the surveillance zone, horse exports to the EU are suspended for a minimum of 2 years.

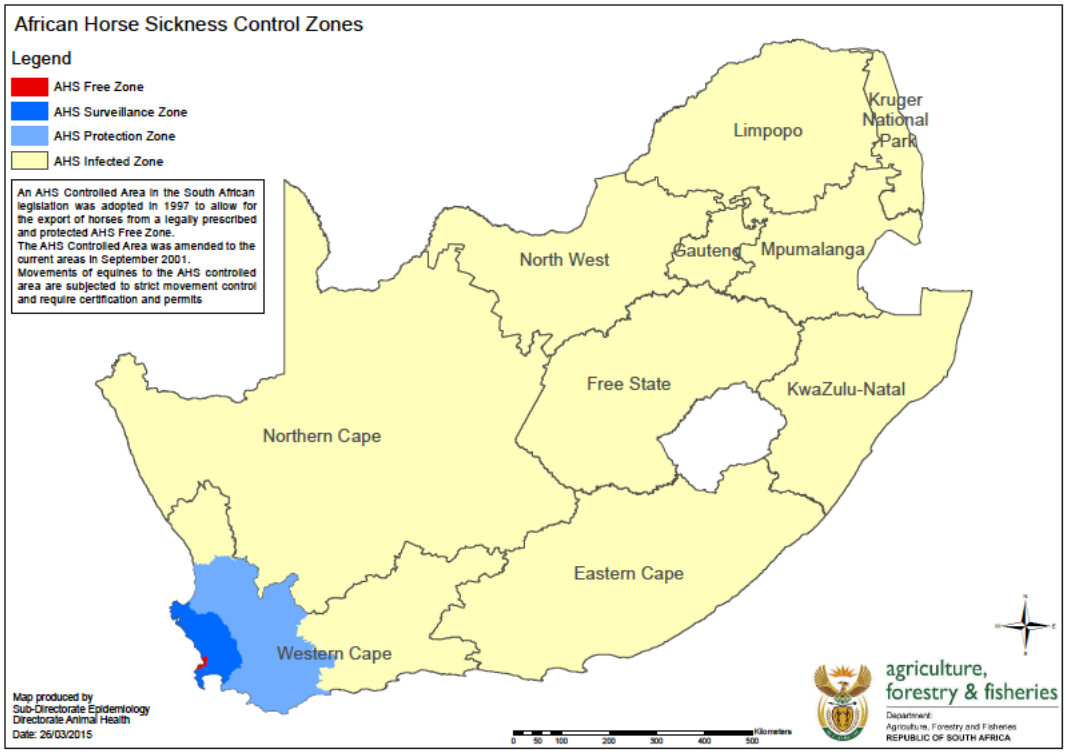

Figure 1.14: Map of the AHS controlled area indicating the free, protection and surveillance zones. (Image retrieved from https://www.nda.agric.za/vetweb/epidemiology/Disease%20Maps/AHSzones%2026Mar2015.pdf)

According to the EU surveillance requirements, every month at least 60 identified unvaccinated horses distributed throughout the free and surveillance zones are serologically tested for AHSV (Weyer 2017). Local law requires all suspected cases of AHS to be reported to the state veterinary authority, and all equine deaths due to AHS undergo official equine necroscopy examination. As a further measure of control, it is compulsory to obtain permission prior to vaccinating horses with the AHS polyvalent live attenuated vaccine (LAV) produced by Onderstepoort Biological Products (OBP, Pretoria) in the free and surveillance zones.

The clinical presentation of AHS is often sufficient to make a tentative diagnosis of the disease; however, particularly in the early stages, differentiation from other equine diseases such as equine encephalosis (EEV), equine viral arteritis (EVA) and West Nile virus (WNV) may not be possible. Traditional methods of virus isolation and serotyping by virus neutralization assay can be used to make a definitive diagnosis, but these tests can take weeks before a result can be obtained, and they rely on the availability of appropriate reference strains and antisera (Sailleau *et al.* 2000). The currently used indirect ELISA test is based on detection of the group-specific VP7 antigen in the serum sample (Maree and Paweska 2005): although the method is accurate, it is not possible to determine the virus serotype using this ELISA test, as each serotype is defined by the sequence of the antigenic determinants present in the outer capsid protein VP2. It is also not possible to differentiate between vaccinated and infected animals using this method as both groups of animals would elicit antibodies to VP7.

Three triplex AHSV type-specific (TS) reverse transcription polymerase chain reaction (RT-qPCR) assays have recently been developed which can be directly applied to nucleic acid extracted from blood samples from AHSV-infected horses (Weyer *et al.* 2015). Using these assays, samples can be extracted and evaluated within 4 hours of their arrival at the laboratory so that the AHSV serotype in a field outbreak can be rapidly determined. This test is most useful in directing the timeous implementation of appropriate vaccination and control strategies.

1.4 Prevention and control

There is no cure for AHS and no specific treatment aside from rest and good animal husbandry. Various interventions, such as non-steroidal anti-inflammatory drugs for alleviating pain and reducing fever, antimicrobials to fight secondary bacterial infection or corticosteroids to help stabilize cell membranes and preserve vascular membrane integrity, have been employed, but all these treatments are supportive rather than curative (African Horse Sickness Trust). Anecdotal reference to homeopathic remedies has also been made, but there is no scientific evidence to prove the efficacy of such treatments in AHS cases. Implementation of certain husbandry modifications such as stabling of animals before dark in vector-proof housing, using insect

repellants and encouraging natural vector predators like fish, frogs and bats, may assist in prevention (Meiswinkel *et al.* 2000; Mellor and Hamblin 2004); however, ultimately vaccination of animals remains the most successful method of prevention and control.

1.4.1 Live attenuated vaccines

Alexander (1934) was the first to demonstrate that a mouse-adapted strain of AHSV could be propagated in chicken embryos, and that serial passage in embryonated hens' eggs caused attenuation of the virus without loss of immunogenicity. His studies also supported the existence of multiple strains of the virus, as he found a large variation (26 - 81%) in the number of horses that were protected after being challenged a second time with a different virus isolate. The successful propagation of AHSV in mammalian tissue culture by Erasmus (1963a), aided by the discovery that viral plaque size could be used as a genetic marker to identify avirulent clones of AHSV from a mixed population (Erasmus 1978), further advanced the development of live-attenuated vaccine (LAV) strains. The polyvalent LAVs that have been successfully used to vaccinate horses over the past six decades are based on these viral formulations. However, although the frequency and severity of outbreaks has declined significantly since these vaccines have come into use, many horse deaths due to AHS still occur in South Africa every year.

The currently used LAV is supplied in two polyvalent vials containing 3 (serotypes 1, 3 and 4) and 4 (serotypes 2, 6, 7 and 8) AHSV serotypes each. Neither AHSV 5 nor AHSV 9 are included in the vaccine (von Teichman and Smit 2008): serotype 5 was originally included, but was withdrawn in 1990 following reports of residual virulence, believed to be the result of re-assortment between serotypes 4 and 5 in the vaccine formulation (von Teichman *et al.* 2010). Serotype 9 has never been included due to its low incidence in southern Africa and, because cross protection between serotypes 1 & 2, 3 & 7, 5 & 8 and 6 & 9 has been documented (Erasmus 1978; Coetzer and Guthrie 2004; von Teichman *et al.* 2010), protection against AHSV 9 is expected to be provided by AHSV 6. There is no cross-protection between AHSV 4 and any of the other serotypes. Of concern however is the fact that in 2006 both AHSV 5 and 9 dominated outbreaks in South Africa, particularly in the Western Cape Province: this raises questions about the competency of the LAV to provide sufficient protection against these two AHSV serotypes.

Although there is little argument that the LAV is still the best option in the fight against AHS, its use has raised concerns with regard to other important issues. The serotype-specific immune response within horse populations as well as between the different serotypes appears to be quite variable, and it may take as many as 8 vaccination courses over 6 years before an animal is fully protected against all nine AHSV serotypes (von Teichman *et al.* 2010; Molini *et al.* 2015; Weyer *et al.* 2017). Furthermore, gene segment re-assortment between outbreak and vaccine strains may lead to the

establishment of new genetic variants or reversion to virulence of attenuated vaccine strains (Mellor and Hamblin 2004). Indeed, a study comparing the whole genome sequences from AHSV isolates responsible for outbreaks between 2004 and 2014 in the controlled area of the Western Cape with LAV and AHSV reference strains, demonstrated conclusive evidence of re-assortment between and reversion to virulence of viruses within the LAV itself (Weyer et al, 2016). The outcome of this study highlights the importance of employing judicious LAV vaccination strategies and genetic screening of circulating field strains during AHS outbreaks.

Another shortcoming of the LAV is the inability to serologically differentiate vaccine-induced immunity from that induced by natural infection, ie. absence of what is known as DIVA capacity. This differentiation is important both for early detection of disease and sero-surveillance and can also limit unnecessary culling of animals in an outbreak situation. A further major issue regarding routine vaccination with the LAV is the fact that it is not licensed for use outside of the African sub-continent, which has a hugely negative impact on the international equine trade and export industry.

1.4.2 Inactivated vaccines

Inactivated or “killed” vaccines have been prepared by treating mammalian cell-cultured AHSV with formaldehyde or ß-propiolactone (Mirchamsy and Taslimi 1968), or with bromoethylenimine (Weyer *et al.* 2013). The latter acts on nucleic acid but not protein, ensuring that the immunogenic properties of the vaccine are not compromised. An inactivated AHSV 9 vaccine tested in guinea pigs and horses (Lelli *et al.* 2013) elicited a comparable neutralizing antibody response in both animal species, confirming the usefulness of the guinea pig as a small animal model to test the efficacy of potential vaccine candidates (Erasmus 1963b). The vaccine proved to be safe, and all horses survived a challenge with the same virus used to generate the killed vaccine.

A formalin-inactivated AHSV vaccine was commercially produced and used during the 1987 - 1991 AHS outbreak in Spain, Portugal and Morocco, but although it proved to be efficacious at the time, this vaccine is no longer available (Mellor and Hamblin 2004). The main drawbacks with regard to inactivated vaccines are firstly, that they are expensive to produce, requiring large-scale isolation of infectious virus, which poses a significant bio-containment risk; secondly, repeated inoculations may be required to ensure long-lasting protective immunity. Furthermore, although the risk of gene segment re-assortment and reversion to virulence are mitigated with this type of vaccine, differentiation between vaccinated and infected animals is not possible.

1.4.3 Recombinant vaccines

Due to raised international awareness and local dissatisfaction with the current vaccine, AHSV research has focussed in recent years on the development of recombinant vaccines. These have largely been based on producing the antigenic AHSV proteins involved in eliciting a protective immune response, particularly the outer capsid proteins VP2 and VP5, and investigating the best ways in which to present them to the host's immune system

1.4.3.1 DNA vaccines

Besides the AHSV proteins themselves, there has been some investigation of the efficacy of using naked AHSV VP2 DNA as a vaccine candidate (Romito *et al.* 1999). Although a VP2-specific humoral and cellular immune response following inoculation of a single horse was observed, and the same horse survived an AHS outbreak during the following rainy season, the neutralizing antibody titre reported was sub-optimal and no experimental challenge ensued. Furthermore, vaccination of hens with cloned VP2 cDNA stimulated the production of egg yolk IgY antibodies with a serum neutralization titre 80-fold less than that obtained following vaccination with purified AHSV. The potential for producing a suitable AHSV DNA vaccine thus seems limited.

1.4.3.2 Subunit vaccines

Recombinant AHSV VP2 produced via the baculovirus expression system has been used either singly or in combination with VP5 and/or VP7 as a subunit vaccine, and was shown to induce protective immunity against the virus (Martinez-Torrecuadrada *et al.* 1996; Roy *et al.* 1996; Kanai *et al.* 2014). However, recombinant soluble antigens are generally poorly immunogenic and the aggregation of baculovirus-expressed VP2 purified from insect cell lysates together with the requirement for repeated boost inoculations (Du Plessis *et al.* 1998), and the use of potent adjuvants to enhance immunogenicity (Scanlen *et al.* 2002), have limited the usefulness and application of this type of vaccine. Furthermore, although subunit vaccines are advantageous in that they permit differentiation between AHSV-vaccinated and infected animals, baculovirus expression requires growth under sterile conditions and is uneconomical for an animal vaccine due to the high cost of the media required to culture insect cells.

1.4.3.3 Poxvirus vectored vaccines

Poxvirus vectored vaccines are recombinant poxvirus strains which have been genetically modified to contain a copy of the gene of interest within the viral genome. The vaccine is delivered directly

to the cells where the viral protein is expressed and presented to the host immune system for the stimulation of both humoral and cellular immunity.

1.4.3.3.1 Canarypox virus

Vaccination of horses with an adjuvant-formulated canarypox vaccine (ALVAC-AHSV) expressing both AHSV 4 VP2 and VP5 was shown to elicit serotype-specific neutralizing antibodies against the virus (Guthrie *et al.* 2009). Upon challenge, horses which received a sufficiently high dose of vaccine developed sterilizing immunity against AHSV 4 with serum neutralization titres ranging from 10 - 80 (expressed as the reciprocal of the highest dilution that provided >50% cell protection). However, stimulation of neutralizing antibodies has yet to be established as a definite correlate of protection: this was emphasized by the survival of a seronegative horse after challenge with virulent AHSV. Furthermore, in a follow-up study using the same vaccine, gamma interferon-producing cells were detected after stimulation with both VP2 and VP5, indicating that cell-mediated immune responses most likely also played a role in protecting against the viral challenge (El Garch *et al.* 2012).

1.4.3.3.2 Modified Vaccinia Ankara (MVA) virus

Since 2009, several studies on the development of an alternative AHSV candidate vaccine based on a modified vaccinia Ankara (MVA) virus have been published (Chiam *et al.* 2009; Castillo-Olivares *et al.* 2011a; Alberca *et al.* 2014; Calvo-Pinilla *et al.* 2014; de la Poza *et al.* 2015; Manning *et al.* 2017; Calvo-Pinilla *et al.* 2018). The MVA strain was originally produced by extensive passage of the chorioallantosis vaccinia virus Ankara (CVA) in chicken embryo fibroblast cells (CEF). This resulted in the loss of 12% of the viral genome, including genes that interfere with the host immune response, and caused inability to replicate in most mammalian cells (Gilbert 2013). However, replication is only blocked after DNA synthesis, so gene expression still occurs, with resulting expression of recombinant antigens inside infected cells. Recombinant MVA vaccines are therefore non-replicative live viral vectors that can induce both a humoral response as well as stimulate T-cell immunity by facilitating intracellular presentation of the antigen of interest via MHC molecules on the cell surface. Interestingly, MVA vaccines have been shown to be most effective in prime-boost regimens, ie. when administered as a heterologous boost following a strong prime vaccination (Cottingham and Carroll 2013). Boosting of an existing T-cell response to a recombinant antigen causes an amplification of the initial response and reduces the response to antigens on the viral vector itself, thus avoiding the issue of pre-existing immunity to the viral vector and allowing re-use of the vaccine.

However, homologous prime-boost vaccination with MVA expressing AHSV VP2 (MVA-VP2) has also been shown to elicit neutralizing antibodies which provided complete protection in both mice and horses (Chiam *et al.* 2009; Castillo-Olivares *et al.* 2011a; Alberca *et al.* 2014; Manning *et al.* 2017). The type 1 interferon receptor knockout (IFNAR -/-) mice used in these experiments were chosen as small animal challenge models as AHSV infection causes similar clinical pathologies and mortality rates to those observed in horses. In these studies, protection was provided by vaccination with MVA vaccines expressing only outer capsid protein VP2, indicating that VP5 is not essential for, but may improve vaccine efficacy.

The role of cell-mediated immunity appears to be less important than antibody responses, as the transfer of splenocytes from MVA-VP2-vaccinated mice to unvaccinated mouse recipients did not cause a statistically significant reduction in viraemia (Calvo-Pinilla *et al.* 2014, 2015). Furthermore, passive immunization with vaccinated donor sera protected recipient mice from infection, demonstrating the primary protective role of the neutralizing antibody response. However, cell-mediated immunity is likely to play an additional protective role to some extent, as mice immunized with either MVA-VP2 or MVA-NS1 have been shown to develop gamma-interferon-producing cells when stimulated with peptide sequences on VP2 and NS1 (de la Poza *et al.* 2015).

In a study to investigate a polyvalent AHSV vaccination approach, horses were immunized and boosted 4 weeks later with either MVA-VP2(4) or MVA-VP2(9) or both, simultaneously or sequentially (Manning *et al.* 2017). Simultaneous vaccination with recombinant MVA-VP2 of both serotypes, induced a statistically significant virus neutralizing antibody (VNAb) response against AHSV 4 and AHSV 9 as well as a cross-protective response to AHSV 6 in the horses which received MVA-VP2(9). Furthermore, 4 months later when the VNAb titres had decreased dramatically, vaccination with MVA-VP2(5) representing a third AHSV serotype, not only elicited VNAb against AHSV 5, but also induced an anamnestic response towards AHSV 4, 6 and 9 as well as the cross-reactive AHSV 8. These results demonstrate the suitability of MVA-VP2 to be used as a polyvalent vaccine mixture providing protection against more than one AHSV serotype. The results also suggest the possibility that other sub-dominant cross-reactive epitopes may exist between AHSV serotypes 5, 6, 8 and 9. This study further confirms that any possible pre-existing immunity to the viral vector does not impact negatively on the usefulness of the MVA-VP2 vaccines.

The immune responses induced by four different AHSV 4 MVA-VP2 vaccines, namely live MVA-VP2, heat - inactivated MVA-VP2, UV - inactivated MVA-VP2 and sucrose gradient-purified MVA-VP2, proved that both pre - formed VP2 in the MVA vaccine and transient expression of VP2 in the vaccinated host's cells, contribute towards inducing a protective immune response (Calvo-Pinilla *et al.* 2018). The inactivated MVA-VP2 vaccines, containing only pre-formed VP2, induced

lower VNAb titres than the live MVA-VP2, yet the gradient purified MVA-VP2, containing no pre-formed VP2, also induced a weaker immune response than that induced by live MVA-VP2. In fact, sterilizing immunity was only induced by the live MVA-VP2 vaccine. It is likely that the transient intracellular expression of conformationally intact VP2 in infected cells activates T-cells, lending credence to the possible supportive role of cellular-mediated immunity in the protective immune response.

1.4.3.4 Reverse genetics vaccines

Over the last decade, reverse genetics systems have been used to generate novel live virus-based BTV and AHSV vaccine candidates, engineered according to a rational design rather than by random serial passage attenuation (Boyce *et al.* 2008; Matsuo *et al.* 2010; Kaname *et al.* 2013; Feenstra *et al.* 2015; van de Water *et al.* 2015; Vermaak *et al.* 2015; Celma *et al.* 2016; Conradie *et al.* 2016; Lulla *et al.* 2016; van Rijn *et al.* 2016; Lulla *et al.* 2017; van Rijn *et al.* 2018). These live vaccine strains depend on the availability of cloned cDNA copies of the viral genes, and are produced in mammalian cell lines via a double transfection strategy. Firstly, a primary viral replication complex is pre-expressed by transfection with expression plasmids encoding the five viral proteins, VP1, VP3, VP4, VP6 and NS2. A second transfection with ten exact copy capped T7 viral RNA transcripts, which serve as effective substitutes for authentic core-derived viral transcripts, then triggers full replication and enables virus rescue. Different AHSV serotypes can be rescued by using the same primary transcription complex, and then exchanging the T7 RNA transcripts of one or more capsid proteins (Kaname *et al.* 2013). More importantly for vaccine purposes, genes encoding these proteins can be incorporated into a common viral genome which has been precisely engineered to contain one or more defective genes.

Two main vaccine platforms to produce defective virus strains have been developed using this technology. Entry Competent Replication Abortive (ECRA) vaccine strains, previously also referred to as Disabled Infectious Single Cycle (DISC) vaccines, lack a functional VP6 gene and are therefore unable to complete even a single replication cycle in infected cells (Lulla *et al.* 2016; Lulla *et al.* 2017). The vaccine is rescued and propagated in a complementary cell line expressing VP6 *in trans* and viral antigens capable of eliciting the expected antibody response are expressed in normal cells, but no active infection ensues. In contrast, Disabled Infectious Single Animal (DISA) vaccine strains lack a functional gene for expression of non-essential non-structural protein NS3/NS3a (Feenstra *et al.* 2015; van de Water *et al.* 2015; van Rijn *et al.* 2018). Absence of these proteins prevents viral egress, thus inhibiting viraemia and allowing only local replication in infected cells with no propagation in nor transmission by midges. Both of these vaccine candidates fulfil the criteria for DIVA compliance, as antibodies to the missing viral protein in each case would be absent in vaccinated animals, but present in animals which have been infected.

The main goal in new AHSV vaccine development is to provide protection against all nine serotypes of the virus. Initially, an attempt was made to develop a set of defective AHSV virus strains each consisting of a common core coated with a different serotype-specific outer capsid protein VP2 (van de Water *et al.* 2015). However, exchange of only a single protein resulted in unequal and significantly lower reassortant viral titres compared to the parental virus strain. To produce suitably-replicating defective vaccine strains for each serotype, it appears necessary to exchange between two (VP2 and VP5) and five (VP2, VP3, VP5, VP7 and NS3) proteins on the common backbone, the number depending on the desired viral serotype (Lulla *et al.* 2016). The safety and immunogenicity of both monospecific (AHSV 4) and multivalent cocktail (AHSV 1/4/6/8) ECRA vaccines was tested in ponies; these were protected against virulent challenge with AHSV 4 (Lulla *et al.* 2017). Pre-challenge serum neutralization titres were in the range of 8 - 64 (expressed as the reciprocal of the highest dilution that provided >50% cell protection), below those generally obtained following vaccination with the AHS LAV (Weyer *et al.* 2017), but nevertheless demonstrating the potential efficacy of a reverse genetics vaccine candidate to protect against the disease. Although the technology looks promising, further research is necessary to determine the minimum dose requirement and longevity of the immune response. Furthermore, the costly high-level biosafety facilities required to produce these types of vaccines, may deter their successful commercialization, particularly in less-developed countries.

1.5 Virus-like particle technology

1.5.1 Virus-like particles as immunogens

Virus-like particles (VLPs) are safe, non-replicating protein complexes which mimic the structure of intact virions. They possess self-adjuvanting properties and have the advantage of being highly immunogenic compared to subunit vaccines, as epitopes are displayed in ordered repetitive arrays on the particle surface (Noad and Roy 2003). The size of VLPs ensures appropriate drainage into the lymph nodes and is also optimal for uptake by antigen-presenting cells and MHC cross presentation (Bachmann *et al.* 1993; Lechner *et al.* 2002). This efficient trafficking of VLPs and their interaction with the host immune cells induces both innate and adaptive humoral and cellular immune responses, making them particularly attractive vaccine candidates (Grgacic and Anderson 2006; Lua *et al.* 2014). Furthermore, such vaccines present no risk of reversion to virulence nor of dsRNA segment re-assortment with wild virus or live vaccine strains, because they do not contain viral RNA or any of the non-structural proteins. Absence of these viral components also makes it possible to distinguish between vaccinated and infected animals using molecular diagnostic techniques, meaning that VLP vaccines would be DIVA compliant.

Several VLP vaccines for human virus diseases have been commercially licensed; namely, Cervarix® (GlaxoSmithKline) and Gardasil® (Merck) against human papillomavirus, Engerix B® (GlaxoSmithKline) and Recombivax HB® (Merck) against hepatitis B virus and Hecolin® (Xiamen Innovax) against hepatitis E virus (Chackerian 2007; Zhu *et al.* 2010).

The production of both BTV and AHSV VLPs is based on the hypothesis that co-synthesis of proteins VP2, VP3, VP5 and VP7 will result in the spontaneous self-assembly of VLPs via various hydrophobic, electrostatic and covalent interactions (Pattenden *et al.* 2005). The successful formation and protective efficacy of BTV VLPs produced by recombinant baculovirus-mediated co-expression of these proteins in insect cells, has been demonstrated (Roy *et al.* 1992; Roy *et al.* 1994a; Stewart *et al.* 2010). More recently, high-level plant-based expression of fully-assembled VLPs of BTV-8 has been reported (Thuenemann *et al.* 2013; van Zyl *et al.* 2016). The VLPs elicited a strong antibody response in sheep which provided protective immunity against challenge with a BTV-8 field isolate.

Until very recently, no reports existed describing the production of AHSV VLPs in any expression system, as an initial investigation regarding the production of AHSV CLPs by co-infection of insect cells with recombinant baculoviruses expressing either AHSV VP3 or VP7, was unsuccessful (Maree *et al.* 1998). In a more recent study, co-expression of AHSV viral proteins and assembly of AHSV CLPs and VLPs was achieved by co-infection with baculovirus recombinants simultaneously expressing two AHSV capsid proteins ie. VP2 and VP3 or VP5 and VP7 (Maree *et al.* 2016). However, the overall VLP yield was very low and precluded quantification. When a mutated version of VP7, modified to increase solubility and reduce VP7 crystal formation (Rutkowska *et al.* 2011) was incorporated into the AHSV CLPs instead of wt VP7, the CLP yield was increased with a concomitant decrease in VP7 crystalline formation. It is therefore possible that VP7 protein engineering may be employed to enhance the production of recombinant AHSV VLPs for vaccine production.

1.5.2 VLPs as carrier molecules

The immunogenic application of VLPs can be extended to include surface presentation of heterologous antigens via chemical conjugation or genetic manipulation of an outer capsid protein (Jennings and Bachmann 2008; Pushko *et al.* 2013). Antigens displayed in this manner assume similar immunogenicity to the particle itself, suggesting that this is an effective mechanism for enhancing the immune response against poorly immunogenic subunit antigens (Chackerian 2007). Antigen conjugation via amino- or carboxyl-groups in amino acid side chains is non-specific, however, preventing directional coupling of the antigen to the VLP. Therefore, conjugation via an exposed sulfhydryl group (Cys) is the most commonly used cross-linking strategy. However, this

method can be complicated by a reactive cysteine residue interfering with pre-existing sulphide bonds in the antigen.

The main disadvantage of genetic fusion strategies is that misfolding of either the capsid protein and/or antigen can result, which can impair VLP assembly and prevent effective display of the antigen. There are also size limitations with regard to the length by which a coat protein (CP) gene can be extended, and the expression system which is optimal for capsid protein synthesis may differ from that which is best for antigen expression. Modular two-step conjugation, in which the VLP and target antigen are first expressed separately and then coupled afterwards, presents a more attractive alternative strategy (Brune and Howarth 2018).

Although no VLP vaccine displaying foreign epitopes has yet been commercialized, the technology is promising and would enable targeting of antigens previously resistant to vaccine-based approaches. In this context, the selection of an expression system permitting high-level VLP production is important both in terms of downstream processing as well as economic viability.

1.6 Plant-based expression systems

In the past, most recombinant proteins have been produced in systems that use microbial fermentation, insect or mammalian cell cultures or transgenic animals. More recently however, there has been an increased interest in utilizing plant-based expression systems - the so-called “biopharming” or “molecular farming” approach - whereby plants are harnessed as mini-factories to produce useful pharmaceutical proteins (Ma et al. 2003; Rybicki 2010; Fischer et al. 2013; Rybicki 2014; Lomonossoff and D’Aoust 2016; Rybicki 2018). Such recombinant proteins may have a wide variety of applications including as therapeutic treatments, diagnostic reagents and prophylactic vaccines.

Compared to the traditional systems mentioned above, a number of advantages are associated with the use of plants for the large-scale production of recombinant proteins. These include lower capital outlay and running costs, increase and speed of scale-up once proof of concept has been established, production of large quantities of recombinant protein, eukaryotic protein processing ability to ensure correct assembly and modification, and especially favourable safety profiles, as plant systems are free from the risk of contaminating animal pathogens and many fall under the “generally regarded as safe” (GRAS) definition (Ma et al. 2003; Twyman et al. 2003; Lai and Chen 2012). Biopharming thus generally offers a more efficient, safer and cost-effective alternative to existing recombinant protein expression technologies. Following the initial production of heterologous proteins in plants in the 1980s, the idea of plants or their organs as cheap edible vaccines was an attractive concept. However, as the science evolved, it became clear that issues

of dose standardization and quality control were likely to prevent this notion from becoming a reality.

As mentioned above, a key consideration when choosing an appropriate expression system for large-scale recombinant protein production, is the cost factor. The simple requirement for natural resources like carbon dioxide, sunlight and water and the ease of scale-up through the cultivation of large areas of land, gives the plant expression platform a huge advantage over insect and mammalian cell systems both of which require costly culture media. Although plant-based expression has no appreciable financial advantage over other cell culture systems in terms of downstream processing, particularly if high protein purity is required, it is estimated that vaccine cost production could be reduced by as much as 31% due to the more economical upstream requirements (Rybicki 2009). This hypothesis is supported by the results of several techno-economic and comparative analyses reported in the literature contrasting different recombinant protein production platforms (Merlin *et al.* 2014; Nandi *et al.* 2014; Gecchele *et al.* 2015; Walwyn *et al.* 2015). However, estimating an actual cost per dose is complicated by the fact that automation of the plant transient expression platform at the lab-scale production level is hardly feasible.

The first recombinant protein to be expressed in plants was the human growth hormone in transgenic tobacco and sunflower plants (Barta et al. 1986). Following this, the correct assembly of a functional human monoclonal antibody in transgenic tobacco demonstrated that complex glycoproteins with several subunits could be successfully expressed in plants (Hiatt et al. 1989). The first indication that transgenic plants could be utilized as low cost vaccine production systems was provided by the plant-based expression of hepatitis B VLPs (Mason et al. 1992) and the VP1 epitope of foot-and-mouth-disease virus (FMDV) on the surface of cowpea mosaic virus (CPMV) VLPs (Usha et al. 1993). Since then, a wide variety of high quality pharmaceutical proteins have been produced in plant-based expression systems with taliglucerase alfa, used for the treatment of Gaucher disease, being the first plant-produced biopharmaceutical to receive FDA approval for human administration (Zimran et al. 2011).

Initially, plant-based expression was accomplished using stable transgenic plant lines whereby the transgene target is incorporated into the plant genome and the recombinant protein can be expressed by successive plant generations (Rybicki 2010). The main disadvantages of this method are the length of time required to achieve successful transgenic expression (3 - 9 months), as well as the relatively low recombinant protein yield compared to traditional expression strategies (Fischer et al. 2013). In recent years, however, there has been a growing interest in either virus-based or *Agrobacterium*-mediated transient protein expression, whereby the transgene is not

integrated into the plant genome, but temporarily directs recombinant protein synthesis while residing as an episome in the plant cell (Rybicki 2010; Chen and Lai 2015).

Virus-based transient expression is achieved by means of vectors based on RNA plant viruses including tobacco mosaic virus (TMV), potato virus X (PVX) and cowpea mosaic virus (CPMV), which contain the gene of interest (Cañizares *et al.* 2006; Giritch *et al.* 2006; Lindbo 2007). These viruses replicate to high titres in infected cells but there are limitations with regard to the size of the gene insert which can be accommodated, as well as biocontainment issues due to the fact that the viral vectors can move throughout the entire plant (Sainsbury and Lomonossoff 2008; Brewer et al. 2018). A further problem with regard to autonomously replicating viral vector constructs, is genetic stability as the transgene is frequently lost as the plant develops (Rybicki 2010).

With *Agrobacterium*-mediated transient protein expression, the recombinant *A. tumefaciens* strain containing the foreign gene within its transfer DNA (T-DNA) region is introduced into the abaxial air spaces of whole plants by means of vacuum or syringe infiltration (agroinfiltration). Recombinant protein production within the plant leaves then starts within 24 hours and continues for several days (Rybicki 2010; Xu et al. 2012). The plant species of choice for transient protein expression is *Nicotiana benthamiana*, which was originally indigenous to Australia, and is a wild relative of the common tobacco plant (Fischer et al. 2004; Goodin et al. 2008). A non-food, non-feed crop with a fast growth rate and leaves which infiltrate easily, this plant appears to have a defective RNA silencing system as well as well characterized regulatory elements for transgene control, making it a highly suitable host for foreign protein expression (Lomonossoff and D'Aoust 2016).

In recent years, the plant-based expression field has been revolutionised by the implementation of agroinfiltration to deliver so-called deconstructed plant virus-derived vectors containing the gene of interest (Rybicki 2018). This strategy, which has become a popular choice for plant-based protein expression, has the added advantage of allowing rapid screening of expression constructs and generally results in high recombinant protein yields once the expression strategy with regard to vector choice, *Agrobacterium* strain, intracellular location and codon usage, has been optimised for the particular protein of interest (Rybicki 2014).

The new generation of deconstructed viral vectors, in which viral genes which are not essential for target gene expression have been removed, have been designed for rapid high-level protein expression in plants (Peyret and Lomonossoff 2015). Two noteworthy deconstructed vectors are the tobacco mosaic virus based magnICON® expression vector (Gleba et al. 2005) and the non-replicating hyper-translational pEAQ-HT™ expression vectors derived from the CPMV RNA 2 (Sainsbury and Lomonossoff 2008; Sainsbury et al. 2009), both of which routinely produce up to

several grams of recombinant protein per kilogram of fresh leaf weight. Furthermore, self-replicating viral vectors derived from the ssDNA bean yellow dwarf mastrevirus (BeYDV), which have been shown to increase protein expression significantly, has also recently been developed by our research group and others (Huang et al. 2009; Regnard et al. 2010).

A number of plant-derived candidate vaccines or therapeutics have thus far been produced by agroinfiltration and transient expression in plants. For example, the swine influenza outbreak in 2009 led Medicago Inc. to develop a rapid response influenza VLP vaccine which, when administered with adjuvant, proved to be well tolerated and induced a strong antibody response (Landry et al. 2010). Furthermore, during the 2014/2015 West African outbreak of Ebola, a plant-produced chimaeric vaccine cocktail of three monoclonal antibodies (MAbs) known as ZMapp™, was administered to patients on compassionate grounds. This vaccine produced positive results in a study using non-human primates (Qiu et al., 2014) and is currently being evaluated for safety and efficacy in randomized clinical trials.

The list of VLP-based vaccines that have been successfully produced in plants thus far includes, but is not limited to, seasonal and pandemic influenza (D'Aoust *et al.* 2010; Landry *et al.* 2010; Shoji *et al.* 2015), Norwalk virus (Lai and Chen 2012), bovine papilloma virus (BPV) (Love et al. 2012), bluetongue virus (BTV) (Thuenemann et al. 2013; van Zyl et al. 2016) and Rift Valley fever virus (RVFV) (Mbewana et al. 2018), demonstrating the significant and exciting potential of the plant expression platform to be a powerful contender in the recombinant biopharmaceutical production arena (Chen and Lai 2013; Fischer et al. 2013; Scotti and Rybicki 2013; Rybicki 2014; Lomonossoff and D'Aoust 2016; Rybicki 2018). The work presented in this thesis will add AHSV to the list.

1.7 Aims of this investigation

The primary aim of this investigation was to develop plant-based virus-like particle (VLP) vaccine candidates against African horse sickness (AHS) as safe, efficacious and cost-effective alternatives to the currently used live attenuated vaccine. To achieve this goal, three specific objectives were addressed.

i) The first objective was to investigate the application of the plant-based expression platform to produce fully-formed VLPs of two different AHSV serotypes in the common tobacco plant *Nicotiana benthamiana* by *Agrobacterium*-mediated transient co-expression of the four capsid protein components which make up the AHSV virion. This involved optimization of the expression platform, identification and evaluation of suitable purification strategies as well as investigating the potential formation of chimaeric AHSV VLPs.

ii) The second objective was to test the safety and immunogenicity of the VLP vaccine candidate in both guinea pigs and horses and to monitor the immune response in horses over a period of 10 months. The preliminary guinea pig study will not be presented in this thesis, but has been published in the peer-accredited Journal of Plant Biotechnology (Dennis *et al.* 2018a).

iii) The third objective was to investigate the potential of utilizing a heterologous VLP carrier strategy to display AHSV serotype-specific antigens on the particle surface in a bid to develop a multivalent vaccine for protection against multiple AHSV serotypes.

C H A P T E R T W O

PLANT-BASED EXPRESSION OF AHSV CAPSID PROTEIN GENES AND SELF-ASSEMBLY OF AHSV VIRUS-LIKE PARTICLES

2.1 Introduction

The African horse sickness virion (AHSV) is a complex, highly organized, multi-layered particle (Figure 1.3) morphologically identical to bluetongue virus (BTV), the *Orbivirus* genus prototype (Bremer 1976; Bremer *et al.* 1990; Grubman and Lewis 1992; Roy *et al.* 1994b). Over the past few decades, the development of increasingly sophisticated electron microscopic and computational software tools has permitted considerable progress towards our understanding of the molecular architecture and biochemical functioning of in particular BTV, but also of AHSV (Manole *et al.* 2012; Roy 2017). The advancement in understanding of the structural composition of these orbiviruses has aided the conceptualization of novel vaccine strategies. One such strategy is the production of virus-like particles (VLPs), particles which exactly mimic the native virion, but are composed purely of the viral capsid proteins without any genetic material (Chackerian 2007; Jennings and Bachmann 2008; Kushnir *et al.* 2012; Pushko *et al.* 2013; Scotti and Rybicki 2013; Fuenmayor *et al.* 2017; Jeong and Seong 2017; Tagliamonte *et al.* 2017). VLPs are thus inherently safe in that they are incapable of replicating or transmitting disease and yet retain the immunogenic character of the functional virus.

The production of orbivirus VLPs is based on the observation that co-expression of the individual capsid proteins that make up the viral particle within the same biological cell, whether it be of bacterial, yeast, insect, plant or mammalian origin, will often result in the spontaneous self-assembly of virus-like particles. The expression and assembly of BTV VLPs in insect cells was first demonstrated in the early 1990s and these VLPs were shown to elicit a long-lasting antibody response in sheep (Roy *et al.* 1992; Roy *et al.* 1994a). The protective efficacy of such VLPs was later confirmed, this time using BTV VLPs produced in tobacco plants (Thuenemann *et al.* 2013). The production of AHSV core-like particles (CLPs) and VLPs in insect cells has also been investigated, but the VLP yield was disappointingly low and indeed, was insufficient for quantification (Maree *et al.* 2016). The successful plant-based expression and assembly of BTV

VLPs provided evidence to suggest that this system might be a more efficient, reliable and cost-effective platform for the production of a potential AHSV VLP vaccine than other more traditionally used expression strategies.

When evaluating the potential usefulness of the plant VLP vaccine platform, it is important to take into consideration the fact that during the assembly process, host cell nucleic acid may be packaged into VLPs or host proteins may adhere to the surface of the VLPs themselves, both of which may impact the immune response (Mohsen *et al.* 2018). Various purification strategies are commonly used to purify the VLPs from host cell contaminants eg. ultracentrifugation and/or chromatographic techniques, although these may not always be economically viable. Alternatively, cell free expression systems (Lourenco and Roy 2011), or a VLP disassembly and subsequent re-assembly strategy (Mach *et al.* 2006; Zhao *et al.* 2012), may be utilized to ensure complete removal of packaged or contaminating host cell components. Disassembly and reassembly is probably not feasible for orbivirus VLPs, given their complexity. However, given that plant-derived components almost certainly present far less risk than those derived from mammalian or even insect cells, removal of these may not be seen as necessary at all.

In this chapter, the *Agrobacterium*-mediated transient co-expression in *N. benthamiana* of the AHSV 5 core capsid proteins VP3 and VP7 and the outer capsid proteins VP2 and VP5, and the possible self-assembly of AHSV 5 VLPs, was investigated. Due to previously documented success with BTV capsid protein expression and VLP assembly in plants, the cowpea mosaic virus-based *HyperTrans* (CPMV-*HT*) and associated pEAQ transient expression system, which targets protein expression to the cytoplasm, was used in this study (Sainsbury *et al.* 2009; Thuenemann *et al.* 2013; van Zyl *et al.* 2016). Besides the high levels of protein expression generally obtainable, the pEAQ vector also encodes the tomato bushy stunt virus (TBSV) p19 silencing suppressor, which is very effective in its ability to inhibit post-transcriptional gene silencing (PTGS) and as a result has been shown to greatly improve transgene expression (Scholthof 2005).

Prior to investigating AHSV VLP formation, expression conditions for the synthesis of the AHSV capsid proteins with regard to protein stoichiometry, *Agrobacterium* strain, concentration of the bacterial recombinants used for leaf infiltration and the period of expression prior to leaf harvesting, were optimised. The VLP purification strategy was then refined to ensure an optimal yield of fully-formed VLPs. Among the nine AHSV serotypes, cross protection has been shown to exist between serotypes 1 and 2, 3 and 7, 5 and 8 and 6 and 9, while serotype 4 does not exhibit cross protection against any other serotype. Therefore, a plant-produced VLP vaccine containing a mixture of five serotypes with a representative from each group, serotypes 1, 4, 5, 6 and 7 for example, would be likely to provide protection against all nine serotypes and is the ultimate goal of this research.

2.2 Materials and Methods

2.2.1 Design and synthesis of plant codon-optimised AHSV 5 and 4 capsid protein genes

A consensus amino acid sequence for each of the AHSV 5 viral capsid proteins VP2, VP3, VP5 and VP7, as well as for AHSV 4 VP2 and VP5 was obtained by aligning the available sequences for these proteins listed in GenBank, using CLC Mainbench bioinformatics software (Qiagen Bioinformatics, Aarhus, Denmark). The accession numbers for the gene sequences from which the amino acid sequences were derived and compared are listed in Table 2.1. The consensus sequences were codon-optimized for expression in *N. benthamiana* and synthesized by GenScript Biotech Corporation (Nanjing, China) with flanking *AgeI* and Xho I restriction enzyme sites.

Table 2.1: GenBank accession numbers for the AHSV sequences used to determine a consensus sequence for the AHSV serotype 4 and 5 capsid proteins.

AHSV protein	Genbank Accession Number					
VP2 Serotype 5	KP009662	KM886345	AY163331	HV742532	KF446278	KT030421
	KT030521	KP00978**2**	HV742525			
VP3 Serotype 5	KP009663	KM886346	KF446260	KP009783	KT030522	KT030612
	KT030422					
VP5 Serotype 5	KP009666	KM886349	KP009786	HV742526	HV742533	KT030524
	KT030424	KT030614				
VP7 Serotype 5	KP009668	KM886350	KP009787	HM035391	HM035399	HM035387
	HM035375	HM035382	HM035374	HM035370	HM035366	HM035362
VP2 Serotype 4	KP009652	HM035362	KP009772	KT030351	KT007169	KT187058
	KT187028	KT003691	KT030511	KT030451	KT030601	KM820850
VP3 Serotype 4	KP009653	KM609467	KP009773	KT187029	KT030352	KF446259
	KT030512	KF446264	KT030602	KT030452		
VP5 Serotype 4	KP009656	KM609470	KP009776	KT187031	KT030354	KT007172
	KT003694	KT187061	KT030514	KT030604	KT030454	
VP7 Serotype 4	KP009657	KM609471	KP009778	KT187033	KT030356	KT007174
	KT003696	KT187063	KT030516	KT030456	KT030606	

2.2.2 Sub-cloning of the AHSV 5 and 4 capsid genes into pEAQ-HT™

The AHSV genes were excised from the pUC19 or pCC1 vector in which they were received using *AgeI* and *XhoI* restriction enzymes (New England Biolabs, Ipswich, MA) according to the manufacturer's instructions. The pEAQ-*HT*™ expression vector (Figure 2.1, obtained from G. Lomonossoff, John Innes Centre, UK (Sainsbury *et al.* 2009)), was linearized using the same two enzymes.

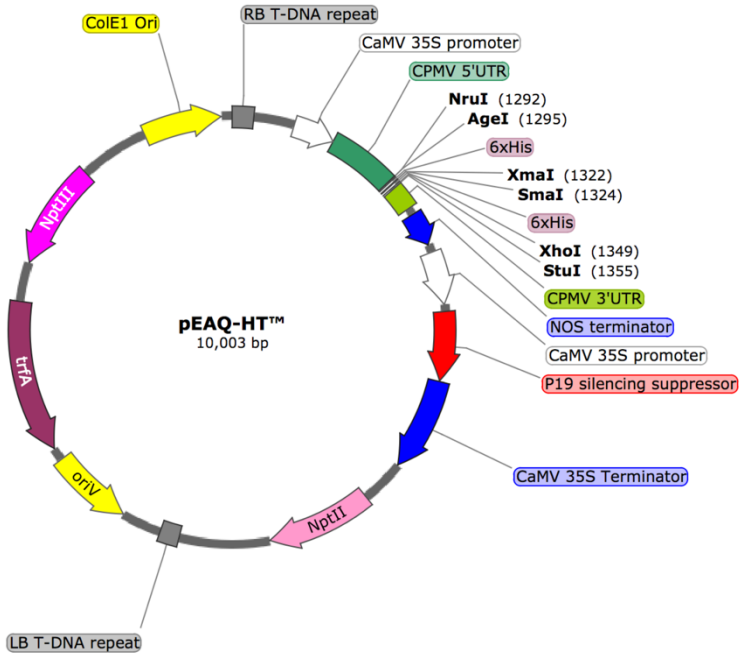

Figure 2.1: Diagrammatic representation of the pEAQ-*HT*™ plant expression vector (Sainsbury *et al.* 2009). T-DNA left (LB) and right (RB) borders, grey boxes; promoter sequences (CaMV, cauliflower mosaic virus), white arrows; CPMV (cowpea mosaic virus) RNA-2 UTRs, green boxes; terminator sequences (nos, nopaline synthase), blue arrows. OriV, pRK2 replication origin and ColEI, pBR322 replication origin, yellow arrows; NPT, neomycin phospho-transferase, pink arrows; TrfA (replication-essential locus), brown arrow and P19 silencing suppressor, red arrow. The plasmid map was compiled using SnapGene (GSL Biotech LLC, Chicago, IL, USA) bioinformatics software.

The restricted DNA species were separated on 1% w/v agarose TBE (89 mM Tris base, 89 mM boric acid and 2 mM EDTA [pH 8]) gels containing 2.5 mg/mL ethidium bromide (EtBr) and visualised under long wavelength ultraviolet (UV) illumination. O'GeneRuler™ 1kb DNA ladder (Fermentas, Waltham, MA, USA) was used as a molecular weight marker on this and all further agarose gels. Linearized vector DNA and the restricted AHSV genes were excised from the agarose gels and purified using a QIAquick® Gel Extraction kit (Qiagen, Hilden, Germany) following the manufacturer's instructions. The purified DNA was then ligated into the pEAQ-*HT*™ expression vector, using T4 DNA ligase (ThermoFisher Scientific, Waltham, MA, USA) and following the manufacturer's quick ligation protocol, to produce pEAQ-AHSV5-VP2, pEAQ-AHSV5-VP3, pEAQ-AHSV5-VP5, pEAQ-AHSV5-VP7, pEAQ-AHSV4-VP2 and pEAQ-AHSV4-VP5.

These pEAQ plasmid constructs were used to transform DH5-α chemically competent *E. coli* cells (E. cloni™, Lucigen, Middleton, WI, USA) following the method described by Sambrook *et al.* (1989). Transformed cells were selected on Luria Bertani (LB) media plates supplemented with kanamycin (50 µg/mL) by incubation for 16 hrs at 37 °C.

Colony PCR using pEAQ vector-specific primers (Table 2.2), was used to confirm successful transformations. In the absence of a DNA insert, these primers will amplify a vector sequence of ±270 bp. A microtip amount of colony material was resuspended in 10 µL double distilled water (ddH2O) by pipetting up and down to dissolve. The PCR reactions consisted of 5 µL resuspended colony material, 200 µM dNTPs, 1 µM of each primer, 1.5 mM $MgCl_2$, 1 x Green GoTaq® Reaction Buffer and 1 unit of GoTaq® DNA polymerase (Promega, Madison, WI, USA). Cloned DNA was amplified by an initial denaturation step at 95 °C for 5 min followed by 30 cycles of denaturation at 95 °C for 30 s, annealing at 54 °C for 30 s and elongation at 72 °C for 90 - 210 s (±60 s per 1000kb DNA) and a final elongation step at 72 °C for 5 min. The amplified products were separated on 1% w/v agarose TBE gels containing 2.5 mg/mL EtBr and visualised under short wavelength UV light.

Table 2.2: Sequences of the vector-specific primers used for PCR amplification to confirm successful cloning of AHSV genes.

Primer	5' – 3' sequence
pEAQ - Forward primer	5 ' -TTCTTCTTCTTGCTGATTGG
pEAQ - Reverse primer	5' -CACAGAAAACCGCTCACC

Transformed cell colonies were inoculated into 5 mL LB broth supplemented with 50 µg/mL kanamycin and incubated with agitation for 16 hrs at 37 °C. Purification of the plasmid constructs was achieved using the QIAprep® Spin Miniprep kit (Qiagen, Hilden, Germany) according to the manufacturer's instructions. Recombinant pEAQ-AHSV clones were verified by digestion of ±500 ng DNA with 1 unit each of *AgeI* and *XhoI* restriction enzymes per reaction for 2 h at 37 ºC followed by separation of the DNA fragments on 1% w/v agarose TBE gels containing 2.5 mg/mL EtBr.

2.2.3 Transformation of *Rhizobium radiobacter*

Agrobacterium strain *Rhizobium radiobacter* (ATCC® BAA101™) (AGL 1) cells (previously known as *Agrobacterium tumefaciens),* were made electrocompetent using the method described by Shen and Forde (1989). The pEAQ-*HT*™ recombinant plasmids (± 400 ng each) were electroporated into 100 µL electrocompetent *AGL1* cells as described previously (Maclean *et al.* 2007) and recombinant clones were selected on LB media plates containing 25 µg/mL carbenicillin and 50 µg/mL kanamycin by incubation for 2 - 3 days at 27 ºC. Successful transformations were confirmed

by colony PCR using pEAQ vector-specific primers as described in **2.2.2**. In order to ensure long term maintenance of the recombinant AGL 1 strains, single recombinant colonies were inoculated into 10 mL LB broth supplemented with 50 µg/mL kanamycin and 25µg/mL carbenicillin and incubated with agitation for 18 hrs at 37 °C. Seed stocks of each recombinant strain were then prepared by mixing 500 µL bacterial culture with 500µL 50% glycerol and freezing at -80 ºC.

2.2.4 *Agrobacterium*-mediated transient protein expression

Starter cultures of the recombinant AGL 1 strains were prepared by inoculating 10mL LB broth supplemented with 50 µg/mL kanamycin and 25 µg/mL carbenicillin with 1 mL glycerol stock and grown by incubating with agitation for 16 hrs at 37 °C. These starter cultures were used to inoculate 50 mL induction media (2.5g/l tryptone, 12.5g/l yeast extract, 5g NaCl/l, 10 mM morpholinoethanesulfonic acid (MES), pH 5.6) supplemented with the appropriate antibiotics and 20 µM acetosyringone. The cultures were incubated for 16 h at 27 °C with agitation. The optical densities (OD_{600}) of the cultures were measured and appropriate volumes were diluted (or combined and diluted for co-expression) in resuspension solution (10 mM MES, pH 5.6, 10 mM MgCl2, 100 µM acetosyringone) to the desired optical density and incubated for 1 h at 22 °C to allow the acetosyringone to induce expression of the *vir* genes.

For single infiltrations, each AHSV AGL 1 suspension was diluted to OD_{600} = 0.5 or 1.0, while co-infiltration suspensions contained all four AHSV recombinants in a ratio VP2:VP3:VP5:VP7 of 1:1:1:1 or 1:1:2:1. For small-scale expression, the top 5 leaves of 5 week-old *N. benthamiana* plants were infiltrated with the relevant recombinant AGL 1 strains, either singly or in combination, by injecting the bacterial suspension into the abaxial leaf spaces using a blunt-ended syringe (Maclean *et al.*, 2007). Plants were grown at 22 °C under 16 hrs / 8 hrs light / dark cycles until harvested.

2.2.5 Protein extraction and analysis

Expression of AHSV 5 VP2, VP3, VP5 and VP7 and AHSV 4 VP2 and VP5 was monitored by taking leaf samples on days 3, 5 and 7 post infiltration (dpi). The leaf samples were weighed and homogenized using a micro pestle in an Eppendorf tube in 2 volumes of PI buffer (1 x PBS [137 mM NaCl, 10 mM Na2HPO4, 2.7 mM KCl, 2 mM KH2PO4, pH 7.4] containing Complete™, EDTA-free protease inhibitor cocktail [Roche, Basel, Switzerland]). Homogenates were incubated on ice for 30 min and then clarified by centrifugation at 13 000 rpm for 15 min in a benchtop microfuge.

To analyse protein expression at the different time points and optical densities, 200 µL crude plant extracts were mixed with 50 µL sample application buffer (Sambrook *et al.* 1989) and denatured at 95 °C for 10 min. Protein samples (40 µL per gel lane) were separated by electrophoresis for ±2 h at 120 V through 10% SDS polyacrylamide gels and then transferred onto HyBond™ C Extra nitrocellulose membranes (AEC - Amersham, South Africa) using a Trans-blot® SD semi-dry transfer cell (Bio-Rad, Irvine, CA). at 15 volts (V) for 1 hr 10 min. Colour Pre-stained Protein Standard, Broad Range Protein Ladder (New England Biolabs, Ipswich, MA) was used as a molecular weight marker. For western blot analysis, the membranes were first blocked in blocking buffer (5% non-fat dairy milk in 1 x PBS containing 0.1% Tween®-20 [PBS-T]) and then probed O/N at 4 °C with with anti-AHSV horse serum raised in a horse vaccinated with an AHSV 5 recombinant vaccine (personal communication and a kind gift from C. Potgieter Deltamune (Pty) Ltd., South Africa) diluted (1: 1000) in blocking buffer. After four washes with blocking buffer for 15 min each, the membranes were incubated in blocking buffer containing anti-horse alkaline phosphatase-conjugated secondary antibody (Sigma-Aldrich, St Louis, MO, USA) at a 1:5000 dilution for 1 hr at 37 °C. The membranes were then washed four times with 1 x PBS-T for 15 min each and the presence of proteins was detected by the addition of 5-bromo-4-chloro-3-indolyl-phosphate and nitroblue tetrazolium phosphatase substrate (BCIP/NBT 1-component, KPL, Milford, MA, USA).

2.2.6 Large-scale vacuum infiltration of *Nicotiana benthamiana*

For large-scale co-expression, the culture volumes were increased by using the 50 mL pre-cultures to inoculate 500 mL induction media supplemented with the appropriate antibiotics and 20 µM acetosyringone and incubating for 16 h at 27 °C with agitation. The infiltration suspensions were prepared as described in **2.2.4** and used to infiltrate 20 - 40 five-week-old *N. benthamiana* plants by applying a vacuum of 100 kPa. For the production of AHSV VLPs, the plants were co-infiltrated with bacterial suspensions containing all four AHSV recombinant AGL 1 strains in a ratio VP2:VP3: VP5:VP7 of 1:1:1:1 at an OD_{600} of 0.5 each. Plants were grown at 22 °C under 16 hrs / 8 hrs light / dark cycles until harvested.

2.2.7 Density gradient purification of AHSV 5 VLPs

The top 3 to 4 leaves of each plant were harvested at 4 dpi, as this time span was shown to be optimal for expression of all four capsid proteins. Harvested leaves were immediately homogenized in two volumes of PI buffer using a Moulinex™ juice extractor. The homogenized leaf pulp was re-incubated with the extracted juice and incubated at 4 °C for 1 h with gentle shaking. Crude plant extracts were filtered through four layers of Miracloth™ (Merck, Darmstadt, Germany) and the filtrate was clarified by centrifugation at 13 000 rpm for 20 min at 4 °C. The homogenates were

incubated at 4 °C for 20 - 24 h to allow AHSV VLPs to mature, followed by a further centrifugation step at 13 000 rpm for 20 min at 4 °C.

AHSV 5 VLPs were purified by ultracentrifugation through discontinuous iodixanol density gradients. Iodixanol (Optiprep™; Sigma Aldrich, St Louis, MO, USA) solutions (20%–40%), prepared in 1 x PBS pH 7.4, were used to create a 9 mL step gradient (3 mL of each gradient in 10% incrementing steps) under 30 mL clarified plant extract and centrifuged at 32 000 rpm for 2 h at 4 °C in an SW32 Ti rotor (Beckman, Brea, CA). Fractions of 500 µL were collected from the bottom of the tubes and 50 µL from fractions representing the 30%–40% region of the gradient was electrophoresed through a 10% SDS-polyacrylamide gel, followed by Coomassie blue staining. Particle quantification was achieved by visual comparison of the four capsid protein bands to known amounts of bovine serum albumin (BSA) run in separate lanes on the same SDS-PAGE gel. To further purify and concentrate VLP samples for use in animal studies, VLP-containing fractions were diluted with PBS to 20% iodixanol and subjected to a second round of ultracentrifugation as per the same protocol described above.

2.2.8 Transmission electron microscopy (TEM)

Glow-discharged copper grids (mesh size 200) were floated on 20 µL crude plant extract or 20 µL density gradient fractions for 5 min and then washed successively by floating on five drops of sterile water. Particles were negatively stained for 30 s with 2% uranyl acetate and then imaged using a Technai G2 transmission electron microscope (TEM).

2.2.9 Gel Densitometry

Plant-produced AHSV VLPs were quantified by SDS-PAGE separation of iodixanol gradient fractions followed by Coomassie blue staining. These samples were electrophoresed alongside serially diluted bovine serum albumin (BSA) (Sigma-Aldrich, St Louis, MO, USA) of known concentration. The amount of protein in individual bands was determined using the SynGene reader – using GeneTools version 3.07.03 software and the AHSV proteins were quantified by extrapolation from the BSA standard curve.

2.2.10 Mass Spectrometry

The identities of the protein species observed on the Coomassie-stained gel were independently determined by the Centre for Proteomic and Genomic Research (CPGR, Cape Town, South Africa). Gel pieces were washed and fragmented by in-gel trypsin digestion as per the protocol described by Shevchenko *et al.* (2007). The peptide solution was analysed using a Dionex Ultimate 3000

nano-HPLC system (ThermoFisher Scientific, Waltham, MA, USA) coupled to a Q Exactive™ Hybrid Quadrupole-Orbitrap Mass Spectrometer (ThermoFisher Scientific). Byonic software (Protein Metrics, San Carlos) was used for comparison of the spectra with sequences retrieved from the UniProt Swissprot protein database. Samples were interrogated against *Nicotiana* spp, *Agrobacterium* spp and African horse sickness virus proteomes.

2.2.11 Cloning of AHSV 5 VP2 by cDNA amplification of AHSV 5 segment 2 dsRNA

AHSV 5 dsRNA was extracted from a current AHSV 5 field isolate (GenBank accession number: KT030421) by P. Coetzee from the Equine Health Institute, Pretoria, South Africa. Primers used for the amplification of AHSV 5 VP2 cDNA are listed in Table 2.3.

Table 2.3: Sequences of the primers used for synthesis of AHSV 5 segment 2 cDNA

Primer	5' – 3' sequence
AHSV 5 VP2 Forward primer	5' AT**ACCGGT**CCATGGCTTCAGAGTTTGGCGT 3'
AHSV 5 VP2 Reverse primer	5' ATCCCGGG**CTCGAG**CTACTTTTCTGTCTTGGCGAGTAATTT 3'
M13 Forward primer	5' CGCCAGGGTTTTCCCAGTCACGAC 3'
M13 Reverse primer	5' GAGCGGATAACAATTTCACACAGG 3'

AgeI and *XhoI* restriction sites in the forward and reverse primers respectively, are underlined and in bold.

AHSV 5 dsRNA (10µl) was denatured with methyl mercury hydroxide (CH_4HgO, ThermoFisher Scientific, Waltham, MA, USA) at a final concentration of 50mM for 20 min at 37 °C. The reaction was stopped by placing on ice and protecting the ssRNA from degradation by the addition of 2-Mercaptoethanol (Sigma Aldrich, St Louis, MO, USA). Twenty pmol of each primer and 1.5 mM dNTPs were then added to 7 µL denatured dsRNA and heated at 65 °C for 5 min. Synthesis of cDNA was achieved by the addition of 1 x cDNA synthesis buffer, 5mM DTT, 40 units of RNAse OUT (ThermoFisher Scientific, Waltham, MA, USA) and 15 units of AMV reverse transcriptase (ThermoFisher Scientific, Waltham, MA, USA) and incubating at 45 °C for 60 min and then at 85 °C for 5 min. The cDNA was amplified by PCR using Phusion™ flash enzyme (ThermoFisher Scientific, Waltham, MA, USA) together with 0.5 µM of the same primers listed in Table 2.3 according to the manufacturer's instructions. For amplification, an initial denaturation step at 98 °C for 10 s was followed by 2 cycles of denaturation at 98 °C for 1 s, annealing at 52 °C for 5 s and elongation at 72 °C for 60 s, and then 28 cycles of denaturation at 98 °C for 1 s, annealing at 64 °C for 5 s and elongation at 72 °C for 60 s, with a final elongation step at 72 °C for 60 s.

The amplified VP2 DNA was separated on a 1% agarose TBE gel and purified using a QIAquick® Gel Extraction kit as described in **2.2.2.** For sub-cloning into the pGEM-T-Easy vector (Promega,

Madison, WI, USA), a 5' A-overhang was added to the purified VP2 gene using 1 x Kapa™ taq A buffer, 0.2mM dATPs and 1 unit of Kapa™ Taq polymerase (Roche, Basel, Switzerland) and incubating at 72 °C for 20min. Ligation was carried out according to the manufacturer's instructions and the recombinant plasmid was transformed into DH5-α chemically competent *E. coli* cells as described previously **(2.2.2)**. Transformed cells were identified by blue/white selection on Luria Bertani (LB) media plates supplemented with ampicillin (100 µg/mL), 80 µg/mL X-gal (5-bromo-4-chloro-3-indolyl-β-D-galactopyranoside) and 0.5 mM IPTG (Isopropylthio - β - D - galactoside,) that were incubated for 16 hrs at 37 °C. Positive recombinants were identified by colony PCR using the M13 primer set (Table 2.3).

The AHSV 5 VP2 gene was excised from the pGEM-T-Easy vector using *AgeI* and *XhoI* restriction enzymes, sub-cloned into the pEAQ-*HT*™ expression vector to produce pEAQ-AHSV5-$VP2_{wt}$, transformed into DH5-α *E. coli* cells and electroporated into *Agrobacterium AGL1* (pEAQ-AHSV5-$VP2_{wt}$ /AGL) as in **2.2.3.** Transient expression of wild-type (wt) AHSV 5 VP2 in *N. benthamiana* plants was achieved following the same protocol as for the plant codon-optimised AHSV recombinant proteins (**2.2.4** and **2.2.5)**.

2.2.12 Purification of AHSV 4 VLPs

For the production of AHSV 4 VLPs, plants were co-infiltrated with bacterial suspensions containing AHSV 4 VP2 and VP5 recombinant AGL 1 strains together with the VP3 and VP7 AGL 1 recombinants used to produce AHSV 5 VLPs as described in **2.2.6**. However, instead of homogenizing the leaves in PI buffer containing PBS pH 7.4, the PI buffer contained 50mM bicine (Sigma Aldrich, St Louis, MO, USA) and 200 mM NaCl, pH 8.4, together with Complete™, EDTA-free protease inhibitor cocktail. The AHSV 4 VLPs were purified by iodixanol density gradient ultracentrifugation as described in **2.2.7** but with the exception that the Optiprep™ gradient solutions were prepared in bicine/NaCl, buffer pH 8.4 instead of 1 x PBS pH 7.4. Proteins were detected by western blot analysis as described in **2.2.5** using anti-AHSV 4 antiserum (a kind gift from C. Potgieter Deltamune (Pty) Ltd., South Africa) diluted (1: 1000) in blocking buffer as the primary antibody. This antiserum was raised in horses vaccinated with a live attenuated AHSV 4 strain rescued by reverse genetics (van de Water *et al.* 2015).

2.2.13 Site directed mutagenesis of the AHSV 4 VP2 gene

The AHSV 4 VP2 gene was altered to replace the A_{1029} nucleotide with a G nucleotide using site directed mutagenesis. This substitution would lead to replacement of the Ile_{343} with a Met moiety in the translated protein. Forward and reverse mutagenesis primers were designed and synthesized for use with the reverse and forward pEAQ primers (Table 2.4) in two separate PCR reactions to

yield a 1052bp and a 2173bp fragment respectively. The PCR reaction consisted of ±400ng pEAQ-AHSV 4-VP2 DNA in 1 x Phusion flash PCR mix with the pEAQ - forward primer and AHSV 4 VP2 mutagenesis reverse primer (0.5 µM) in the first mix and the pEAQ - reverse primer and AHSV 4 VP2 mutagenesis forward primer (0.5 µM) in the second mix. For amplification, an initial denaturation step at 98 °C for 4 min was followed by 30 cycles of denaturation at 98 °C for 1 s, annealing at 51 °C for 10 s and elongation at 72 °C for 60 s, with a final elongation at 72 °C for 60s.

Table 2.4: Sequences of the primers used for site-directed mutagenesis of AHSV 4 VP2

Primer	**5' – 3' sequence**
pEAQ - Forward primer	5 ' -TTCTTCTTCTTGCTGATTGG
AHSV 4 VP2 mutagenesis Reverse primer	5' GAAATCCATGTACGG**C**ATTCTTTTAACC 3'
AHSV 4 VP2 mutagenesis Forward primer	5' GTTAAAAGAAT**G**CCGTACATGGATTTCA 3'
pEAQ - Reverse primer	5' -CACAGAAAACCGCTCACC

The nucleotide base substitution is underlined and in bold.

The amplified VP2 PCR products were separated on a 1% agarose TBE gel and purified using a QIAquick® Gel Extraction kit as described in **2.2.2.** These 2 products served as combined templates in a second PCR reaction with the pEAQ forward and reverse primers (0.5 µM each) under the same cycle conditions as above. The resulting PCR product was gel extracted and purified followed by digestion with *AgeI* and *XhoI* according to the manufacturer's instructions.

The digested DNA was purified over a QIAquick® spin column and then sub-cloned into the pEAQ-*HT*™ expression vector to produce pEAQ-AHSV 4-VP2$_{mu}$, transformed into DH5-α *E. coli* cells and electroporated into *Agrobacterium* AGL1 as in **2.2.2** and **2.2.3.**

2.2.14 *In vitro* assembly of AHSV 5 VLPs

The expression of individual AHSV 5 capsid proteins was achieved by vacuum infiltration of *N. benthamiana* plants with AGL 1 transformants each carrying one of the AHSV 5 capsid protein genes (VP2, VP3, VP5 or VP7) in the pEAQ-*HT* expression vector. Alternatively, half the plants were co-infiltrated with strains carrying the VP3, VP5 and VP7 pEAQ constructs while the other half were infiltrated with the AHSV 5 VP2 recombinant strain alone.

At 4 days post infiltration, leaves from singly infiltrated plants were harvested and homogenized together in two volumes of PI buffer. Or, leaves co-infiltrated with VP3, VP5 and VP7 recombinant strains were homogenized together with leaves infiltrated only with the AGL 1 strain carrying the pEAQ-AHSV 5 VP2 construct in two volumes of PI buffer. The homogenates were incubated at 4^{o}C

for 60 min with gentle agitation and then filtered through four layers of Miracloth™ (Merck). The crude plant extracts were clarified by centrifugation at 13 000 rpm for 20 min in a JA14 rotor (Beckman) and incubated for ± 20 h at 4^{o} C to allow spontaneous VLP assembly to occur. The crude homogenates were then again clarified by centrifugation at 13 000 rpm for 20 min before purifying by density gradient ultracentrifugation (as in **2.2.7)**. Fractions (500 µL) collected from the bottom of the tubes were analyzed by SDS-PAGE and TEM as before.

2.3 Results

2.3.1 Design, synthesis and cloning of plant codon-optimised AHSV capsid protein genes

To investigate whether AHSV capsid proteins could be transiently co-expressed and lead to spontaneous self-assembly of intact VLPs within individual plants, recombinant plasmids containing the AHSV 5 VP2, VP3, VP5 and VP7 and AHSV 4 VP2 and VP5 genes were constructed. A consensus sequence of each gene was obtained by aligning all the known sequences listed in GenBank; these were codon optimized for *Nicotiana* spp. translation and synthesized with flanking *Age I* and *Xho I* restriction enzyme sites by GenScript Biotech Corporation, China. A comparison of the AHSV 5 and 4 amino acid consensus sequences for the four capsid proteins revealed 51.5%, 100%, 85.5% and 99.7% sequence identity for the VP2, VP3, VP5 and VP7 proteins respectively. This demonstrates and confirms the high degree of variability known to exist between the serotype-specific VP2 capsid proteins (Potgieter *et al.* 2003).

The genes were cloned into the multiple cloning site of the pEAQ-*HT*^{TM} vector (Sainsbury *et al.* 2009), and transformed into *E. coli* to yield six different constructs, pEAQ-AHSV5-VP2, pEAQ-AHSV5-VP3, pEAQ-AHSV5-VP5, pEAQ-AHSV5-VP7, pEAQ-AHSV4-VP2 and pEAQ-AHSV4-VP5 (Figure 2.3). The consensus sequences of AHSV VP3 of both serotypes 4 and 5 were identical, while that of AHSV 5 VP7 differed from that of AHSV 4 VP7 by only a single amino acid. Therefore, only the AHSV 5 VP3 and VP7 gene sequences were synthesized and cloned.

VP2

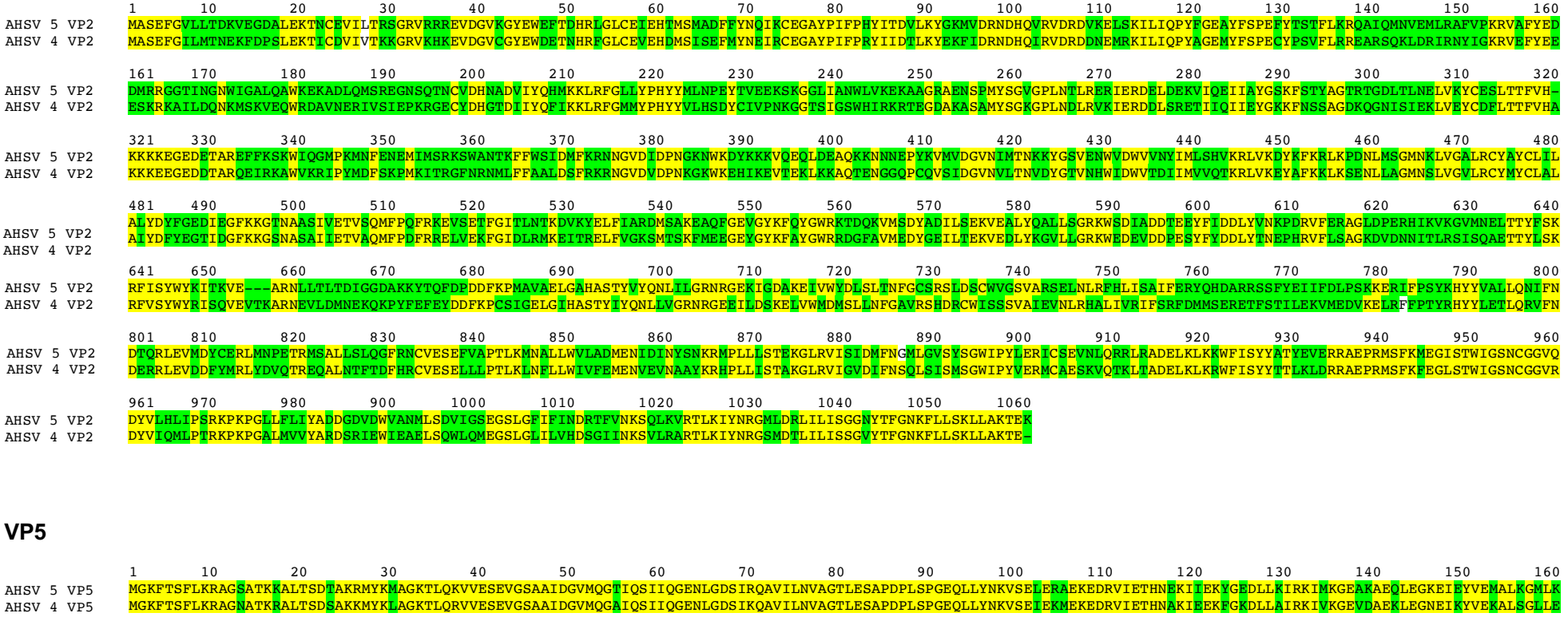

VP5

(Cont. overleaf)

VP3

```
                1       10        20        30        40        50        60        70        80        90        100       110       120       130       140       150       160
AHSV 5 VP3      MSGNERIQDKNEKEKAYAPYLDGASVSTDNGPILSVFALQEIMQKIRQNQSDMAAHAPDVDGAIPEVMTIISGIKGLLEEKDYKVINAPPNSFRTIPMQSTEYVLQVNTFYERMSEIGGPVDETDPIGFYALILEKLKFLKSEGAFILQGIATKDYRGAE
AHSV 4 VP3      MSGNERIQDKNEKEKAYAPYLDGASVSTDNGPILSVFALQEIMQKIRQNQSDMAAHAPDVDGAIPEVMTIISGIKGLLEEKDYKVINAPPNSFRTIPMQSTEYVLQVNTFYERMSEIGGPVDETDPIGFYALILEKLKFLKSEGAFILQGIATKDYRGAE

                161     170       180       190       200       210       220       230       240       250       260       270       280       290       300       310       320
AHSV 5 VP3      IADPEIIGVSFQNALSHLAAIDRQIIQDTLNGMIIENGLVADRNVDVFRAAMSDPIYRIHNVLQGYIEGIQYGELRESVNWLMRLGLRKRIEFANDFLTDFRRADTIWIISQRLPINANVIWNVPRCHIANLITNVALCLPTGEYLMPNPRINSITITQR
AHSV 4 VP3      IADPEIIGVSFQNALSHLAAIDRQIIQDTLNGMIIENGLVADRNVDVFRAAMSDPIYRIHNVLQGYIEGIQYGELRESVNWLMRLGLRKRIEFANDFLTDFRRADTIWIISQRLPINANVIWNVPRCHIANLITNVALCLPTGEYLMPNPRINSITITQR

                321     330       340       350       360       370       380       390       400       410       420       430       440       450       460       470       480
AHSV 5 VP3      ITQTNPFSIISGLTPTAVQMNDVRKIYLALMFPNQIILDIKPDSSHAVDPVLRMVAGVLGHVMFTYGPIMTNITPTMAELLDAALSDYLLYMYNNRIPINYGPTGQPLDFRIGARNQYDCNAFRADPQTGRGYNGWGVVDVQRVQPSPYDHVQRVIRYCD
AHSV 4 VP3      ITQTNPFSIISGLTPTAVQMNDVRKIYLALMFPNQIILDIKPDSSHAVDPVLRMVAGVLGHVMFTYGPIMTNITPTMAELLDAALSDYLLYMYNNRIPINYGPTGQPLDFRIGARNQYDCNAFRADPQTGRGYNGWGVVDVQRVQPSPYDHVQRVIRYCD

                481     490       500       510       520       530       540       550       560       570       580       590       600       610       620       630       640
AHSV 5 VP3      IDSREIIDPRTYGMNMTYPIFREMLRMLVAAGKDQEAAYLRQMLPFHMIRFARINQIINEDLLSAFSLPDQNFDVVLHNLIDSREIIDPRTYGMNMTYPIFREMLRMLVAAGKDQEAAYLRQMLPFHMIRFARINQIINEDLLSAFSLPDQNFDVVLHNL
AHSV 4 VP3      IDSREIIDPRTYGMNMTYPIFREMLRMLVAAGKDQEAAYLRQMLPFHMIRFARINQIINEDLLSAFSLPDQNFDVVLHNLIDSREIIDPRTYGMNMTYPIFREMLRMLVAAGKDQEAAYLRQMLPFHMIRFARINQIINEDLLSAFSLPDQNFDVVLHNL

                641     650       660       670       680       690       700       710       720       730       740       750       760       770       780       790       800
AHSV 5 VP3      IQGNFGETDPVVLEVSWASIWFAFVRRFEPIARSDLLEAAPLIEARYAAELSTMQMDVQQLRMMRARVPDTVINATPSQCWKAVLKNAPEPIKNLMNLSHSFSFVNVRDIVRWSQQRDIQESLAYVLNREAWAIANDFEDLMLVDHVYIQRTMLPEPRLD
AHSV 4 VP3      IQGNFGETDPVVLEVSWASIWFAFVRRFEPIARSDLLEAAPLIEARYAAELSTMQMDVQQLRMMRARVPDTVINATPSQCWKAVLKNAPEPIKNLMNLSHSFSFVNVRDIVRWSQQRDIQESLAYVLNREAWAIANDFEDLMLVDHVYIQRTMLPEPRLD

                801     810       820       830       840       850       860       870       880       890       900       910       920       930       940       950       960
AHSV 5 VP3      DINEFRRQGFFHTNMIDGAPPIGDVTHYTYAIANLQANMGQFRAAIRRTLDDNGWIQFGGMLRNIKIKFFDSRPPDEILTAMPYVYTEEERDGVRMVAFKYATTATAYFLLYNVEYSNTPDTLITVNPTFTMTKIHMRKKIVRRVRAPDVLSQVNKRLVA
AHSV 4 VP3      DINEFRRQGFFHTNMIDGAPPIGDVTHYTYAIANLQANMGQFRAAIRRTLDDNGWIQFGGMLRNIKIKFFDSRPPDEILTAMPYVYTEEERDGVRMVAFKYATTATAYFLLYNVEYSNTPDTLITVNPTFTMTKIHMRKKIVRRVRAPDVLSQVNKRLVA

                961     970       980
AHSV 5 VP3      YKGKMRLMDVTKCLKTGVQ
AHSV 4 VP3      YKGKMRLMDVTKCLKTGVQ
```

VP7

```
                1       10        20        30        40        50        60        70        80        90        100       110       120       130       140       150       160
AHSV 5 VP7      MDAIAARALSVVRACVTVTDARVSLDPGVMETLGIAINRYNGLTNHSVSMRPQTQAERNEMFFMCTDMVLAALNVQIGNISPDYDQALATVGALATTEIPYNVQAMNDIVRITGQMQTFGPSKVQTGPYAGAAEVQQSGRYYVPQGRTRGGYINSNIAEV
AHSV 4 VP7      MDAIAARALSVVRACVTVTDARVSLDPGVMETLGIAINRYNGLTNHSVSMRPQTQAERNEMFFMCTDMVLAALNVQIGNISPDYDQALATVGALATTEIPYNVQAMNDIVRITGQMQTFGPSKVQTGPYAGAVEVQQSGRYYVPQGRTRGGYINSNIAEV

                161     170       180       190       200       210       220       230       240       250       260       270       280       290       300       310       320
AHSV 5 VP7      CMDAGAAGQVNALLAPRRGDAVMIYFVWRPLRIFCDPQGASLESAPGTFVTVDGVNVAAGDVVAWNTIAPVNVGNPGARRSILQFEVLWYTSLDRSLDTVPELAPTLTRCYAYVSPTWHALRAVIFQQMNMQPINPPIFPPTERNEIVAYLLVASLADVY
AHSV 4 VP7      CMDAGAAGQVNALLAPRRGDAVMIYFVWRPLRIFCDPQGASLESAPGTFVTVDGVNVAAGDVVAWNTIAPVNVGNPGARRSILQFEVLWYTSLDRSLDTVPELAPTLTRCYAYVSPTWHALRAVIFQQMNMQPINPPIFPPTERNEIVAYLLVASLADVY

                321     330       340       349
AHSV 5 VP7      AALRPDFRMNGVVAPVGQINRALVLAAYH
AHSV 4 VP7      AALRPDFRMNGVVAPVGQINRALVLAAYH
```

Figure 2.2: Comparison of the consensus amino acid sequences of AHSV 5 and 4 capsid protein genes. A consensus sequence for each of the AHSV 5 and 4 capsid proteins, VP2, VP3, VP5 and VP7 was obtained by alignment of known sequences listed in GenBank. These were codon optimized for *Nicotiana* spp. and synthesized by GenScript Biotech Corporation, China. Areas of amino acid identity between each of the AHSV 5 and 4 proteins are highlighted in yellow, while regions of amino acid variability are highlighted in green.

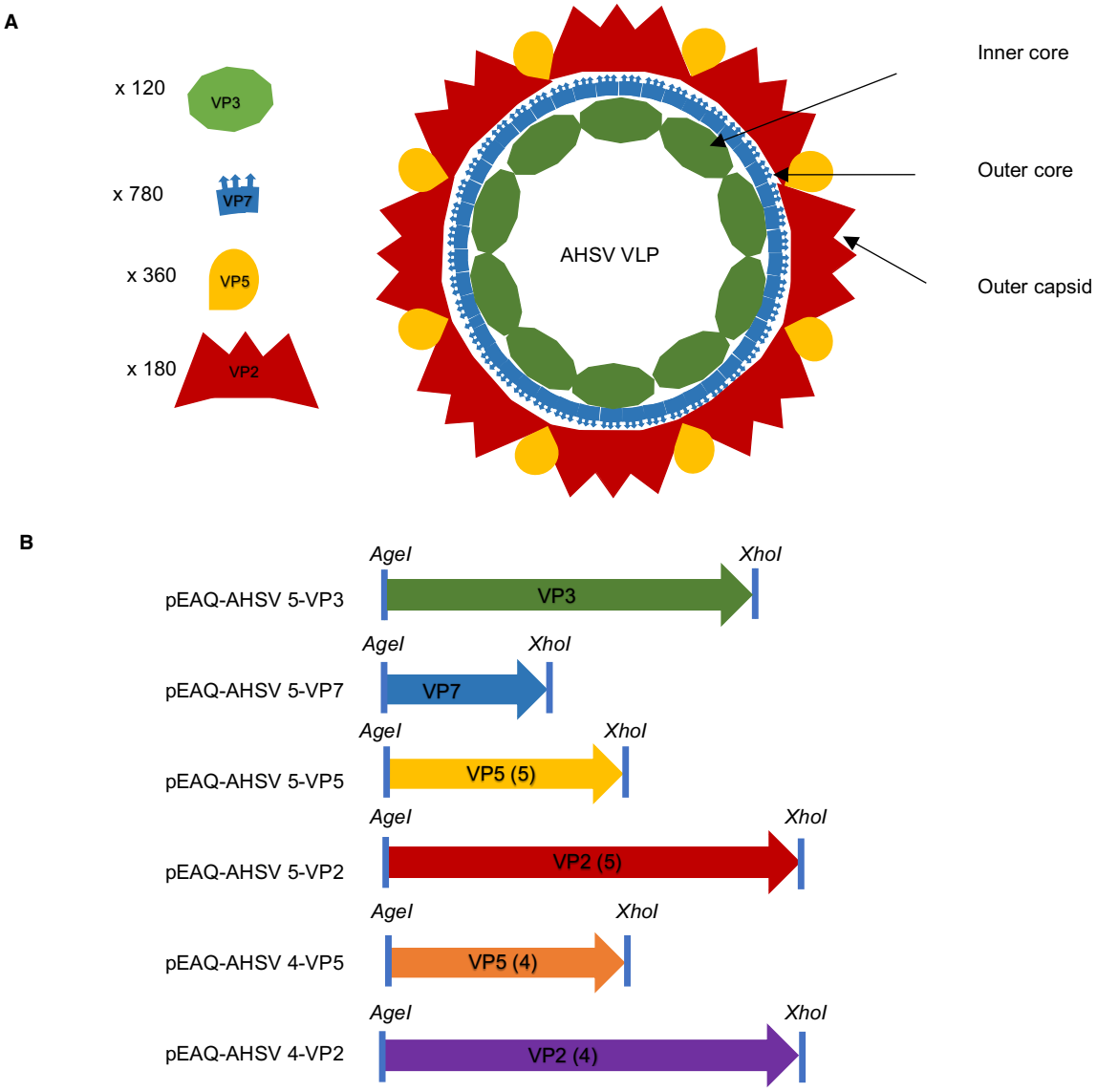

Figure 2.3: Schematic representation of the constructs created for *Agrobacterium*-mediated expression of African horse sickness (AHSV) serotype 4 & 5 structural proteins in *N.benthamiana* and their resultant assembly into virus-like particles. (A) Stoichiometric diagram of virus-like particle formation. (B) Codon-optimized genes for AHSV 5 VP2, VP3, VP5 & VP7 and AHSV 4 VP2 & VP5 were cloned into the pEAQ-HT^{TM} plant expression vector (Sainsbury *et al.* 2009).

Successful cloning of the AHSV genes was demonstrated by colony PCR and small-scale plasmid isolation from O/N cultures followed by restriction enzyme digestion with *Age I* and *Xho I* (results not shown). Colony PCR resulted in bands of ±3.47 kb (3.2 + 0.27 kb vector sequence), ±2.97 kb, (2.7 + 0.27 kb vector sequence), ±1.77 kb (1.5 + 0.27 kb vector sequence) and ±1.27 kb (1 + 0.27kb vector sequence), representing the correct sizes of AHSV VP2, VP3, VP5 and VP7 respectively (Figure 2.4 A). The AHSV pEAQ constructs were electroporated into *Agrobacterium* AGL 1, and successful transformations were again confirmed by colony PCR (Figure 2.4 B).

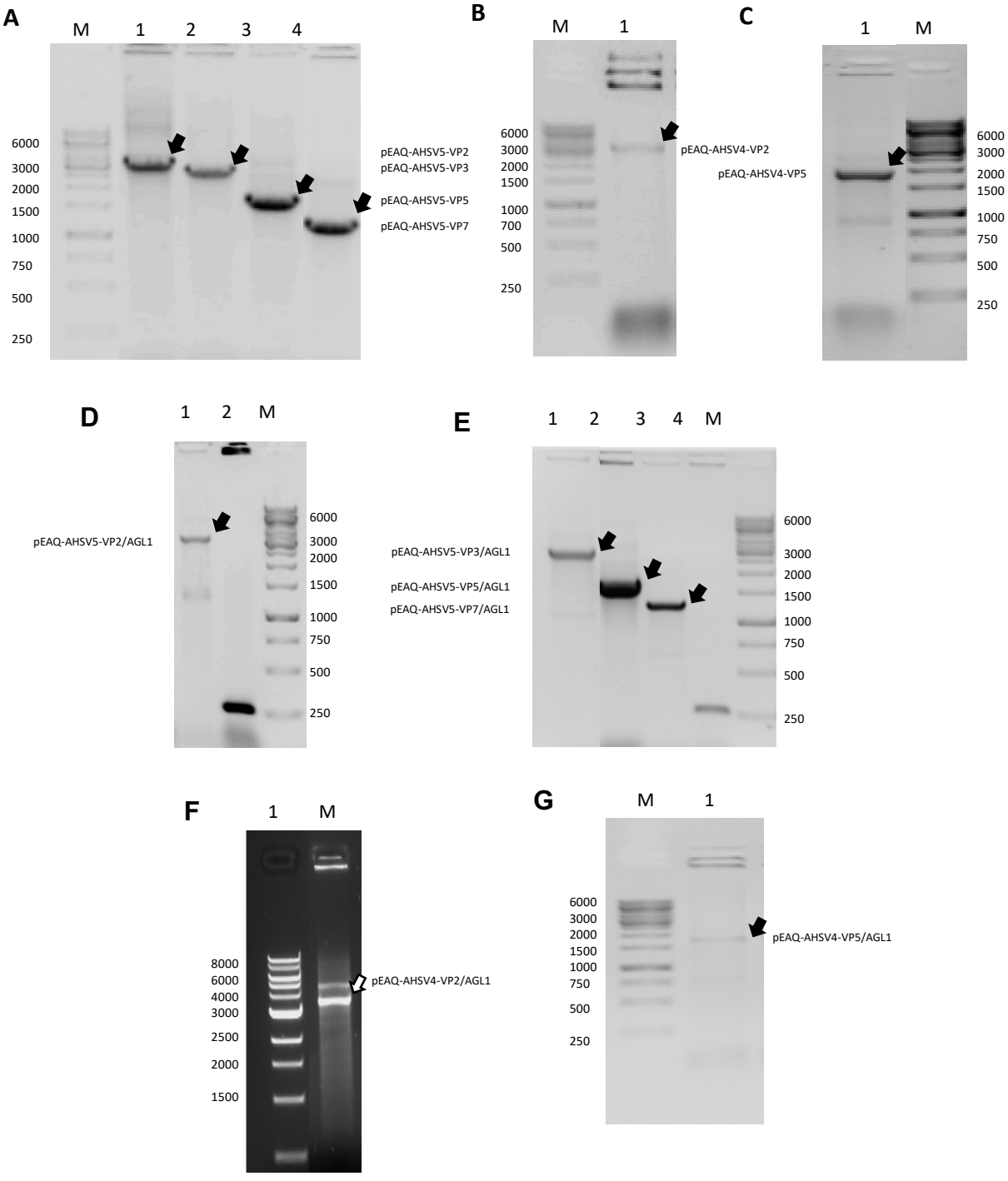

Figure 2.4: Verification of recombinant AHSV strains. Colony PCR amplification using the pEAQ vector-specific primer set was used to verify the successful cloning of the AHSV capsid protein genes and transformation of *E. coli* (A - C) and *Agrobacterium* AGL 1 (D - G). PCR of the AHSV recombinants amplified a ±3.47 kb (3.2 + 0.27 kb vector sequence) fragment (A, lane 1 & D, lane 1) for AHSV 5 VP2, a ±3.47 kb (3.2 + 0.27 kb vector sequence) fragment (B, lane 1 & F, lane 1) for AHSV 4 VP2, a ±2.97 kb, (2.7 + 0.27 kb vector sequence) fragment (A, lane 2 & E, lane 1) for VP3, a ±1.77 kb (1.5 + 0.27 kb vector sequence) fragment (A, lane 3 & E, lane 2) for VP5, a ±1.77 kb (1.5 + 0.27 kb vector sequence) fragment (C, lane 1 & G, lane 1) for VP5 serotype 4 and a ±1.27 kb (1 + 0.27 kb vector sequence) fragment for VP7 (A, lane 4 & E, lane 3). Transformation with the pEAQ plasmid lacking a goi was used as a negative control (D, lane 2 & E, lane 4). The molecular weight markers are indicated adjacent to each gel.

2.3.2 Assembly of AHSV 5 capsid proteins transiently expressed in *Nicotiana benthamiana*

Small-scale transient expression of the serotype 5 AHSV proteins was tested first. Five leaves of each *N. benthamiana* plant were syringe-infiltrated with *Agrobacterium* strains carrying the individual AHSV 5 constructs, or co-infiltrated with all four recombinant-carrying strains. All infiltrated leaf tissue exhibited chlorosis, but little if any necrosis was observed (Figure 2.5). *Agrobacterium* suspensions carrying recombinants in two different VP2:VP3:VP5:VP7 ratios were tested, namely 1:1:1:1 and 1:1:2:1, as the latter ratio has been previously shown (van Zyl *et al.* 2016) to give a better yield of bluetongue virus (BTV) VLPs.

Three leaf discs were clipped per expression test using an Eppendorf vial lid, and extracted on 3, 5- and 7-days post-infiltration (dpi), to determine the optimal expression conditions.

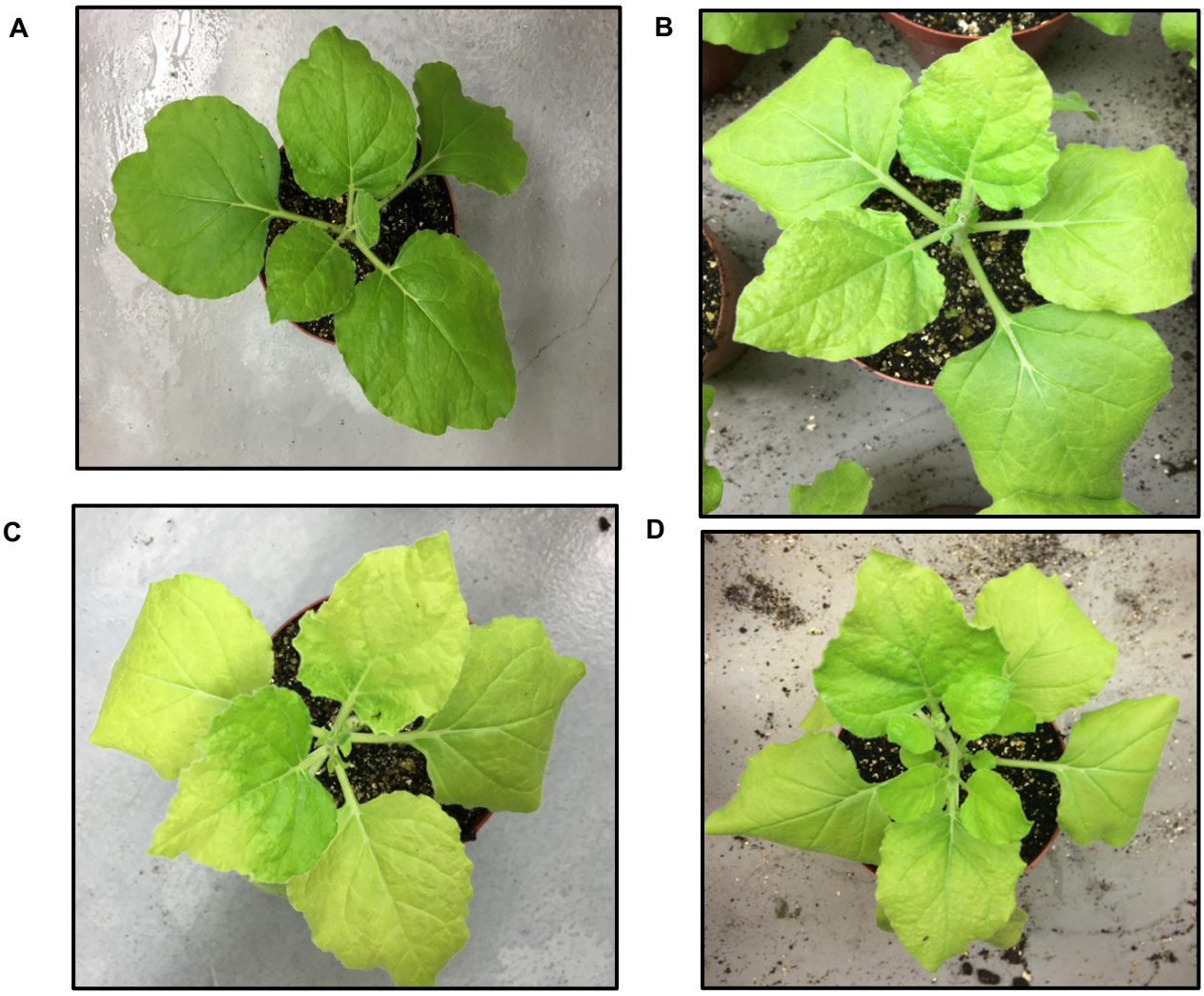

Figure 2.5: Infiltration of *N. benthamiana* plants with all 4 AHSV 5 *Agrobacterium* recombinants. Healthy five-week-old tobacco plants (A) were co-infiltrated with the bacterial suspension and the plant condition was recorded 3 (B), 5 (C) and 7 (D) days post infiltration.

Western blots using anti-AHSV 5 antiserum showed that crude leaf extracts infiltrated with *Agrobacterium*-carrying recombinants at an OD_{600} of 0.5 each and prepared 5 - 7 days after infiltration yielded some protein expression (Figure 2.6, black arrows). There was no apparent difference in expression between the two construct mixture ratios used (Figure 2.6, lanes 6 & 7); therefore, plants were infiltrated with each recombinant at OD_{600} = 0.5 in all subsequent experiments.

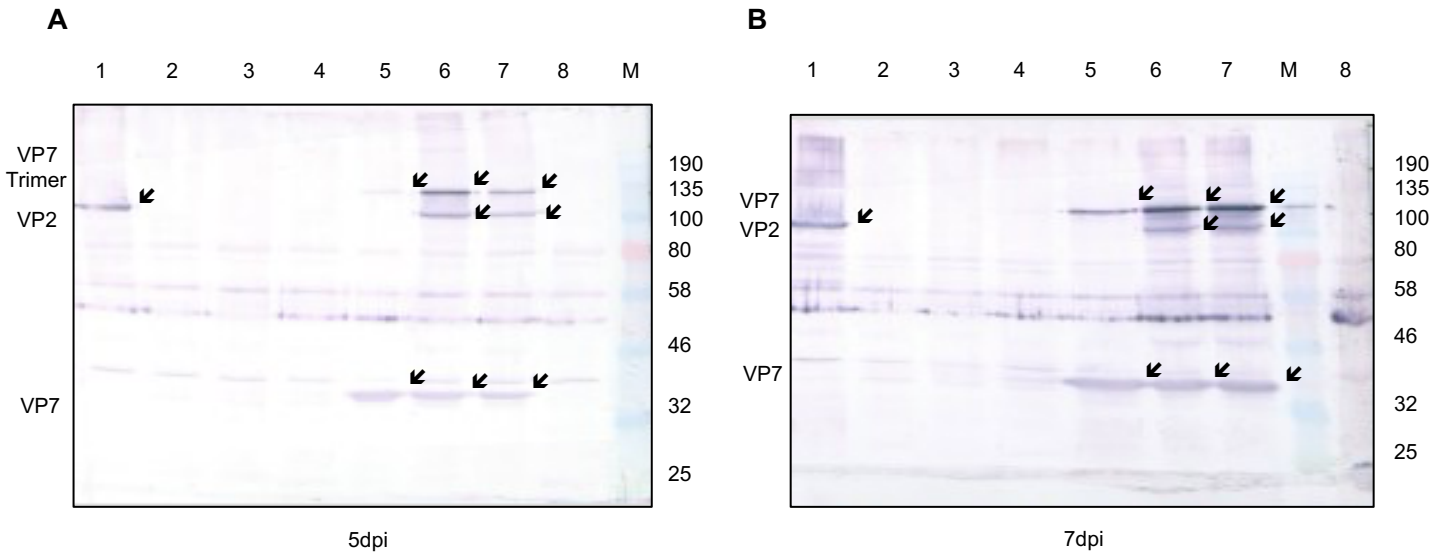

Figure 2.6 Optimization of plant-based expression of recombinant AHSV-5 structural proteins. Western blot analysis of crude leaf extracts obtained 5 (A) and 7 (B) days after plants were infiltrated with *Agrobacterium* AGL1 containing pEAQ-AHSV5 VP2 (lane 1), pEAQ-AHSV5 VP3 (lane 2), pEAQ-AHSV5 VP5, OD_{600}=0.5 (lane 3), pEAQ-AHSV5 VP5, OD_{600}=1.0 (lane 4), pEAQ-AHSV5 VP7 (lane 5) or co-infiltrated with all 4 AHSV-5 recombinants in the ratio 1:1:1:1 (lane 6) or in the ratio 1:1:2:1 (lane 7). A crude extract from a plant infiltrated with the empty pEAQ-*HT* expression vector, was used as a negative control (lane 8). An anti-AHSV 5 antiserum, which proved unable to detect either VP3 or VP5, was used as the primary antibody. VP2 and VP7 (trimer and monomer) proteins (123, 135 and 38 kDa respectively) are indicated by arrow heads. Colour pre-stained protein standard, broad range (New England Biolabs, Massachusetts, USA) indicated to the right of the blots, was used as a molecular weight marker.

Expression of VP2 (123 kD) and VP7 (37 kD) as well as a VP7 trimer (135 kD) was demonstrated (Figure 2.7, black arrows), the proteins being visualized as distinct bands of the correct expected molecular weight in these western blot analyses of crude plant extracts. Apparent differences in gel loading can be observed as a result of natural leaf - to - leaf and plant-to-plant total soluble protein (TSP) variation. Bands corresponding to VP3 (103 kD) and VP5 (57 kD) were not detected due to a peculiarity of the available antiserum which, for an unknown reason was shown to detect only VP2 and VP7.

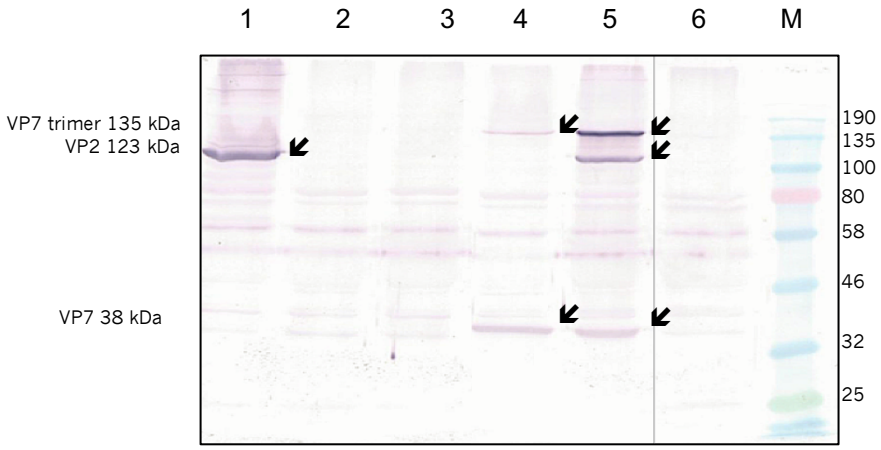

Figure 2.7: Expression of recombinant AHSV 5 structural proteins in *N. benthamiana*. Western blot analysis of crude leaf extracts obtained 7 dpi with *Agrobacterium* AGL1 containing pEAQ-AHSV5 VP2 (lane 1), pEAQ-AHSV5 VP3 (lane 2), pEAQ-AHSV5 VP5 (lane 3), pEAQ-AHSV5 VP7 (lane 4) or co-infiltrated with all 4 AHSV-5 recombinants (lane 5). Crude extract from leaves infiltrated with *Agrobacterium* transformed with pEAQ-*HT* expression vector lacking any gene of interest (goi), was used as a negative control (lane 6). Anti-AHSV 5 antiserum (1:1000), which was unable to detect either VP3 or VP5, was used as the primary antibody. VP7 trimer (135 kDa), VP2 (123 kDa) and VP7 monomer (38 kDa) are indicated by black arrows. Colour pre-stained protein standard, broad range (New England Biolabs, MA, USA) indicated to the right of the blot was used as a molecular weight marker.

However, fully formed AHSV 5 VLPs ± 80 nm in size were imaged by TEM analysis of these crude extracts, indicating that all four capsid proteins were expressed and indeed had self-assembled into complete particles (Figure 2.8).

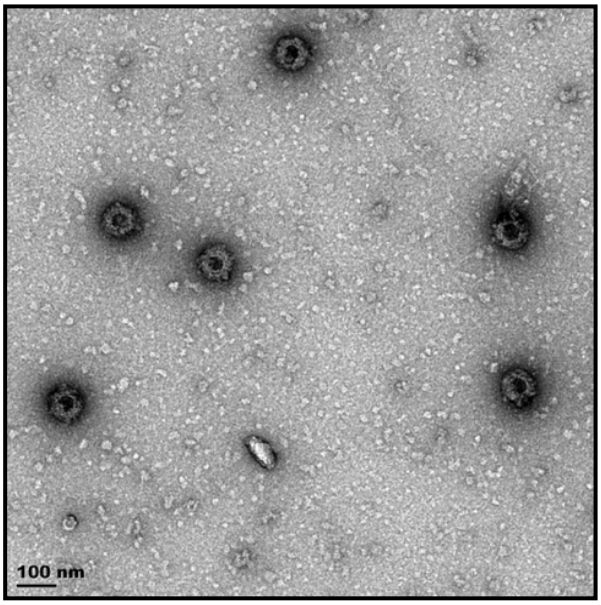

Figure 2.8: Fully assembled AHSV 5 virus-like particles imaged by TEM analysis of crude extracts from plants co-infiltrated with pEAQ-AHSV5 VP2, pEAQ-AHSV5 VP3, pEAQ-AHSV5 VP5 and pEAQ-AHSV5 VP7. Scale bar, 100nm.

2.3.3 Purification of plant-produced AHSV 5 VLPs

To produce an AHSV 5 VLP preparation of sufficient purity and concentration for immunization of horses, several modifications were made to the small-scale expression protocol. Firstly, the process was upscaled to infiltrate 24 whole plants with the recombinant constructs at an OD_{600} of 0.5 each. Secondly, a vacuum infiltrator was used to introduce the *Agrobacterium* suspension into the leaf intercellular spaces as this was much less labour-intensive than syringe infiltration and resulted in more uniform infiltration of plant leaves. Thirdly, clarified leaf extracts were fractionated by iodixanol density gradient ultracentrifugation.

Following ultracentrifugation, it was observed that green-coloured impurities settled in the upper 30% region of the gradient, while a single iridescent band (green arrow) was observed at a higher density, near the 30%–40% interface (Figure 2.9 A). Fractions (1 ml) were collected from the bottom of the tubes and four distinct bands corresponding to the correct molecular weight sizes of the AHSV capsid proteins were observed following separation of fractions 6–8 by SDS-PAGE and Coomassie blue staining (Figure 2.9 B).

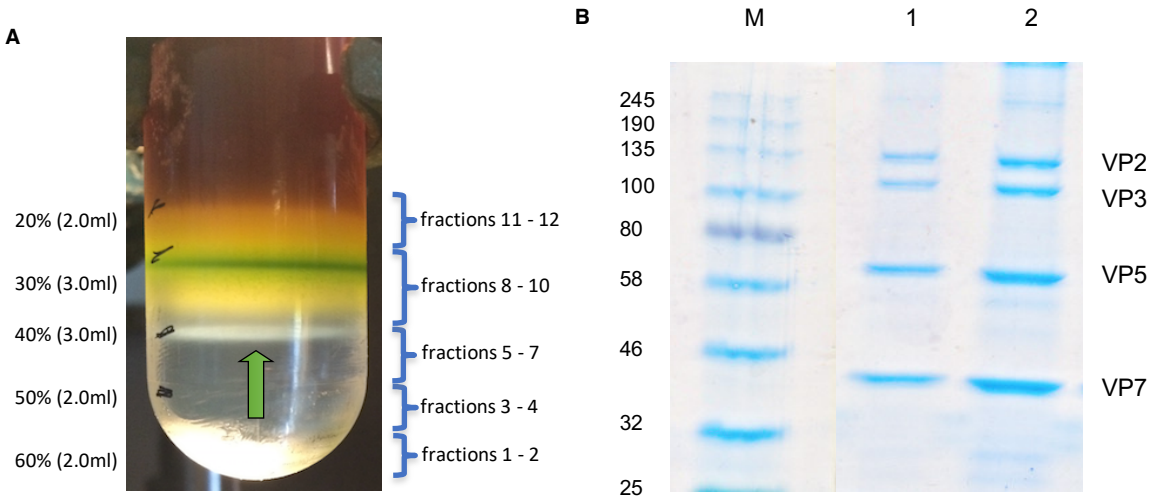

Figure 2.9: Purification of AHSV-5 VLP's. A) Crude homogenates from plants 7 days after co-infiltration with all 4 AHSV 5 *Agrobacterium* recombinants, were subjected to iodixanol density gradient ultra-centrifugation. (B) Gradient fractions were collected from the bottom and fractions 7 (lane 1) and 8 (lane 2) were separated by denaturing SDS-PAGE followed by Coomassie blue staining. The AHSV viral proteins VP2, VP3, VP5 and VP7 are indicated to the right of the gel, while the molecular weight marker sizes are shown on the left.

Expression of VP2 and VP7 as well as the VP7 trimer was demonstrated by western blotting using the available AHSV 5 antiserum (Figure 2.10).

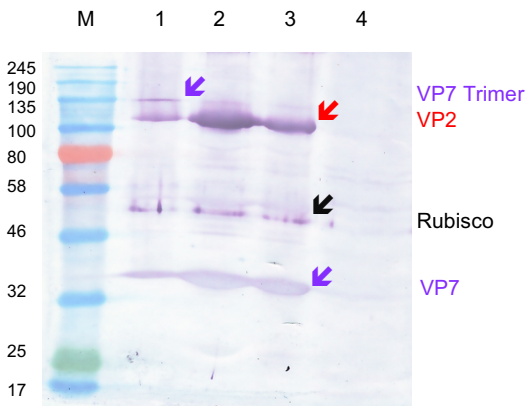

Figure 2.10: Western blot analysis of AHSV 5 VLPs. Gradient fractions 6 (lane 1), 7 (lane 2) and 8 (lane 3) were separated by denaturing SDS-PAGE followed by western blot analysis using the same AHSV 5 antiserum, which does not detect VP3 or VP5, only VP2 and VP7 (1:1000). Crude extract from leaves infiltrated with *Agrobacterium* transformed with pEAQ-HT expression vector lacking any goi, was used as a negative control (lane 4). The location of the detected AHSV viral proteins, VP2 and VP7, are indicated to the right of the gel together with the plant protein, rubisco, while the molecular weight marker sizes are shown on the left.

As AHSV serotype 5 is one of the serotypes not included in the LAV, we did not have access to a positive control for this study. Therefore, the identity of the four protein species was further confirmed by mass spectrometry (Figure 2.10).

Figure 2.11: Mass spectrometry analysis of the 4 protein bands recovered from SDS-PAGE separation of density gradient fractions from leaves co-infiltrated with *Agrobacterium* AGL1 pEAQ recombinants for co-expression of AHSV capsid proteins VP2, VP3, VP5 and VP7. Highlighted regions represent sequence identity of the peptides with the respective AHSV proteins.

The co-sedimentation of all four proteins was highly suggestive of the presence of VLPs, and this was confirmed by TEM analysis (Figure 2.12). An estimated 40%–50% of the viral structures were seen to be complete AHSV VLPs (white arrows in Figure 2.12) or contained at least a partial VP2 outer layer, although some particles appear to have been slightly damaged during the purification process. Assembly intermediates representing core-like particles (CLPs), or CLPs in the process of acquiring the two outer coat proteins, were also observed (yellow arrows in Figure 2.12).

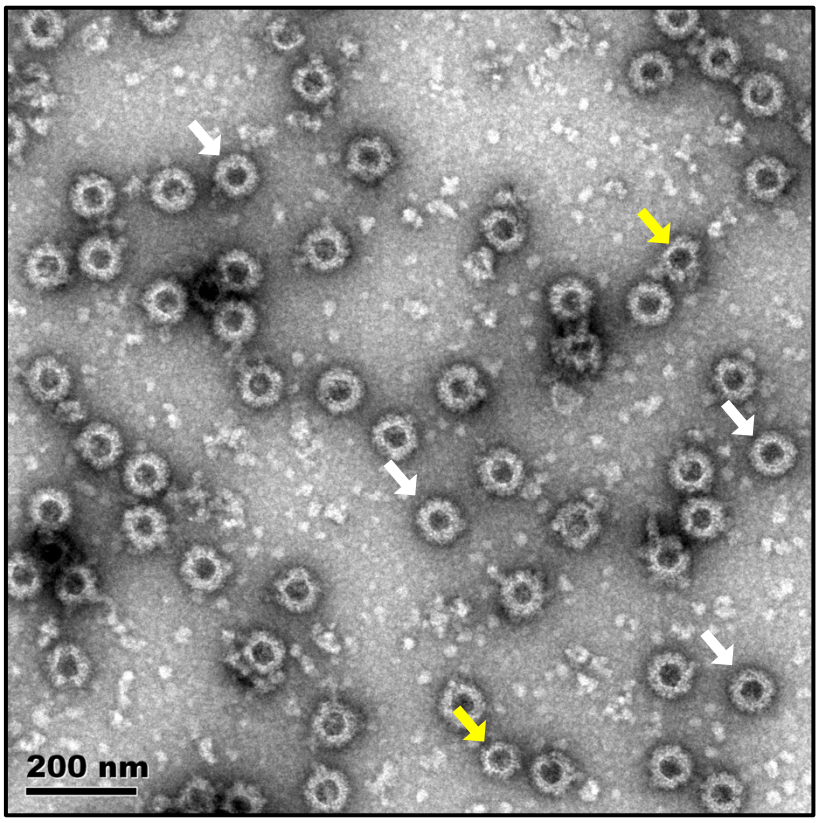

Figure 2.12: TEM analysis of gradient fractions of crude extracts from leaves co-infiltrated with *Agrobacterium* AGL1 pEAQ recombinants for co-expression of the four AHSV 5 capsid proteins. Gradient fraction 8 (Figure 2.9) revealed the presence of fully assembled VLPs (white arrows) together with some assembly intermediates (yellow arrows). Scale bars, 200nm.

Gel densitometry was used to estimate the VLP concentration (Figure 2.13). The purification was repeated several times and typically, 70 g infiltrated leaf material yielded ± 0.4 mg highly purified VLPs, which equates to ± 5.7 mg purified VLPs/kg leaf biomass.

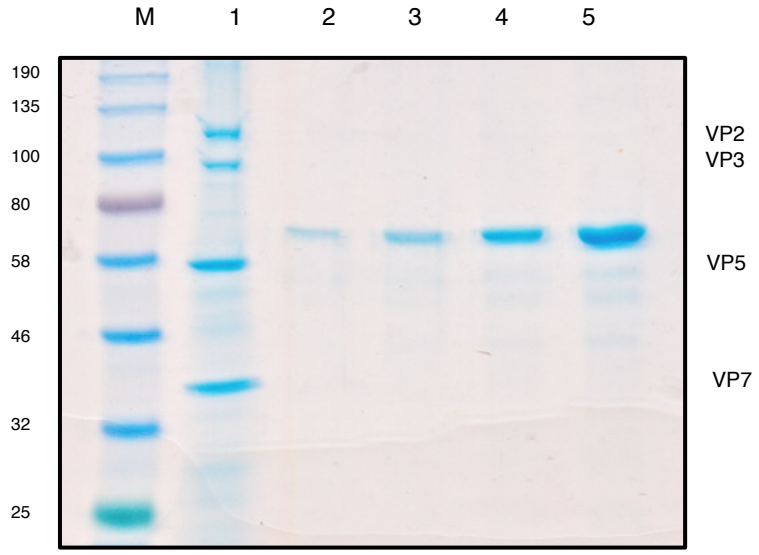

Figure 2.13: Quantification of AHSV 5 VLPs by gel densitometry. Particle quantification was achieved by visual comparison of the four capsid protein bands (lane 1) to known amounts of bovine serum albumin (BSA), 315 ng (lane 2), 625 ng (lane 3), 1.25 ug (lane 4) and 2.5 ug (lane 5) run separately on the same SDS-PAGE gel. The location of the AHSV viral proteins VP2, VP3, VP5 and VP7 are indicated to the right of the gel, while molecular weight marker sizes (kDa) are shown on the left.

2.3.4 Stability of plant-produced AHSV 5 VLPs

Aliquots (1 – 5 mL) of purified AHSV 5 VLPs were stored at -80 ^{o}C until ready for vaccination into animals. A grid depicting AHSV 5 VLPs compared well to another prepared from the same sample after storage at -80 ^{o}C for 18 months (Figure 2.14, A & B). Although an accurate determination and comparison of the proportion of fully-formed VLPs versus assembly intermediates was not possible due to the insufficient number of grid frames documented at the earlier timepoint, a qualitative visual assessment suggests that the VLPs are stable for long periods of time at this temperature. Furthermore, AHSV 5 VLPs that had been stored for 23 months and then analysed by SDS-PAGE and western blot with AHSV 5 antiserum from horses vaccinated with plant-produced AHSV 5 VLPs (1:5000), indicated that the integrity of the individual capsid protein components had been maintained during the almost 2-year storage period (Figure 2.14, C).

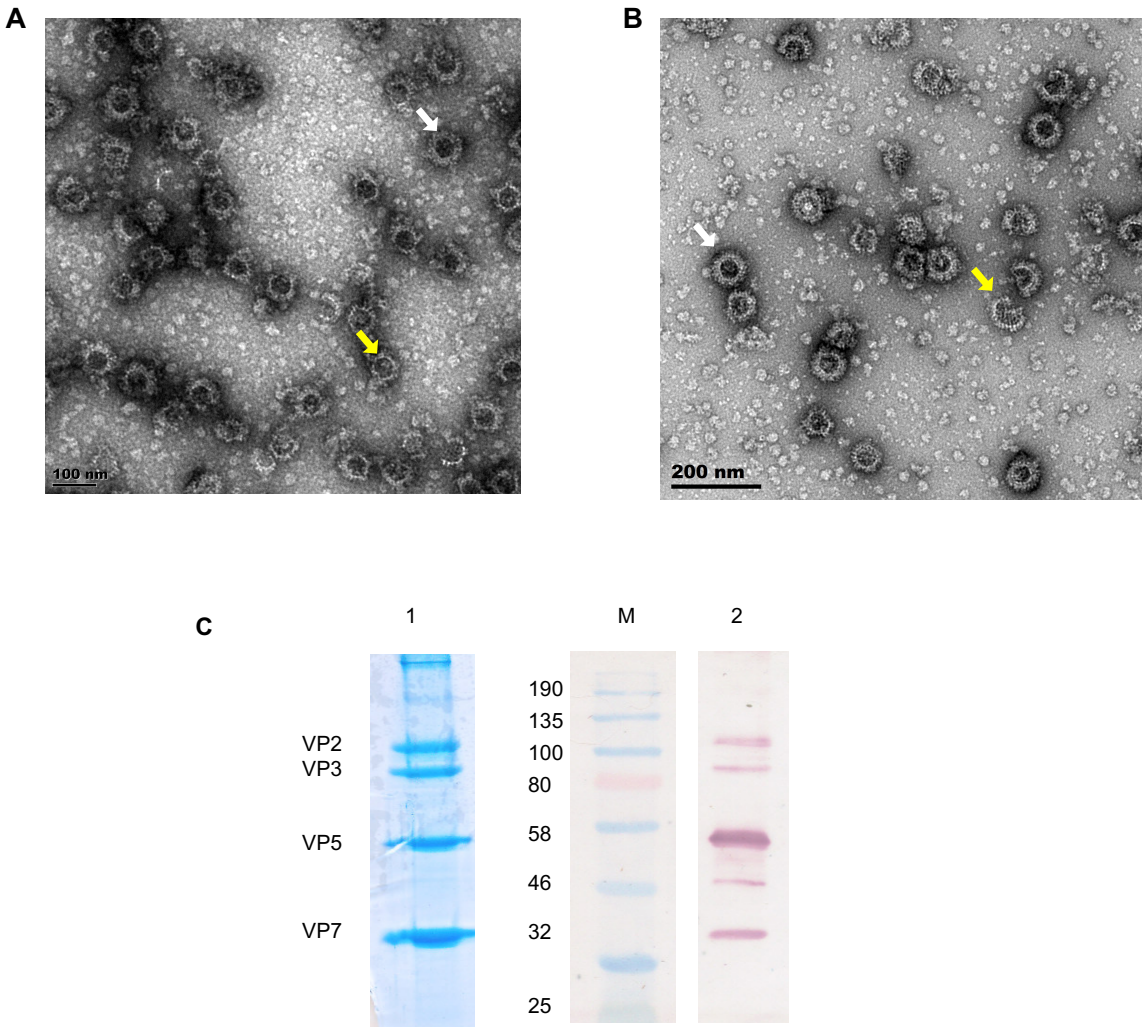

Figure 2.14: Stability of AHSV 5 VLPs and capsid protein components. TEM analysis of a mixture of gradient fractions of crude extracts from leaves co-infiltrated with *Agrobacterium* AGL1 pEAQ recombinants for co-expression of the four AHSV 5 capsid proteins on the day of preparation (A) and 18 months after storage at -80 ° C (B). The presence of fully assembled VLPs (white arrows) together with some assembly intermediates (yellow arrows) was visualized both before and after storage. Scale bars, 100 - 200nm. AHSV 5 VLPs stored for 23 months at -80 °C were analysed by SDS-PAGE (C, lane 1) and western blot (C, lane 2) using AHSV 5 antiserum from horses vaccinated with plant-produced AHSV 5 VLPs (1:5000). The location of the AHSV viral proteins VP2, VP3, VP5 and VP7 are indicated to the left of the gel, while molecular weight marker sizes are shown adjacent to the marker in lane M.

2.3.5 Expression of wild-type AHSV 5 VP2

To investigate whether plant codon-optimization of VP2 for expression in *N. benthamiana* promotes better translation compared to the wt mammalian gene sequence, a cDNA copy of the wild-type AHSV 5 VP2 gene was synthesized from dsRNA extracted from a recent AHSV 5 field isolate, cloned into the pEAQ vector and electroporated into *Agrobacterium* AGL 1. Transient expression

in *N. benthamiana* leaves was demonstrated by western blotting of crude leaf extracts infiltrated either with pEAQ-AHSV5-VP2/AGL or pEAQ-AHSV5-VP2$_{wt}$/AGL in the same experiment. Expression of AHSV 5 VP2 from the wt gene was observed, but the protein seems to be expressed more efficiently from the plant codon-optimised gene as judged by the density of the VP2 bands in the western blot result (Figure 2.1 A). However, it should be noted that the protein sequence encoded by the wt mammalian gene was also found to differ from the AHSV 5 VP2 amino acid consensus sequence (and the plant codon-optimised gene product) by 22 amino acids (data not shown).

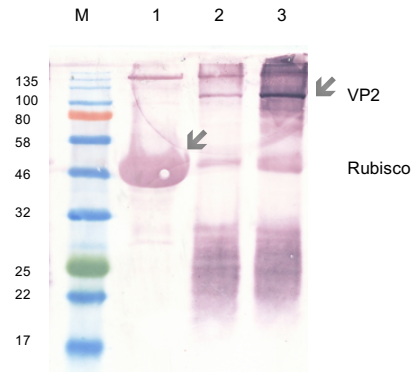

Figure 2.15: Comparison of wild-type versus plant codon-optimised AHSV 5 VP2 expression in *N. benthamiana.* Western blot analysis of crude leaf extracts obtained 5 dpi infiltration with *Agrobacterium* AGL1 containing wildtype pEAQ-AHSV 5 VP2 (A, lane 2) and plant codon-optimised pEAQ-AHSV5 VP2 (A, lane 3). Crude extract from leaves infiltrated with *Agrobacterium* transformed with pEAQ-*HT* expression vector lacking any goi, was used as a negative control (A, lane 1). Anti-AHSV 5 antiserum raised in guinea pigs vaccinated with plant-produced AHSV 5 VLPs (1:1000) was used as the primary antibody. VP2 (123 kDa) is indicated to the right of the gel, while molecular weight marker sizes are shown to the left.

2.3.6 Formation of AHSV 4 VLPs with the same AHSV 5 VP3/VP7 core

To investigate the spontaneous self-assembly in plants of VLPs representing a second AHSV serotype, whole plants were co-infiltrated with recombinant *Agrobacterium* strains carrying the AHSV 4 VP2 and VP5 constructs together with the AHSV VP3 and VP7 constructs. These AHSV serotype 4 VLPs would thus share a common core with the AHSV 5 VLPs, the outer capsid shell identifying the particular serotype.

As successful expression of AHSV 5 VP3 and VP7 had previously been demonstrated, small-scale transient expression of AHSV 4 VP2 and VP5 was tested first as described for the four AHSV 5 capsid proteins (**2.3.2**). AHSV 4 antiserum detected both AHSV 4 VP2 and VP5 in western blot experiments (Figure 2.16).

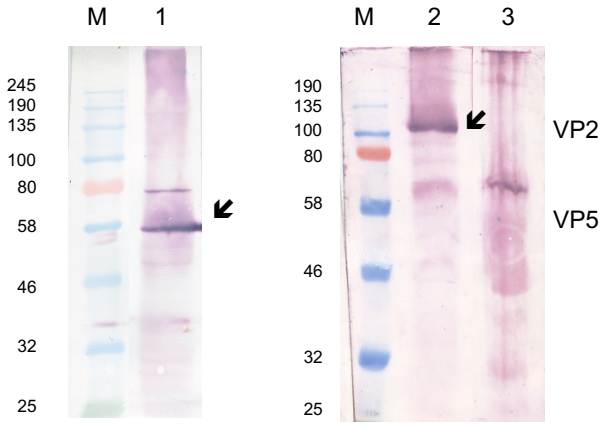

Figure 2.16: Expression of recombinant AHSV 4 structural proteins in *N. benthamiana*. Western blot analysis of crude leaf extracts obtained 7 dpi with *Agrobacterium AGL1* containing pEAQ-AHSV4 VP5 (lane 1) and pEAQ-AHSV4 VP2 (lane 2). Crude extract from leaves infiltrated with *Agrobacterium* transformed with pEAQ-*HT* expression vector lacking any goi, was used as a negative control (lane 3). Anti-AHSV 4 antiserum (1:1000) raised in horses vaccinated with a live attenuated AHSV 4 strain that had been rescued by reverse genetics, was used as the primary antibody (van de Water *et al.* 2015). VP2 (123 kDa) and VP5 (57 kDa) are indicated by black arrows. Colour pre-stained protein standard indicated to the left of the blots was used as a molecular weight marker.

To produce an AHSV 4 VLP preparation of sufficient purity and concentration for immunization of horses, the same procedure as for AHSV 5 VLPs (**2.3.3**) was initially followed. Twenty-four plants were co-infiltrated with bacterial suspensions containing AHSV 4 VP2 and VP5 recombinant AGL 1 strains together with the VP3 and VP7 AGL 1 recombinants used to produce AHSV 5 VLPs. Clarified leaf extracts were then purified by iodixanol density gradient ultracentrifugation. However, only the inner core capsid proteins VP3 and VP7 could be visualized by SDS-PAGE separation of the gradient fractions (Figure 2.17).

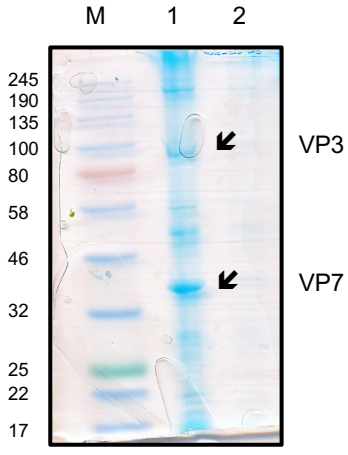

Figure 2.17: Purification of AHSV 4 VLPs. (a) Gradient fractions were collected from the bottom of the tubes and fractions 7 (lane 2) and 8 (lane 1) were separated by denaturing SDS-PAGE followed by Coomassie blue staining. The location of the AHSV viral proteins VP3 and VP7 are indicated with black arrows, while the molecular weight marker sizes are shown on the left of the gel.

Furthermore, the presence of core-like particles (CLPs) only, was confirmed by TEM imaging of gradient fraction 8 (Figure 2.18).

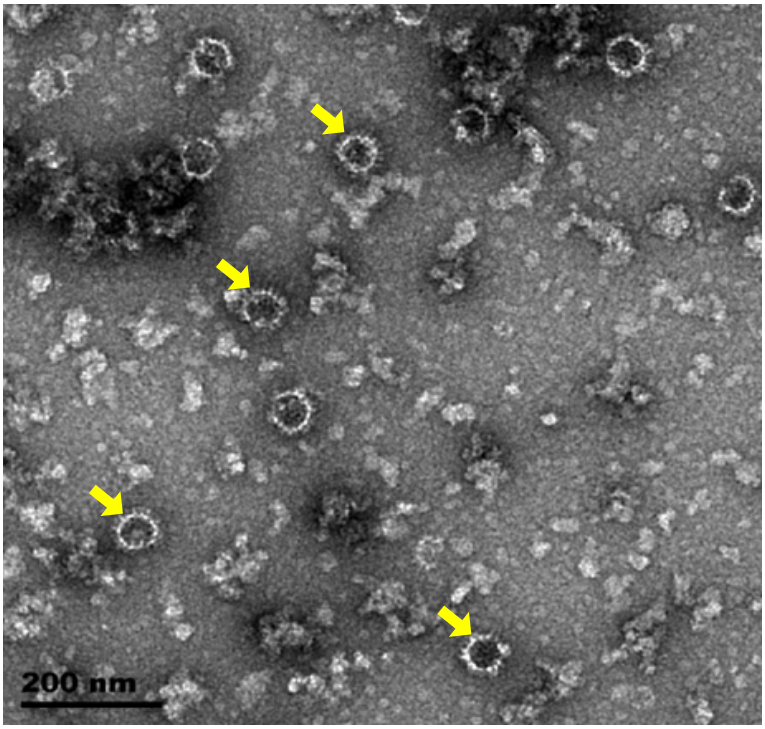

Figure 2.18: TEM analysis of gradient fractions of crude extracts from leaves co-infiltrated with *Agrobacterium* AGL1 pEAQ recombinants for co-expression of the two AHSV 4 outer capsid proteins together with the AHSV 5 inner core proteins. Gradient fraction 8 (Figure 2.16) revealed only the presence of core-like particles (yellow arrows). Scale bar, 200nm.

From the western blot analysis result (2.16), it was clear that AHSV 4 VP2 and VP5 were being expressed, but for some reason, VLPs were not assembling. Therefore, two strategies were employed to encourage self-assembly of these AHSV 4 VLPs. Firstly, the pH of the homogenization buffer was increased and secondly, a single amino acid was substituted to produce an AHSV 4 VP2 sequence with 100% identity to that used by van de Water *et al.* (2015), who reported the successful recovery of virulent AHSV 4 using a reverse genetics strategy.

To test the impact that changing the buffer conditions might have on the ability of the AHSV 4 capsid proteins to self-assemble, the PBS buffer (pH 7.4) used in the leaf homogenization and density gradient preparation was replaced with a bicine/NaCl buffer having an increased pH of 8.4. Under these buffer conditions, four distinct bands corresponding to the correct molecular weight sizes of the AHSV 4 capsid proteins were observed following separation of gradient fractions 6 - 8 by SDS-PAGE and Coomassie blue staining (Figure 2.19).

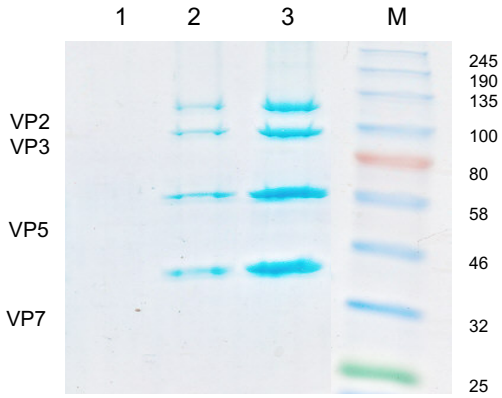

Figure 2.19: Purification of AHSV 4 VLPs. Gradient fractions were collected from the bottom of the tubes and fractions 6 (lane 1), 7 (lane 2) and 8 (lane 3) were separated by denaturing SDS-PAGE followed by Coomassie blue staining. The location of the AHSV viral proteins are indicated to the left of the gel, while the molecular weight marker sizes are shown on the right.

Furthermore, fully formed AHSV 4 VLPs were visualized by TEM, together with some assembly intermediates (Figure 2.20 A). The identity of the four protein species was further confirmed by western blotting using AHSV 4 antiserum (Figure 2.20 B).

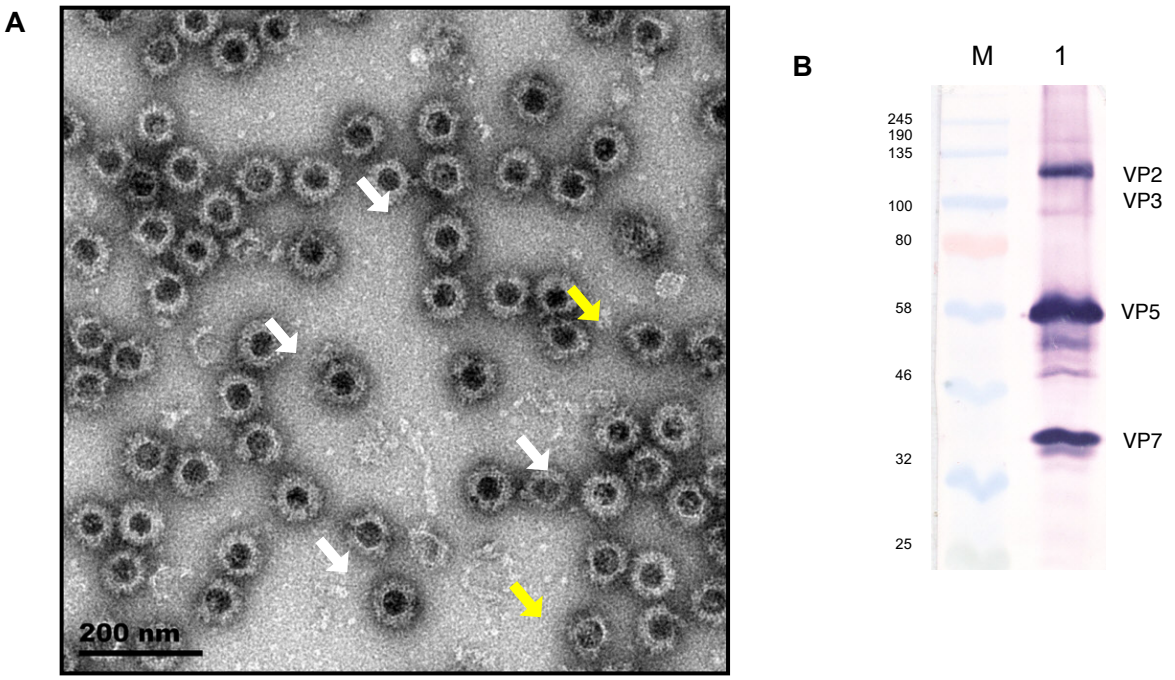

Figure 2.20: TEM and western blot analysis of gradient fractions of crude extracts from leaves co-infiltrated with *Agrobacterium* AGL1 pEAQ recombinants for co-expression of the four AHSV 4 capsid proteins. Gradient fraction 8 (Figure 2.17) revealed the presence of fully assembled VLPs (figure 2.18 A, white arrows) together with some assembly intermediates (figure 2.19 A, yellow arrows). Scale bar, 200nm. For western blot analysis of AHSV 4 VLPs (figure 2.19 B), Gradient fraction 8 was separated by denaturing SDS-PAGE and probed with AHSV 4 antiserum (1:1000) raised in horses vaccinated with a live attenuated AHSV 4 strain that had been rescued by reverse genetics. The location of the AHSV viral proteins are indicated to the right of the gel while the molecular weight marker sizes are shown on the left.

To align the AHSV 4 VP2 amino acid consensus sequence with the sequence used by van de Water *et al.* (2015) (GenBank accession number: KM820850), the Ile_{343} moiety of the AHSV 4

recombinant VP2 was replaced with Met_{343} by site directed mutagenesis of the pEAQ-AHSV-4-VP2 construct. The pEAQ-AHSV-4-$VP2_{mu}$ recombinant plasmid was sequenced with the pEAQ forward and reverse primers to obtain sequence data for the sequence area encompassing the nucleotide base change. Sequences were analysed using CLC Mainbench software (QIAGEN Bioinformatics) by alignment of the sequence data with the original and mutated AHSV-4-VP2 sequences. Sequence analysis confirmed that the A/G mutation had been correctly effected (Figure 2.21)

```
5'MASEFGILMTNEKFDPSLEKTICDVIVTKKGRVKHKEVDGVCGYEWDETNHRFGLCEVEHDMSISEFMY
NEIRCEGAYPIFPRYIIDTLKYEKFIDRNDHQIRVDRDDNEMRKILIQPYAGEMYFSPECYPSVFLRREAR
SQKLDRIRNYIGKRVEFYEEESKRKAILDQNKMSKVEQWRDAVNERIVSIEPKRGECYDHGTDIIYQFIKK
LRFGMMYPHYYVLHSDYCIVPNKGGTSIGSWHIRKRTEGDAKASAMYSGKGPLNDLRVKIERDDLSRETII
QIIEYGKKFNSSAGDKQGNISIEKLVEYCDFLTTFVHAKKKEEGEDDTARQEIRKAWVKRMPYMDFSKPMK
ITKGLIETCYFP.....RARTLKIYNRGSMDTLILISSGVYTFGNKFLLSKLLAKTE 3'
```

Figure 2.21: Sequence analysis of the pEAQ-AHSV5-$VP2_{mu}$ construct. The pEAQ set of primers was used to read the sequence of the cloned gene in both directions. The translated sequence is depicted above where the Met_{343} moiety is underlined and in bold.

The AHSV-4-$VP2_{mu}$/AGL recombinant strain was also used in co-infiltration experiments for incorporation of AHSV 4 $VP2_{mu}$ into VLPs. SDS-PAGE and TEM analysis demonstrated that the AHSV 4 VLPs self-assembled equally well regardless of whether VP2 or $VP2_{mu}$ was expressed (results not shown).

Gel densitometry was used to estimate the AHSV 4 VLP concentration (Figure 2.22). Repeated purifications typically yielded ± 0.58 mg highly purified AHSV 4 VLPs per 90 g infiltrated leaf material, which equates to ± 6.4 mg purified VLPs/kg leaf biomass.

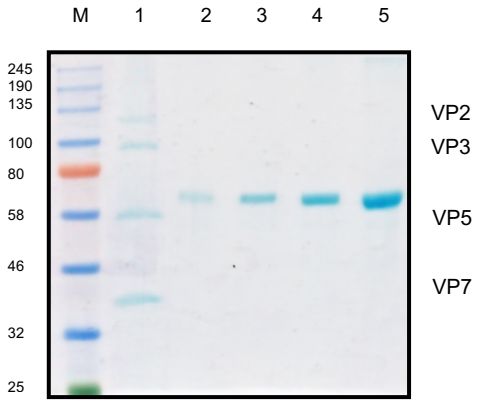

Figure 2.22: Quantification of AHSV 4 VLPs by gel densitometry. Particle quantification was achieved by visual comparison of the four capsid protein bands (lane 1) to known amounts of bovine serum albumin (BSA), 315 ng (lane 2), 625 ng (lane 3), 1.25 ug (lane 4) and 2.5 ug (lane 5) run separately on the same SDS-PAGE gel. The location of the AHSV viral proteins VP2, VP3, VP5 and VP7 are indicated to the right of the gel, while molecular weight marker sizes are shown on the left.

2.3.7 *In vitro* assembly of AHSV 5 VLPs

Both the AHSV 4 and 5 VLPs were assembled *in planta* by the transient co-expression of the 4 AHSV capsid proteins within the same plant. To investigate the possibility of using a cell-free *in vitro* system as opposed to *in planta* VLP self-assembly, clarified extracts from plants which had been singly infiltrated with the individual recombinant *Agrobacterium* strains, each carrying a different AHSV 5 pEAQ construct, were mixed together and incubated for 20 - 24 h at 4 ^{o}C. Iodixanol density gradient ultracentrifugation of the combined plant homogenate mixture followed by separation of gradient fractions 6 – 8 by SDS - PAGE and Coomassie blue staining, revealed four distinct protein bands corresponding to the AHSV 5 capsid proteins (Figure 2.23 A). The successful *in vitro* assembly of AHSV 5 VLPs was confirmed by TEM analysis of these gradient fractions. (Figure 2.23 B & C).

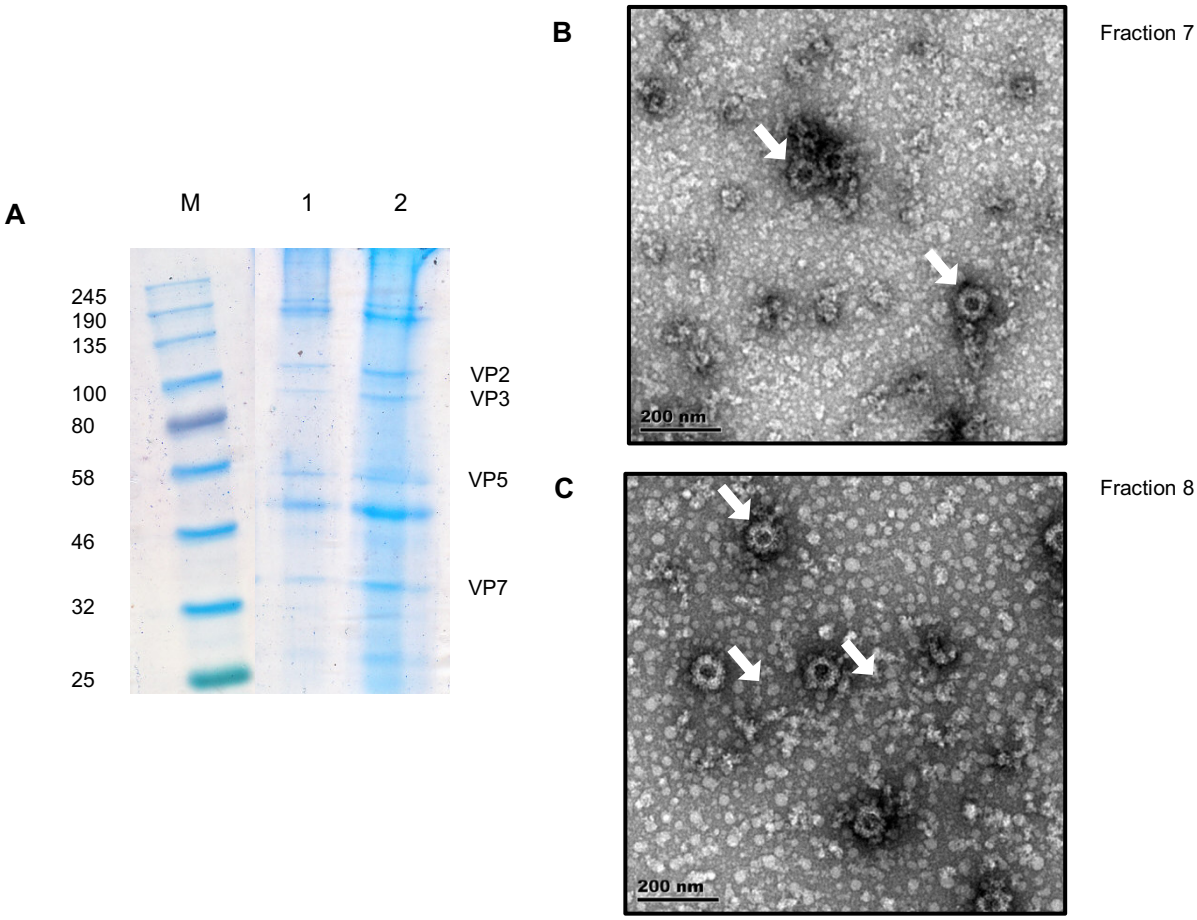

Figure 2.23: *In vitro* assembly of AHSV 5 VLPs. Combined crude extracts from plants each infiltrated with one of the AHSV 5 *Agrobacterium* constructs were purified by density gradient ultracentrifugation. Gradient fractions 7 & 8 were separated by SDS-PAGE followed by Coomassie blue staining (A, lanes 1 and 2). The location of the AHSV viral proteins are indicated to the right of the gel, while the molecular weight marker sizes are shown on the left. Fully assembled VLPs were imaged by TEM analysis of these fractions (B, white arrows). Scale bar, 200nm.

This *in vitro* VLP assembly was also tested by combining clarified plant extracts from leaves that had been co-infiltrated with the AHSV 5 VP3, VP5 and VP7 recombinant *Agrobacterium* strains and leaves that had been infiltrated with the AHSV 5 VP2 recombinant strain alone. Once again, SDS-PAGE (Figure 2.24 A) and TEM (Figure 2.24 B) analysis demonstrated the successful *in vitro* formation of AHSV 5 VLPs.

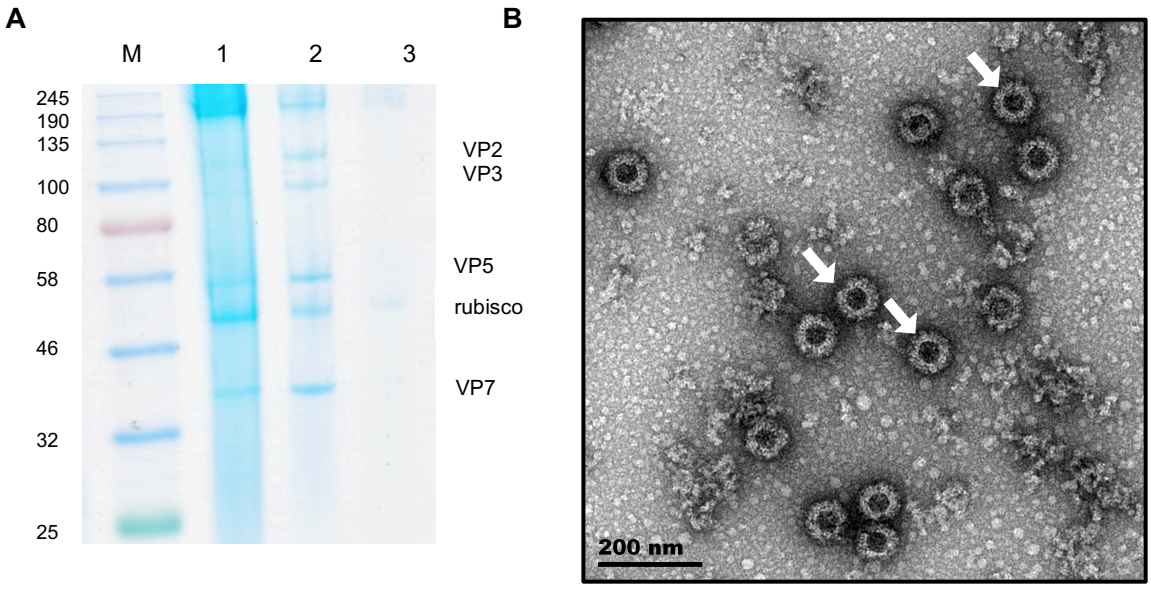

Figure 2.24: *In vitro* assembly of AHSV 5 VLPs. Combined crude extracts from plants co-infiltrated with the AHSV 5 VP3, VP5 and VP7 *Agrobacterium* constructs and plants that were infiltrated with the AHSV 5 VP2 *Agrobacterium* construct alone, were purified by density gradient ultracentrifugation. Gradient fractions 7, 8 & 9 (A, lanes 1, 2 and 3) were separated by SDS-PAGE followed by Coomassie blue staining (A). The location of the AHSV viral proteins are indicated to the right of the gel, while the molecular weight marker sizes are shown on the left. Fully assembled VLPs were imaged by TEM analysis of fraction 8 (B, white arrows). Scale bar, 200nm.

2.4 Discussion

Several different strategies have been adopted by research groups worldwide in the quest to develop new, safe, efficacious and cost-effective replacements for the currently used live attenuated AHSV vaccine. These include inactivated vaccines as well as recombinant vaccines, ranging from DNA and protein subunit vaccines to poxviral vectors and vaccines utilizing sophisticated reverse genetics technologies. Simple in design, but morphologically most similar to the live AHSV virion, VLP vaccines represent perhaps the most promising potential candidates.

VLP technology is based on the spontaneous self-assembly of particles following co-expression of the constituent structural protein(s) in a particular expression system. In choosing an appropriate expression platform, it is important to select the one that is most likely to yield the safest, yet biologically effective product at the lowest cost. In comparison to fermentation systems and mammalian or insect cell culture, plant-based expression is more economical and recombinant proteins can be produced at industrial scale levels (Streatfield 2007; Nandi *et al.* 2014). Furthermore, they are free from the risk of contaminating animal pathogens or toxins.

The results presented in this chapter show that the four capsid proteins of AHSV 5 spontaneously assembled into virus-like particles (VLPs) following recombinant DNA expression of these proteins within transiently transfected plant cells (Figure 2.12). The VLPs are non-infectious and inherently safe, as they assemble in the absence of any viral genetic material or of other viral proteins. This work is the first known report of AHSV VLPs being produced in plants (Dennis *et al.* 2018a).

The VLP component proteins were each expressed for 5 – 7 days from different pEAQ recombinant gene-carrying *Agrobacterium* strains, co-infiltrated in equal concentrations. The pEAQ vector, containing both the P19 silencing suppressor and the gene of interest, which was strategically positioned to ensure hyper translation of the viral protein (Sainsbury *et al.* 2009), proved to be a suitable expression vehicle.

VLPs seen in crude extracts resulting from small-scale expression in a single plant were almost all fully formed, whereas larger scale expression and subsequent iodixanol gradient purification produced a more heterogeneous mix of particles including assembly intermediates as well as some partially damaged particles. Density gradient ultracentrifugation proved to be a useful purification strategy for confirming the successful assembly of VLPs within the plants, but it is possible that the high centrifugal force may be damaging to the particles. This, together with the high cost of iodixanol, the expensive and sensitive equipment required and the labour-intensive centrifugation and fractionation step, makes it important to consider alternative purification strategies for large-scale centrifuge-free production of VLPs for use in animal studies. These

include depth filtration and tangential flow cytometry and will be discussed further in Chapter Three.

A yield of ± 5.7mg highly purified VLPs/kg infiltrated leaf material was routinely obtained during large-scale purifications, which means that 1 kg of leaves (which equates to roughly 300 plants) would provide sufficient vaccine to inoculate about 30 horses at a dose of 100 μg x 2 (prime and boost) per horse, ie. 10 plants per horse. Furthermore, a comparison of EM images, Coomassie-stained gels and western blots taken before and after long-term storage of the VLPs at - 80 ^{o}C, indicated both the long-term integrity of the capsid protein components as well as the stability of the particles. The plant-produced AHSV VLPs were shown to be stable for a period of at least 18 months but would more than likely remain so for even longer.

There is evidence to suggest that codon-optimization of the gene of interest, whereby rare codons are replaced by codons which occur more commonly in the host organism, may enhance expression of recombinant proteins in heterologous systems (Gustafsson *et al.* 2004; Kudla *et al.* 2009). To determine whether this might be the case for AHSV gene translation too, expression of AHSV 5 VP2 cDNA prepared by reverse transcription of dsRNA purified from a naturally occurring field isolate was compared with that of the plant codon-optimised VP2 gene. The results demonstrated here indicate that VP2 synthesis occurred following infiltration with either of the two recombinant *Agrobacterium* strains, but that codon optimization did indeed appear to result in improved expression levels.

As it would be advantageous for a vaccine alternative to the currently used live vaccine to provide protection against all nine serotypes of the virus, the formation of so-called chimeric VLPs, where the outer capsid proteins were replaced with those of a different serotype, in this case AHSV serotype 4, was also investigated. Initial attempts to produce these VLPs containing the original VP3/VP7 core and a serotype 4 VP2/VP5 outer shell using the same transient transfection method employed to produce homologous AHSV 5 VLPs, was unsuccessful. Although evidence was obtained for the synthesis of all four proteins within the infiltrated plant host cells, only CLPs but not VLPs could be purified from homogenized leaf tissue (Figure 2.18).

Others had shown that it was possible to recover AHSV serotype 4 particles using a reverse genetics approach (van de Water *et al.* 2015), and therefore two strategies were employed to promote successful AHSV 4 VLP assembly. Firstly, site-directed mutagenesis was used to align the AHSV 4 VP2 consensus sequence (Figure 2.1) with the sequence used by van de Water *et al.* (2015). This involved replacing Ile_{343} with a Met residue. Secondly, due to the fact that it is a reduction in pH which causes uncoating of the virus particle in infected cells ie. removal of VP2 and later VP5, the buffer used for homogenization and iodixanol gradient purification (PBS pH 7.4)

was replaced with a bicine buffer having a higher pH of 8.4. Both buffers have a pH higher than that in the endosome where uncoating takes place (±pH 6.5), but it was reasoned that a pH higher than 7.4 may be more likely to encourage and maintain VLP assembly. The increased pH indeed resulted in the formation of correctly assembled chimeric AHSV 4 VLPs, demonstrating that buffer pH seems to play an important role in successful VLP assembly (Figure 2.20). This will have important implications regarding the development of a heterotypic AHSV VLP vaccine. Furthermore, these AHSV 4 VLPs assembled successfully regardless of whether the original VP2 or the sequence-adjusted VP2 was used in infiltration experiments, indicating that pH was more important for VLP assembly than a slight sequence variability.

In considering the development of a heterotypic AHSV VLP vaccine, it was of interest to discover whether the structural protein components of the AHSV particle would only self-assemble if co-expressed within a living system ie. *in planta* or whether simply mixing the four proteins *in vitro* would also permit formation of functional VLPs. With this in mind, plants were infiltrated individually with the different AHSV 5 *Agrobacterium* recombinants or combinations thereof, and crude homogenates, prepared 3 – 4 days post infiltration, were then mixed and incubated overnight at 4^{o}C to allow the possibility of spontaneous VLP assembly. The results above show that AHSV 5 VLPs could be purified both from a mixture of individual protein-containing homogenates, (Figure 2.23) as well as from an homogenate prepared from leaves co-infiltrated with VP3, VP5 and VP7 pEAQ recombinant-carrying *Agrobacterium* strains mixed with an homogenate prepared from leaves infiltrated with the VP2 *Agrobacterium* strain only (Figure 2.24). This is the first known evidence of multimeric VLP assembly *in vitro* in any expression system and may prove useful in the rapid screening of possible chimaeric VLPs, and subsequent preparation of potential AHSV VLP vaccine candidates for protection against multiple serotypes.

C H A P T E R T H R E E

SAFETY AND IMMUNOGENICITY OF THE PLANT- PRODUCED AHSV VLP VACCINE CANDIDATES IN HORSES

3.1 Introduction

As a highly infectious notifiable viral disease, AHS poses a substantial challenge to horse owners in sub-Saharan Africa. The situation is further complicated by the 9 different serotypes of the aetiological agent, AHSV, that have been isolated in the region (Coetzer and Guthrie 2004; Mellor and Hamblin 2004). Immunisation with live attenuated vaccines (LAVs) (Alexander 1934) has been the primary control strategy to date, but recent research has shown that vaccines of this nature carry the inherent risk of reverting to virulence, as well as the possibility of gene segment re-assortment between outbreak and vaccine strains (Weyer *et al.* 2016).

Neither AHSV 5 nor AHSV 9 are included in the current vaccine (von Teichman and Smit 2008), but because of the existence of cross protection between serotypes 1 & 2, 3 & 7, 5 & 8 and 6 & 9 (Erasmus 1978; Coetzer and Guthrie 2004; von Teichman *et al.* 2010), protection against AHSV 5 and 9 is expected to be provided by AHSV 8 and 6 respectively. Of concern, however, is the fact that in 2006 both AHSV 5 and 9 dominated outbreaks (Weyer *et al.* 2016), particularly in the Western Cape Province, which raises doubts about the competency of the LAV to provide sufficient protection against these two AHSV serotypes. Moreover, besides the inability to differentiate between natural and vaccine-induced immunity (non-DIVA), the LAV is restricted to use within southern Africa, and this has significant implications for both the horse export industry as well as the equestrian sporting arena.

Although research demonstrating the efficacy of various alternative vaccine candidates has been published, none of these have yet been commercialised (Guthrie *et al.* 2009; Lulla *et al.* 2017; Manning *et al.* 2017; van Rijn *et al.* 2018). In Chapter Two of this thesis, the successful purification of fully-assembled AHSV 5 and 4 VLPs in plants via a transient expression strategy, was demonstrated. As inherently safe, DIVA compliant, non-replicating protein assemblies, essentially identical in size and shape to the intact virions, these VLPs are promising new additions to the arsenal of potential AHSV vaccines. Indeed, the ability of plant-produced AHSV 5 VLPs to elicit a

strong serotype-specific neutralising antibody response in guinea pigs has been demonstrated in a preliminary study (Dennis *et al.* 2018a).

Two small animal models have been shown by others to be useful laboratory models for evaluating the antigenic properties of AHSV vaccines namely, the guinea pig (Erasmus 1978; Du Plessis *et al.* 1998; Ronchi *et al.* 2012; Lelli *et al.* 2013; Kanai *et al.* 2014) and the mouse, specifically immunocompetent Balb/C and immunodeficient type 1 interferon receptor knockout (IFNAR -/-) mice (Castillo-Olivares *et al.* 2011b; Calvo-Pinilla *et al.* 2014; de la Grandiere *et al.* 2014; Aksular *et al.* 2018). The latter are a particularly useful small animal model due to their high clinical susceptibility to AHSV infection, and the guinea pig has been shown to be an excellent small animal screening model due to the high levels of neutralizing antibodies elicited in immunogenicity experiments (Du Plessis *et al.* 1998; Dennis *et al.* 2018a). The use of these small animal models in preliminary studies is ethically and economically beneficial in reducing experiments in horses, but ultimately it is necessary to test the immunogenicity and efficacy of candidate vaccines in the main target animal itself. The aim of this chapter, therefore, was to test the safety and immunogenicity of both AHSV 5 and 4 plant-produced VLPs in horses, with a view to producing a supplemental vaccine to complement the currently used live vaccine mixture.

A small area of the Cape Town Metropole is the only area in South Africa where no cases of AHS have ever been recorded, and in order to maintain the country's positive horse export status, movement of horses into this area and the surrounding surveillance and protection zones is strictly monitored (Weyer *et al.* 2016). As the University of Cape Town (UCT) is in the Western Cape, research using infectious virus is prohibited and therefore it is not possible to conduct an AHSV challenge study here. However, as the plant-produced AHSV VLP vaccine is composed entirely of a protein shell and contains no viral genetic material, safety and immunogenicity testing is permitted. The test regime is complicated by the fact that many horses in the Western Cape have been vaccinated with the LAV at some point and this therefore needs to be taken into consideration when designing the study protocol and analyzing the data obtained. In this chapter, the safety and immunogenicity in horses of AHSV VLPs of two different serotypes was investigated.

Iodixanol density gradient ultracentrifugation may be a suitable purification method for the preparation of plant-produced AHSV VLPs, but due to the expensive reagents and equipment required, this labour-intensive method is impractical and not economically viable for large-scale vaccine production. Therefore, an alternative purification strategy was employed and tested alongside conventional ultracentrifugation to prepare the VLP vaccines used in this study. The efficacy of the candidate vaccines was evaluated by virus neutralisation analysis of serum from vaccinated horses. These assessments were conducted at the University of Pretoria, again due to the prohibition of working with live virus in the Western Cape province of South Africa.

In the case of AHSV serotype 5, horse sera were regularly taken and analysed over a time period of 42 weeks to gain a clearer understanding of the quality and longevity of the immune response elicited by the plant-produced AHSV VLPs. This will facilitate comparisons with the immune responses reported in studies by others where horses were vaccinated with the LAV (von Teichman *et al.* 2010; Crafford *et al.* 2014; Weyer *et al.* 2017) and will provide evidence of the value of this VLP vaccine candidate as a suitable alternative or adjunct therapy to the currently used vaccine.

3.2 Materials and Method

3.2.1 Vaccine preparation for safety and immunogenicity testing in horses

Two different AHSV 5 VLP vaccine formulations were used in this study. Firstly, AHSV 5 VLPs were purified from *N. benthamiana* plants co-infiltrated with all four recombinant AHSV 5 *Agrobacterium* strains by iodixanol discontinuous density gradient ultracentrifugation of crude plant lysates as described in Chapter Two.

For the second formulation, crude plant lysates containing AHSV 5 VLPs were prepared using a bicine/NaCl buffer (20 mM NaCl, 50 mM bicine pH 8.4, 1 mM dithiothreitol (DTT) (Thermo Fisher Scientific) and 1x protease inhibitor (PI) cocktail P2714 (Sigma Life Science) instead of PBS buffer (137 mM NaCl, 10 mM Na2HPO4, 2.7 mM KCl, 2 mM KH2PO4, pH 7.4) containing Complete™, EDTA-free protease inhibitor cocktail (Roche, Basel, Switzerland). These crude plant lysates were then filtered through a depth filter (Sartoclean GF sterile midicap, 3 µM + 8 µM) using a Masterflex console drive 4 peristaltic pump (Cole-Parmer Instrument Company).

To further purify and concentrate the VLPs, the lysate was filtered through a 300 K Minimate™ TFF capsule (Pall Life Sciences) with the pressure not exceeding 2 Bar. The latter removes all proteins smaller than 300 K. The filtrate was washed with two volumes of bicine buffer lacking DTT. Finally, the extract was filter-sterilised through a 0.45 µM + 0.2 µM Sartobran 300 sterile capsule (Sartorius Stedim Biotech GmbH) using a peristaltic pump.

Particle quantification was achieved by purification of a sample of the filtered VLP preparation by iodixanol discontinuous density gradient ultracentrifugation and then visual comparison of the four capsid protein bands to known amounts of bovine serum albumin (BSA) run in separate lanes on the same SDS-PAGE gel.

Prior to vaccination, AHSV 5 and 4 VLP samples were adjuvanted with 5% Pet Gel A (SEPPIC, Paris, France) by mixing 290 µl adjuvant with 5.51 ml VLP sample and pipetting gently up and down, to produce 5.8 ml vaccine per horse. This allows a 5 ml vaccine preparation with sufficient extra to account for the dead volume in the syringe. The sample and adjuvant were mixed on the day of vaccination and stored for ±2 h on ice until ready to be injected.

3.2.2 Immunisation of horses

3.2.2.1 Horses used in the study

Ten horses were used in the study and approval for immunisation was obtained from both the Faculty of Health Sciences Animal Ethics Committee, University of Cape Town (FHS AEC Ref No.: 017/006) and the South African Medical Research Council Ethics Committee for Research on Animals (SAMRC ECRA Ref No.:07/17). Furthermore, permission to conduct the study in terms of Section 20 of the Animal Diseases Act 1984 (ACT NO. 35 of 1984) was obtained from the South African Department of Agriculture, Forestry and Fisheries (DAFF Ref No.:12/11/1/7).

The horses were all housed at the SA MRC facility in Cape Town: as the early history of these horses was not well documented, blood samples were drawn from the animals prior to vaccination (day 0) in order to ascertain the pre-vaccination immune status of the selected animals. A positive pre-vaccination ELISA score would be an indication of prior exposure to the virus either by vaccination with the currently used live attenuated vaccine (LAV) mixture, or by natural infection. AHSV protein VP7 is the group-specific antigen used in these ELISA-based diagnostic tests (Chuma *et al.* 1992), and the test is based on the principle that AHSV-infected or vaccinated animals will produce IgG antibodies, which will bind to the recombinant VP7 antigen in the ELISA plate wells.

Furthermore, the presence or absence of virus neutralizing antibodies in the pre-vaccination serum samples against AHS, was also determined. These tests were conducted at the Department of Veterinary Tropical Diseases at the University of Pretoria.

Vaccinations were carried out at the South African Medical Research Council (SA MRC) facility by the registered facility veterinarian Dr J Neuland, who was also responsible for monitoring the well-being of the horses. On day 0, the ten horses each received a deep intra muscular injection of 5 mL vaccine or control vaccine preparation and this was boosted on day 27 by a second vaccination. Temperatures were monitored daily for 6 weeks and weekly thereafter.

3.2.2.2 Vaccination Schedule

The ten horses were vaccinated according to the schedule described in Table 3.1.

Table 3.1: Vaccination schedule. Horses were vaccinated with either gradient-purified (Group 1) or filtered (Group 2) plant-produced AHSV 5 VLPs, PBS (Group 3), bicine buffer (Group 4) or gradient-purified plant-produced AHSV 4 VLPs (Group 5), all adjuvanted with 5% Pet Gel A (SEPPIC, Paris, France) and administered by deep intra-muscular injection.

Group	Horses	Vaccine	Protein Content	Dose and route of administration
1	Horse 1 Horse 2	Gradient-purified AHSV 5 VLPs	AHSV 5 VP2, VP3, VP5 & VP7	± 200 µg total protein in 5 mL PBS pH 7.4 with 5% Pet Gel A adjuvant, intra-muscular
2	Horse 3 Horse 4	Filtered AHSV 5 VLPs	AHSV 5 VP2, VP3, VP5& VP7	± 100 µg total protein in 5 mL bicine buffer pH 8.4 with 5% Pet Gel A adjuvant, intra-muscular
3	Horse 5 Horse 6	PBS	Nil	5 mL PBS pH 7.4 with 5% Pet Gel A adjuvant intra-muscular
4	Horse 7 Horse 8	Bicine	Nil	5 mL bicine buffer pH 8.4 with 5% Pet Gel A adjuvant, intra-muscular
5	Horse 9 Horse 10	Gradient-purified AHSV 4 VLPs	AHSV 4 VP2, VP3, VP5 & VP7	± 200 µg total protein in 5mL bicine buffer pH 8.4 with 5% Pet Gel A adjuvant intra-muscular

3.2.3 iELISA for detection of VP7 serotype-specific antibodies

Blood samples drawn from the horses were analysed by routine VP7 indirect ELISA at the Onderstepoort Veterinary Research Institute (ARC-OVI) in Pretoria, South Africa. Ninety-six well plates (Nunc Maxisorp, ThermoFisher Scientific) were coated with 50 ng recombinant VP7 antigen (100 µL/well) diluted in coating buffer (10 mM Tris, pH 8.5) and incubated overnight at 4°C with gentle shaking. Plates were blocked with 300 µL blocking buffer (1x Tris-Cl, pH 7.5, 5% non-fat dairy milk powder) for 2 h at room temperature after which they were washed 4x with 1x TST (1x TBS, 0.05% Tween 20) wash buffer using an ELx50 Autostrip washer (Bio-Tek Instruments Inc).

Horse serum samples to be tested were diluted (1:100) and added to each well and the plates were incubated at 37°C for 1 h. The plates were washed 4x with 1x TST, followed by the addition of 100 µL anti-horse Protein-G horseradish peroxidase-conjugated secondary antibody (1:10000, Sigma-Aldrich, St Louis, MO, USA) to each well and incubated at 37°C for 1 h. For the final washes, plates were washed with 1x TBS (pH 9) after which 200 µL TMB (3,3′,5,5′-tetramethylbenzidine) substrate (Sigma-Aldrich) was added to each well and incubated in the dark for 30 min.

The absorbance at a single wavelength of 450 nm was measured using an ELISA plate reader (BIOTEK ELx *808*, Winooski, VT, USA). High positive control sera pooled from vaccinated horses inoculated with live attenuated vaccine (bottle 1) obtained from Onderstepoort Biological Products (OBP, Pretoria, South Africa) was used as a positive control, while commercial HyClone™ Donor Equine serum (ThermoFisher Scientific, Waltham, MA, USA) was used as a negative control. Control sera were diluted (1:100) in diluent-buffer (10 mM Tris, pH 8.5).

The results were rounded off to the nearest digit where applicable. Sample Percentage Positive (PP) values less than 5.0 were classified as negative for AHSV Ab, while Sample Percentage Positive (PP) values greater than or equal to 5.0, but less than 10.0 were considered suspect for AHSV antibodies. Sample Percentage Positive (PP) values greater than 10.0 were classified as positive for AHSV Ab.

3.2.4 Neutralisation assay of vaccinated horse sera

Antisera from vaccinated horses were analysed for virus neutralisation against AHSV 5, AHSV 4 and AHSV 8 by Carina Lourens from the Department of Veterinary Tropical Diseases at the University of Pretoria, South Africa. Horse sera to be tested were diluted 1:5 in 1 x PBS (137 mM NaCl, 10 mM Na2HPO4, 2.7 mM KCl, 2 mM KH2PO4, pH 7.4) and heat-inactivated for 30min at 56°C. The 1:5 dilution was serially diluted further in minimal essential medium MEM, containing

5% foetal calf serum and 1% antibiotics (Gentamycin 50) and 100 µl of each dilution was added to the test wells in a 96 well plate (Nunc Maxisorp, ThermoFisher Scientific).

The stock virus was diluted in 5% MEM (containing foetal calf serum and antibiotics) and 100µl of the AHSV (100$TCID_{50}$) was added to each well. As a virus control 100$TCID_{50}$ AHSV antigen, as well as serial dilutions thereof, were added to control wells (no antisera). The plates were incubated for one hour at 37ºC in a humid atmosphere of 5% CO_2 in air. Vero cells with a concentration of 480 000 cells/ml were added (80µl) to each well. For the cell control, 200µl of 5% MEM (containing foetal calf serum and antibiotics) was mixed with 80µl of the cell suspension.

The plates were incubated at 37ºC in a humid atmosphere of 5% CO_2 in air for a further 5 days when the back titration indicated that the stock virus showed 50% cytopathic effect (CPE). The presence of specific antibodies in the test serum inhibits the production of CPE and the end point was thus taken as the dilution at which 50% of the cells were infected. Sheep serum from animals vaccinated with live AHSV was used as a positive control.

3.2.5 Western blot detection of anti-AHSV antibodies

Sera were tested for antibodies by western blot analysis as per the protocol described in **2.2.5**. AHSV VLPs were separated by SDS-PAGE and individual lanes were probed with different horse serum samples at a 1:1000 dilution. Detection of bound alkaline phosphatase secondary antibodies was measured by incubation of the membrane strips in BCIP substrate at room temperature for 15 - 60 min under no light conditions.

3.3 Results

3.3.1 Pre-immune status of the horses used in the study

The indirect ELISA results (Table 3.2) indicated that only half of the horses (horses 1, 2, 5, 9 and 10) were naïve prior to the study. The other five horses (horses 3, 4, 6, 7 and 8) all had positive VP7 iELISA scores, most likely indicating prior vaccination with the LAV. However, the virus neutralisation titres (vnts) were negative for all ten horses, and these horses were therefore used in the safety and immunogenicity study.

Table 3.2: VP7 indirect ELISA results and virus neutralizing antibody titers (vnts) of the pre-vaccination sera. Pre-vaccination sera of all 10 horses used in the experiment were assessed for AHSV antibodies (Ab) by indirect ELISA. The horse sera were assayed for neutralisation capability against AHSV 4, AHSV 5 and AHSV 8 and all horses were shown to be negative against all three serotypes tested.

Horse	iELISA - S/P %	vnt
Horse 1	Negative	Negative
Horse 2	Negative	Negative
Horse 3	83	Negative
Horse 4	34	Negative
Horse 5	Negative	Negative
Horse 6	35	Negative
Horse 7	39	Negative
Horse 8	44	Negative
Horse 9	Negative	Negative
Horse 10	Negative	Negative

3.3.2 Immunisation of horses

Plant-produced AHSV 4 and 5 VLPs used to vaccinate the horses in Groups 1 and 5, were prepared and purified by iodixanol discontinuous density gradient ultracentrifugation of crude plant lysates as described in Chapter 2 **(2.2.7).** Each of the horses in these two groups received ± 200µg adjuvanted AHSV VLPs (Figure 3.1).

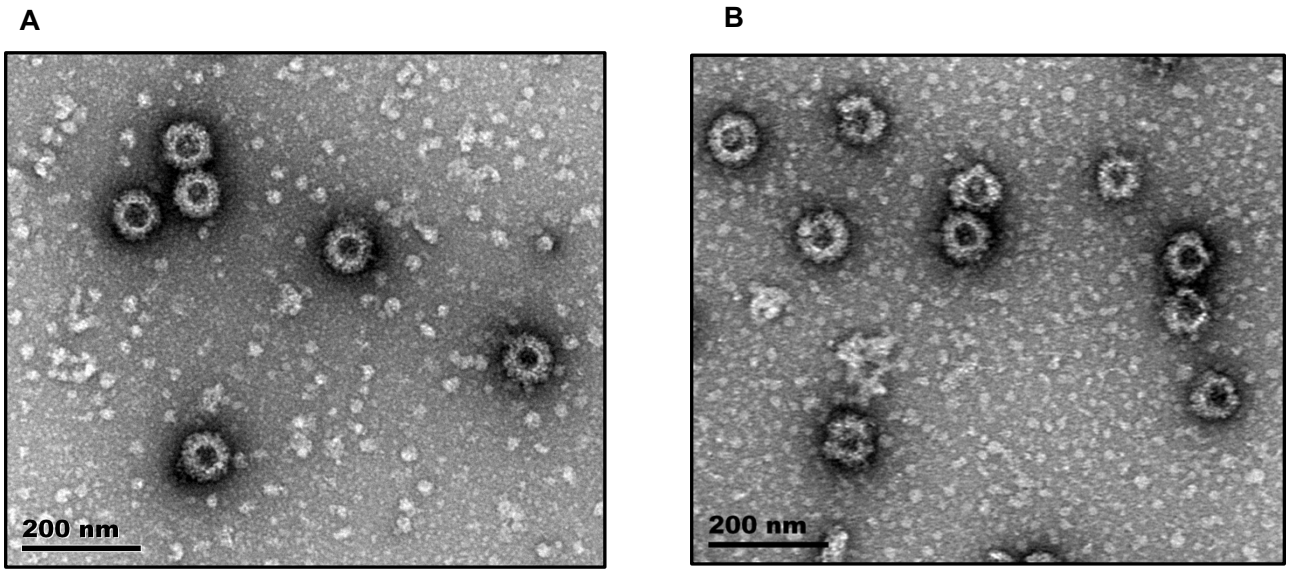

Figure 3.1: Plant-produced AHSV VLP vaccines. Electron-micrograph images of (A) iodixanol density gradient-purified AHSV 5 VLPs used to vaccinate horses 1 and 2 and (B) iodixanol density gradient-purified AHSV 4 VLPs used to vaccinate horses 9 and 10. The scale bar is 200 nm.

To make the method more scalable, by obviating the need to use the expensive equipment and reagents required for labour-intensive high-speed centrifugation, an alternative purification strategy was utilised to prepare the vaccine for the horses in Group 2. This method entailed purifying the crude AHSV 5-infiltrated plant lysate by a combination of depth- and tangential flow filtration (TFF). These filtered vaccine samples were prepared by M. O'Kennedy, D. Rutkowska and T. Tsekoa at the Council for Scientific and Industrial Research (CSIR) in Pretoria using the recombinant *Agrobacterium* constructs detailed in Chapter 2 (**2.2.2** and **2.2.3**).

With this strategy, leaves were homogenised using a bicine extraction buffer (pH 8.4) instead of 1 x PBS (pH 7.4) as using a higher pH buffer seemed to stabilise the assembled VLPs. To determine the particle concentration in the TFF-purified lysates, a sample was purified by iodixanol density gradient ultracentrifugation and quantified by gel densitometry (Figure 3.2).

The two horses in Group 2 each received ± 100 µg adjuvanted AHSV 5 VLPs prepared in this manner, a lower dose than that received by the horses in Groups 1 and 5 due to the inability to achieve an equivalently high concentration of VLPs in the allowed dose volume using this alternative purification method (Figure 3.3). Groups 3 and 4 were the control vaccinated horses, receiving either adjuvanted PBS or bicine buffer.

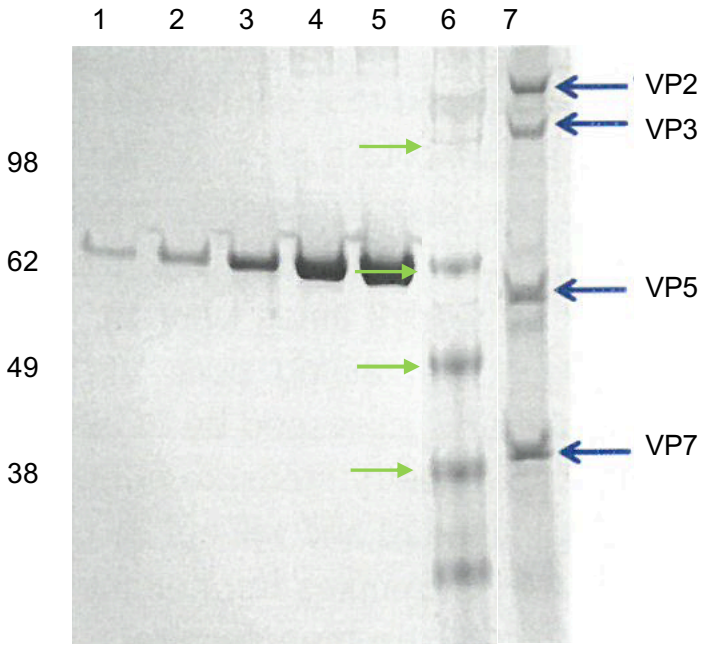

Figure 3.2: Quantification of AHSV 5 VLPs in TFF plant lysates by gel densitometry. For quantification purposes, filtered plant lysates were purified by iodixanol gradient centrifugation and gradient fraction 8 was separated by SDS-PAGE (lane 7). Quantification was achieved by visual comparison of the four capsid protein bands to known amounts of bovine serum albumin (BSA), 100 ng (lane 1), 200 ng (lane 2), 400 ng (lane 3), 800 ng (lane 4) and 1.6 ug (lane 5) run separately on the same SDS-PAGE gel. The location of the AHSV viral proteins VP2, VP3, VP5 and VP7 are indicated to the right of the gel, while sizes of molecular weight markers in lane 6 are shown to the left (green arrows).

Upon vaccination, both Group 2 horses (depth filtration preparation) developed slight neck stiffness in the region where the vaccine was administered, but this subsided after 2 days. This was most likely due to the rather crude nature of the filtered vaccine preparation, which was clear but olive green in colour. It was not possible to visualise the VLPs in the crude extract by TEM analysis, nor to see the constituent protein bands on an SDS-PAGE gel. The VLPs could only be observed following density gradient ultracentrifugation of a sample of the filtered VLP preparation. Besides the slight neck stiffness, no other side effects of the vaccinations were observed. Body temperatures were monitored daily and remained normal.

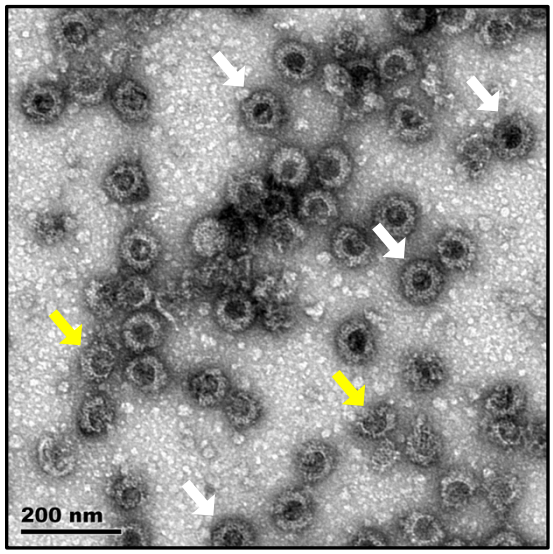

Figure 3.3: Electron-micrograph image of AHSV 5 VLPs prepared by iodixanol density gradient ultracentrifugation of TFF-purified plant lysates co-infiltrated with *Agrobacterium* AGL1 pEAQ recombinants for co-expression of the four AHSV 5 capsid proteins. The crude TFF lysates were used to vaccinate horses 3 and 4. Gradient fraction 8 (Figure 3.2) revealed the presence of fully assembled VLPs (white arrows) together with some assembly intermediates (yellow arrows). The scale bar is 200 nm.

On day 27, blood samples were drawn from all the horses in order to monitor the immune status after the primary vaccination. Immediately after bloods were drawn, the horses all then received a boost vaccination according to the same schedule described above. No side-effects were observed after the boost vaccination, even in the horses in Group 2, and the body temperatures of the horses continued to remain normal. On day 41, blood samples were again drawn for western blot analysis and virus neutralisation testing.

3.3.3 Plant-produced AHSV VLPs induce a strong immunogenic response in horses

Pre - (day 0) and post- (day 41) vaccination horse sera were used to probe a western blot of AHSV 4 and 5 VLPs used in the initial inoculations and separated by SDS-PAGE (Figure 3.4). Strong signals for VP2, VP3, VP5 and VP7 were detected by post-vaccination sera from all of the VLP-vaccinated horses (lanes 3, 5, 7, 9, 12 and 14) but not by the control-vaccinated horses (results not shown) nor by the pre-vaccination sera (lanes 2, 4, 6, 8, 11 and 13) from any of the horses.

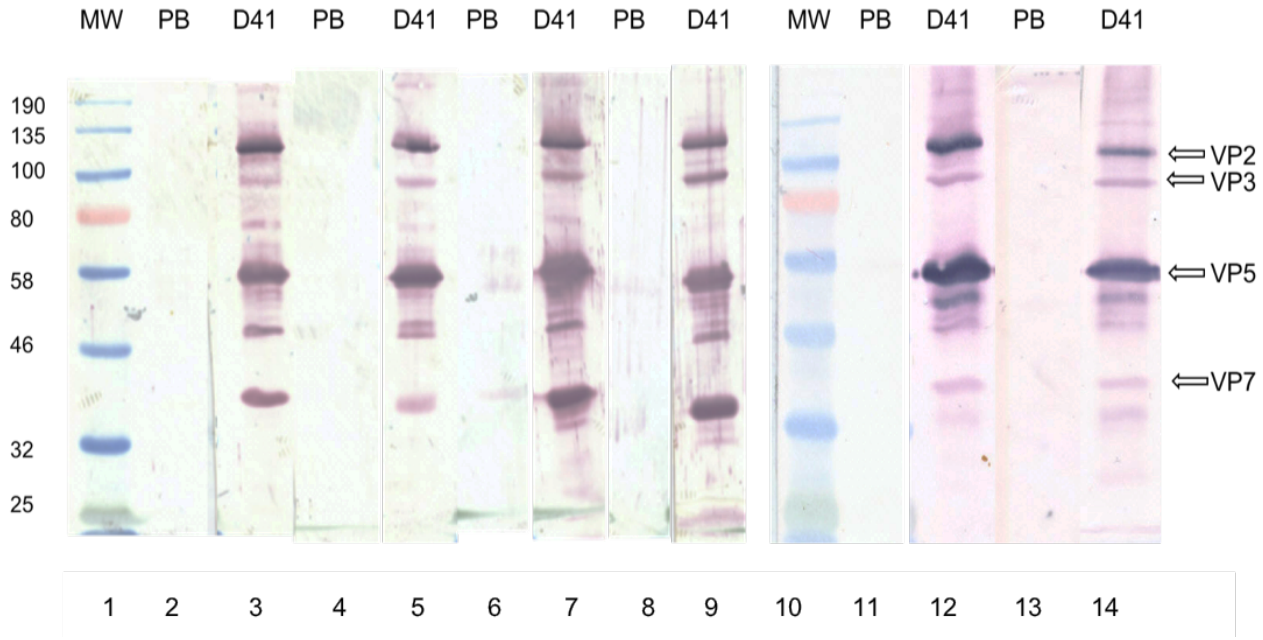

Figure 3.4: Western blot analysis of pre- and post- (day 41) vaccination antisera. Pre- and post- (day 41) vaccination antisera (1:5000 dilution) from horse 1 (lanes 2 and 3), horse 2 (lanes 4 and 5), horse 3 (lane 6 and 7), horse 4 (lanes 8 and 9), horse 9 (lanes 11 and 12) and horse 10 (lanes 13 and 14) were used to detect AHSV 5 (lanes 2 - 9) or AHSV 4 (lanes 11 - 14) VLP proteins in a standard western blot analysis. No AHSV proteins were detected in any of the pre-vaccination sera (PB) (lanes 2, 4, 6, 8, 11 and 13) but all four were detected in serum sampled at days 41 post vaccination (D41) (lanes 3, 5, 7, 9, 12 and 14). Protein bands of AHSV viral proteins VP2, VP3, VP5 and VP7 are indicated with arrows; colour pre-stained protein molecular weight marker (New England Biolabs, Massachusetts, USA) is shown in lanes 1 and 10.

3.3.4 Neutralisation assay with antiserum from horses immunised with plant-produced AHSV VLPs

Blood samples from all 10 horses (groups 1 to 5) were drawn again on days 69 and 97 post-vaccination and also on days 125, 153, 188, 225, 267 and 298 from the horses in groups 1 - 4. Sera from the 8 horses in groups 1 – 4 were thus monitored for a period of 42 weeks in total, while sera from the horses in group 5 were analysed for 14 weeks only, as these horses were vaccinated at a later time frame than the other 8 and further monitoring was precluded due to time constraints and the validity period of the ethics approval certificate.

Together with the pre-vaccination sera (day 0), all the serum samples drawn were analysed for virus neutralisation against AHSV 4, AHSV 5 and AHSV 8, as serological cross-protection has been shown *in vitro* between AHSV 5 and AHSV 8 (von Teichman *et al.* 2010). No cross-protection has been shown between AHSV 4 and any of the other serotypes.

The virus neutralisation results are detailed in Table 3.3 and graphically depicted in Figures 3.5.

Table 3.3: Virus neutralising antibody titers and VP7 iELISA scores of VLP-vaccinated and control horse sera. Pre- and post-vaccination sera were assayed for neutralisation capability against AHSV 4, AHSV 5 and AHSV 8. Sheep serum from animals vaccinated with live AHSV virus was used as a positive control. The pre- and post-vaccination iELISA S/P scores of sera sampled prior to vaccination and 41 days post-vaccination are shown in the right-hand column. High positive control sera pooled from vaccinated horses inoculated with live attenuated vaccine (bottle 1) obtained from OBP, was used as a positive control. A negative value (-) in the iELISA column indicates that measurements were not taken at those time points.

Horse	Immunogen	Day	AHSV 4	AHSV 5	AHSV 8	iELISA
Horse 1	AHSV 5	0	Negative	Negative	Negative	Negative
		27	Negative	1:56	1:40	-
		41	1:20	1:320	1:320	120
		69	1:20	1:224	1:224	-
		97	1:20	1:160	1:80	-
		125	1:10	1:160	1:160	-
		153	1:10	1:160	1:160	-
		188	Negative	1:112	1:80	-
		225	Negative	1:112	1:56	-
		267	Negative	1:56	1:28	-
		298	Negative	1:40	1:20	-
Horse 2	AHSV 5	0	Negative	Negative	Negative	Negative
		27	Negative	1:28	1:14	-
		41	Negative	1:320	1:224	97
		69	Negative	1:112	1:56	-
		97	Negative	1:112	1:40	-
		125	Negative	1:112	1:80	-
		153	Negative	1:56	1:80	-
		188	Negative	1:80	1:40	-
		225	Negative	1:80	1:40	-
		267	Negative	1:40	1:20	-
		298	Negative	1:40	1:20	-
Horse 3	AHSV 5	0	Negative	Negative	Negative	83
		27	1:80	1:20	1:28	-
		41	1:112	1:160	1:160	124
		69	1:112	1:56	1:224	-
		97	1:112	1:56	1:160	-
		125	1:56	1:80	1:160	-
		153	1:56	1:80	1:160	-
		188	1:40	1:56	1:56	-
		225	1:28	1:56	1:56	-
		267	1:20	Negative	1:28	-
		298	1:40	Negative	1:28	-
Horse 4	AHSV 5	0	Negative	Negative	Negative	34
		27	1:28	1:56	1:80	-
		41	1:112	1:160	1:224	122
		69	1:112	1:56	1:112	-
		97	1:56	1:56	1:112	-
		125	1:28	1:112	1:160	-
		153	1:28	1:80	1:160	-
		188	1:14	1:80	1:56	-
		225	1:10	1:28	1:40	-
		267	1:14	1:20	1:20	-
		298	1:28	Negative	1:20	-

(Cont. overleaf)

Horse 5	Nil	0	Negative	Negative	Negative	Negative
		27	Negative	Negative	Negative	-
		41	Negative	Negative	Negative	Negative
		69	Negative	Negative	Negative	-
		97	Negative	Negative	Negative	-
		125	Negative	Negative	Negative	-
		153	Negative	Negative	Negative	-
		188	Negative	Negative	Negative	-
		225	Negative	Negative	Negative	-
		267	Negative	Negative	Negative	-
		298	Negative	Negative	Negative	-
Horse 6	Nil	0	Negative	Negative	Negative	35
		27	Negative	Negative	Negative	-
		41	Negative	Negative	Negative	29
		69	Negative	Negative	Negative	-
		97	Negative	Negative	Negative	-
		125	Negative	Negative	Negative	-
		153	Negative	Negative	Negative	-
		188	Negative	Negative	Negative	-
		225	Negative	Negative	Negative	-
		267	Negative	Negative	Negative	-
		298	Negative	Negative	Negative	-
Horse 7	Nil	0	Negative	Negative	Negative	39
		27	Negative	Negative	Negative	-
		41	Negative	Negative	Negative	124
		69	Negative	Negative	Negative	-
		97	Negative	Negative	Negative	-
		125	Negative	Negative	1:40	-
		153	Negative	Negative	1:40	-
		188	Negative	Negative	1:10	-
		225	Negative	Negative	Negative	-
		267	Negative	Negative	Negative	-
		298	Negative	Negative	Negative	-
Horse 8	Nil	0	Negative	Negative	Negative	44
		27	Negative	Negative	Negative	-
		41	Negative	Negative	Negative	38
		69	Negative	Negative	Negative	-
		97	Negative	Negative	Negative	-
		125	Negative	Negative	1:20	-
		153	Negative	Negative	1:28	-
		188	Negative	Negative	1:10	-
		225	Negative	Negative	Negative	-
		267	Negative	Negative	Negative	-
		298	Negative	Negative	Negative	-
Horse 9	AHSV 4	0	Negative	Negative	Negative	Negative
		27	Negative	Negative	Negative	-
		41	1:320	1:10	Negative	96
		69	1:320	1:10	Negative	-
		97	1:224	Negative	Negative	-
Horse 10	AHSV 4	0	Negative	Negative	Negative	Negative
		27	Negative	Negative	Negative	-
		41	1:160	Negative	Negative	104
		69	1:160	Negative	Negative	-
		97	1:80	Negative	Negative	-
AHSV (+) control			>1:320	1:320	>1:320	-

A

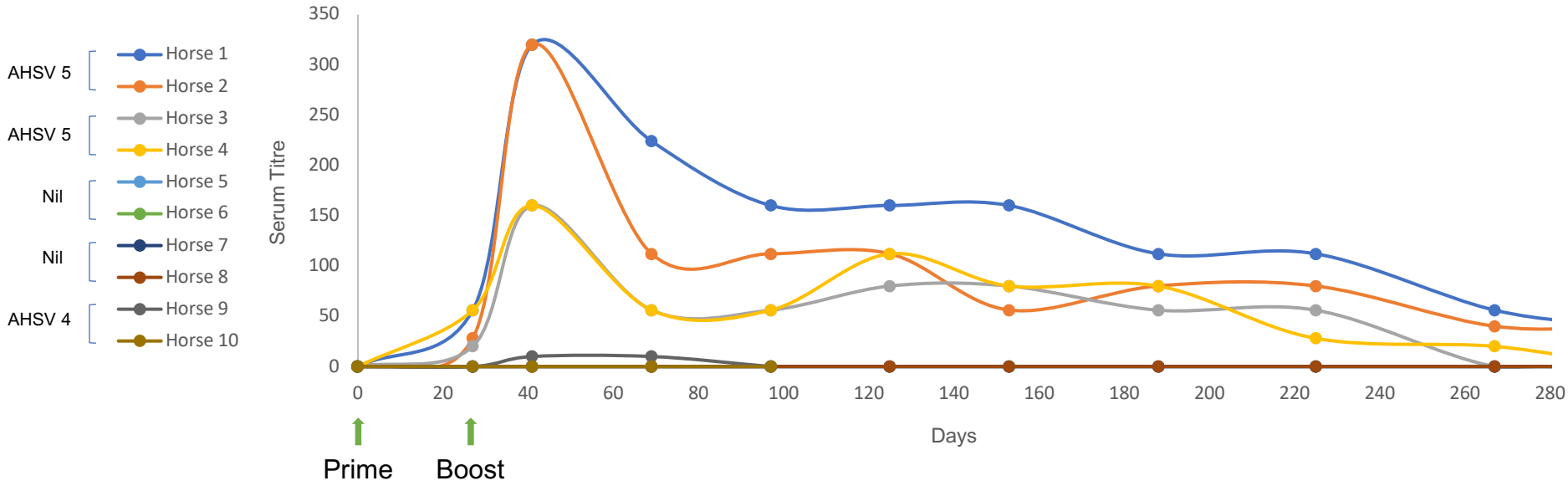

B

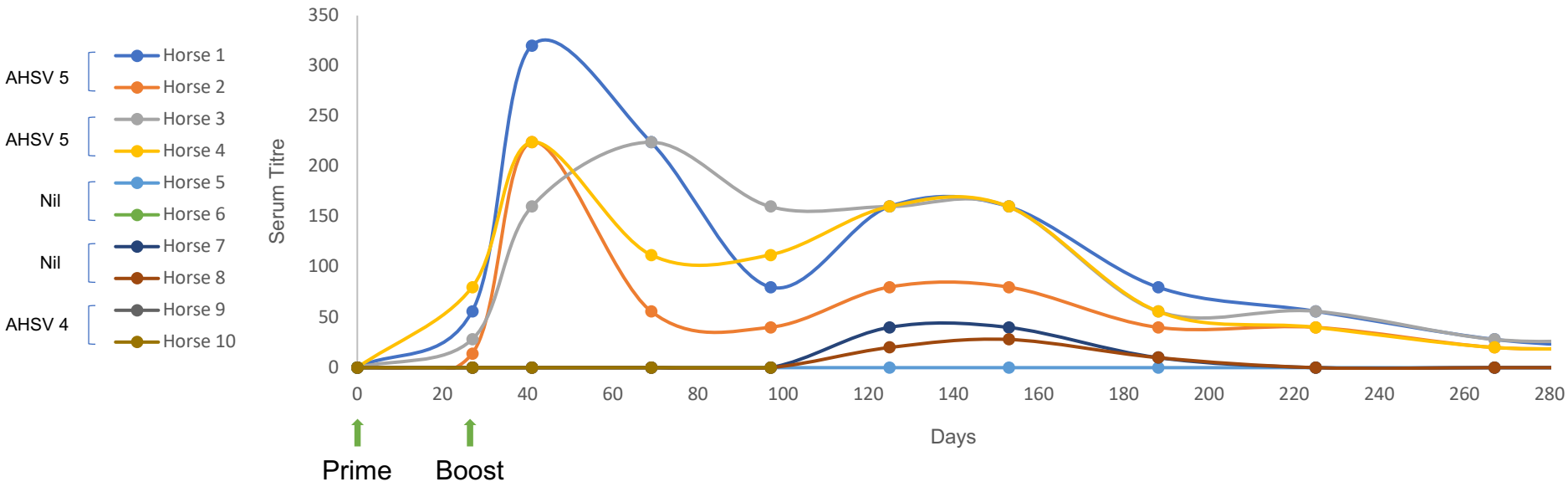

(Cont. overleaf)

C

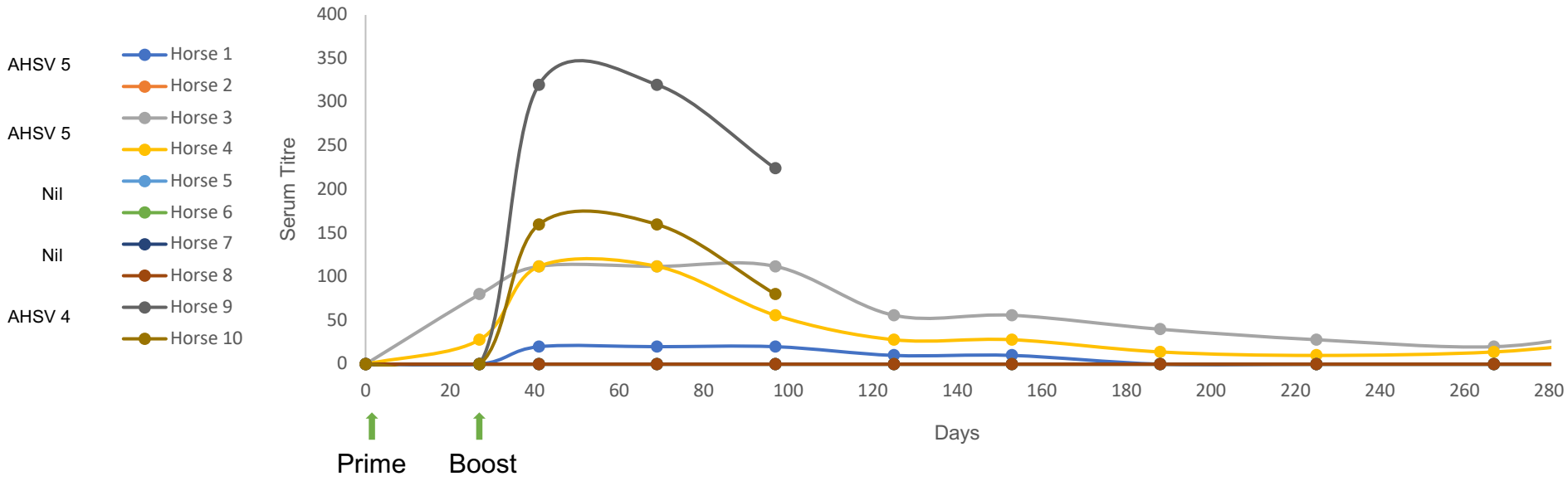

Figure 3.5: Virus neutralising antibody titers of AHSV 5 and 4 VLP-vaccinated and control horse sera against AHSV serotypes 4, 5 and 8. All horses were vaccinated on day 0 and received a boost vaccination on day 27. Pre- (day 0) and post- (days 27, 41, 69, 97, 125, 153, 188, 225, 267 and 298 in the case of the AHSV 5 VLP vaccine and days 27, 41, 69 and 97 in the case of the AHSV 4 VLP vaccine) virus neutralisation titres (vnt) against serotypes 5 (A), 8 (B) and 4 (C) for all VLP- and control vaccinated horses were determined. The vnt is taken as the dilution at which 50% of the cells are infected

All AHSV 5 VLP-vaccinated horse sera neutralised both AHSV 5 and AHSV 8 to titres of 1:160 – 1:320 (log10 2.2 – 2.5). Interestingly, neutralisation titres in serum from group 2 horses were notably lower than those from group 1 after the boost (Table 3.3). Furthermore, these sera also neutralised AHSV 4, although to a lesser extent.

Serum from the previously naïve horse 2 did not neutralise AHSV 4, although surprisingly, serum from horse 1, another horse naïve prior to vaccination, exhibited a low neutralisation titre (1:20 or $\log_{10}$ 1.3) against AHSV 4 after boosting (Figure 1C). Although none of the four control horse sera neutralised AHSV 5, there was a very low neutralisation response measured when tested against ASHV 8 by the control horses in group 4 (Figure 1B).

Analysis of sera drawn on day 69 indicated a drop in viral neutralisation titres in all four VLP-vaccinated horses against AHSV 5 and a subsequent plateauing effect for days 97 to 225 post vaccination. Interestingly, the vnt response against AHSV 4 in horses 3 and 4 which were not naïve prior to vaccination, plateaued for up to 97 and 69 days post boost vaccination, respectively before declining. In the case of AHSV 8, both horses had titres which plateaued at a value of 1:160 ($\log_{10}$ 2.2.).

The AHSV 4 VLP-vaccinated horse sera neutralised AHSV 4 to titres of 1:160 –1:320 (log10 2.2 – 2.5), the same range as observed for the AHSV 5 VLP vaccine. However, this maximum titre was maintained for a longer period of time in the AHSV 4 VLP-vaccinated horses in Group 5, as the titres only started falling after 10 weeks as opposed to 6 weeks, which was the case observed for the Group 1 and 2 horses. The AHSV positive control serum elicited a vnt of 1:320, indicating that the titres obtained for all the VLP-vaccinated horses were in the protective range.

3.4 Discussion

There is no cure for AHS, and vaccination remains the most effective means of resisting and controlling the disease. In spite of the fact that a large majority of horses in South Africa are vaccinated annually with the AHSV LAV, many horses still get infected and frequently succumb to the disease. Strict measures have been in place since 1997 to try to prevent the incidence of AHS in the Western Cape region of South Africa at least, but in recent years outbreaks have occurred regularly in both the surveillance and protection zones notably in 1999, 2004, 2006, 2011, 2013, 2014 and 2016 (Grewar *et al.* 2013; Weyer *et al.* 2013; Weyer *et al.* 2016; Grewar *et al.* 2018). Most of these outbreaks have been conclusively shown to have occurred as a result of re-assortment between and reversion to virulence of viruses within the LAV itself (Weyer *et al.* 2016), lending credence to the belief that the development of a new and safer vaccine alternative should be regarded as a matter of urgency and grave importance.

The investigation into the safety and immunogenicity of two plant-produced AHSV VLP vaccine candidates presented in this chapter yielded positive and exciting results. All six horses vaccinated with either the plant-produced AHSV 5 or 4 VLPs, seroconverted after two doses of the vaccine. The maximum viral neutralisation titre of 1:320 achieved for three of the naïve horses (horses 1, 2 and 9) is comparable to that generally obtained when inoculating horses with the AHSV LAV (Weyer *et al.* 2017) and the titre of 1:160 demonstrated for the fourth naïve horse (horse 10), also falls well within what is regarded as the acceptable range of protection.

The same lower neutralisation titre (1:160) was measured in the sera from horses 3 and 4. This is most likely due to the fact that, because of the lower concentration of VLPs in the allowed dose volume obtained using the alternative filtration strategy, these horses received half the dose that horses 1, 2, 9 and 10 received. Analysis of the results indicates that the vnt response in all the AHSV 5 VLP-vaccinated horses seemed to peak at two weeks post final vaccination before declining, which concurs with the findings of others (Manning *et al.* 2017; Weyer *et al.* 2017). However, it was interesting to note that the high vnt response was maintained for at least 6 weeks post final vaccination in the horses which were vaccinated with the AHSV 4 VLP vaccine, indicating perhaps that a variable response may be elicited by vaccination with different AHSV serotypes and some may be longer-lasting than others.

The unexpected yet low vnts against AHSV 4 observed for the previously naïve horse 1, together with the late vnt response against AHSV 8 in both control horses 7 and 8 after 125 and 153 days, suggests that a vnt less than 1:40 could be regarded as a cut-off titre when drawing any conclusions with regard to the protective efficacy of the AHSV vaccine. A minimum cut-off titre of 16 has been stated for the commercially available LAV and it is likely that protection of individual

horses will be effected by varying vnt titres (Crafford *et al.* 2014). This should be an important point of consideration when evaluating future potential AHSV vaccine candidates.

Overall, the virus neutralisation titres obtained indicate that the plant-produced AHSV 5 and 4 VLP vaccines may be at least as effective as the current LAV in protecting against AHSV 5 and 4, but without any of the associated risks of a live vaccine such as reversion to virulence or genetic re-assortment with field or vaccine strains. Furthermore, a similarly strong protective response against AHSV 8 was also elicited by the four horses vaccinated with the AHSV 5 VLP vaccine, confirming the cross-protection between these two AHSV serotypes.

Sera from horses which were vaccinated with the AHSV 5 VLPs prepared by depth and tangential flow filtration unexpectedly demonstrated strong neutralizing capability against AHSV 4. However, as could be seen from their positive iELISA scores prior to vaccination, they had obviously had some prior exposure to AHSV and it is possible that immunisation with the plant-produced VLPs boosted an earlier immune activation (one which would have included AHSV 8 and 4, but not AHSV 5 as the OBP LAV does not contain AHSV 5 (Weyer *et al.* 2017)) resulting in an anamnestic response to the non-cross-reactive serotype 4. These results are in agreement with those published by Manning *et al.* (2017), who demonstrated a similar immune boosting of an earlier vaccination with MVA VP2 (serotype 4) and MVA VP2 (serotype 9) when they subsequently vaccinated the same animals with the MVA VP2 (serotype 5) vaccine.

Aside from a transient local stiffness in the necks of the two horses that received the filtered plant extract, vaccination did not cause any adverse reactions, and all horses have remained healthy to date. These results demonstrate that the filtration strategy to purify the plant-produced AHSV 5 VLPs is potentially a cost-effective alternative to purification by high speed density gradient ultracentrifugation, which makes this vaccine platform even more attractive. Further efforts are currently being made to refine this technique to produce cleaner, more concentrated vaccine samples and also to test the long-term stability of preparations.

The results in this chapter indicate that the plant-produced AHSV VLP vaccine candidates are both safe and effective in eliciting a strong neutralizing antibody response in vaccinated horses. To determine the ultimate protective efficacy of these vaccines in the field, it will be necessary to conduct a challenge study outside of the AHS controlled region. Such a study should determine whether a high neutralizing antibody response is a sufficient correlate of protection to defend animals against infection and whether equal protection is afforded against cross-reactive serotypes and/or more than one serotype administered in the same vaccine.

C H A P T E R F O U R

INVESTIGATING THE POSSIBILITY OF A NOVEL MULTIVALENT AHSV VACCINE CANDIDATE

4.1 Introduction

To provide complete and effective protection against African horse sickness, it would be advantageous for a new vaccine to recognize and defend the host against all nine serotypes of the virus. Outer capsid protein VP2 is the most variable protein and contains the major neutralizing epitopes which elicit the serotype-specific immune response (Burrage *et al.* 1993; Stone-Marschat *et al.* 1996; Potgieter *et al.* 2003). Therefore, this protein, with particular emphasis on those sequences associated with virus neutralization, should be the main focus of any design aimed at the development of a multivalent AHSV vaccine candidate. Various research groups have conducted studies to identify the location of the antibody-binding epitopic regions on VP2 (Martinez-Torrecuadrada and Casal 1995; Bentley *et al.* 2000; Venter *et al.* 2000; Martinez-Torrecuadrada *et al.* 2001; Manole *et al.* 2012) and their data suggest that most of the neutralizing antibody sites are located towards the N-terminal region of the protein between amino acids 279 and 483.

This region is believed to comprise the VP2 tip domain (Chapter 1, Figure 1.8) and comprises the region with lowest degree of sequence identity between the different serotypes (Potgieter *et al.* 2003; Manole *et al.* 2012). Furthermore, amino acids 340 to 360 have been implicated in determining tissue tropism, and it has been hypothesized that amino acid changes in this region can confer virulence or attenuation, particularly as VP2 is believed to play a role in host cell entry and apoptosis (Potgieter *et al.* 2009). The nature of AHSV virulence is likely to be more complex than this, however, which is borne out by the fact that a high degree of variation in clinical severity is frequently observed within individual outbreaks (Weyer *et al.* 2016), and there is also no real evidence to suggest that any one serotype is more virulent than another.

Much attention has been focused on the development of recombinant AHSV VP2 proteins and investigating how best to utilize them to evoke a protective immune response in the animal host (Martinez-Torrecuadrada *et al.* 1996; Roy *et al.* 1996; Stone-Marschat *et al.* 1996; Guthrie *et al.* 2009; Alberca *et al.* 2014; Kanai *et al.* 2014; van de Water *et al.* 2015; Manning *et al.* 2017). Besides the expression, assembly and purification of VLPs composed only of the AHSV structural

proteins themselves, as described in the previous chapters, VLP technology can be further extended to include the surface presentation of an important viral antigen like VP2 on the surface of a heterologous display platform.

The antigenic moieties can either be chemically linked to the particle surface, or the coat protein (CP) that assembles to form the VLPs can be genetically modified to be a CP/antigen fusion protein, so that the chosen antigen is appropriately displayed on the surface of the assembled particle (Jennings and Bachmann 2008; Pushko *et al.* 2013). In this way, it is possible to display multiple copies of one or maybe even more antigens of interest on a carrier VLP for effective presentation to the host immune system, which has potential in the development of a multivalent AHSV vaccine.

Research on the use of recombinant VLPs as carriers of foreign antigens began around the mid-1980s, with hepatitis B surface and core antigen particles, tobacco mosaic virus (TMV) particles, yeast Ty VLPs and poliovirus particles all being shown to act as effective display platforms for attached antigens of interest (Valenzuela *et al.* 1985; Delpeyroux *et al.* 1986; Haynes *et al.* 1986; Adams *et al.* 1987; Clarke *et al.* 1987; Martin *et al.* 1988; Rutgers *et al.* 1988). For the purposes of this study, both TMV and *Acinetobacter* phage AP205 VLPs were investigated as potential carriers of AHSV 5 VP2 antigen (Haynes *et al.* 1986; Smith *et al.* 2009; Brune *et al.* 2016; Gasanova *et al.* 2016; Thrane *et al.* 2016; Lam and Steinmetz 2018).

TMV has a positive sense RNA genome which encodes four proteins, including the 17.5 kDa coat protein (CP), the sole component of the viral capsid (Turner *et al.* 1988; Gaddipati and Siegel 1990). The genome is enclosed by a rigid, rod-shaped structure ± 300nm in length and composed of approximately 2 130 of these CP subunits. This large number of subunit components was what first suggested that the TMV particle may be a suitable vaccine display platform for multiple heterologous antigens. Each CP subunit allows the insertion of a foreign epitope at either the N-terminus, the C-terminus, or in two surface-exposed loops corresponding to amino acids (aa) 59–65 and 152-156 (Smith *et al.* 2009; Gasanova *et al.* 2016). In initial studies, extensions or insertions of up to 20 aa were shown to be tolerated (Fitchen *et al.* 1995; Bendahmane *et al.* 1999), but more recently, the fusion of a 133-aa foreign peptide to the CP C-terminus of Turnip vein clearing virus (TVCV) via a flexible linker sequence, has also been reported (Werner *et al.* 2006).

A further interesting phenomenon with regard to TMV is the observation that heating TMV rods at a high temperature before cooling on ice, causes a conformational change resulting in the production of TMV spherical particles (SPs) (Atabekov *et al.* 2011; Bruckman *et al.* 2015; Trifonova *et al.* 2017). These SPs are uniquely able to non-specifically bind a variety of foreign proteins on

their surface and have also been shown to act as effective adjuvants, stimulating an immune response to the adsorbed antigens (Karpova *et al.* 2012; Nikitin *et al.* 2014).

Like TMV, *Acinetobacter* phage AP205 also has a positive sense RNA genome encoding four proteins. The isometric VLP is ± 23 nm in size and is formed from 180 copies of the 14 kD CP. The AP205 CP has both termini surface-exposed, which confers an increased and potentially advantageous tolerance for long N- and/or C-terminal fusions.

A novel conjugation system has recently been described which has been successfully implemented to couple a variety of pre-formed antigens produced in different expression systems to the surface of AP205 VLPs produced in *E. coli* (Brune *et al.* 2016; Thrane *et al.* 2016). This system makes use of two peptide sequences from the fibronectin-binding protein FbaB of the gram-positive bacterium *Streptococcus pyogenes.* The so-called SpyTag (ST) peptide (13 amino acids) interacts within minutes with its SpyCatcher (SC) peptide partner (116 amino acids) to form an irreversible highly stable isopeptide bond under a wide range of pH and temperature conditions. Fusion of either the SC or ST peptide to one of the coat protein termini of a suitable phage or viral carrier thus allows irreversible coupling with an antigen fused to the appropriate partner ST or SC peptide, and facilitates display of the antigen on the VLP surface (Figure 4.1).

This ST/SC coupling strategy was used by researchers in Denmark to construct a Spy VLP vaccine presenting the malaria transmission blocking antigen Pfs25, which when used to vaccinate mice successfully blocked malaria transmission to mosquitoes (Thrane *et al.* 2016). Furthermore, Spy VLP display also enabled breaking of tolerance against various self-antigens: mice that were prophylactically vaccinated with SC-HER2 displayed on ST AP205 VLPs were protected against a HER2-positive cancer challenge. In another study, it was shown that the level and quality of the vaccine-induced humoral response following vaccination with ST AP205 VLPs displaying the malaria circumsporozoite protein (CSP), was significantly increased compared to a control vaccine consisting of unconjugated soluble CSP and untagged AP205 VLPs (Janitzek *et al.* 2016).

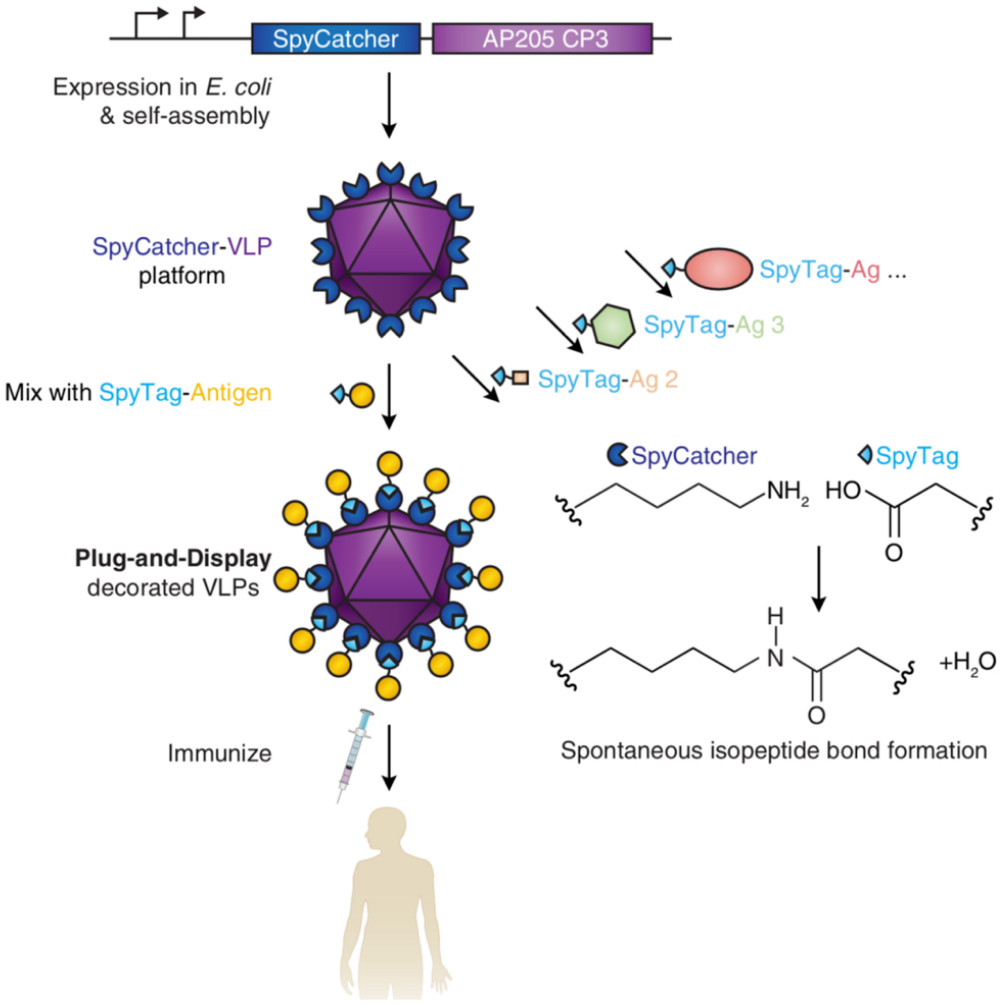

Figure 4.1: Schematic representation of SpyTag/SpyCatcher VLP technology. SpyCatcher (SC) is genetically fused to the AP205 phage coat protein (CP) and expressed in *E. coli* where SC-CP monomers self-assemple to generate VLPs. When mixed with a ST-antigen, a spontaneous isopeptide bond is formed with SC -VLPs, to produce decorated particles for immunization (Brune *et al.* 2016). *Image under the Creative Commons Attribution (CC-BY) license*

The success of the ST/SC technology reported in these and other studies (Brune *et al.* 2016; Singh *et al.* 2017; Palladini *et al.* 2018) is an indication that the use of a modular VLP conjugation approach may hold potential for the development of a multivalent VP2 AHSV vaccine. With this in mind, the plant-based expression system was used to produce so-called “Spy VLPs” for coupling to and display of a Spy-tagged AHSV 5 VP2 antigen. Such a vaccine, incorporating spy-tagged VP2 antigens from different AHSV serotypes, would potentially provide protection against all nine serotypes of the virus, and the investigation of the possibility of producing such antigens from both AP205 phage-derived VLPs and from recombinant TMV, forms the basis of the work presented in this chapter.

4.2 Materials and Methods

4.2.1 Design, synthesis and cloning of plant codon-optimized Spy genes

The *Acinetobacter* AP205 CP gene (GenBank Accession number NC_002700.2) was modified to contain either a ST or SC gene sequence (Brune *et al.* 2016) at the N-terminus. Constructs were designed to contain a flexible linker between the binding tag and the AP205 coat protein, namely GSGTAGGGSGS for ST AP205 and GGSGS for SC AP205 (Thrane *et al.* 2016). The native TMV CP gene (Goelet *et al.* 1982) (GenBank Accession number: V01408.1) was modified to contain the ST gene sequence at either the N- or C-terminus. For ST TMV, the ST was separated from the TMV CP N- terminus by the GSGTAGGGSGS linker sequence and the origin of assembly (OOA) sequence was included downstream from the CP gene. For TMV ST, the OOA sequence was included downstream from the ST sequence which was separated from the TMV CP C-terminus by the same linker.

The AHSV 5 VP2 consensus sequence was modified to contain either the ST or SC sequence on either the N- or the C-terminus. In each case, the Spy sequence was separated from the VP2 gene by a short glycine/serine linker (GGS), and a 6-x histidine (His) tag was added to the opposite terminus. The sequences were codon-optimized for expression in *N. benthamiana* and synthesized by GenScript Biotech Corporation (Nanjing, China) with flanking *AgeI* and *XhoI* restriction enzyme sites (Figure 4.2). The Spy-tagged genes were sub-cloned into the pEAQ plant expression vector and transformed into DH5-α *E. coli* cells (as in **2.2.2)** before being electroporated into *Agrobacterium AGL1* (as in **2.2.3)**.

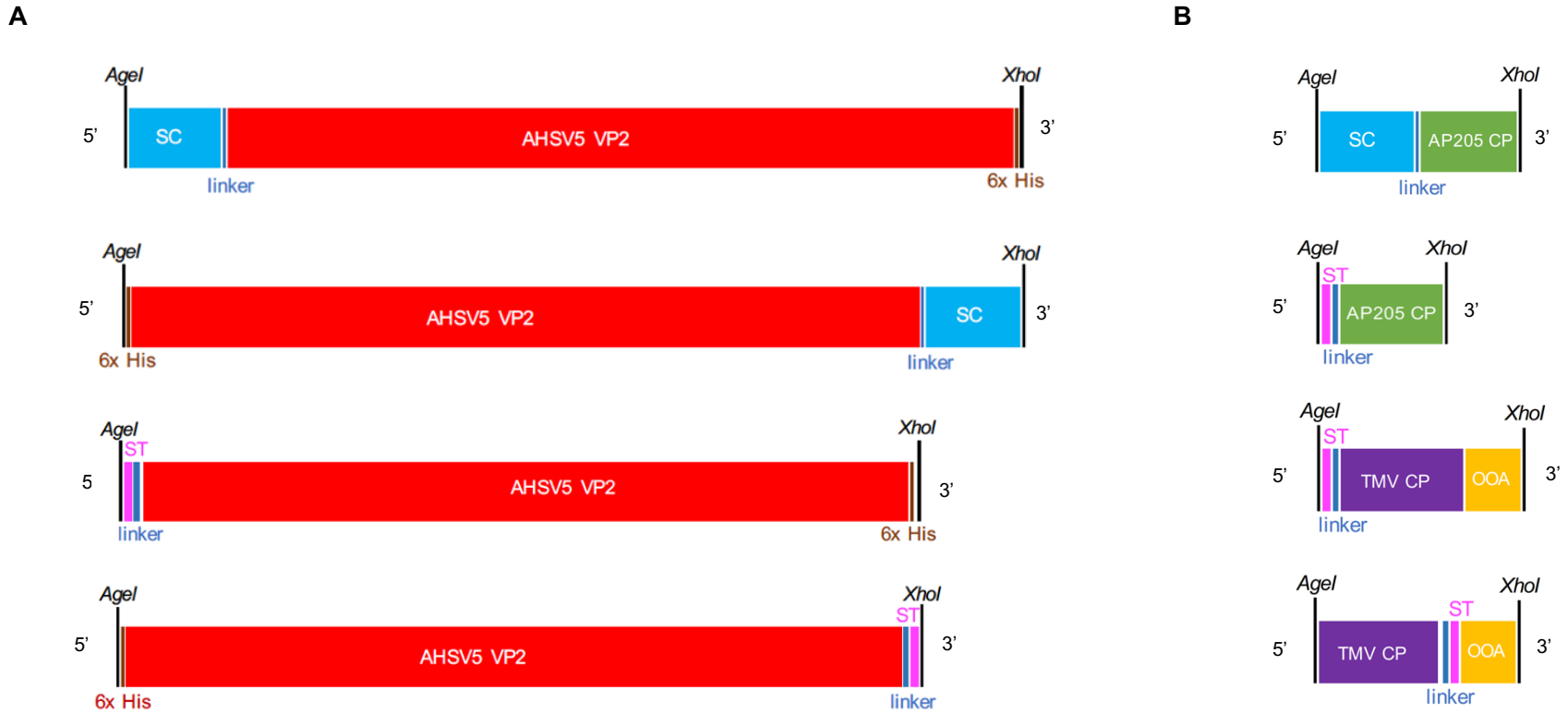

Figure 4.2: Schematic representation of the constructs created for *Agrobacterium*-mediated expression of Spy-tagged AHSV serotype 5 VP2 and Spy-tagged carrier VLPs in *N. benthamiana*. (A) Codon-optimized genes for AHSV-5 VP2 (red box) containing either the ST (pink box) or SC (turquoise box) peptide at either the 5' or 3' ends and separated from VP2 by a glycine/serine (GGS) linker sequence (blue box), were cloned into the pEAQ-HT plant expression vector (Sainsbury et al. 2009) and expressed in tobacco plants. All 4 VP2 constructs were synthesized with a 6 x His tag (brown box) at the opposite end to the ST or SC peptide. (B) Codon-optimized genes for the AP205 CP (green box) with either the SC or ST peptide at the 5' end and TMV CP (purple box) with ST peptide at either the 5' or 3' ends, were similarly cloned into pEAQ for plant-based expression. The OOA (orange box) was included downstream of the CP gene to facilitate assembly of the Spy-tagged TMV rod particles and the ST and SC peptides were separated from the CP genes by one of two different linker sequences (GSGTAGGGSGS or GGSGS)

4.2.2 Expression and purification of plant-produced Spy VLPs

4.2.2.1 Plant-based expression and purification of AP205 Spy VLPs

The AGL 1 recombinant ST- and SC AP205 CP strains were cultured and prepared for infiltration as described in **2.2.4.** The suspensions were diluted to either OD_{600} = 0.25 or 0.5 and used to infiltrate 15 - 30 five-week-old *N. benthamiana* plants by applying a vacuum of 100kPa. Plants were grown at 22 °C under 16 hrs / 8 hrs light / dark cycles until harvested.

The top 3 to 4 leaves of each plant were harvested at 3- 6 dpi and leaves were immediately homogenized in two volumes of PI buffer using a Moulinex™ juice extractor. The homogenized leaf pulp was re-incubated with the extracted juice and incubated at 4 °C for 1h with gentle shaking. Crude plant extracts were filtered through four layers of Miracloth™ (Merck, Darmstadt, Germany) and the filtrate was clarified by centrifugation at 13 000 rpm for 20 min at 4 °C.

ST and SC VLPs were purified by ultracentrifugation through discontinuous iodixanol density gradients. Iodixanol (Optiprep™; Sigma Aldrich, St Louis, MO, USA) solutions (23, 29 and 35 %) prepared in 1 x PBS pH 7.4, were used to create a 7 mL step gradient (2, 3 and 2 mL of each gradient solution respectively) under 30 mL clarified plant extract and centrifuged at 32 000 rpm for 2 h at 4 °C in an SW32 Ti rotor (Beckman, Brea, CA). Fractions of 500 µL were collected from the bottom of the tubes and 50 µL of each fraction was electrophoresed through 10% SDS-polyacrylamide gels, followed by Coomassie blue staining. Samples from the fractions were also analysed by western blot using AP205 antiserum (a kind gift from C. Janitzek, Centre for Medical Parasitology (CMP), University of Copenhagen, Denmark) diluted (1:600) in blocking buffer and imaged by TEM (as in **2.2.5** and **2.2.8)**. VLPs were quantified by gel densitometry (as in **2.2.9).**

4.2.2.2 Plant-based expression and purification of TMV Spy VLPs

The AGL 1 recombinant ST TMV and TMV ST strains were cultured and used to infiltrate *N. benthamiana* plants as described above (**4.2.2.1).** The suspensions were diluted to either OD_{600} = 0.25 or 0.5 and the top 3 to 4 leaves of each plant were harvested at 3 - 6 dpi. Crude plant lysates were clarified by centrifugation at 13 000 rpm for 20 min at 4 °C and TMV Spy VLPs were allowed to precipitate O/N at 4 °C by the addition of 4 % Polyethylene glycol (PEG) 6000 (Sigma Aldrich, St Louis, MO, USA) and 4 % NaCl. The VLPs were pelleted by centrifugation at 4 °C for 10 min at 10 000 rpm and resuspended in 1/10th volume Dulbecco's PBS (Sigma Aldrich, St Louis, MO, USA). They were precipitated a second time with 4 % PEG/NaCl for 6 h at 4 °C followed by centrifugation at 10 000 rpm for 10 min and 4 °C. The TMV Spy VLP pellet was resuspended in ½ volume 1 x Dulbecco's PBS and 50 µL samples were analysed by SDS-PAGE followed by

Coomassie blue staining. Samples were also analysed by western blot using TMV antiserum diluted (1: 5000) in blocking buffer and imaged by TEM (as in **2.2.5** and **2.2.8)**.

4.2.3 Expression and purification of Spy AHSV 5 VP2 proteins

The AGL 1 recombinant Spy-tagged AHSV 5 VP2 strains were cultured and used to infiltrate *N. benthamiana* plants as described above (**4.2.2.1).** The suspensions were diluted to either OD_{600} = 0.25 or 0.5 and the top 3 to 4 leaves of each plant were harvested at 3- 6 dpi. Crude plant lysates were clarified by centrifugation at 13 000 rpm for 20 min at 4 °C and Spy-tagged AHSV 5 VP2 was purified by ammonium sulphate $(NH_4)_2SO_4$ precipitation (20 - 80% in 20% incrementing steps). The amount of solid $(NH_4)_2SO_4$ required was calculated using the online tool at: https://www.encorbio.com/protocols/AM-SO4-new.htm. In each case, protein was precipitated at 4 °C for 30 min followed by centrifugation at 13 000 rpm for 20 min at 4 °C. Protein pellets were resuspended in 1/6th volume Dulbecco's PBS and dialysed O/N against 1 x PBS at 4 °C. Samples were analysed by Western blot using AHSV 5 antiserum diluted (1: 5000) in blocking buffer (as in **2.2.5)**.

4.2.4 Coupling of AHSV 5 VP2 Spy antigen to AP205 VLPs

To investigate coupling of AHSV 5 VP2-ST to both plant- and *E. coli* produced SC AP205 VLPs, the Spy VLPs and dialysed Spy-tagged VP2 antigen were incubated overnight at 4 °C at 5 different VLP:antigen ratios - 1:1.5, 1:5, 1:10, 1:20 and 1:40 in 400 µL reaction volumes. Samples (50 µL) from each reaction were centrifuged at 13 000 rpm for 5 min in a benchtop microfuge to eliminate any protein aggregates. Both spun and unspun samples were analysed by western blot using AHSV 5 antiserum diluted (1: 5000) in blocking buffer (as in **2.2.5).**

4.2.5 Thermal transition of native TMV and TMV Spy VLPs into spherical nanoparticles

The transition of wild-type TMV (purified from TMV-infected cowpea plants in 1978 by E. Rybicki) and Spy-tagged TMV rods into spherical VLPs was investigated by heating samples (50 µL) of each for 2 min at 96 °C and then cooling on ice for 10 sec. Glow-discharged copper grids (mesh size 200) were floated on 20 µL heated or unheated samples for 5 min and then washed successively by floating on three drops of sterile water. The grids were not stained but imaged directly by TEM.

4.2.6 Expression and purification of AP205 Spy VLPs in *E. coli*

Recombinant *E. coli* expression plasmids containing a cloned copy of either the SC AP205 or the ST AP205 CP gene in pET15c, were a kind gift from C. Janitzek, Centre for Medical Parasitology, Denmark. These plasmids were used to transform BL21 chemically competent *E. coli* (New England Biolabs, Ipswich, MA) following the method described by Sambrook *et al.* (1989). Transformed cells were selected on Luria Bertani (LB) media plates supplemented with ampicillin (100 µg/mL) and chloramphenicol (100) by incubation for 16 hrs at 37 °C.

Starter cultures of the recombinant AP205 *E. coli* strains were prepared by inoculating 10mL LB supplemented with 100 µg/mL ampicillin and 100 µg/mL chloramphenicol with 1 mL glycerol stocks and grown by incubating with agitation for 16 hrs at 37 °C. These starter cultures were used to inoculate 1 L of LB supplemented with 100 µg/mL ampicillin and 100 µg/mL chloramphenicol and grown at 37 °C with agitation until they reached an OD_{600} = 0.6. Protein expression was induced with 1 mM Isopropyl β-D-1-thiogalactopyranoside (IPTG, Sigma Aldrich, St Louis, MO, USA) for 4 h at 30 °C with gentle shaking and cells were harvested by centrifugation at 13 000 rpm for 10 min at 4 °C in a JA14 rotor (Beckman, Brea, CA).

The cell pellet was resuspended in 1/25th volume of sodium phosphate buffer (0.3 M NaCl, 50 mM Na_2HPO_4 pH 7.2) and cells were lysed by addition of 1 mg/ mL lysozyme (ThermoFisher Scientific, Waltham, MA, USA) and sonication at 80% power with 3 pulsations for 90 sec each on ice. Lysates were clarified by centrifugation at 13 000 rpm for 10 min at 4 °C and ST and SC AP205 VLPs were purified by ultracentrifugation through discontinuous iodixanol density gradients. Iodixanol solutions (23, 29 and 35 %) prepared in 1 x PBS pH 7.4, were used to create a 2.25 mL step gradient (750 µL of each gradient) under 3.75 mL clarified plant extract and centrifuged at 44 000 rpm for 6 h and 16 °C in an SW55 Ti rotor (Beckman, Brea, CA). Fractions of 500 µL were collected from the bottom of the tubes and 50 µL of each fraction was analysed by SDS-PAGE followed by Coomassie blue staining. Samples from the fractions were analysed by western blot using AP205 antiserum diluted 1:600 in blocking buffer and imaged by TEM (as in **2.2.5** and **2.2.8)**.

4.2.7 Coupling of SC to ST AP205 or TMV ST VLPs

Coupling of a SC antigen to both plant-produced ST AP205 and TMV ST VLPs was tested as described (**4.2.5.1**) by C. Janitzek at CMP, Denmark due to the unsuccessful expression of a SC-conjugated AHSV 5 VP2 antigen.

4.3 Results

4.3.1 Design, synthesis and cloning of plant codon-optimised Spy genes

4.3.1.1 Spy AP205

To determine whether *Acinetobacter* phage AP205 VLPs displaying either a ST or SC peptide on the particle surface could be produced within individual *N. benthamiana* plants, recombinant plasmids were constructed containing the AP205 coat protein gene modified by the addition of a ST or SC gene sequence at the N-terminus. The constructs were sub-cloned into the multiple cloning site of the pEAQ-*HT*^{TM} plant expression vector to produce pEAQ-ST AP205 and pEAQ-SC AP205. Successful cloning of the Spy AP205 CP genes was demonstrated by colony PCR (Figure 4.3 A & B). PCR amplification using the pEAQ primer set, resulted in bands of ± 690 bp (420 bp +270 bp vector sequence) and ±1 kb (770 bp + 270 bp vector sequence) representing the correct sizes of the ST AP205 CP and SC AP205 CP genes respectively. The tagged AP205 pEAQ constructs were electroporated into *Agrobacterium* AGL 1 (pEAQ - ST AP205/AGL and pEAQ - SC AP205/AGL) and successful transformations were again confirmed by colony PCR (Figure 4.3 C).

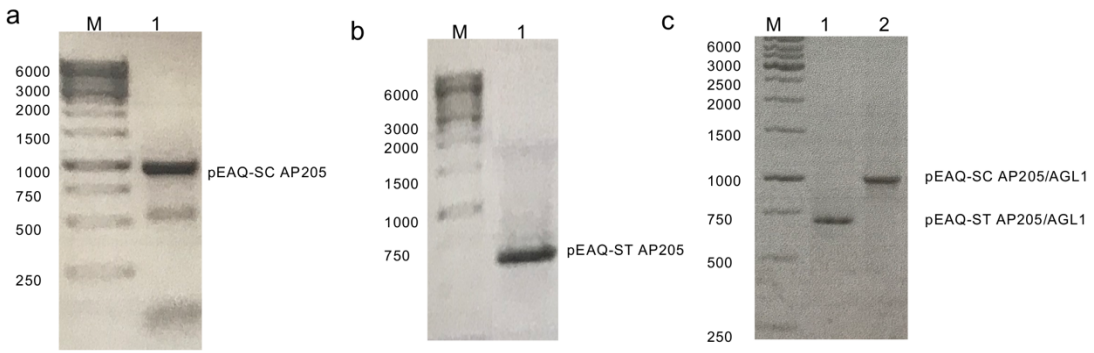

Figure 4.3: Verification of recombinant Spy AP205 strains. Colony PCR amplification using the pEAQ vector-specific primer set was used to verify the successful cloning of the ST AP205 and SC AP205 coat protein (CP) genes and transformation of *E. coli* (A & B) and *Agrobacterium* AGL 1 (C). PCR of the Spy AP205 recombinants amplified a ±1 kb (770 bp + 270 bp vector sequence) fragment (A, lane 1 & C, lane 2) for SC AP205 CP and a ± 690 kb (770 bp + 270 bp vector sequence) fragment for ST AP205 (B, lane 1 & C, lane 1). The molecular weight markers are indicated adjacent to each gel.

4.3.1.2 Spy TMV

To determine whether TMV Spy VLP rods could self-assemble in *N. benthamiana* plants, Spy-tagged versions of the TMV CP gene with the ST sequence on either the N- or C- terminus were constructed with flanking *Age I* and *Xho I* restriction enzyme sites and sub-cloned into the pEAQ expression vector to produce pEAQ-ST TMV and pEAQ-TMV ST. Successful cloning of the Spy TMV CP gene was demonstrated by colony PCR and amplification using the pEAQ primer set and resulted in a band of ± 1 kb (777 bp +270 bp vector sequence) representing the correct size of both Spy-tagged TMV CP/OOA sequences (Figure 4.4). The tagged TMV pEAQ constructs were electroporated into *Agrobacterium* AGL 1 (pEAQ-ST TMV/AGL and pEAQ-TMV ST/AGL) and successful transformations were again confirmed by colony PCR.

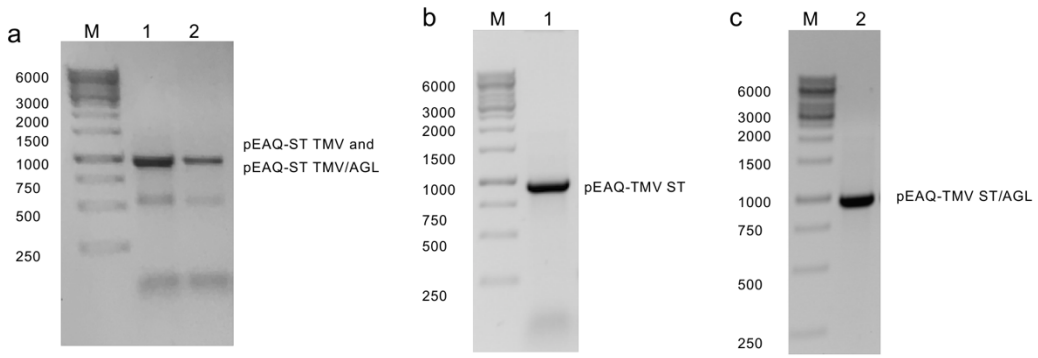

Figure 4.4: Verification of the recombinant Spy TMV strains. Colony PCR amplification using the pEAQ vector-specific primer set was used to verify the successful cloning of the ST TMV CP/OOA and TMV ST CP/OOA genes and transformation of *E. coli* (A & B, lane 1) and *Agrobacterium* AGL1 (A & C, lane 2). PCR of the Spy TMV recombinants amplified a ±1 kb (777 bp +270 bp vector sequence) fragment in each case. The molecular weight markers are indicated adjacent to each gel.

4.3.1.3 AHSV 5 Spy VP2

To facilitate display of the AHSV 5 VP2 antigen on the surface of the AP205 or TMV Spy VLPs, the VP2 gene was modified to contain the ST or SC sequence on either the N- or the C-terminus. The genes were synthesized with flanking *Age I* and *Xho I* restriction enzyme sites and sub-cloned into the pEAQ expression vector to produce pEAQ-ST VP2, pEAQ-VP2 ST, pEAQ-SC VP2 and pEAQ-VP2 SC. In each case, the Spy sequence was separated from the VP2 gene by a short glycine/serine linker and a 6 x His tag was added to the opposite gene terminus. Successful cloning of the Spy VP2 genes was demonstrated by colony PCR and amplification using the pEAQ primer set resulted in bands of ± 3.8 kb (3.5 kb + 270 bp vector sequence) or ± 3.5 kb (3.2 kb + 270 bp vector sequence) representing the correct sizes of the SC VP2 or the ST VP2 constructs respectively (Figure 4.5). The tagged VP2 constructs were electroporated into *Agrobacterium*

AGL 1 (pEAQ-ST VP2/AGL, pEAQ-VP2 ST/AGL, pEAQ-SC VP2/AGL and pEAQ-VP2 SC/AGL) and successful transformations were again confirmed by colony PCR.

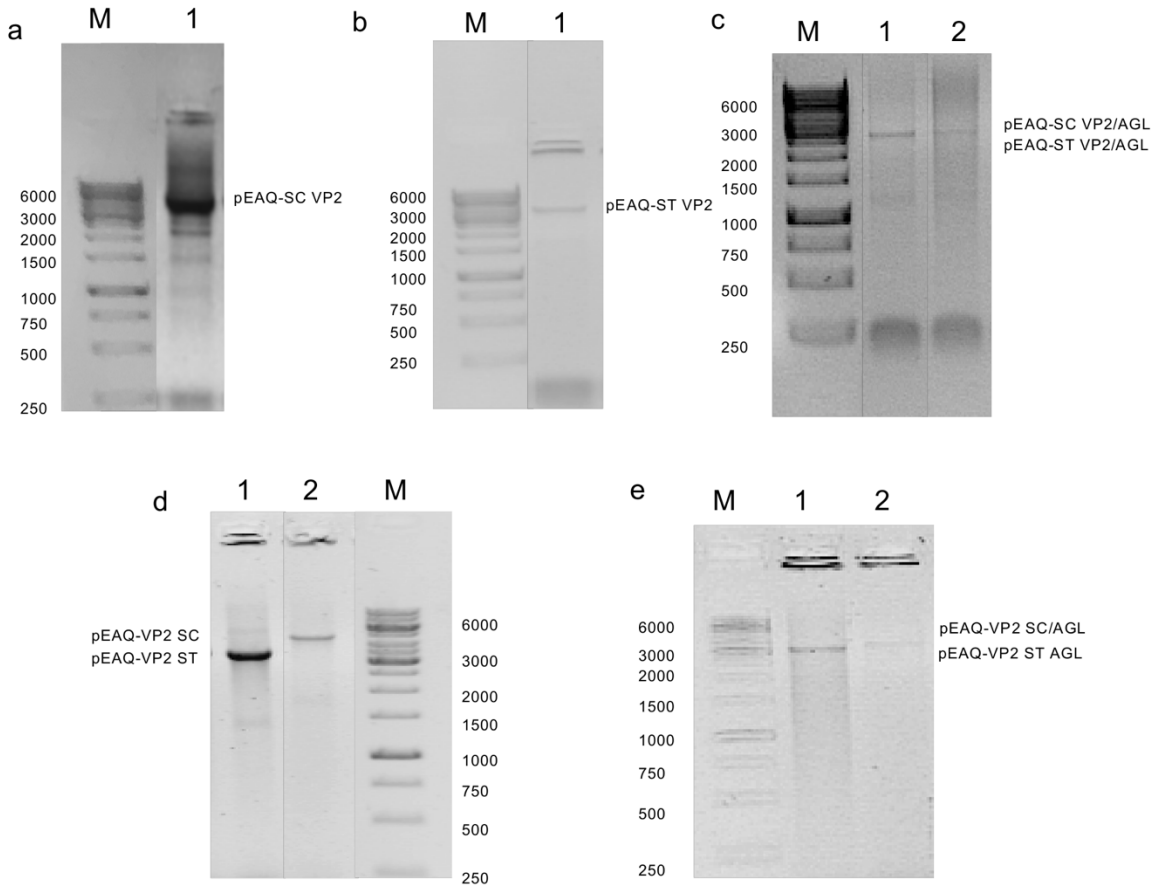

Figure 4.5: Verification of the recombinant AHSV 5 Spy VP2 strains. Colony PCR amplification using the pEAQ vector-specific primer set was used to verify the successful cloning of the ST VP2, VP2 ST, SC VP2 and VP2 SC genes and transformation of E. coli (A, B & D, lanes 1 & 2) and *Agrobacterium* AGL 1 (C & E, lanes1 & 2). PCR of the Spy VP2 recombinants amplified a ± 3.8 kb (3.5 kb +270 bp vector sequence) fragment or a ± 3.5 kb (3.2 kb +270 bp vector sequence) fragment in each case. The molecular weight markers are indicated adjacent to each gel.

4.3.2 Expression and purification of Spy VLPs

4.3.2.1 ST and SC AP205

Transient expression and assembly of the AP205 Spy VLPs in *N. benthamiana* was investigated by vacuum-infiltrating whole plants with either *Agrobacterium* recombinant pEAQ-ST AP205/AGL or pEAQ-SC AP205/AGL. Due to the unavailability of a suitable antiserum to test expression of the AP205 CP in crude leaf extracts, it was not possible to do a small-scale investigation and instead, putative AP205 Spy VLPs were purified directly by iodixanol density gradient ultracentrifugation. Expression of Spy-AP205 coat proteins was confirmed by SDS-PAGE analysis

of fractions collected following density gradient ultracentrifugation. A protein band of the expected size for ST AP205 CP (±16.5 kD) was observed in fractions across the gradient (Figure 4.6A, lanes 1 - 4) while the protein band for SC AP205 CP (±27 kD) was less apparent (Figure 4.6B). Spontaneous self-assembly of each AP205 Spy VLP was evaluated by TEM which revealed particles with an estimated size of ±28 nm for ST AP205 VLPs (Figure 4.6 C) and ±34 nm for SC AP205 VLPs (Figure 4.6 D).

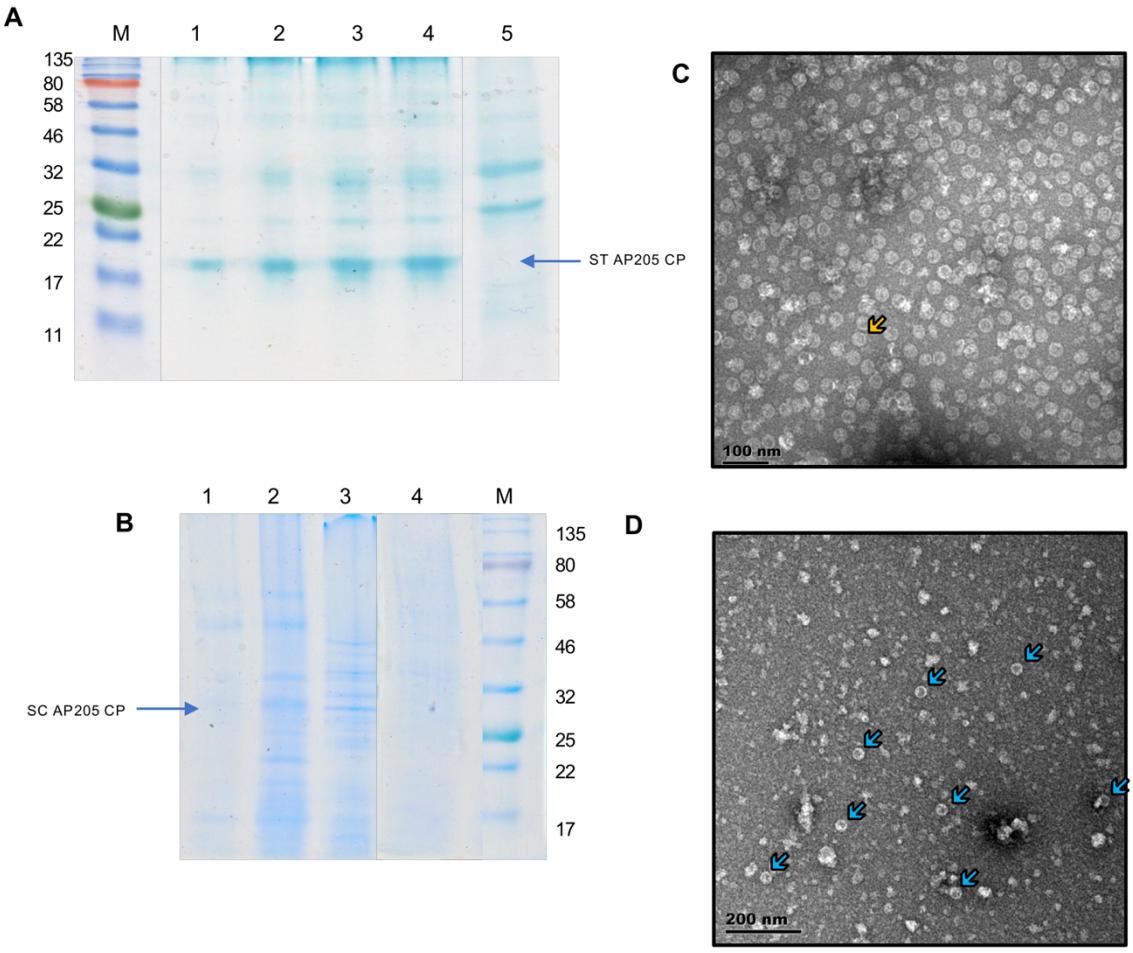

Figure: 4.6: Purification of AP205 Spy VLPs. Crude homogenates from plants 6 days after infiltration with either ST AP205 (A) or SC AP205 (B) recombinants, were subjected to iodixanol density gradient ultra-centrifugation and fractions 2 - 5 (A & B, lanes 1 - 4) were separated by denaturing SDS-PAGE followed by Coomassie blue staining. Crude extract from leaves infiltrated with *Agrobacterium* transformed with pEAQ-*HT* expression vector lacking any goi, was used as a negative control (lane 5). In each case gradient fraction 2 (cleanest fraction) was imaged by TEM and revealed the presence of SpyTag - (C, orange arrow) or SpyCatcher (D, cyan arrows) AP205 VLPs respectively. Scale bars: 100nm - 200nm.

Subsequently, a small aliquot of AP205 antiserum was received from C. Janitzek, (CMP, Denmark) and this was used in an attempt to optimize the expression of the Spy-tagged AP205 CP by syringe infiltrating leaves at two different OD_{600} concentrations and testing expression at 3 - 6 dpi. Western blot analysis using this antiserum (1:600) detected a protein band of the correct ±27 kD size for

SC AP205 CP in crude plant extracts, with expression being best on day 4 at an OD_{600} = 0.25 (Figure 4.7 A). The additional ±58kD and ±17kD bands detected on the blot may possibly represent a SC AP205 CP dimer and a CP monomer which has lost the SC peptide, respectively.

In a later western blot experiment, using the infiltration criteria shown to be optimal for SC AP205 CP expression, a protein species of the expected ±16.5 kD size of ST AP205 CP was detected using the anti-AP205 serum (Figure 4.7 B).

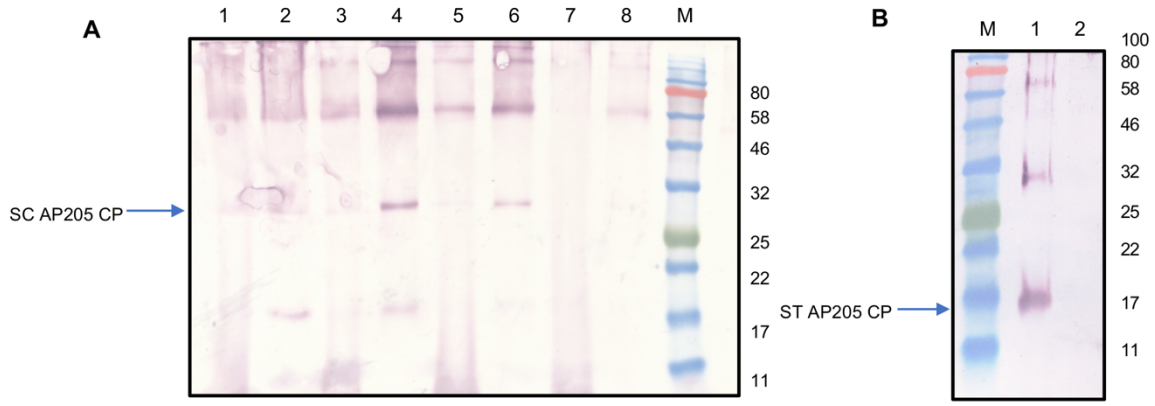

Figure: 4.7: Optimization of plant-based expression of recombinant Spy-tagged AP205 coat proteins. Western blot analysis of crude leaf extracts obtained 3 (A, lanes 1 & 2), 4 (A, lanes 3 & 4), 5 (A, lanes 5 & 6) and 6 (A, lanes 7 & 8) days after plants were infiltrated with *Agrobacterium* AGL1 containing pEAQ-SC AP205 at an OD_{600}=0.25 (lanes 2, 4 ,6 & 8) or at an OD_{600}=0.5 (lanes 1, 3 ,5 & 7). Analysis of crude leaf extracts from plants infiltrated with the pEAQ-ST AP205 recombinant at OD_{600}=0.25 and harvested 4 dpi (B, lane 1). Crude extract from leaves infiltrated with *Agrobacterium* transformed with pEAQ-*HT* expression vector lacking any goi, was used as a negative control (B, lane 2). Anti AP205 serum (1:600) was used as the primary antibody. Colour pre-stained protein standard, broad range, indicated adjacent to the blots, was used as a molecular weight marker.

4.3.2.2 Spy-tagged TMV

TMV virion assembly has been shown to initiate by the binding of a two-layer protein disc, consisting of 34 CP monomers, to the origin of assembly (OOA) sequence in viral genomic ssRNA (Fraenkel-Conrat and Williams 1955; Turner *et al.* 1988). The latter is a specific region of the viral RNA 75 bp in length situated about 1kb from its 3' end (Goelet *et al.* 1982). Thereafter, protein subunit discs are added sequentially to the growing rod with assembly proceeding bidirectionally, although elongation towards the 5' end is believed to occur more rapidly and prior to that in the 3' direction (Gaddipati and Siegel 1990). As it lengthens, the growing rod encapsidates the viral RNA, interacting with 3 nucleotides for every CP monomer (Turner *et al.* 1988). However, it has been shown that, provided it contains the OOA sequence, essentially any RNA molecule can be encapsidated by the TMV CP, which has interesting potential for the design of TMV VLP rods that can act as carrier molecules for antigens of interest (Smith *et al.* 2007; Maharaj *et al.* 2014; Zhou

et al. 2015; Gasanova *et al.* 2016). This strategy was employed to synthesize TMV VLPs displaying ST peptides on the particle surface for binding to and presentation of AHSV 5 VP2 antigen.

Small-scale transient expression of the Spy-tagged TMV coat protein genes was tested first. Five leaves of each *N. benthamiana* plant were syringe-infiltrated with *Agrobacterium* strains carrying either ST TMV or TMV ST constructs. Three leaf discs were clipped per expression test using an Eppendorf vial lid and extracted 6 days post-infiltration (dpi) when the leaves were chlorotic but had no signs of necrosis. These crude extracts were imaged by TEM and typical TMV rod-shaped structures were observed for TMV ST but not for ST TMV (Figure 4.8, A & B). Therefore, expression of TMV-ST only was optimized by infiltrating at two different OD_{600} concentrations and testing expression at 3 - 6 dpi. Western blot analysis using antiserum against wild-type TMV was used to detect the presence of the TMV ST CP in crude plant extracts (Figure 4.8 C).

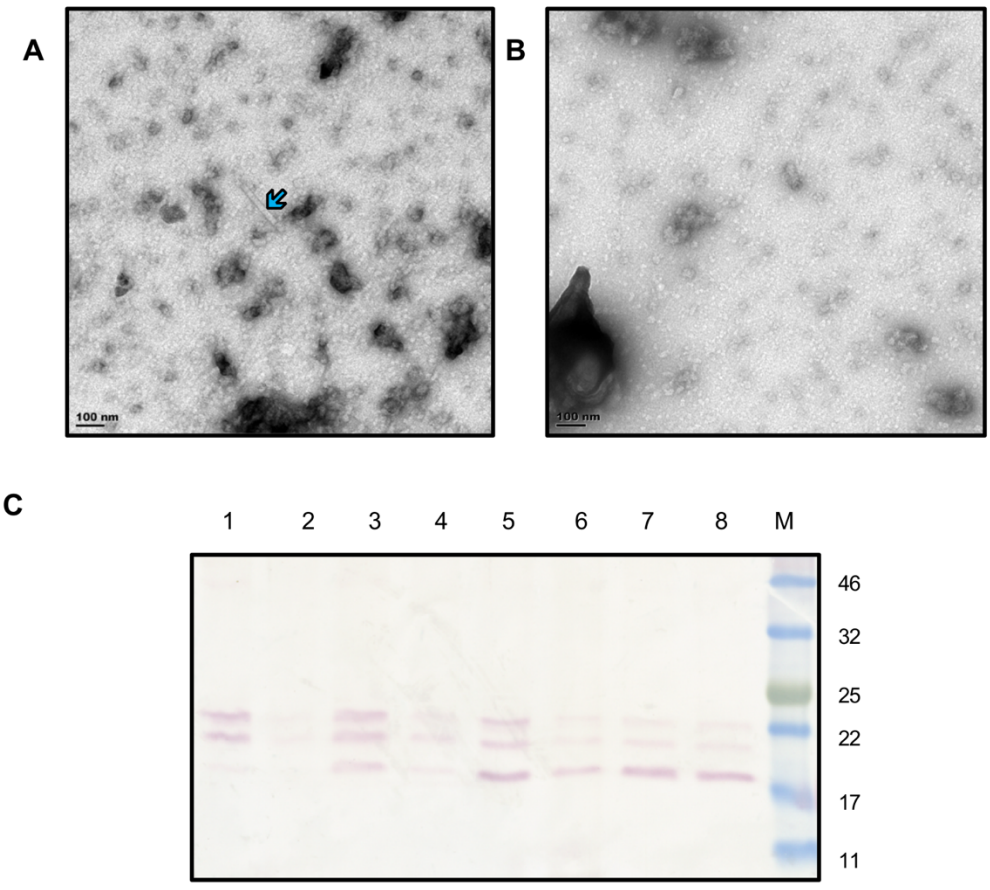

Figure 4.8: Optimization of plant-based expression of recombinant TMV ST coat protein. TMV rods were imaged by TEM for TMV ST (A, blue arrow) but not for ST TMV (B). Crude leaf extracts obtained 3 (lanes 1 & 2), 4 (lanes 3 & 4), 5 (lanes 5 & 6) and 6 (lanes 7 & 8) days after plants were infiltrated with *Agrobacterium* AGL1 containing pEAQ-TMV-ST at an OD_{600}=0.25 (lanes 1, 3 ,5 & 7) or at an OD_{600}=0.5 (lanes 2, 4 ,6 & 8), were analysed by western blot. TMV antiserum (1:5000) was used as the primary antibody and molecular weight markers are shown on the right.

TMV antiserum detected 3 protein species in western blots, the smallest of which corresponded to the approximately correct size for the TMV-ST coat protein (±19 kD). Expression of this protein species was best at 5 - 6 dpi, while expression of the two larger protein species (±21 & ±23 kD) was best at 3 dpi. Better expression was observed at an OD_{600} = 0.25 on days 3, 4 & 5, but by day 6, there was no observable difference between the two concentrations.

For large-scale purification of TMV-ST, the VLPs were purified from the crude leaf extract by double precipitation with 4% PEG/NaCl. The resuspended VLP pellet was analysed by SDS-PAGE and Coomassie blue staining of the gel revealed a single protein band representing the correct molecular weight of the Spy-tagged TMV coat protein (Figure 4.9, A). Typical TMV rod-shaped VLPs varying in length from ± 80 - 350 nm with a diameter of ± 20 nm, were imaged by TEM (Figure 4.9 B, blue arrow) together with thinner rod-shaped particles with a diameter of ±10 nm (Figure 4.9 B, orange arrow).

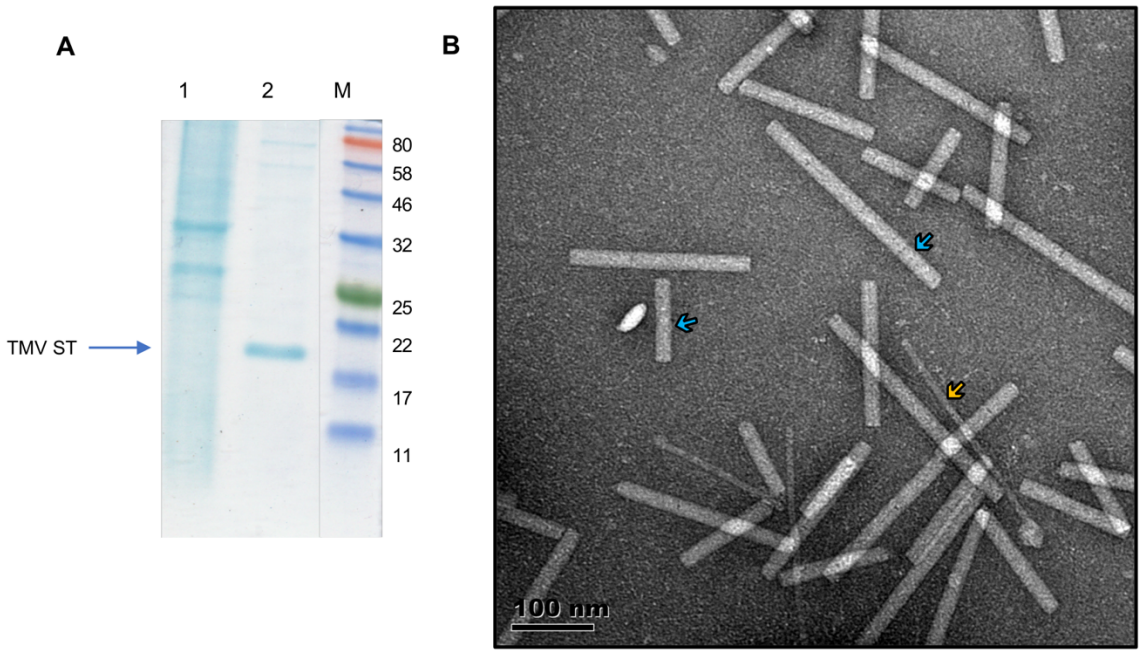

Figure 4.9: Purification of TMV ST VLPs. PEG precipitates of crude extracts from leaves infiltrated with the *Agrobacterium* pEAQ-TMV-ST recombinant were analysed by SDS-PAGE and Coomassie blue staining (A, lane 2). Crude extract from leaves infiltrated with *Agrobacterium* transformed with pEAQ-*HT* expression vector lacking any goi, was used as a negative control (lane 1), while molecular weight marker sizes are shown to the right of the gel. TEM analysis of the PEG-precipitated preparation revealed the presence of rod-shaped TMV Spy VLPs (B) varying in length from ± 80 - 350 nm with a diameter of ± 20 nm (blue arrows) together with thinner rod-shaped particles with a diameter of ± 10 nm (orange arrow). Scale bars: 100nm.

Given the previously-mentioned possibility of using heat-denatured TMV as an immunogen, an attempt was made to reproduce this both with a TMV preparation isolated in the 1970s, as well as with the TMV ST VLPs, with a view to comparing the immunogenic capacity of Spy-tagged TMV SPs with Spy-tagged TMV rods. Both the native TMV and Spy TMV rods were modified by the heat treatment to form TMV SPs (Figure 4.10).

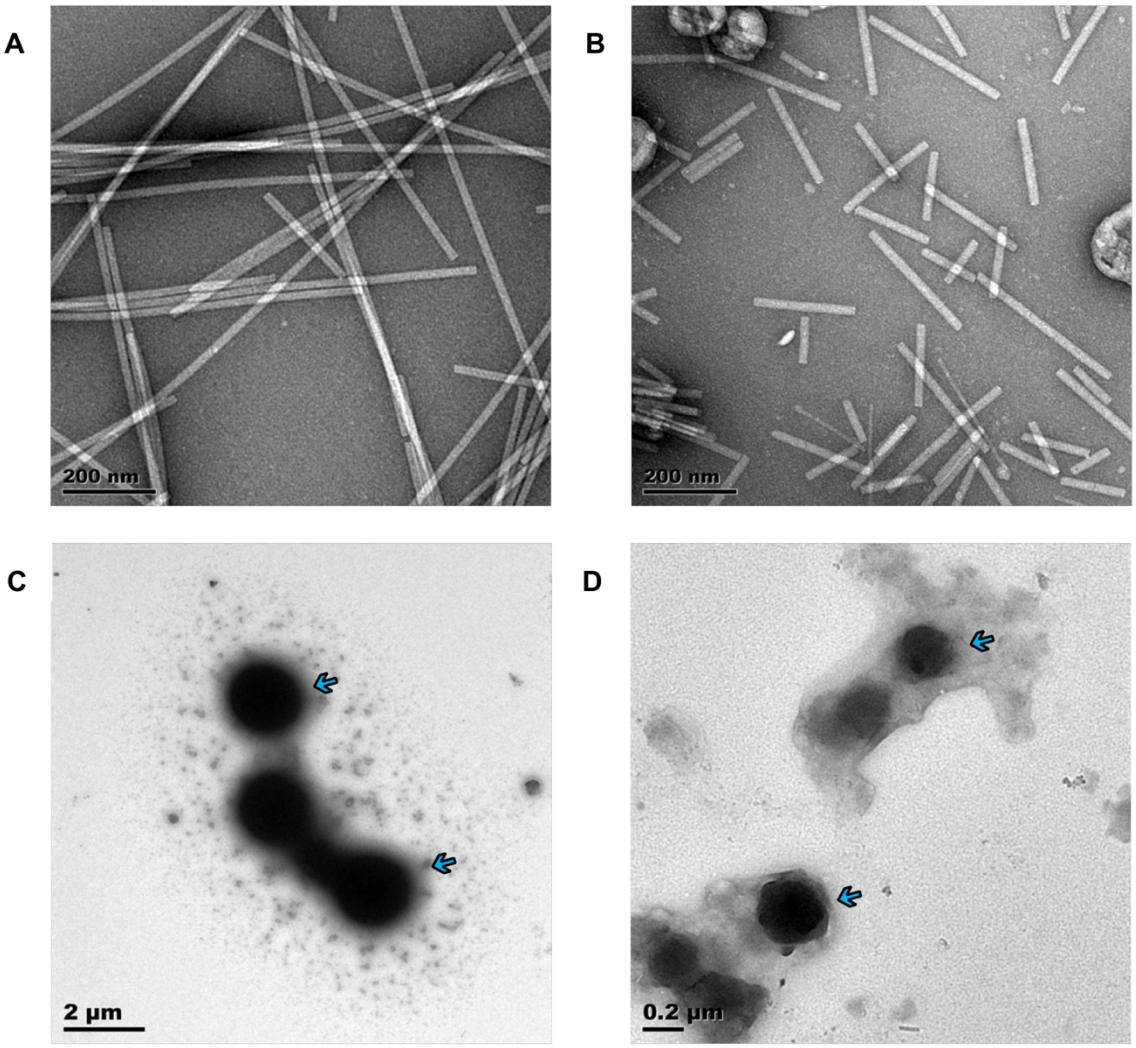

Figure 4.10: Transition of native TMV into spherical nanoparticles. Untreated and heat-treated native TMV (A) and Spy TMV (B) rods were imaged by TEM (The image in B is the full-size image shown in Figure 4.9B captured at a lower magnification). A conformational change of the TMV rods resulting in spherical wild-type TMV (C) or Spy TMV VLPs (SPs) (D) respectively, was observed (cyan arrows). Scale bars 200nm - 200µm.

4.3.2.3 Quantification of Spy VLPs

Unlike the SC AP205 coat protein, the ST AP205 and TMV ST coat proteins were expressed in sufficiently high amounts to enable visualization of the protein bands on a Coomassie-stained gel. Therefore, gel densitometry was used to estimate the protein concentrations (Figure 4.11). A typical purification yielded ±144 mg ST AP205 VLPs and ±186 mg TMV ST VLPs per 25 g infiltrated leaf material, which equates to ±5.7 mg and ±7.4 mg purified VLPs/kg leaf biomass respectively.

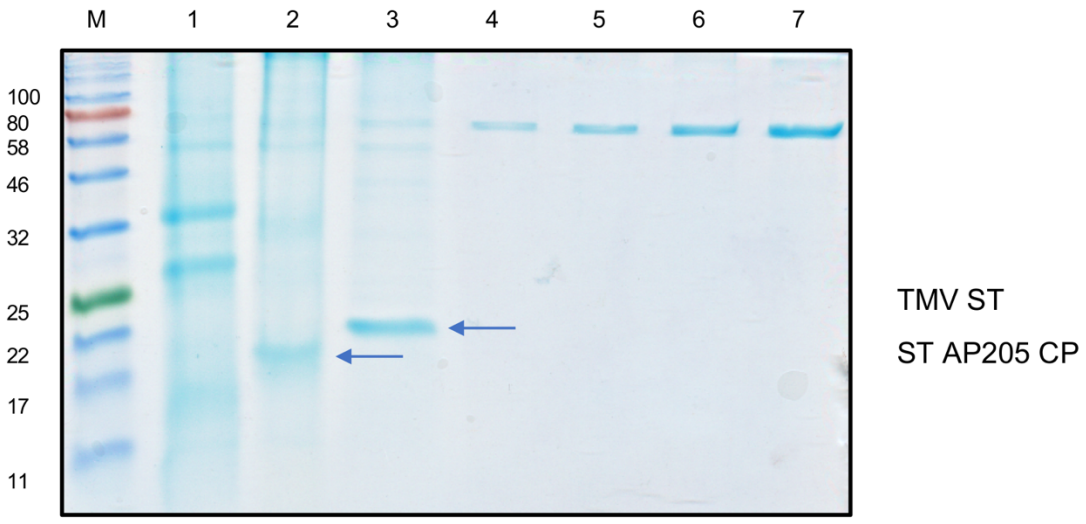

Figure 4.11: Quantification of Spy VLPs by gel densitometry. Particle quantification was achieved by visual comparison of the ST AP205 (lane 2) and TMV ST CP bands (lane 3) to known amounts of bovine serum albumin (BSA), 312 ng (lane 4), 625 ng (lane 5), 1.25 ug (lane 6) and 2.5 ug (lane 7) run separately on the same SDS-PAGE gel. Crude extract from leaves infiltrated with *Agrobacterium* transformed with the pEAQ expression vector lacking any goi, was used as a negative control (lane 1). The location of the Spy proteins TMV ST (±19 kD) and ST AP205 (±16.5 kD) are indicated to the right and by blue arrows, while molecular weight marker sizes are shown on the left.

4.3.3 Expression of AHSV 5 Spy VP2 antigens

Small-scale transient expression of the Spy-tagged AHSV 5 VP2 genes was tested first. Five leaves of each *N. benthamiana* plant were syringe-infiltrated with *Agrobacterium* strains carrying either pEAQ-ST VP2, pEAQ-VP2 ST, pEAQ-SC VP2 or pEAQ-VP2 SC at OD_{600} = 0.25 or 0.5 each. Three leaf discs were clipped per expression test using an Eppendorf vial lid, and extracted 4, 5- and 6-days post-infiltration (dpi) when the leaves were chlorotic but had no signs of necrosis.

Western blot analysis using AHSV 5 antiserum (1:5000) detected a protein band of ±124 kD, the correct size for AHSV5 VP2-ST in crude plant extracts with expression being best on day 3 at an OD_{600} = 0.5 (Figure 4.12 A). However, this protein, which should contain an N-terminal 6 x His tag, could not be detected by anti-His antibody (Figure 4.12 B). Furthermore, no expression of any of the other three Spy-VP2 proteins (with expected sizes of either ±124 kD, for AHSV5 ST-VP2 or ±135 kD for AHSV5 SC-VP2 or AHSV5 VP2-SC) was observed under any of the conditions tested. A western blot comparison of expression levels of the various AHSV5 VP2 antigens used in this study is shown in Figure 4.13.

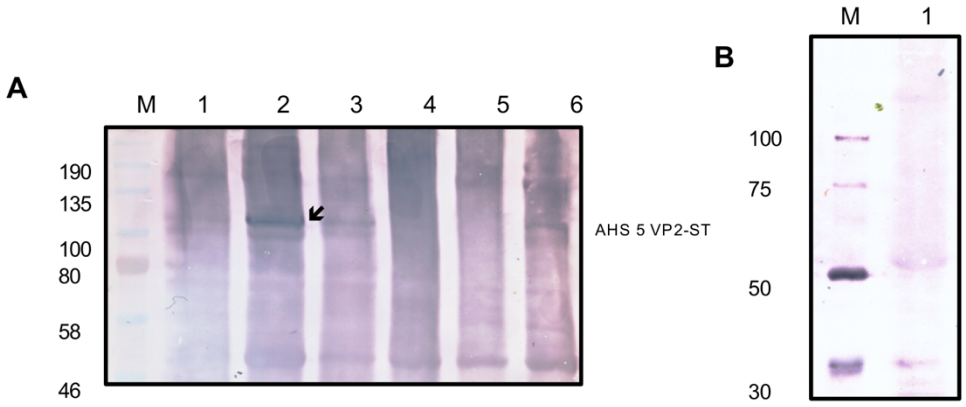

Figure 4.12: Optimization of plant-based expression of recombinant AHSV 5 VP2-ST. A) Western blot analysis of crude leaf extracts obtained 3 (lanes 1 & 2), 5 (lanes 3 & 4) and 7 (lanes 5 & 6) days after plants were infiltrated with *Agrobacterium* AGL1 containing pEAQ-AHSV 5 VP2-ST at OD600=0.5 (lanes 2, 3 & 6) or OD600=0.25 (lanes 1, 4 & 5). Anti-AHSV 5 serum (1:5000) raised in guinea pigs inoculated with plant-produced AHSV 5 VLPs, was used as the primary antibody and the position of AHSV 5 VP2-ST (± 124kD) is indicated by the black arrow. B) Western blot analysis of crude leaf extract obtained 3 days after plants were infiltrated with the pEAQ-AHSV5 VP2-ST *Agrobacterium* recombinant at OD600=0.5, using AP-conjugated anti-His serum (lane 1) showing no detectable band for AHSV5 VP2-ST. Molecular weight marker sizes in both blots are shown on the left.

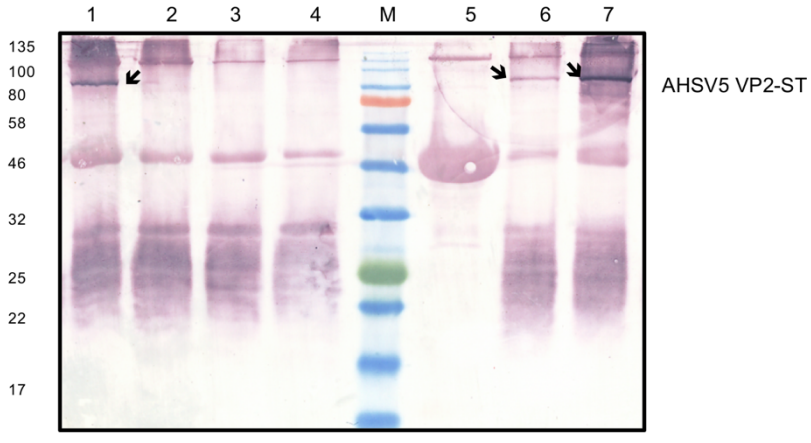

Figure 4.13: Plant-based expression of AHSV 5 VP2 antigens. Western blot analysis of crude leaf extracts obtained 3 days after plants were infiltrated with *Agrobacterium* AGL1 containing pEAQ-AHSV5 VP2-ST (lane 1), pEAQ-AHSV5 VP2-SC (lane 2), pEAQ-AHSV5 ST-VP2 (lane 3), pEAQ-AHSV5 SC-VP2 (lane 4), pEAQ-AHSV 5 VP2 (wildtype) (lane 6) or pEAQ-AHSV 5 VP2 (plant codon- optimized) (lane 7) at OD600=0.5. Anti-AHSV 5 serum (1:5000) raised in guinea pigs inoculated with plant-produced AHSV 5 VLPs was used as the primary antibody and AHSV 5 VP2 antigens are indicated by black arrows. Crude extract from leaves infiltrated with *Agrobacterium* transformed with pEAQ-HT expression vector lacking any goi, was used as a negative control (lane 5). Molecular weight marker sizes are shown on the left.

As AHSV 5 VP2-ST was the only VP2 Spy antigen to be successfully expressed, production was upscaled to include infiltration of 24 plants and the VP2-ST antigen was purified by ammonium sulphate ($(NH_4)_2SO_4$) precipitation. AHSV 5 VP2-ST was thus precipitated by sequential addition of increasing concentrations of $(NH_4)_2SO_4$ to a crude leaf extract obtained 3 days after plants were infiltrated with the pEAQ-AHSV5 VP2-ST *Agrobacterium* recombinant. The $(NH_4)_2SO_4$ precipitated fractions were dialysed overnight against PBS and then analysed by western blotting (Figure 4.14). The majority of the plant-expressed VP2-ST was precipitated by the addition of 40% $(NH_4)_2SO_4$ and therefore this VP2-ST fraction was used in the coupling experiments.

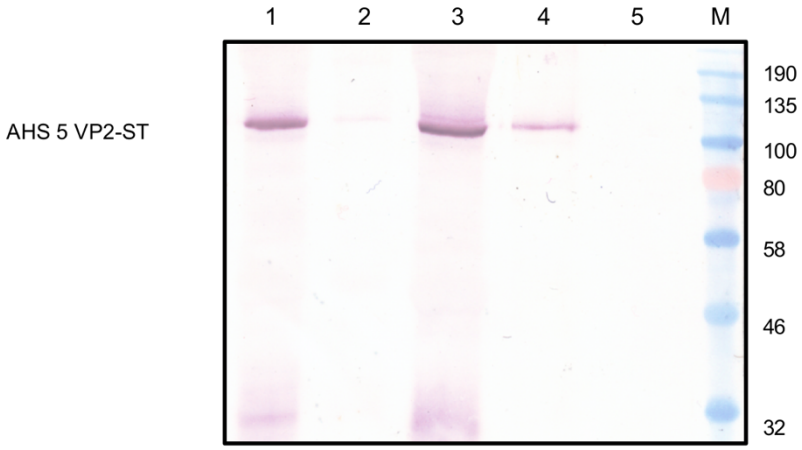

Figure 4.14: Purification of recombinant of Spy-tagged AHSV 5 VP2 antigen. Plant-expressed VP2-ST was precipitated from infiltrated crude leaf extract by sequential addition of 20% (lane 2), 40% (lane 3), 60% (lane 4) and 80% $(NH_4)_2SO_4$ and analysed by western blot using AHSV 5 antiserum (1:5000) raised in guinea pigs inoculated with plant-produced AHSV 5 VLPs as the primary antibody. Dialysed crude extract prior to $(NH_4)_2SO_4$ precipitation was used to demonstrate expression of VP2-ST in the plants (lane 1) and molecular weight marker sizes are shown on the right.

4.3.4 ST - SC coupling experiments

The expression results of the different ST and SC constructs detailed in the preceding sections are summarized in Table 4.1. AP205 VLPs putatively displaying either a SC or a ST peptide on the VLP surface, have been successfully expressed. The assembly of TMV VLPs with ST attached to the C'-terminus of the CP monomers, has also been demonstrated. Lastly, AHSV 5 VP2 has been expressed with the ST peptide fused to its C'-Terminus. Display of Spy-tagged antigen on the surface of a Spy VLP requires coupling via a covalent bond between the ST and its corresponding SC partner. As AHSV 5 VP2-ST was the only tagged VP2 protein that was successfully expressed in *N. benthamiana,* it was only possible to test coupling of this plant-produced Spy-tagged VP2 antigen to the SC AP205 VLPs.

Table 4.1: Plant-based expression of AHSV 5 Spy VP2 antigens and AP205 and TMV Spy VLPs. Western blot analysis was used to test the expression of both AHSV 5 Spy VP2 antigens and Spy VLPs in crude leaf extracts 3 – 5 days after plants were infiltrated with the corresponding pEAQ AGL1 recombinants.

Construct	WB detection	Purification Strategy
ST-AP205	+++	Iodixanol density gradient centrifugation
SC-AP205	+	Iodixanol density gradient centrifugation
ST-TMV	-	-
TMV-ST	+++	PEG/NaCl precipitation
ST-VP2	-	-
VP2-ST	++	$(NH_4)_2SO_4$ precipitation
SC-VP2	-	-
VP2-SC	-	-

4.3.4.1 Coupling of plant-produced AHSV 5 VP2-ST to plant-produced SC AP205 VLPs

Since the concentration of Spy-tagged antigen to Spy VLP is known to influence conjugation, the ratio of Spy VLP: VP2 antigen in the different coupling reactions between AHSV 5 VP2-ST and the plant-produced SC AP205 VLPs, was varied. Western blot analysis of the reactions using AHSV 5 antiserum (1:5000), revealed the presence of an additional band representing a protein species of ± 80 kD instead of the expected size of ±150 kD (Figure 4.15). Increasing concentrations of the Spy VLP in the coupling reactions correlated with more of the input VP2-ST antigen being converted to this smaller ± 80 kD species (Figure 4.15). The experiment was repeated with two different SC AP205 preparations and the same result was obtained in both cases.

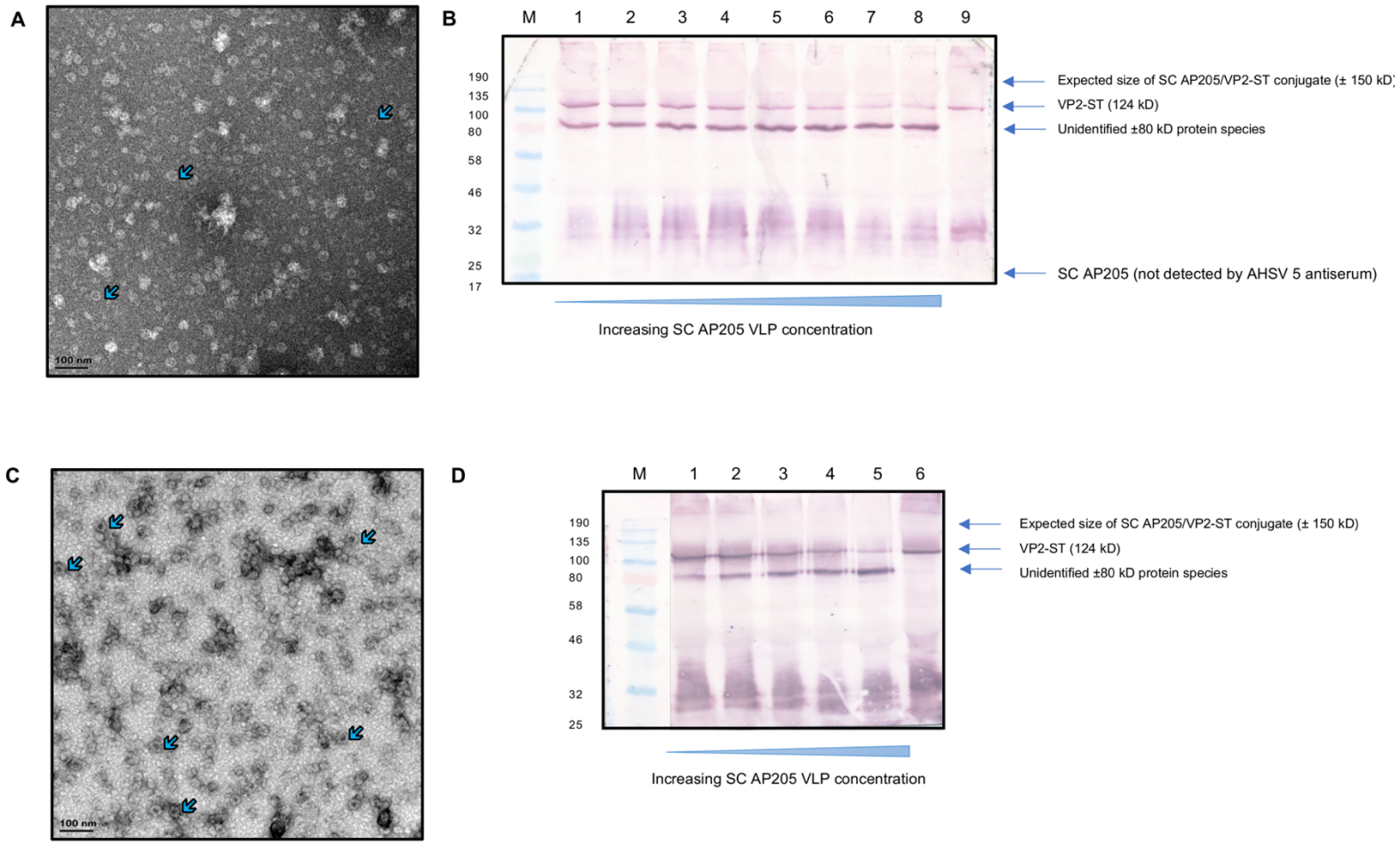

Figure 4.15 Coupling of AHSV 5 VP2-ST antigen to SC AP205 VLPs. Spy VLPs (A) were mixed with tagged AHSV 5 VP2 antigen in four different combinations with increasing ratios of Spy VLP: VP2 antigen (B). These were analysed by western blot using AHSV 5 antiserum (1:5000) raised in guinea pigs inoculated with plant-produced AHSV 5 VLPs as the primary antibody either directly (lanes 2, 4, 6 & 8) or spun to remove aggregates before analyzing the resulting supernatant (lanes 1, 3, 5 & 7). A different Spy VLP sample preparation (C) was mixed with tagged AHSV 5 VP2 antigen in five different combinations with increasing ratios of Spy VLP: VP2 antigen (D, lanes 1 - 5) and directly analysed. In both B and D, input VP2 -ST antigen (B, lane 9 and D, lane 6) was included as an uncoupled control and molecular weight marker sizes are shown to the left.

4.3.4.2 Coupling of SC antigen to plant-produced ST AP205 VLPs

Although ST AP205 VLPs were successfully produced in plants, it was not possible to test coupling of an AHSV VP2 antigen to these VLPs, due to the unavailability of a SC-VP2 antigen. Therefore, a sample of these plant-produced ST AP205 VLPs was sent to C. Janitzek at the Centre for Medical Parasitology (CMP), University of Copenhagen, Denmark, to test their ability to conjugate this to one of their SC-tagged antigen candidates, in this case an *E. coli*- produced SC protein. The plant-produced Spy VLPs were mixed with the tagged SC antigen and the formation of antigen-VLP subunit conjugates was analysed by denaturing SDS-PAGE followed by Coomassie blue staining. Analysis revealed the presence of a protein band matching the combined size of the SC antigen and ST AP205 VLP subunit (28kD) (Figure 4.16, lanes 3 & 4), demonstrating successful coupling of the antigen to the Spy VLP.

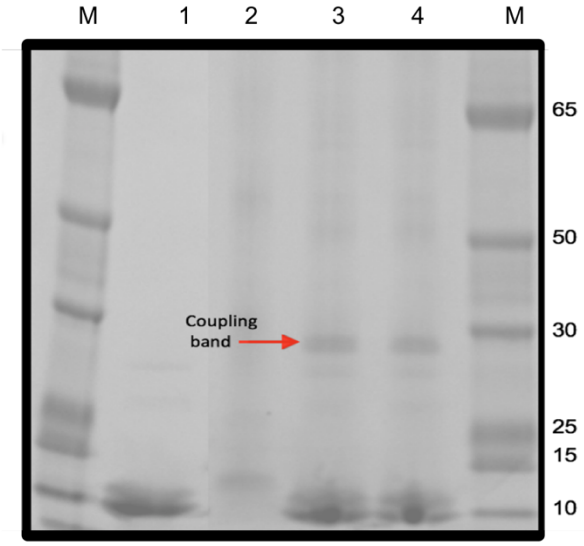

Figure 4.16: Coupling of SC antigen to plant produced ST AP205 VLPs. Spy VLPs were mixed with tagged SC antigen and analysed directly (lane 3) or spun to remove aggregates before analyzing the resulting supernatant (lane 4). Input SpyCatcher (±12kD) (lane 1) and input ST AP205 VLPs (±16kD) (lane 2) were included as uncoupled controls and molecular weight marker sizes are shown to the left and right of the gel.

4.3.4.3 Coupling of AHSV 5 VP2-ST to SC AP205 VLPs produced in *E. coli*

As coupling of plant-produced VP2-ST with the plant-produced SC AP205 VLPs had been unsuccessful, an alternative Spy VLP platform was investigated for the production of tagged AP205 VLPs. Recombinant *E.coli* expression plasmids containing a cloned copy of either the SC AP205 or the ST AP205 coat protein gene (a kind gift from C. Janitzek, CMP, Denmark) were transformed into *E.coli* and cultured for expression of Spy VLPs. The putative AP205 Spy VLPs were purified by density gradient ultracentrifugation and evaluated by TEM. Particles with an estimated size of ± 29 nm for ST AP205 VLPs (Figure 4.17 A) and ± 34 nm for SC AP205 VLPs (Figure 4.17 B) were visualised under the electron microscope.

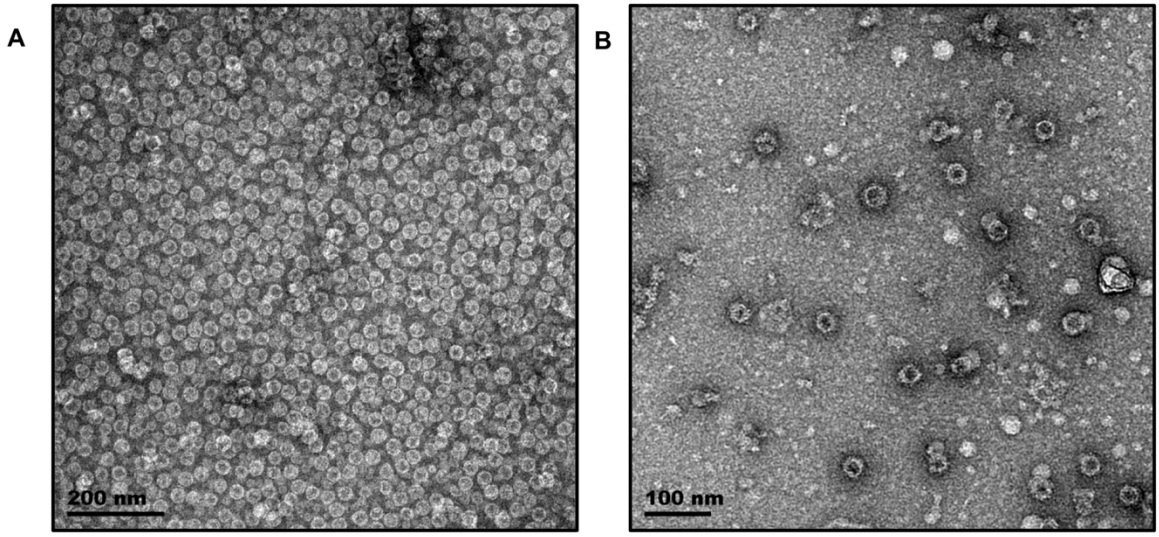

Figure 4.17: Expression and purification of AP205 Spy VLPs in *E. coli.* Clarified bacterial lysates of *E. coli* recombinant ST AP205 or SC AP205 strains were subjected to iodixanol density gradient ultra-centrifugation followed by imaging of the gradient fractions by TEM. Fully-formed Spy VLPs were observed for both SpyTag - (A) and SpyCatcher (B) AP205 VLPs respectively. Scale bars: 100nm - 200nm.

The *E. coli* expressed SC VLPs were mixed with plant-produced AHSV 5 VP2-ST antigens in different ratios and the formation of antigen-VLP subunit conjugates was analysed by western blotting. However, detection with AHSV 5 antiserum did not reveal the presence of a 150 kD protein conjugate species, as would be expected if coupling had occurred between the VP2-ST antigen and the SC AP205 VLP (Figure 4.18).

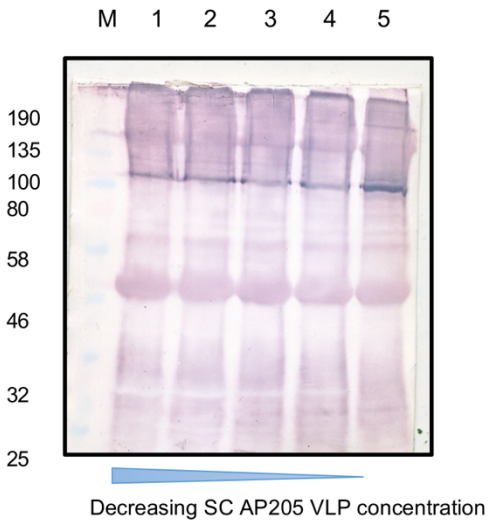

Figure 4.18: Coupling of AHSV 5 VP2-ST antigen to *E. coli*-produced SC AP205 VLPs. Spy VLPs were mixed with tagged AHSV 5 VP2-ST antigen in four different combinations with increasing ratios of Spy VLP:VP2 antigen and analysed western blot using AHSV 5 antiserum (1:5000) raised in guinea pigs inoculated with plant-produced AHSV 5 VLPs as the primary antibody (lanes 1 - 4). Input AHSV 5 VP2-ST (lane 5) was included as an uncoupled control and molecular weight marker sizes are shown to the left of the blot.

4.3.4.4 Coupling of SC antigen to plant-produced TMV ST VLPs

Although the generation of TMV-ST VLPs in plants was highly successful, it was not possible to test conjugation of a SC antigen to these particles, as neither of the SC-conjugated AHSV 5 VP2 antigens was successfully expressed. To prove the concept that the plant-produced Spy-tagged TMV VLPs could at least bind to an *E. coli* - produced SC antigen, a sample of the plant-produced TMV ST VLPs was sent to C. Janitzek at CMP for coupling investigations. The Spy TMV VLP rods were mixed with the tagged SC antigen and antigen-VLP subunit conjugate formation was analysed by SDS-PAGE followed by Coomassie blue staining (Figure 4.19).

No clear evidence of coupling between the SC antigen and the TMV VLPs was evident as determined by the lack of an additional antigen-VLP subunit conjugate band of the correct size (±31kD). However, a possible change in molecular weight of the SC antigen following mixing with the plant-produced TMV ST VLPs was observed (Figure 4.19). This change did not occur when the TMV ST VLPs rods were modified by heating to form spherical TMV bodies.

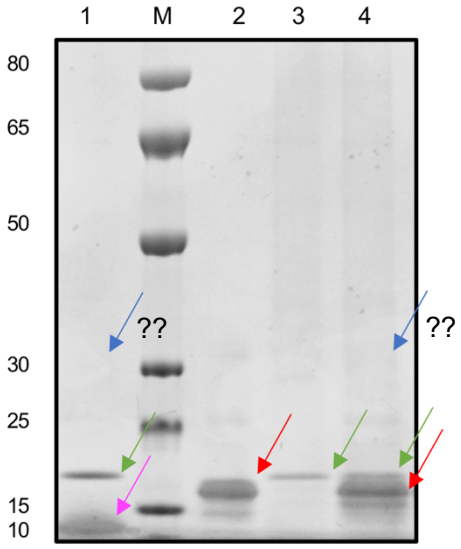

Figure 4.19: Coupling of *E. coli*-produced SC antigen to plant-produced TMV-ST VLPs. Spy VLPs were mixed with SC antigen either directly (lane 1) or after heat treatment to alter the conformation of the tagged TMV rods to form SPs (lanes 4). Input SC antigen (lane 2, red arrow) and input TMV-ST VLPs (lane 3, green arrow) were included as uncoupled controls. The blue arrows indicate the 31 kD expected size of a coupled SC-TMV-ST conjugate, while the pink arrow represents the appearance of an additional band, in place of the SC antigen band which is absent. Molecular weight marker sizes are indicated to the left of the gel and in lane M.

4.4 Discussion

Vaccination with VLPs assembled from AHSV structural proteins is a safe and potentially effective way to defend horses against infection with AHSV and protect them from contracting the disease. However, advances in genetic engineering have also raised the possibility of developing an AHSV vaccine candidate consisting of VLPs derived from an unrelated pathogen, to which an AHSV antigenic protein has been linked. Outer capsid protein VP2 is the natural antigen of choice for the development of such chimaeric VLPs, as it is the major determinant of serotype-specificity and contains the epitopes which elicit a neutralizing antibody response.

Genetic fusion strategies for the coupling of two proteins have become commonplace in many areas of molecular biology, one of the best known examples being the incorporation of green fluorescent protein (GFP) into proteins to study their biological functions (Lippincott-Schwartz et al. 2001). Furthermore, the most advanced candidate vaccine against human malaria, RTS,S consists of sequences from the malaria circumsporozoite protein (CSP) which have been genetically fused to the hepatitis B surface antigen (HBsAg), resulting in display of these peptides on the surface of HBV VLPs (Rutgers et al. 1988). However, fusing VP2 to a heterologous CP monomer for subsequent multimerization is unlikely to be successful as it is a large protein (124kD) and the possibility of misfolding is high, which would probably affect VLP assembly and thus prevent display of the antigen on the particle surface. The concept of a modular two-step conjugation, in which VP2 and the VLP monomer are expressed separately first and VP2 is then coupled to the assembled VLP afterwards, is a more attractive alternative (Brune and Howarth 2018).

The novel SpyTag / SpyCatcher conjugation system, or “bacterial superglue” as it has come to be known (Thrane et al. 2016), is a versatile platform which has been shown to permit coupling of a wide variety of antigens to the surface of different VLPs. This covalent coupling strategy has the added advantage of stability under a wide range of physiological conditions, an important consideration in vaccine production for third world countries where cold chain maintenance can be problematical. In this chapter, the plant-based expression system was used to produce Spy VLPs consisting of either Acinetobacter phage AP205 VLPs or TMV particles displaying a ST or SC peptide. In addition, AHSV 5 VP2 displaying ST was also expressed in plants and for comparison, Spy AP205 VLPs were produced in *E. coli.*

Both ST- and SC AP205 CPs spontaneously assembled into VLPs following recombinant DNA expression of these proteins within transiently transfected plant cells. The yield of ST AP205 VLPs was greater than that of SC AP205, possibly due to the larger size of the SC tag which may have caused reduced recombinant protein expression (Fig 4.6). Indeed, this was seen to be true for the

E. coli expression system as well, which also permitted successful assembly of Spy AP205 VLPs (Figure 4.17).

Anti-AP205 sera raised in mice vaccinated with AP205 VLPs detected multiple protein bands following western blot analysis, two of which corresponded to the correct molecular weight sizes of the ST- and SC AP205 CP monomers (±16.5 and ±27 kD, respectively) (Figure 4.7). The sizes of the larger protein species detected on the blots are in the region of the expected sizes of SC AP205 dimers (±54 kD) and ST AP205 dimers (±33 kD) and trimers (±50 kD), although it is unclear what the smaller band on the SC AP205 blot represents (Figure 4.7). The presence of multiple bands complicated the interpretation of results, but Spy AP205 VLPs of both types were clearly visualized by TEM. Iodixanol density gradient centrifugation was used to purify the Spy AP205 VLPs produced in both expression systems, although it appeared to be difficult to remove all contaminating plant proteins using this method (Figure 4.6).

The formation of Spy TMV rods was observed within transiently transfected plant cells following recombinant DNA expression of TMV with ST fused to the C-terminus (Figure 4.9). No protein expression was observed when the coding sequence for the ST peptide was fused to the N-terminus of the TMV CP gene (Figure 4.8). This is in agreement with the results of others who also reported successful expression of TMV CP fusion products only when the fused protein was attached to the C-terminus (Werner et al. 2006). TMV Spy VLPs were effectively purified from contaminating plant proteins by PEG/NaCl precipitation and were clearly imaged by TEM (Figure 4.9).

Western blot analysis again detected 3 protein species using TMV-specific antiserum, the smallest of which corresponded to the correct size of the Spy-tagged TMV CP (Figure 4.8). The identity of the two larger protein species on the western blots is unclear, as they are too small to represent CP dimers. However, it was interesting to observe that two unique species of TMV rods, with differing widths, were visualised by TEM (Figure 4.9). It is possible that the thinner rod represents a different arrangement of TMV CP monomers around the helical axis or that the Spy-tagged CP has been cleaved to form a truncated TMV CP, but one which still has the ability to self-assemble into mutant TMV rods. It was not possible to determine with certainty by TEM analysis whether the ST peptide is present on the surface of either species of TMV rod, as the peptide is too small to notice an observable difference by TEM. No antiserum to detect the ST moiety by western blot analysis was available either, meaning that the only conclusive evidence of the successful display of ST on the TMV rod surface would be demonstrated by successful coupling to a SC antigen.

The TMV rod length is determined by the length of the encapsidated RNA. Thus, the length of the recombinant Spy-tagged TMV rods was expected to be about 83 nm as the mRNA transcribed

from the cloned gene, including vector sequences, was calculated to be 1785 bp long, with transcription initiating at the CaMV 35S promotor and ending at the NOS terminator. TMV rods of ± 80 - 350nm were visualised by TEM, the presence of the longer lengths presumed to be a result of end-to-end arrangement of shorter rods as is likely to be the case with the wt TMV rods observed in Figure 4.8 A, many of which appear longer than the presumptive 300nm length of wt TMV (Gasanova et al. 2016).

The genetic fusion of the SC peptide to either the 5' or 3' end of AHSV 5 VP2 apparently prevented recombinant DNA expression of this protein within transiently infected plant cells. The reason for this is unclear but it is most likely due to the relatively large size of the SC peptide and its location at one of the gene termini, which may hinder correct folding of VP2. No expression was observed when the ST peptide was fused to the N-terminus of the VP2 gene either, but the expression of Spy-tagged AHSV 5 VP2 was detected by western blot analysis when the ST peptide was fused to the C-terminus of the VP2 gene (Figure 4.10). However, as this gene was genetically manipulated to express the VP2 protein with an N-terminal His-tag, it was surprising that it was not detected by anti-His antibodies. This would seem to suggest that either the His tag was cleaved off during expression, or it has become hidden during post-translational folding of the VP2-ST protein.

The unexpected result obtained when an attempt was made to covalently attach VP2 ST to the surface of plant-produced SC AP205 VLPs is puzzling (Figure 4.16). The fact that a protein species of ± 80 kD, roughly half the size of the expected band of ± 150 kD, was detected by western blot analysis using AHSV 5 antiserum, can perhaps only be explained by the cleavage of the Spy-tagged VP2/AP205 CP conjugate by the activity of a plant protease. The fact that increasing the concentration of SC AP205 VLPs in the coupling reaction caused exponentially more of the VP2 ST to be converted to the smaller protein species, is a clear indication that the SC AP205 preparation is implicated in some way. The supposed presence of a serum-type protease site in the AHSV VP2 hub domain (Chapter 1, Figure 1.10) which, if cleaved, would split the Spy-tagged VP2/AP205 CP conjugate into roughly two equal halves, lends further credence to the hypothesis that the Spy-tagged VP2/AP205 CP conjugate has been cleaved.

If this is the case, then unfortunately the part of AHSV VP2 which would remain attached to the Spy AP205 VLP would be the C-terminal region of the protein. As the epitopes which induce neutralizing antibodies are believed to be positioned in the N-terminal half of the protein, this VP2/AP205 conjugate would not be suitable as a potential vaccine candidate.

A further effort to effect plant-produced AHSV 5 VP2 display on AP205 VLPs, this time using SC AP205 VLPs produced in E. coli, was also unsuccessful. This result was most disappointing as it

indicated the probable failure of AHSV VP2 to be accommodated on the Spy AP205 VLP surface. The fact that plant-produced ST AP205 VLPs were shown by our Danish colleagues to couple successfully to a SC antigen in their laboratory, was proof that Spy-tagged VLPs, capable of coupling to a suitable antigen, can be successfully produced in plants. However, due to its intrinsic nature and size, coupling of the full length AHSV VP2 appears to be precluded using this strategy. Further investigation is required to determine whether coupling of smaller VP2 peptides representing one or more neutralizing epitopes, may perhaps be a more feasible approach and one that will be met with greater success.

The failure of SC VP2 to be transiently expressed in plant cells meant that it was not possible to test coupling of VP2 to either the plant produced Spy-tagged TMV rods or to the spherical TMV particles produced by heat treatment of these rods. However, once again a sample of the TMV Spy VLPs was sent to our colleagues in Denmark for coupling with their SC antigen. The results of these experiments were rather ambiguous as, although a SC VP2/TMV ST VLP coupling band of the expected 31 kD was not observed, there was once again evidence of a possible change in molecular weight of the SpyCatcher antigen following mixing with the plant-produced TMV-ST VLPs (Figure. 4.19).

It would thus appear that coupling to the TMV Spy VLPs was not achieved, but possible cleavage of the SC antigen occurred, again perhaps due to the presence of a contaminating plant protease. The heat treatment applied to modify the Spy TMV rods to spherical particles is likely to have destroyed this protease and therefore, the SC antigen in reactions with the spherical VLPs remained unaffected. It is unclear, however, why coupling with this was unsuccessful. Two possible explanations are that either the ST was cleaved off during the expression and assembly process, or that for some reason the ST is hidden from the rod surface and not available for coupling with the SC antigen.

Concurrently, but independently of the investigations presented here, Saunders and Lomonossoff (2017) reported the synthesis and assembly of different length TMV “nano-wires” also using the pEAQ plant transient expression system. They successfully expressed TMV CP which incorporated a metal-binding peptide at its C’-terminus and demonstrated the production of TMV rods of defined length coated with cobalt-platinum. However, when they investigated the expression and assembly of TMV CP incorporating a 6 x His tag at its C’-terminus, they found that the process was very inefficient in comparison to wt TMV assembly and the level of VLP rod assembly was too low to permit further characterization. This peptide is half the size of the ST peptide used in the fusion strategy presented here and so together these studies indicate that there are limiting factors with regard to incorporating modified TMV CPs into RNA-containing

particles. As described above, the possibility exists that in both these studies, the additional peptides have been post-translationally removed from the CP monomers by protease degradation.

Although presentation of AHSV 5 VP2 on a heterologous display system was not proven in these experiments, this research has demonstrated the successful expression of two different Spy VLP carriers in plants as well as the successful coupling of a SC antigen to the surface of plant-produced ST AP205 VLPs. These findings have paved the way towards further investigations regarding the coupling of smaller VP2 epitope sequences of different AHSV serotypes to the surface of Spy VLPs. This would allow optimal presentation of these protein peptides to the animal's immune system with a view to developing a multivalent vaccine that would provide protection against all nine AHSV serotypes.

C H A P T E R F I V E

GENERAL DISCUSSION AND CONCLUDING REMARKS

5.1 General Discussion

African horse sickness is a lethal and debilitating disease of domestic equids, that doesn't discriminate. Farm horses, thoroughbreds, show horses, ponies - all are susceptible, and in a country like South Africa, with a horse population of around 300 000 horses, many of them working animals, it is a very real concern. The measure of control afforded by the currently used live attenuated vaccine at least provides some level of confidence. However, production of this vaccine uses very old technology and production volumes cannot meet the current demand, with only approximately 50% of the national herd of horses presently being vaccinated. Furthermore, the fact that many horses still contract the disease and often die in spite of vaccination, has obliged the equine community to look to the scientific world, particularly to the field of molecular biology, for new hope and alternative options.

Four types of alternative AHS vaccine platforms have been described in recent years. Two of these, the ECRA (Entry Competent Replication Abortive) (Lulla *et al.* 2017) and DISA (Disabled Infectious Single Animal) (van Rijn *et al.* 2018) candidate vaccines, stem from research in the area of reverse genetics technology, while the third and fourth are based on modified pox viruses (Guthrie *et al.* 2009; Calvo-Pinilla *et al.* 2018). Although the results obtained in experimental trials with these vaccines look promising, issues of cost and scalability have thus far prevented any from being commercialized. A fifth AHS vaccine option is presented in this thesis, one which is believed to be as efficacious as the currently used live attenuated vaccine, but which is free from the latter's accompanying risks and shortcomings.

Confidence in this novel AHSV VLP vaccine hinges largely on the fact that it is a vaccine comprised entirely of protein, free from infectious genetic material, and produced using a cost-effective plant transient expression system. Furthermore, the vaccine platform mimics field exposure to the naturally immunogenic AHS virion, but without endangering the immunised animal in any way and being completely free of the possibilities of reversion to virulence, or reassortment with other vaccine or wild-type viruses. Significant progress has been made in this project with regard to the plant-based expression of different serotypes of AHSV VLPs that can be safely administered to horses. The goal of developing a multivalent vaccine capable of protecting animals against

multiple AHSV serotypes simultaneously has also been appreciably advanced, with the two serotype VLPs that have been tested potentially being able to protect against three wild-type viruses.

The propensity of orbivirus capsid proteins to self-assemble into VLPs when co-expressed has been demonstrated for BTV in both insect cells and in plants (French *et al.* 1990; Hewat *et al.* 1994; Stewart *et al.* 2010; Thuenemann *et al.* 2013). However, the only previous attempt at producing AHSV VLPs, in this case in insect cells, was less successful and the resulting low VLP yield precluded quantification (Maree *et al.* 2016). In this study, transient co-expression of the four capsid proteins of two different AHSV serotypes in *N. benthamiana,* resulted in the efficient self-assembly of well-formed AHSV VLPs. Moreover, these VLPs were shown to be both safe and highly immunogenic in guinea pigs (serotype 5 only) (Dennis *et al.* 2018a) and in horses (Dennis *et al.* 2018b). From a comparison of EM images taken before and after long-term storage of the VLPs at -80 ^{o}C, the particles were shown to be stable for a period of at least 18 months but would more than likely remain so for even longer.

Although density gradient ultracentrifugation proved to be a very useful strategy for purifying AHSV VLPs from infiltrated plant lysates, the relatively high costs of materials and requirement for specialised equipment that would probably not scale very well, prompted the decision to evaluate other centrifuge-free approaches. The filtration strategy employed to prepare one of the AHSV-5 VLP vaccines used in this study yielded a formulation which, besides being more cost-effective, was both well-tolerated by the recipient horses and immunologically effective. This is a clear indication of the potential of production of the plant-based vaccine to meet the upscaling conditions required to economically inoculate a substantial percentage of the national herd. For example, it was shown that ± 5.7 mg purified VLPs can be produced from 1 kg of leaves (± 300 plants), which is sufficient to inoculate about 30 horses at a dose of 100 μg x 2 (prime and boost) per horse. Therefore, 10 tonnes of leaf material would be required to produce sufficient vaccine to immunize the 300 000 horses in South Africa annually – which production level is within the capability of several facilities presently in operation in the USA and elsewhere.

Only a few studies evaluating the AHSV antibody dynamics of horses vaccinated in the field with the LAV have been published (von Teichman *et al.* 2010; Crafford *et al.* 2014; Weyer *et al.* 2017). From these studies, it is apparent that the antibody responses in vaccinated horses are very variable, and while one serotype may have been reported to be the most immunogenic in one study, in another study, more horses seroconverted to a different serotype. In the horse study presented in this thesis, the maximum virus neutralization titres acquired by horses immunized with either plant-produced AHSV 5 or AHSV 4 VLPs, fell comfortably within the range observed

for the most immune responsive horses following vaccination with the LAV in other published reports, in all horses tested.

Furthermore, sera from horses immunized with AHSV 5 VLPs also elicited a comparative immune response towards AHSV 8, confirming reports of cross protection between these two serotypes. The immune responses against serotypes 4, 5 and 8 was highest immediately after the boost vaccination. They then plateaued to levels which, in three of the four horses vaccinated with AHSV 5 VLPS, were still above the minimum protective titre stated by the manufacturer of the LAV, eleven months after the initial vaccination (Crafford *et al.* 2014). Serum neutralisation titres in horses vaccinated with AHSV 4 VLPs demonstrated even longer-lasting initial immunity, with values only falling below the maximum titres 2 months after the boost vaccinations. These results demonstrate the importance of pursuing further investigation into the exciting potential and suitability of this candidate AHSV vaccine.

Of particular significance in these studies was the demonstration that the outer capsid proteins VP2 and VP5 of two different serotypes could be assembled interchangeably onto a common VP3/VP7 core. However, it was clear that AHSV 4 VLPs had more stringent assembly requirements than AHSV 5, as the latter assembled under both buffer pH conditions tested, whereas evidence of AHSV 4 VLP formation was only apparent under higher pH conditions. The precise interactions between VP2 and the underlying VP7 layer, and possibly also the interactions between the VP2 trimers and between the VP2 and VP5 trimers in the outer core, may be quite complex and definitely appear to differ between the serotypes. It will be interesting to discover whether the outer capsid proteins of the other seven serotypes can also be assembled onto this same common core, and if so, under which pH or other external buffer conditions.

Although others have also shown that co-expression of the capsid proteins of multi-capsid protein component viruses in several expression systems results in the spontaneous self-assembly of VLPs, a review of the relevant literature shows that in each case, the viral capsid proteins were always co-expressed, and assembly is believed to have occurred within the same cells of the expression vehicle (plants, insect cells, mammalian cells etc.) (Roy and Sutton 1998; Thuenemann *et al.* 2013; Maree *et al.* 2016; van Zyl *et al.* 2016; Brillault *et al.* 2017). A highly novel finding to emerge from this investigation, therefore, was the demonstration that if each AHSV protein is expressed separately in different plants and the infiltrated crude plant lysates are mixed together, spontaneous VLP assembly occurs *in vitro* during an overnight incubation at a cool temperature.

It was surprising to discover that four different proteins could be expressed separately in plant leaf cells and then could assemble outside of the expression platform to form whole particles, and this

may have useful implications when considering the development of chimaeric AHSV VLPs. One could thus conceivably express AHSV VP2 proteins representing serotypes other than 5 and then incubate these overnight with individually-expressed AHSV serotype 5 VP3, VP5 and VP7 proteins to encourage chimaeric VLP assembly, thereby resulting in the production of VLPs which represent other AHSV serotypes. These could all be combined to form a multivalent vaccine for horses which would provide protection against more than one viral serotype, while obviating the necessity for expressing all four proteins of every serotype.

Although vaccination with AHSV VLPs is a safe and potentially effective way to protect horses against infection with AHSV, and the concept of vaccinating horses with a polyvalent mixture of AHSV serotypes would certainly not be a new one, an alternative approach to the development of a multivalent particulate AHSV vaccine was also addressed in this thesis. This involved the adoption of a modular conjugation strategy, where it was proposed that outer capsid protein VP2, which contains the antigenic determinants responsible for eliciting a serotype-specific immune response, should be covalently attached to the surface of either phage AP205 or TMV VLPs, both produced in plants. The coupling strategy investigated involved the use of the SpyTag / SpyCatcher or bacterial "superglue" methodology (Brune *et al.* 2016; Thrane *et al.* 2016), according to which Spy-tagged antigens are irreversibly bound to Spy VLPs for efficient presentation to the host's immune system.

Using this approach, one of the protein partners is fused to the SpyCatcher (SC) peptide while the other is fused to the SpyTag (ST) peptide. Both ST- and SC AP205 and TMV ST VLPs were successfully expressed in plants, as was AHSV 5 VP2 ST antigen. However, as it was only possible to synthesize VP2 fused to the smaller ST modality and not to the larger SC peptide, the only plant-produced Spy VLP that could be investigated in the coupling reactions was SC AP205, given that TMV SC particles were not made. Unfortunately, this strategy was more complicated than originally envisaged. From western blot analysis it appeared that although conjugation between AHSV 5 VP2 and SC AP205 occurred, the resultant protein product was cleaved, more than likely by a plant protease, meaning that the full-length coupling of AHSV 5 VP2 to the phage particle was unsuccessful. Even when a prokaryotic expression system (as opposed to plants) was utilised to produce SC AP205, no coupling of the *E coli*-produced Spy VLPs to VP2 ST was apparent. In this case, however, as no unexpected cleavage products were observed by western blot analysis, the lack of coupling was thought to be related to the large size of the VP2 ST antigen.

Although coupling tests between a SC antigen and the plant-produced ST AP205 and TMV ST VLPs could not be conducted at UCT, Danish colleagues at the Centre for Medical Parasitology in Copenhagen were willing to test the concept that the plant-produced Spy-tagged VLPs could at least bind to an *E. coli*-produced SC antigen. Their experiments demonstrated the successful

coupling of plant-produced ST AP205 to the SC antigen, a 12 kD protein, which is considerably smaller than the size of the 124 kD AHSV 5 VP2. Coupling of this *E coli*-produced SC antigen to the plant-produced TMV ST VLPs however, was not successful. This is believed to be due to one of three factors: either the ST was cleaved off the TMV CP monomers during the expression and VLP assembly process, or the ST is somehow hidden from the surface of the VLP preventing coupling with the SC antigen, or coupling occurred and, as observed in coupling experiments between plant-produced SC AP205 and AHSV 5 VP2 ST, the coupled coat protein/SC conjugate was cleaved by the action of a plant protease. Even though less successful than anticipated, the results of the modular conjugation experiments presented here, have opened the door to future investigations regarding optimal size and presentation of AHSV 5 VP2 antigens to the animal's immune system. These studies should thus provide further impetus towards attaining the goal of developing a multivalent vaccine that would provide protection against all nine AHSV serotypes.

5.2 Future Prospects

There is little doubt that the live attenuated vaccine (LAV) that has been used in South Africa to defend horses against AHSV for the past 6 decades (House 1993; MacLachlan *et al.* 2007), has ensured their continued existence in this country. Although the traditional vaccine dominates the commercial market place, there has been an increasing demand for a new, safer and more cost-effective vaccine which would not only address the concerns of South African horse owners, but also be acceptable in the wider European context where live vaccines for the disease would not be acceptable. Biotechnological advances over the past few decades have paved the way for new generation vaccines which lack the associated negative features of the LAV, and which could potentially serve as adequate replacement vaccines.

An ideal AHSV vaccine would activate both humoral and cell-mediated immune responses and provide rapid and long-lasting protective immunity against all nine serotypes of the virus. It would block viraemia, disallow transmission by the midge vector, ensure that no risk of reversion to virulence nor re-assortment with outbreak strains was possible, and permit accurate differentiation between vaccinated and infected animals. It should be possible to safely, consistently and economically produce sufficient doses of such a vaccine to meet the demands of both the private and rural sectors. Importantly, the vaccine should hold sufficient interest and market potential to capture the attention of the manufacturing industry. The vaccine candidates developed and described in this thesis meet most, if not all of these criteria.

A vital next step in assessing the potential of the plant-produced AHSV 5 and 4 VLP vaccines to provide adequate and durable protection against infection with the respective AHSV serotypes, would be to conduct a challenge study. This would involve vaccination and subsequent virulent

challenge of horses in an area outside of the Western Cape Province of South Africa, due to the restrictions imposed with regard to research using the live virus in this region. It will be important also to investigate the formation of AHSV VLPs of the other serotypes, together with their ability to safely induce a protective immunogenic response in horses. Concomitant investigations into refining and upscaling the VLP filtration purification strategy are important to ensure the economical production of quality-controlled vaccine preparations. All production processes would need to meet the requirements of the relevant regulatory authorities.

An indirect ELISA test based on the detection of antibodies to VP7 in the serum sample is currently used to diagnose AHSV infection (Maree and Paweska 2005). However, although accurate, it is neither possible to determine the virus serotype nor to differentiate between vaccinated and infected animals using this method. As the plant-produced VLPs contain VP7, antibodies to this protein would be found in the sera of both vaccinated and infected animals alike, making it unsuitable as a complementary diagnostic test. It will therefore be necessary to develop an alternative diagnostic test that can be used alongside the plant-produced VLP vaccine to ensure DIVA compliance. Potential candidates for such a new test include either non-structural protein NS4 or protein VP6, the viral helicase, both of which are highly conserved across the serotypes and which are not contained within the VLP vaccine. Plant-produced VP7 alone could be used as a reagent in current or future serological assays for AHSV diagnosis, however, and would almost certainly be cheaper to produce than the current reagent.

As cellular immune mechanisms almost certainly play an important additional role in protection against AHSV, it would furthermore be of benefit to identify and characterize potential AHSV immunodominant T-cell epitopes in horses. Virus-specific CD8+ T-cells have previously been detected in peripheral blood mononuclear cells (PBMC) in vaccinated horses (El Garch *et al.* 2012; Pretorius *et al.* 2012), and AHSV VP2 and NS1 CD8+ epitopes have also been identified in immunized IFNAR(-/-) mice (Calvo-Pinilla *et al.* 2015). An investigation into the induction of cell-mediated immune responses by the plant-produced AHSV VLP vaccines described here was beyond the scope of this thesis, but it is an important avenue to be explored in future studies.

A very interesting aspect of the studies presented in this thesis was the observation that assembly of AHSV 5 VLPs was less constrained by the buffer pH conditions than that of AHSV 4 VLPs. This had led to curiosity with regard to the nature of the VP2 interactions within the particles of the different AHSV serotypes. An understanding of these interactions at the molecular level would provide useful information with regard to the development of chimaeric AHSV VLPs and would have important implications regarding the development of a multivalent vaccine. Efforts in our group will now be concentrated on investigating the 3D structures of one or more AHSV VLPs,

with particular focus on the connections made between the trimers of VP2, and between the VP2 trimers and the other viral protein components.

The latter studies will also provide valuable insight regarding those regions of VP2 located on the surface of the particle that are likely to play a role in serotype specificity and immunogenicity. The unsuccessful coupling of Spy-tagged AHSV 5 VP2 to plant-produced AP205 Spy VLPs has prompted the need to consider designing VP2-epitope moieties, which can be fused to either the ST or SC peptides, and expressed in plants for coupling to plant-produced Spy VLPs. If successful, a mixture of serotype-specific Spy VLPs will provide an alternative candidate vaccine to the self-assembled AHSV VLPs and may simplify development of a multivalent AHSV vaccine platform.

Both the self-assembled AHSV VLPs and the AHSV Spy VLP vaccine platforms rely on the plant-based expression of the protein components that comprise the individual vaccines. "Biopharmed" AHSV vaccine candidates have the advantages of reduced cost compared to those produced in insect or mammalian cell expression systems, and correct post-translational processing, something which is difficult if not impossible to achieve in prokaryotic systems. Plant transient expression strategies have drawn increased scientific attention in recent years and are likely to pave the way towards the development of innovative vaccine designs and therapeutic products. The research presented in this thesis and recently published (Dennis *et al.* 2018a; Dennis *et al.* 2018b) is the first report of AHSV VLPs being produced in plants and their immunogenicity in horses; this holds significant implications for the successful development of an alternative AHSV vaccine candidate.

Bibliography

Adams, SE, Dawson, KM, Gull, K, Kingsman, SM, Kingsman, AJ (1987) The expression of hybrid HIV: Ty virus-like particles in yeast. *Nature* **329**, 68.

Aksular, M, Calvo-Pinilla, E, Marín-López, A, Ortego, J, Chambers, AC, King, LA, Castillo-Olivares, J (2018) A single dose of African horse sickness virus (AHSV) VP2 based vaccines provides complete clinical protection in a mouse model. *Vaccine* **36**, 7003-7010.

Alberca, B, Bachanek-Bankowska, K, Cabana, M, Calvo-Pinilla, E, Viaplana, E, Frost, L, Gubbins, S, Urniza, A, Mertens, P, Castillo-Olivares, J (2014) Vaccination of horses with a recombinant modified vaccinia Ankara virus (MVA) expressing African horse sickness (AHS) virus major capsid protein VP2 provides complete clinical protection against challenge. *Vaccine* **32**, 3670-4.

Alexander, RA (1934) The immunization of horses and mules against Horse Sickness by means of the neurotropic virus of mice and guinea-pigs. *Onderstepoort J Vet Sci Anim Ind* **2**, 375-391.

Alexander, RA (1935) Studies on the neurotropic virus of horsesickness III: The intracerebral protection test and its application to the study of immunity. *Onderstepoort Journal of veterinary Science and animal Industry* **4**, 349 - 377.

Atabekov, J, Nikitin, N, Arkhipenko, M, Chirkov, S, Karpova, O (2011) Thermal transition of native tobacco mosaic virus and RNA-free viral proteins into spherical nanoparticles. *Journal of General Virology* **92**, 453-456.

Bachmann, MF, Rohrer, UH, Kundig, TM, Burki, K, Hengartner, H, Zinkernagel, RM (1993) The influence of antigen organization on B cell responsiveness. *Science* **262**, 1448.

Barnard, BJH (1998) Epidemiology of African horse sickness and the role of the zebra in South Africa. In: Mellor P.S., Baylis M., Hamblin C., Mertens P.P.C., Calisher C.H. (eds) African Horse Sickness, Springer, Vienna. 13-19.

Barta, A, Sommergruber, K, Thompson, D, Hartmuth, K, Matzke, MA, Matzke, AJM (1986) The expression of a nopaline synthase—human growth hormone chimaeric gene in transformed tobacco and sunflower callus tissue. *Plant Molecular Biology* **6**, 347-357.

Basak, AK, Gouet, P, Grimes, J, Roy, P, Stuart, D (1996) Crystal structure of the top domain of African horse sickness virus VP7: comparisons with bluetongue virus VP7. *J Virol* **70**, 3797-3806.

Basak, AK, Grimes, JM, Gouet, P, Roy, P, Stuart, DI (1997) Structures of orbivirus VP7: implications for the role of this protein in the viral life cycle. *Structure* **5**, 871-883.

Beaton, AR, Rodriguez, J, Reddy, YK, Roy, P (2002) The membrane trafficking protein calpactin forms a complex with bluetongue virus protein NS3 and mediates virus release. *Proceedings of the National Academy of Sciences* **99**, 13154-13159.

Bendahmane, M, Koo, M, Karrer, E, Beachy, RN (1999) Display of epitopes on the surface of tobacco mosaic virus: impact of charge and isoelectric point of the epitope on virus-host interactions1. *Journal of molecular biology* **290**, 9-20.

Bentley, L, Fehrsen, J, Jordaan, F, Huismans, H, Du Plessis, DH (2000) Identification of antigenic regions on VP2 of African horsesickness virus serotype 3 by using phage-displayed epitope libraries. *Journal of General Virology* **81**, 993-1000.

Boorman, J, Mellor, PS, Penn, M, Jennings, M (1975) The growth of African horse-sickness virus in embryonated hen eggs and the transmission of virus byCulicoides variipennis Coquillett (Diptera, Ceratopogonidae). *Archives of virology* **47**, 343-349.

Boyce, M, Celma, CCP, Roy, P (2008) Development of reverse genetics systems for bluetongue virus: recovery of infectious virus from synthetic RNA transcripts. *J Virol* **82**, 8339-8348.

Boyce, M, Celma, CP, Roy, P (2012) Bluetongue virus non-structural protein 1 is a positive regulator of viral protein synthesis. *Virol J* **9**, 178.

Boyce, M, Wehrfritz, J, Noad, R, Roy, P (2004) Purified recombinant bluetongue virus VP1 exhibits RNA replicase activity. *J Virol* **78**, 3994-4002.

Bremer, CW (1976) A gel electrophoretic study of the protein and nucleic acid components of African horsesickness virus. *Onderstepoort J Vet Res* **43**, 193-199.

Bremer, CW, Huismans, H, Van Dijk, AA (1990) Characterization and cloning of the African horsesickness virus genome. *Journal of General Virology* **71**, 793-799.

Brewer, HC, Hird, DA-O, Bailey, AA-O, Seal, SA-O, Foster, GA-O (2018) A guide to the contained use of plant virus infectious clones. *Plant biotechnology journal* **16**, 832-843.

Brillault, L, Jutras, PV, Dashti, N, Thuenemann, EC, Morgan, G, Lomonossoff, GP, Landsberg, MJ, Sainsbury, F (2017) Engineering Recombinant Virus-like Nanoparticles from Plants for Cellular Delivery. *ACS Nano* **11**, 3476 - 3484.

Bruckman, MA, VanMeter, A, Steinmetz, NF (2015) Nanomanufacturing of Tobacco Mosaic Virus-Based Spherical Biomaterials Using a Continuous Flow Method. *ACS Biomaterials Science & Engineering* **1**, 13-18.

Brune, KD, Howarth, M (2018) New Routes and Opportunities for Modular Construction of Particulate Vaccines: Stick, Click, and Glue. *Frontiers in Immunology* **9**, 1432.

Brune, KD, Leneghan, DB, Brian, IJ, Ishizuka, AS, Bachmann, MF, Draper, SJ, Biswas, S, Howarth, M (2016) Plug-and-Display: decoration of Virus-Like Particles via isopeptide bonds for modular immunization. *Scientific Reports* **6**, 19234.

Burrage, TG, Laegreid, WW (1994) African horsesickness: Pathogenesis and immunity. *Comparative immunology, microbiology and infectious diseases* **17**, 275-285.

Burrage, TG, Trevejo, R, Stone-Marschat, M, Laegreid, WW (1993) Neutralizing epitopes of African horsesickness virus serotype 4 are located on VP2. *Virology* **196**, 799-803.

Burroughs, JN, O'Hara, RS, Smale, CJ, Hamblin, C, Walton, A, Armstrong, R, Mertens, PP (1994) Purification and properties of virus particles, infectious subviral particles, cores and VP7 crystals of African horsesickness virus serotype 9. *J Gen Virol* **75 (Pt 8)**, 1849-57.

Calisher, CH, Mertens, PP (1998) Taxonomy of African horse sickness viruses. In: Mellor P.S., Baylis M., Hamblin C., Mertens P.P.C., Calisher C.H. (eds) African Horse Sickness. Springer, Vienna

Calvo-Pinilla, E, de la Poza, F, Gubbins, S, Mertens, PP, Ortego, J, Castillo-Olivares, J (2014) Vaccination of mice with a modified Vaccinia Ankara (MVA) virus expressing the African horse sickness virus (AHSV) capsid protein VP2 induces virus neutralising antibodies that confer protection against AHSV upon passive immunisation. *Virus Res* **180**, 23-30.

Calvo-Pinilla, E, de la Poza, F, Gubbins, S, Mertens, PP, Ortego, J, Castillo-Olivares, J (2015) Antiserum from mice vaccinated with modified vaccinia Ankara virus expressing African horse sickness virus (AHSV) VP2 provides protection when it is administered 48h before, or 48h after challenge. *Antiviral Res* **116**, 27-33.

Calvo-Pinilla, E, Gubbins, S, Mertens, P, Ortego, J, Castillo-Olivares, J (2018) The immunogenicity of recombinant vaccines based on modified Vaccinia Ankara (MVA) viruses expressing African horse sickness virus VP2 antigens depends on the levels of expressed VP2 protein delivered to the host. *Antiviral Res* **154**, 132-139.

Cañizares, MC, Liu, L, Perrin, Y, Tsakiris, E, Lomonossoff, GP (2006) A bipartite system for the constitutive and inducible expression of high levels of foreign proteins in plants. *Plant biotechnology journal* **4**, 183-193.

Carpenter, S, Mellor, PS, Fall, AG, Garros, C, Venter, GJ (2017) African Horse Sickness Virus: History, Transmission, and Current Status. *Annu Rev Entomol* **62**, 343-358.

Caspar, DLD, Klug, A (1962) Physical principles in the construction of regular viruses. *Cold Spring Harbor symposia on quantitative biology* **27**, 1-24.

Castillo-Olivares, J, Calvo-Pinilla E Fau - Casanova, I, Casanova I Fau - Bachanek-Bankowska, K, Bachanek-Bankowska K Fau - Chiam, R, Chiam R Fau - Maan, S, Maan S Fau - Nieto, JM, Nieto Jm Fau - Ortego, J, Ortego J Fau - Mertens, PPC, Mertens, PP (2011a) A modified vaccinia Ankara virus (MVA) vaccine expressing African horse sickness virus (AHSV) VP2 protects against AHSV challenge in an IFNAR -/- mouse model. *PLoS One* **6**, e 16503.

Castillo-Olivares, J, Calvo-Pinilla E Fau - Casanova, I, Casanova I Fau - Bachanek-Bankowska, K, Bachanek-Bankowska K Fau - Chiam, R, Chiam R Fau - Maan, S, Maan S Fau - Nieto, JM, Nieto Jm Fau - Ortego, J, Ortego J Fau - Mertens, PPC, Mertens, PP (2011b) A modified vaccinia Ankara virus (MVA) vaccine expressing African horse sickness virus (AHSV) VP2 protects against AHSV challenge in an IFNAR -/- mouse model.

Celma, CC, Stewart, M, Wernike, K, Eschbaumer, M, Gonzalez-Molleda, L, Breard, E, Schulz, C, Hoffmann, B, Haegeman, A, De Clercq, K (2016) Replication-deficient particles: New insights into the next generation of bluetongue virus vaccines. *J Virol* **91**, e 01892-16.

Celma, CCP, Roy, P (2009) A viral nonstructural protein regulates bluetongue virus trafficking and release. *J Virol* **83**, 6806-6816.

Celma, CCP, Roy, P (2011) Interaction of calpactin light chain (S100A10/p11) and a viral NS protein is essential for intracellular trafficking of non-enveloped Bluetongue virus. *J Virol* **85**, 4783 - 4791.

Chackerian, B (2007) Virus-like particles: flexible platforms for vaccine development. *Expert review of vaccines* **6**, 381-390.

Chen, Q, Lai, H (2013) Plant-derived virus-like particles as vaccines. *Human vaccines & immunotherapeutics* **9**, 26-49.

Chen, Q, Lai, H (2015) Gene delivery into plant cells for recombinant protein production. *BioMed research international* **2015**,

Chiam, R, Sharp, E, Maan, S, Rao, S, Mertens, P, Blacklaws, B, Davis-Poynter, N, Wood, J, Castillo-Olivares, J (2009) Induction of antibody responses to African horse sickness virus (AHSV) in ponies after vaccination with recombinant modified vaccinia Ankara (MVA). *PLoS One* **4**, e5997.

Chuma, T, Le Blois, H, Sanchez-Vizcaino, JM, Diaz-Laviada, M, Roy, P (1992) Expression of the major core antigen VP7 of African horsesickness virus by a recombinant baculovirus and its use as a group-specific diagnostic reagent. *J Gen Virol* **73 (Pt 4)**, 925-31.

Clarke, BE, Newton, SE, Carroll, AR, Francis, MJ, Appleyard, G, Syred, AD, Highfield, PE, Rowlands, DJ, Brown, F (1987) Improved immunogenicity of a peptide epitope after fusion to hepatitis B core protein. *Nature* **330**, 381.

Coetzer, JAW, Erasmus, BJ (1994) African horse sickness. In: Coetzer J.A.W., Thomson, G.R. and Tustin, R.C. (Eds), Infectious diseases of livestock with special reference to southern Africa, Oxford Uiversity Press, Oxford **1**, 460-475.

Coetzer, JAW, Guthrie, AJ (2004) African horse sickness. In: Infectious Diseases of Livestock. (Eds) J.A.W. Coetzer and R.C. Tustin, 2nd Ed. Oxford University Press, Cape Town. **2**, 1231-1246.

Conradie, AM, Stassen, L, Huismans, H, Potgieter, CA, Theron, J (2016) Establishment of different plasmid only-based reverse genetics systems for the recovery of African horse sickness virus. *Virology* **499**, 144-155.

Cottingham, MG, Carroll, MW (2013) Recombinant MVA vaccines: dispelling the myths. *Vaccine* **31**, 4247-4251.

Crafford, JE, Lourens, CW, Smit, TK, Gardner, IA, MacLachlan, NJ, Guthrie, AJ (2014) Serological response of foals to polyvalent and monovalent live-attenuated African horse sickness virus vaccines. *Vaccine* **32**, 3611-6.

D'Aoust, MA, Couture, MMJ, Charland, N, Trepanier, S, Landry, N, Ors, F, Vézina, LP (2010) The production of hemagglutinin-based virus-like particles in plants: a rapid, efficient and safe response to pandemic influenza. *Plant biotechnology journal* **8**, 607-619.

Darpel, K, Batten, C, Veronesi, E, Shaw, A, Anthony, S, Bachanek-Bankowska, K, Kgosana, L, Bin-Tarif, A, Carpenter, S, Müller-Doblies, U (2007) Clinical signs and pathology shown by British sheep and cattle infected with bluetongue virus serotype 8 derived from the 2006 outbreak in northern Europe. *Vet Rec* **161**, 253-261.

de la Grandiere, MA, Dal Pozzo, F, Tignon, M, Zonta, W, Thiry, D, Mauroy, A, Mathijs, E, Caij, AB, Saegerman, C, Thiry, E (2014) Study of the virulence of serotypes 4 and 9 of African horse sickness virus in IFNAR(-/-), Balb/C and 129 Sv/Ev mice. *Vet Microbiol* **174**, 322-32.

de la Poza, F, Marin-Lopez, A, Castillo-Olivares, J, Calvo-Pinilla, E, Ortego, J (2015) Identification of CD8 T cell epitopes in VP2 and NS1 proteins of African horse sickness virus in IFNAR(-/-) mice. *Virus Res* **210**, 149-53.

de Vos, CJ, Hoek, CA, Nodelijk, G (2012) Risk of introducing African horse sickness virus into the Netherlands by international equine movements. *Prev Vet Med* **106**, 108-22.

Delpeyroux, F, Chenciner, N, Lim, A, Malpiece, Y, Blondel, B, Crainic, R, Van der Werf, S, Streeck, RE (1986) A poliovirus neutralization epitope expressed on hybrid hepatitis B surface antigen particles. *Science* **233**, 472-475.

Dennis, S, J., Meyers, A, E., Guthrie, A, J., Hitzeroth, I, I., Rybicki, E, P. (2018a) Immunogenicity of plant-produced African horse sickness virus-like particles: implications for a novel vaccine. *Plant biotechnology journal* **16**, 442-450.

Dennis, SJ, O'Kennedy, MM, Rutkowska, D, Tsekoa, T, Lourens, CW, Hitzeroth, II, Meyers, AE, Rybicki, EP (2018b) Safety and immunogenicity of plant-produced African horse sickness virus-like particles in horses. *Veterinary research* **49**, 105.

Du Plessis, M, Cloete, M, Aitchison, H, Van Dijk, AA (1998) Protein aggregation complicates the development of baculovirus-expressed African horsesickness virus serotype 5 VP2 subunit vaccines. *Onderstepoort Journal of Veterinary Research* **65**, 321-329.

Du Toit, RM (1944) The transmission of bluetongue and horse sickness by Culicoides. *Onderstepoort Journal of veterinary Science and animal Industry* **19**, 7-16.

El Garch, H, Crafford, JE, Amouyal, P, Durand, PY, Edlund Toulemonde, C, Lemaitre, L, Cozette, V, Guthrie, A, Minke, JM (2012) An African horse sickness virus serotype 4 recombinant canarypox virus vaccine elicits specific cell-mediated immune responses in horses. *Vet Immunol Immunopathol* **149**, 76-85.

Erasmus, B (1978) A new approach to polyvalent immunization against African horsesickness. In:Proceedings of the 4th International Conference on Equine Infectious Diseases. Eds: J.T. Bryans & H. Gerber, Veterinary Publications, Princeton. 401-403.
Erasmus, BJ (1963a) Cultivation of horsesickness virus in tissue culture. *Nature* **200**, 716.
Erasmus, BJ (1963b) Preliminary observations on the value of the guinea-pig in determining the innocuity and antigenicity of neurotropic attenuated horsesickness strains. *Onderstepoort Journal of Veterinary Research* **30**, 11 - 22.
Erasmus, BJ (1974) The pathogenesis of African horsesickness. In 'Equine Infectious Diseases.' pp. 1-11. (Karger Publishers)
Feenstra, F, Pap, JS, van Rijn, PA (2015) Application of bluetongue Disabled Infectious Single Animal (DISA) vaccine for different serotypes by VP2 exchange or incorporation of chimeric VP2. *Vaccine* **33**, 812-8.
Fischer, R, Schillberg, S, F Buyel, J, M Twyman, R (2013) Commercial aspects of pharmaceutical protein production in plants. *Current pharmaceutical design* **19**, 5471-5477.
Fischer, R, Stoger, E, Schillberg, S, Christou, P, Twyman, RM (2004) Plant-based production of biopharmaceuticals. *Current opinion in plant biology* **7**, 152-158.
Fitchen, J, Beachy, RN, Hein, MB (1995) Plant virus expressing hybrid coat protein with added murine epitope elicits autoantibody response. *Vaccine* **13**, 1051-1057.
Forzan, M, Marsh, M, Roy, P (2007) Bluetongue virus entry into cells. *J Virol* **81**, 4819-4827.
Forzan, M, Wirblich, C, Roy, P (2004) A capsid protein of nonenveloped Bluetongue virus exhibits membrane fusion activity. *Proceedings of the National Academy of Sciences* **101**, 2100-2105.
Fraenkel-Conrat, H, Williams, RC (1955) Reconstitution of active tobacco mosaic virus from its inactive protein and nucleic acid components. *Proceedings of the National Academy of Sciences* **41**, 690-698.
French, TJ, Marshall, JJ, Roy, P (1990) Assembly of double-shelled, viruslike particles of bluetongue virus by the simultaneous expression of four structural proteins. *J Virol* **64**, 5695-5700.
Fuenmayor, J, Gòdia, F, Cervera, L (2017) Production of virus-like particles for vaccines. *New Biotechnology* **39**, 174-180.
Gaddipati, JP, Siegel, A (1990) Study of TMV assembly with heterologous RNA containing the origin-of-assembly sequence. *Virology* **174**, 337-344.
Gasanova, T, Petukhova, N, Ivanov, P (2016) Chimeric particles of tobacco mosaic virus as a platform for the development of next-generation nanovaccines. *Nanotechnologies in Russia* **11**, 227-236.
Gecchele, E, Merlin, M, Brozzetti, A, Falorni, A, Pezzotti, M, Avesani, L (2015) A comparative analysis of recombinant protein expression in different biofactories: bacteria, insect cells and plant systems. *J Vis Exp*
Gilbert, SC (2013) Clinical development of Modified Vaccinia virus Ankara vaccines. *Vaccine* **31**, 4241-4246.
Giritch, A, Marillonnet, S, Engler, C, van Eldik, G, Botterman, J, Klimyuk, V, Gleba, Y (2006) Rapid high-yield expression of full-size IgG antibodies in plants coinfected with noncompeting viral vectors. *Proceedings of the National Academy of Sciences* **103**, 14701-14706.
Gleba, Y, Klimyuk, V, Marillonnet, S (2005) Magnifection—a new platform for expressing recombinant vaccines in plants. *Vaccine* **23**, 2042-2048.
Goelet, P, Lomonossoff, G, Butler, P, Akam, M, Gait, M, Karn, J (1982) Nucleotide sequence of tobacco mosaic virus RNA. *Proceedings of the National Academy of Sciences* **79**, 5818-5822.
Goodin, MM, Zaitlin, D, Naidu, RA, Lommel, SA (2008) Nicotiana benthamiana: its history and future as a model for plant–pathogen interactions. *Molecular plant-microbe interactions* **21**, 1015-1026.
Gouet, P, Diprose, JM, Grimes, JM, Malby, R, Burroughs, JN, Zientara, S, Stuart, DI, Mertens, PP (1999) The highly ordered double-stranded RNA genome of bluetongue virus revealed by crystallography. *Cell* **97**, 481-490.
Grewar, JD, Weyer, CT, Guthrie, AJ, Koen, P, Davey, S, Quan, M, Visser, D, Russouw, E, Bührmann, G (2013) The 2011 outbreak of African horse sickness in the African horse sickness controlled area in South Africa. *J S Afr Vet Assoc* **84**, 1-7.
Grewar, JD, Weyer, CT, Venter, GJ, van Helden, LS, Burger, P, Guthrie, AJ, Coetzee, P, Labuschagne, K, Bührmann, G, Parker, BJ, Thompson, PN (2018) A field investigation of an African horse sickness outbreak in the controlled area of South Africa in 2016. *Transbound Emerg Dis* **0**,
Grgacic, EV, Anderson, DA (2006) Virus-like particles: passport to immune recognition. *Methods* **40**, 60-65.

Grimes, J, Basak, AK, Roy, P, Stuart, D (1995) The crystal structure of bluetongue virus VP7. *Nature* **373**, 167.
Grimes, JM, Burroughs, JN, Gouet, P, Diprose, JM, Malby, R, Zientara, S, Mertens, PPC, Stuart, DI (1998) The atomic structure of the bluetongue virus core. *Nature* **395**, 470-478.
Grimes, JM, Jakana, J, Ghosh, M, Basak, AK, Roy, P, Chiu, W, Stuart, DI, Prasad, BVV (1997) An atomic model of the outer layer of the bluetongue virus core derived from X-ray crystallography and electron cryomicroscopy. *Structure* **5**, 885-893.
Grubman, MJ, Lewis, SA (1992) Identification and characterization of the structural and nonstructural proteins of African horsesickness virus and determination of the genome coding assignments. *Virology* **186**, 444-451.
Gustafsson, C, Govindarajan, S, Minshull, J (2004) Codon bias and heterologous protein expression. *Trends in Biotechnology* **22**, 346-353.
Guthrie, AJ, Quan, M, Lourens, CW, Audonnet, JC, Minke, JM, Yao, J, He, L, Nordgren, R, Gardner, IA, Maclachlan, NJ (2009) Protective immunization of horses with a recombinant canarypox virus vectored vaccine co-expressing genes encoding the outer capsid proteins of African horse sickness virus. *Vaccine* **27**, 4434-8.
Hassan, SH, Wirblich, C, Forzan, M, Roy, P (2001) Expression and functional characterization of bluetongue virus VP5 protein: role in cellular permeabilization. *J Virol* **75**, 8356-8367.
Haynes, JR, Cunningham, J, Von Seefried, A, Lennick, M, Garvin, RT, Shen, S-H (1986) Development of a Genetically–Engineered, Candidate Polio Vaccine Employing the Self–Assembling Properties of the Tobacco Mosaic Virus Coat Protein. *Nature Biotechnology* **4**, 637.
Henning, MW (1956) African Horse Sickness, Perdesiekte, Pestis Equorum. In: Animal Diseases of South Africa, Central News agency Ltd., Pretoria, South Africa **2**, 785 - 808.
Herholz, C, Fussel, AE, Timoney, P, Schwermer, H, Bruckner, L, Leadon, D (2008) Equine travellers to the Olympic Games in Hong Kong 2008: A review of worldwide challenges to equine health, with particular reference to vector-borne diseases. *Equine Vet J* **40**, 87-95.
Hewat, EA, Booth, TF, Roy, P (1992) Structure of bluetongue virus particles by cryoelectron microscopy. *Journal of Structural Biology* **109**, 61-69.
Hewat, EA, Booth, TF, Roy, P (1994) Structure of Correctly Self-Assembled Bluetongue Virus-like Particles. *Journal of Structural Biology* **112**, 183-191.
Hiatt, A, Caffferkey, R, Bowdish, K (1989) Production of antibodies in transgenic plants. *Nature* **342**, 76.
Hopley, R, Toth, B (2013) Focus on: African horse sickness. *Vet Rec* **173**, 13-4.
House, JA (1993) Recommendations for African horse sickness vaccines for use in nonendemic areas. *Revue d'élevage et de médecine vétérinaire des pays tropicaux* **46**, 77 - 81.
Howell, PG (1962) The isolation and identification of further antigenic types of African horsesickness virus. *Onderstepoort Journal of Veterinary Research* **29**, 139 - 149.
Huang, Z, Chen, Q, Hjelm, B, Arntzen, C, Mason, H (2009) A DNA replicon system for rapid high-level production of virus-like particles in plants. *Biotechnology and bioengineering* **103**, 706-714.
Iwata, H, Yamagaw, M, Roy, P (1992) Evolutionary relationships among the gnat-transmitted orbiviruses that cause African horse sickness, bluetongue, and epizootic hemorrhagic disease as evidenced by their capsid protein sequences. *Virology* **191**, 251-261.
Janitzek, CM, Matondo, S, Thrane, S, Nielsen, MA, Kavishe, R, Mwakalinga, SB, Theander, TG, Salanti, A, Sander, AF (2016) Bacterial superglue generates a full-length circumsporozoite protein virus-like particle vaccine capable of inducing high and durable antibody responses. *Malaria Journal* **15**, 545.
Jennings, GT, Bachmann, MF (2008) The coming of age of virus-like particle vaccines. *Biol Chem* **389**, 521-536.
Jeong, H, Seong, BL (2017) Exploiting virus-like particles as innovative vaccines against emerging viral infections. *J Microbiol* **55**, 220-230.
Kanai, Y, van Rijn, PA, Maris-Veldhuis, M, Kaname, Y, Athmaram, TN, Roy, P (2014) Immunogenicity of recombinant VP2 proteins of all nine serotypes of African horse sickness virus. *Vaccine* **32**, 4932-7.
Kaname, Y, Celma, CC, Kanai, Y, Roy, P (2013) Recovery of African horse sickness virus from synthetic RNA. *J Gen Virol* **94**, 2259-65.
Kar, AK, Bhattacharya, B, Roy, P (2007) Bluetongue virus RNA binding protein NS2 is a modulator of viral replication and assembly. *BMC molecular biology* **8**, 4.
Karpova, O, Nikitin, N, Chirkov, S, Trifonova, E, Sheveleva, A, Lazareva, E, Atabekov, J (2012) Immunogenic compositions assembled from tobacco mosaic virus-generated spherical particle platforms and foreign antigens. *Journal of General Virology* **93**, 400-407.

Kudla, G, Murray, AW, Tollervey, D, Plotkin, JB (2009) Coding-sequence determinants of gene expression in Escherichia coli. *Science (New York, N.Y.)* **324**, 255-258.
Kushnir, N, Streatfield, SJ, Yusibov, V (2012) Virus-like particles as a highly efficient vaccine platform: diversity of targets and production systems and advances in clinical development. *Vaccine* **31**, 58-83.
Lai, H, Chen, Q (2012) Bioprocessing of plant-derived virus-like particles of Norwalk virus capsid protein under current Good Manufacture Practice regulations. *Plant Cell Reports* **31**, 573-584.
Lam, P, Steinmetz, NF (2018) Plant viral and bacteriophage delivery of nucleic acid therapeutics. *Wiley Interdisciplinary Reviews: Nanomedicine and Nanobiotechnology* **10**, e1487.
Landry, N, Ward, BJ, Trépanier, S, Montomoli, E, Dargis, M, Lapini, G, Vézina, L-P (2010) Preclinical and clinical development of plant-made virus-like particle vaccine against avian H5N1 influenza. *PLoS One* **5**, e15559.
Lechner, F, Jegerlehner, A, Tissot, AC, Maurer, P, Sebbel, P, Renner, WA, Jennings, GT, Bachmann, MF (2002) Virus-Like Particles as a Modular System for Novel Vaccines. *Intervirology* **45**, 212-217.
Lelli, R, Molini, U, Ronchi, GF, Rossi, E, Franchi, P, Ulisse, S, Armillotta, G, Capista, S, Khaiseb, S, Di Ventura, M (2013) Inactivated and adjuvanted vaccine for the control of the African horse sickness virus serotype 9 infection: evaluation of efficacy in horses and guinea-pig model. *Veterinaria italiana* **49**, 89-98.
Limn, C-K, Roy, P (2003) Intermolecular interactions in a two-layered viral capsid that requires a complex symmetry mismatch. *J Virol* **77**, 11114-11124.
Limn, C-K, Staeuber, N, Monastyrskaya, K, Gouet, P, Roy, P (2000) Functional dissection of the major structural protein of bluetongue virus: identification of key residues within VP7 essential for capsid assembly. *J Virol* **74**, 8658-8669.
Lindbo, JA (2007) TRBO: a high-efficiency tobacco mosaic virus RNA-based overexpression vector. *Plant physiology* **145**, 1232-1240.
Lippincott-Schwartz, J, Snapp, E, Kenworthy, A (2001) Studying protein dynamics in living cells. *Nature reviews Molecular cell biology* **2**, 444.
Lomonossoff, GP, D'Aoust, M-A (2016) Plant-produced biopharmaceuticals: a case of technical developments driving clinical deployment. *Science* **353**, 1237-1240.
Lourenco, S, Roy, P (2011) In vitro reconstitution of Bluetongue virus infectious cores. *Proceedings of the National Academy of Sciences* **108**, 13746-13751.
Love, AJ, Chapman, SN, Matic, S, Noris, E, Lomonossoff, GP, Taliansky, M (2012) In planta production of a candidate vaccine against bovine papillomavirus type 1. *Planta* **236**, 1305-1313.
Lua, LHL, Connors, NK, Sainsbury, F, Chuan, YP, Wibowo, N, Middelberg, APJ (2014) Bioengineering virus-like particles as vaccines. *Biotechnology and bioengineering* **111**, 425-440.
Lubroth, J (1988) African Horsesickness and the epizootic in Spain, 1987. *Equine Practices* **10**, 26-33.
Lulla, V, Losada, A, Lecollinet, S, Kerviel, A, Lilin, T, Sailleau, C, Beck, C, Zientara, S, Roy, P (2017) Protective efficacy of multivalent replication-abortive vaccine strains in horses against African horse sickness virus challenge. *Vaccine* **35**, 4262-4269.
Lulla, V, Lulla, A, Wernike, K, Aebischer, A, Beer, M, Roy, P (2016) Assembly of Replication-Incompetent African Horse Sickness Virus Particles: Rational Design of Vaccines for All Serotypes. *J Virol* **90**, 7405-14.
M'Fadyean, J (1900) African horse-sickness. *Journal of Comparative Pathology and Therapeutics* **13**, 1-20.
Ma, JKC, Drake, PMW, Christou, P (2003) Genetic modification: the production of recombinant pharmaceutical proteins in plants. *Nature Reviews Genetics* **4**, 794.
Mach, H, Volkin, DB, Troutman, RD, Wang, BEI, Luo, Z, Jansen, KU, Shi, L (2006) Disassembly and reassembly of yeast-derived recombinant human papillomavirus virus-like particles (HPV VLPs). *Journal of pharmaceutical sciences* **95**, 2195-2206.
MacLachlan, NJ, Balasuriya, UB, Davis, NL, Collier, M, Johnston, RE, Ferraro, GL, Guthrie, AJ (2007) Experiences with new generation vaccines against equine viral arteritis, West Nile disease and African horse sickness. *Vaccine* **25**, 5577-5582.
Maclean, J, Koekemoer, M, Olivier, A, Stewart, D, Hitzeroth, I, Rademacher, T, Fischer, R, Williamson, A, Rybicki, E (2007) Optimization of human papillomavirus type 16 (HPV-16) L1 expression in plants: comparison of the suitability of different HPV-16 L1 gene variants and different cell-compartment localization. *Journal of General Virology* **88**, 1460-1469.
Maharaj, PD, Mallajosyula, JK, Lee, G, Thi, P, Zhou, Y, Kearney, CM, McCormick, AA (2014) Nanoparticle encapsidation of Flock house virus by auto assembly of Tobacco mosaic virus coat protein. *International journal of molecular sciences* **15**, 18540-18556.

Manning, NM, Bachanek-Bankowska, K, Mertens, PPC, Castillo-Olivares, J (2017) Vaccination with recombinant Modified Vaccinia Ankara (MVA) viruses expressing single African horse sickness virus VP2 antigens induced cross-reactive virus neutralising antibodies (VNAb) in horses when administered in combination. *Vaccine* **35**, 6024-6029.

Manole, V, Laurinmaki, P, Van Wyngaardt, W, Potgieter, CA, Wright, IM, Venter, GJ, van Dijk, AA, Sewell, BT, Butcher, SJ (2012) Structural insight into African horsesickness virus infection. *J Virol* **86**, 7858-66.

Marchi, PR, Rawlings, P, Burroughs, JN, Wellby, M, Mertens, PPC, Mellor, PS, Wade-Evans, AM (1995) Proteolytic cleavage of VP2, an outer capsid protein of African horse sickness virus, by species-specific serum proteases enhances infectivity in Culicoides. *Journal of General Virology* **76**, 2607-2611.

Maree, S, Durbach, S, Huismans, H (1998) Intracellular production of African horsesickness virus core-like particles by expression of the two major core proteins, VP3 and VP7, in insect cells. *J Gen Virol* **79 (Pt 2)**, 333-7.

Maree, S, Maree, FF, Putterill, JF, de Beer, TA, Huismans, H, Theron, J (2016) Synthesis of empty african horse sickness virus particles. *Virus Res* **213**, 184-94.

Maree, S, Paweska, JT (2005) Preparation of recombinant African horse sickness virus VP7 antigen via a simple method and validation of a VP7-based indirect ELISA for the detection of group-specific IgG antibodies in horse sera. *J Virol Methods* **125**, 55-65.

Martin, A, Wychowski, C, Couderc, T, Crainic, R, Hogle, J, Girard, M (1988) Engineering a poliovirus type 2 antigenic site on a type 1 capsid results in a chimaeric virus which is neurovirulent for mice. *The EMBO journal* **7**, 2839-2847.

Martinez-Torrecuadrada, JL, Casal, JI (1995) Identification of a linear neutralization domain in the protein VP2 of African horse sickness virus. *Virology* **210**, 391-9.

Martinez-Torrecuadrada, JL, Diaz-Laviada, M, Roy, P, Sanchez, C, Vela, C, Sanchez-Vizcaino, JM, Casal, JI (1996) Full protection against African horsesickness (AHS) in horses induced by baculovirus-derived AHS virus serotype 4 VP2, VP5 and VP7. *J Gen Virol* **77 (Pt 6)**, 1211-21.

Martinez-Torrecuadrada, JL, Langeveld, JP, Meloen, RH, Casal, JI (2001) Definition of neutralizing sites on African horse sickness virus serotype 4 VP2 at the level of peptides. *J Gen Virol* **82**, 2415-24.

Mason, HS, Lam, DM, Arntzen, CJ (1992) Expression of hepatitis B surface antigen in transgenic plants. *Proceedings of the National Academy of Sciences* **89**, 11745-11749.

Mathebula, EM, Faber, FE, van Wyngaardt, W, van Schalkwyk, A, Pretorius, A, Fehrsen, J (2017) B-cell epitopes of African horse sickness virus serotype 4 recognised by immune horse sera. *Onderstepoort Journal of Veterinary Research* **84**, 1-12.

Matsuo, E, Celma, CC, Roy, P (2010) A reverse genetics system of African horse sickness virus reveals existence of primary replication. *FEBS Lett* **584**, 3386-91.

Mbewana, S, Meyers, AE, Rybicki, EP (2018) Chimaeric Rift Valley fever virus-like particle vaccine candidate production in Nicotiana benthamiana. *Biotechnol J* 1800238.

McIntosh, BM (1955) Horsesickness antibodies in the sera of dogs in enzootic areas. *J S Afr Vet Assoc* **26**, 269-272.

McIntosh, BM (1958) Immunological types of horsesickness virus and their significance in immunization. *Onderstepoort Journal of Veterinary Research* **27**, 465 - 536.

Meiswinkel, R, Baylis, M, Labuschagne, K (2000) Stabling and the protection of horses from Culicoides bolitinos (Diptera: Ceratopogonidae), a recently identified vector of African horse sickness. *Bulletin of Entomological Research* **90**, 509-515.

Mellor, P (1993) African horse sickness: transmission and epidemiology. *Vet Res* **24**, 199-212.

Mellor, PS, Boorman, J, Jennings, M (1975) The multiplication of African horse-sickness virus in two species ofCulicoides (Diptera, Ceratopogonidae). *Archives of virology* **47**, 351-356.

Mellor, PS, Hamblin, C (2004) African horse sickness. *Vet Res* **35**, 445-66.

Merlin, M, Gecchele, E, Capaldi, S, Pezzotti, M, Avesani, L (2014) Comparative evaluation of recombinant protein production in different biofactories: the green perspective. *BioMed research international* **2014**,

Mertens, PPC, Burroughs, JN, Walton, A, Wellby, MP, Fu, H, O'Hara, RS, Brookes, SM, Mellor, PS (1996) Enhanced infectivity of modified bluetongue virus particles for two insect cell lines and for TwoCulicoidesVector species. *Virology* **217**, 582-593.

Mirchamsy, H, Hazrati, A (1973) A review on etiology and pathogeny of African horse sickness. *Arch Razi Inst* **25**, 23-46.

Mirchamsy, H, Taslimi, H (1968) Inactivated African horse sickness virus cell culture vaccine. *Immunology* **14**, 81.

Modrof, J, Lymperopoulos, K, Roy, P (2005) Phosphorylation of bluetongue virus nonstructural protein 2 is essential for formation of viral inclusion bodies. *J Virol* **79**, 10023-10031.
Mohl, B-P, Roy, P (2016) Cellular casein kinase 2 and protein phosphatase 2A modulate replication site assembly of bluetongue virus. *Journal of Biological Chemistry* jbc-M116.
Mohsen, MA-O, Gomes, AC, Vogel, M, Bachmann, MF (2018) Interaction of Viral Capsid-Derived Virus-Like Particles (VLPs) with the Innate Immune System. *Vaccines (Basel)* **6**, 37.
Molini, U, Marucchella, G, Maseke, A, Ronchi, GF, Di Ventura, M, Salini, R, Scacchia, M, Pini, A (2015) Immunization of horses with a polyvalent live-attenuated African horse sickness vaccine: Serological response and disease occurrence under field conditions. *Trials in Vaccinology* **4**, 24-28.
Nandi, S, McDonald, KA, Hefferon, K (2014) Expression of Recombinant Proteins in Plant Cell Culture. *Plant-derived Pharmaceuticals: Principles and Applications for Developing Countries* 20.
Nason, EL, Rothagel, R, Mukherjee, SK, Kar, AK, Forzan, M, Prasad, BV, Roy, P (2004) Interactions between the inner and outer capsids of bluetongue virus. *J Virol* **78**, 8059-8067.
Nikitin, NA, Malinin, AS, Trifonova, EA, Rakhnyanskaya, AA, Yaroslavov, AA, Karpova, OV, Atabekov, JG (2014) Proteins immobilization on the surface of modified plant viral particles coated with hydrophobic polycations. *Journal of Biomaterials Science, Polymer Edition* **25**, 1743-1754.
Noad, R, Roy, P (2003) Virus-like particles as immunogens. *Trends in Microbiology* **11**, 438-444.
Oellermann, R, Els, H, Erasmus, B (1970) Characterization of African horsesiekness virus. *Arch Gesamte Virusforsch* **29**, 163-174.
Palladini, A, Thrane, S, Janitzek, CM, Pihl, J, Clemmensen, SB, de Jongh, WA, Clausen, TM, Nicoletti, G, Landuzzi, L, Penichet, ML, Balboni, T, Ianzano, ML, Giusti, V, Theander, TG, Nielsen, MA, Salanti, A, Lollini, PL, Nanni, P, Sander, AF (2018) Virus-like particle display of HER2 induces potent anti-cancer responses. *Oncoimmunology* **7**, e1408749.
Patel, A, Roy, P (2014) The molecular biology of Bluetongue virus replication. *Virus Res* **182**, 5-20.
Pattenden, LK, Middelberg, APJ, Niebert, M, Lipin, DI (2005) Towards the preparative and large-scale precision manufacture of virus-like particles. *Trends in Biotechnology* **23**, 523-529.
Peyret, H, Lomonossoff, GP (2015) When plant virology met Agrobacterium: the rise of the deconstructed clones. *Plant biotechnology journal* **13**, 1121-1135.
Potgieter, AC, Cloete, M, Pretorius, PJ, van Dijk, AA (2003) A first full outer capsid protein sequence data-set in the Orbivirus genus (family Reoviridae): cloning, sequencing, expression and analysis of a complete set of full-length outer capsid VP2 genes of the nine African horsesickness virus serotypes. *J Gen Virol* **84**, 1317-26.
Potgieter, AC, Page, NA, Liebenberg, J, Wright, IM, Landt, O, Van Dijk, AA (2009) Improved strategies for sequence-independent amplification and sequencing of viral double-stranded RNA genomes. *Journal of General Virology* **90**, 1423-1432.
Pretorius, A, Van Kleef, M, Van Wyngaardt, W, Heath, J (2012) Virus-specific CD8+ T-cells detected in PBMC from horses vaccinated against African horse sickness virus. *Vet Immunol Immunopathol* **146**, 81-86.
Pushko, P, Pumpens, P, Grens, E (2013) Development of virus-like particle technology from small highly symmetric to large complex virus-like particle structures. *Intervirology* **56**, 141-165.
Quan, M, Van Vuuren, M, Howell, PG, Groenewald, D, Guthrie, AJ (2008) Molecular epidemiology of the African horse sickness virus S10 gene. *Journal of General Virology* **89**, 1159-1168.
Ramadevi, N, Burroughs, NJ, Mertens, PPC, Jones, IM, Roy, P (1998) Capping and methylation of mRNA by purified recombinant VP4 protein of bluetongue virus. *Proceedings of the National Academy of Sciences* **95**, 13537-13542.
Ratinier, M, Caporale, M, Golder, M, Franzoni, G, Allan, K, Nunes, SF, Armezzani, A, Bayoumy, A, Rixon, F, Shaw, A (2011) Identification and characterization of a novel non-structural protein of bluetongue virus. *PLoS pathogens* **7**, e1002477.
Regnard, GL, Halley-Stott, RP, Tanzer, FL, Hitzeroth, II, Rybicki, EP (2010) High level protein expression in plants through the use of a novel autonomously replicating geminivirus shuttle vector. *Plant biotechnology journal* **8**, 38-46.
Rodriguez, M, Hooghuis, H, Castaño, M (1992) African horse sickness in Spain. *Veterinary Microbiology* **33**, 129-142.
Romito, M, Du Plessis, DH, Viljoen, GJ (1999) Immune responses in a horse inoculated with the VP2 gene of African horsesickness virus. *Onderstepoort J Vet Res* **66**, 139-44.
Ronchi, GF, Ulisse, S, Rossi, E, Franchi, P, Armillotta, G, Capista, S, Peccio, A, Di Ventura, M, Pini, A (2012) Immunogenicity of two adjuvant formulations of an inactivated African horse sickness vaccine in guinea-pigs and target animals. *Vet Ital* **48**, 55-76.

Roy, P (2004) Genetically engineered structure-based vaccine for bluetongue disease. *Vet Ital* **40**, 594-600.
Roy, P (2017) Bluetongue virus structure and assembly. *Current Opinion in Virology* **24**, 115-123.
Roy, P, Bishop, DH, Howard, S, Aitchison, H, Erasmus, B (1996) Recombinant baculovirus-synthesized African horsesickness virus (AHSV) outer-capsid protein VP2 provides protection against virulent AHSV challenge. *J Gen Virol* **77 (Pt 9)**, 2053-7.
Roy, P, Bishop, DHL, LeBlois, H, Erasmus, BJ (1994a) Long-lasting protection of sheep against bluetongue challenge after vaccination with virus-like particles: evidence for homologous and partial heterologous protection. *Vaccine* **12**, 805-811.
Roy, P, French, T, Erasmus, B (1992) Protective efficacy of virus-like particles for bluetongue disease. *Vaccine* **10**, 28-32.
Roy, P, Hirasawa, T, Fernandez, M, Blinov, VM, Rodrique, S-VJM (1991) The complete sequence of the group-specific antigen, VP7, of African horsesickness disease virus serotype 4 reveals a close relationship to bluetongue virus. *Journal of General Virology* **72**, 1237-1241.
Roy, P, Mertens, PP, Casal, I (1994b) African horse sickness virus structure. *Comparative immunology, microbiology and infectious diseases* **17**, 243-273.
Roy, P, Noad, R (2006) Bluetongue virus assembly and morphogenesis. In: Roy P. (eds) Reoviruses: Entry, Assembly and Morphogenesis. Current Topics in Microbiology and Immunology, Springer, Berlin, Heidelberg **309**, 87-116.
Roy, P, Sutton, G (1998) New generation of African horse sickness virus vaccines based on structural and molecular studies of the virus particles. *Arch Virol Suppl* **14**, 177-202.
Ruoslahti, E (1996) RGD AND OTHER RECOGNITION SEQUENCES FOR INTEGRINS. *Annual Review of Cell and Developmental Biology* **12**, 697-715.
Rutgers, T, Gordon, D, Gathoye, AM, Hollingdale, M, Hockmeyer, W, Rosenberg, M, Wilde, MD (1988) Hepatitis B Surface Antigen as Carrier Matrix for the Repetitive Epitope of the Circumsporozoite Protein of Plasmodium Falciparum. *Bio/Technology* **6**, 1065-1070.
Rutkowska, DA, Meyer, QC, Maree, F, Vosloo, W, Fick, W, Huismans, H (2011) The use of soluble African horse sickness viral protein 7 as an antigen delivery and presentation system. *Virus Res* **156**, 35-48.
Rybicki, E (2018) History and Promise of Plant-Made Vaccines for Animals. In 'Prospects of Plant-Based Vaccines in Veterinary Medicine.' (Ed. J MacDonald.) pp. 1-22. (Springer International Publishing: Cham)
Rybicki, EP (2009) Plant-produced vaccines: promise and reality. *Drug discovery today* **14**, 16-24.
Rybicki, EP (2010) Plant-made vaccines for humans and animals. *Plant biotechnology journal* **8**, 620-637.
Rybicki, EP (2014) Plant-based vaccines against viruses. *Virol J* **11**, 205.
Sailleau, C, Hamblin, C, Paweska, J, Zientara, S (2000) Identification and differentiation of the nine African horse sickness virus serotypes by RT–PCR amplification of the serotype-specific genome segment 2. *Journal of General Virology* **81**, 831-837.
Sainsbury, F, Lomonossoff, GP (2008) Extremely high-level and rapid transient protein production in plants without the use of viral replication. *Plant Physiol* **148**, 1212-8.
Sainsbury, F, Thuenemann, EC, Lomonossoff, GP (2009) pEAQ: versatile expression vectors for easy and quick transient expression of heterologous proteins in plants. *Plant Biotechnol J* **7**, 682-93.
Sambrook, J, Fritsch, EF, Maniatis, T (1989) 'Molecular cloning: a laboratory manual.' (Cold spring harbor laboratory press:
Saunders, K, Lomonossoff, GP (2017) In Planta Synthesis of Designer-Length Tobacco Mosaic Virus-Based Nano-Rods That Can Be Used to Fabricate Nano-Wires. *Frontiers in Plant Science* **8**,
Scanlen, M, Paweska, JT, Verschoor, JA, van Dijk, AA (2002) The protective efficacy of a recombinant VP2-based African horsesickness subunit vaccine candidate is determined by adjuvant. *Vaccine* **20**, 1079-88.
Scholthof, HB (2005) Plant virus transport: motions of functional equivalence. *Trends in plant science* **10**, 376-382.
Scotti, N, Rybicki, EP (2013) Virus-like particles produced in plants as potential vaccines. *Expert review of vaccines* **12**, 211-224.
Shen, W-J, Forde, BG (1989) Efficient transformation of Agrobacterium spp. by high voltage electroporation. *Nucleic acids research* **17**, 8385.
Shevchenko, A, Tomas, H, Havli, J, Olsen, JV, Mann, M (2007) In-gel digestion for mass spectrometric characterization of proteins and proteomes. *Nature protocols* **1**, 2856-2860.
Shoji, Y, Prokhnevsky, A, Leffet, B, Vetter, N, Tottey, S, Satinover, S, Musiychuk, K, Shamloul, M, Norikane, J, Jones, RM, Chichester, JA, Green, BJ, Streatfield, SJ, Yusibov, V (2015)

Immunogenicity of H1N1 influenza virus-like particles produced in Nicotiana benthamiana. *Human vaccines & immunotherapeutics* **11**, 118-123.
Singh, SK, Thrane, S, Janitzek, CM, Nielsen, MA, Theander, TG, Theisen, M, Salanti, A, Sander, AF (2017) Improving the malaria transmission-blocking activity of a Plasmodium falciparum 48/45 based vaccine antigen by SpyTag/SpyCatcher mediated virus-like display. *Vaccine* **35**, 3726 - 3732.
Smith, M, Fitzmaurice, W, Turpen, T, Palmer, K (2009) Display of peptides on the surface of tobacco mosaic virus particles. In: Karasev A.V. (eds) Plant-produced Microbial Vaccines. Current Topics in Microbiology and Immunology, Springer, Berlin, Heidelberg **332**, 13-31.
Smith, ML, Corbo, T, Bernales, J, Lindbo, JA, Pogue, GP, Palmer, KE, McCormick, AA (2007) Assembly of trans-encapsidated recombinant viral vectors engineered from Tobacco mosaic virus and Semliki Forest virus and their evaluation as immunogens. *Virology* **358**, 321-333.
Stewart, M, Bhatia, Y, Athmaran, TN, Noad, R, Gastaldi, C, Dubois, E, Russo, P, Thiéry, R, Sailleau, C, Bréard, E, Zientara, S, Roy, P (2010) Validation of a novel approach for the rapid production of immunogenic virus-like particles for bluetongue virus. *Vaccine* **28**, 3047-3054.
Stone-Marschat, MA, Moss, SR, Burrage, TG, Barber, ML, Roy, P, Laegreid, WW (1996) Immunization with VP2 is sufficient for protection against lethal challenge with African horsesickness virus Type 4. *Virology* **220**, 219-22.
Streatfield, SJ (2007) Approaches to achieve high-level heterologous protein production in plants. *Plant biotechnology journal* **5**, 2-15.
Stuart, D, Grimes, J (2006) Structural studies on orbivirus proteins and particles. In: Roy P. (eds) Reoviruses: Entry, Assembly and Morphogenesis. Current Topics in Microbiology and Immunology, Springer, Berlin, Heidelberg **309**, 221-244.
Stuart, DI, Gouet, P, Grimes, J, Malby, R, Diprose, J, Zientara, S, Burroughs, JN, Mertens, PP (1998) Structural studies of orbivirus particles. *Arch Virol Suppl* **14**, 235-50.
Tagliamonte, M, Tornesello, ML, Buonaguro, FM, Buonaguro, L (2017) Virus-Like Particles. 205-219.
Theiler, A (1910) The susceptibility of the dog to african horse-sickness. *Journal of Comparative Pathology and Therapeutics* **23**, 315-325.
Thompson, GM, Jess, S, Murchie, AK (2012) A review of African horse sickness and its implications for Ireland. *Irish Veterinary Journal* **65**, 9.
Thrane, S, Janitzek, CM, Matondo, S, Resende, M, Gustavsson, T, de Jongh, WA, Clemmensen, S, Roeffen, W, van de Vegte-Bolmer, M, van Gemert, GJ, Sauerwein, R, Schiller, JT, Nielsen, MA, Theander, TG, Salanti, A, Sander, AF (2016) Bacterial superglue enables easy development of efficient virus-like particle based vaccines. *Journal of Nanobiotechnology* **14**, 30.
Thuenemann, EC, Meyers, AE, Verwey, J, Rybicki, EP, Lomonossoff, GP (2013) A method for rapid production of heteromultimeric protein complexes in plants: assembly of protective bluetongue virus-like particles. *Plant biotechnology journal* **11**, 839-846.
Trifonova, EA, Zenin, VA, Nikitin, NA, Yurkova, MS, Ryabchevskaya, EM, Putlyaev, EV, Donchenko, EK, Kondakova, OA, Fedorov, AN, Atabekov, JG, Karpova, OV (2017) Study of rubella candidate vaccine based on a structurally modified plant virus. *Antiviral Res* **144**, 27-33.
Turner, DR, Joyce, LE, Butler, PJG (1988) The tobacco mosaic virus assembly origin RNA: functional characteristics defined by directed mutagenesis. *Journal of molecular biology* **203**, 531-547.
Twyman, RM, Stoger, E, Schillberg, S, Christou, P, Fischer, R (2003) Molecular farming in plants: host systems and expression technology. *Trends in Biotechnology* **21**, 570-578.
Usha, R, Rohll, JB, Spall, VE, Shanks, M, Maule, AJ, Johnson, JE, Lomonossoff, GP (1993) Expression of an animal virus antigenic site on the surface of a plant virus particle. *Virology* **197**, 366-374.
Valenzuela, P, Coit, D, Medina-Selby, MA, Kuo, CH, Van Nest, G, Burke, RL, Bull, P, Urdea, MS, Graves, PV (1985) Antigen engineering in yeast: synthesis and assembly of hybrid hepatitis B surface antigen-herpes simplex 1 gD particles. *Nature Biotechnology* **3**, 323.
van de Water, SG, van Gennip, RG, Potgieter, CA, Wright, IM, van Rijn, PA (2015) VP2 Exchange and NS3/NS3a Deletion in African Horse Sickness Virus (AHSV) in Development of Disabled Infectious Single Animal Vaccine Candidates for AHSV. *J Virol* **89**, 8764-72.
van Rijn, PA, Maris-Veldhuis, MA, Potgieter, CA, van Gennip, RGP (2018) African horse sickness virus (AHSV) with a deletion of 77 amino acids in NS3/NS3a protein is not virulent and a safe promising AHS Disabled Infectious Single Animal (DISA) vaccine platform. *Vaccine* **36**, 1925-1933.
van Rijn, PA, van de Water, SG, Feenstra, F, van Gennip, RG (2016) Requirements and comparative analysis of reverse genetics for bluetongue virus (BTV) and African horse sickness virus (AHSV). *Virol J* **13**, 119.

Van Staden, V, Theron, J, Greyling, B, Huismans, H, Nel, L (1991) A comparison of the nucleotide sequences of cognate NS2 genes of three different orbiviruses. *Virology* **185**, 500-504.
van Zyl, AR, Meyers, AE, Rybicki, EP (2016) Transient Bluetongue virus serotype 8 capsid protein expression in Nicotiana benthamiana. *Biotechnology Reports* **9**, 15-24.
Venter, E, Van der Merwe, CF, Buys, AV, Huismans, H, Van Staden, V (2014) Comparative ultrastructural characterization of African horse sickness virus-infected mammalian and insect cells reveals a novel potential virus release mechanism from insect cells. *Journal of General Virology* **95**, 642-651.
Venter, M, Napier, G, Huismans, H (2000) Cloning, sequencing and expression of the gene that encodes the major neutralisation-specific antigen of African horsesickness virus serotype 9. *J Virol Methods* **86**, 41-53.
Vermaak, E, Paterson, DJ, Conradie, A, Theron, J (2015) Directed genetic modification of African horse sickness virus by reverse genetics. *South African Journal of Science* **111**, 1-8.
von Teichman, BF, Dungu, B, Smit, TK (2010) In vivo cross-protection to African horse sickness Serotypes 5 and 9 after vaccination with Serotypes 8 and 6. *Vaccine* **28**, 6505-17.
von Teichman, BF, Smit, TK (2008) Evaluation of the pathogenicity of African Horsesickness (AHS) isolates in vaccinated animals. *Vaccine* **26**, 5014-21.
Walwyn, DR, Huddy, SM, Rybicki, EP (2015) Techno-Economic Analysis of Horseradish Peroxidase Production Using a Transient Expression System in Nicotiana benthamiana. *Applied Biochemistry and Biotechnology* **175**, 841-854.
Werner, S, Marillonnet, S, Hause, G, Klimyuk, V, Gleba, Y (2006) Immunoabsorbent nanoparticles based on a tobamovirus displaying protein A. *Proceedings of the National Academy of Sciences* **103**, 17678-17683.
Weyer, CT (2017) PhD thesis: African horse sickness outbreak investigation and disease surveillance using molecular techniques. University of Pretoria.
Weyer, CT, Grewar, JD, Burger, P, Joone, C, Lourens, C, MacLachlan, NJ, Guthrie, AJ (2017) Dynamics of African horse sickness virus nucleic acid and antibody in horses following immunization with a commercial polyvalent live attenuated vaccine. *Vaccine* **35**, 2504-2510.
Weyer, CT, Grewar, JD, Burger, P, Rossouw, E, Lourens, C, Joone, C, le Grange, M, Coetzee, P, Venter, E, Martin, DP, MacLachlan, NJ, Guthrie, AJ (2016) African Horse Sickness Caused by Genome Reassortment and Reversion to Virulence of Live, Attenuated Vaccine Viruses, South Africa, 2004-2014. *Emerg Infect Dis* **22**, 2087-2096.
Weyer, CT, Joone, C, Lourens, CW, Monyai, MS, Koekemoer, O, Grewar, JD, van Schalkwyk, A, Majiwa, PO, MacLachlan, NJ, Guthrie, AJ (2015) Development of three triplex real-time reverse transcription PCR assays for the qualitative molecular typing of the nine serotypes of African horse sickness virus. *J Virol Methods* **223**, 69-74.
Weyer, CT, Quan, M, Joone, C, Lourens, CW, MacLachlan, NJ, Guthrie, AJ (2013) African horse sickness in naturally infected, immunised horses. *Equine Vet J* **45**, 117-9.
Wohlsein, P, Pohlenz, JF, Davidson, FL, Salt, JS, Hamblin, C (1997) Immunohistochemical demonstration of African horse sickness viral antigen in formalin-fixed equine tissues. *Veterinary pathology* **34**, 568-574.
Xu, J, Dolan, MC, Medrano, G, Cramer, CL, Weathers, PJ (2012) Green factory: plants as bioproduction platforms for recombinant proteins. *Biotechnology advances* **30**, 1171-1184.
Zhang, X, Boyce, M, Bhattacharya, B, Zhang, X, Schein, S, Roy, P, Zhou, ZH (2010) Bluetongue virus coat protein VP2 contains sialic acid-binding domains, and VP5 resembles enveloped virus fusion proteins. *Proceedings of the National Academy of Sciences* **107**, 6292-6297.
Zhang, X, Patel, A, Celma, CC, Yu, X, Roy, P, Zhou, ZH (2016) Atomic model of a nonenveloped virus reveals pH sensors for a coordinated process of cell entry. *Nature structural & molecular biology* **23**, 74-80.
Zhao, Q, Modis, Y, High, K, Towne, V, Meng, Y, Wang, Y, Alexandroff, J, Brown, M, Carragher, B, Potter, CS (2012) Disassembly and reassembly of human papillomavirus virus-like particles produces more virion-like antibody reactivity. *Virol J* **9**, 52.
Zhou, Y, Maharaj, PD, Mallajosyula, JK, McCormick, AA, Kearney, CM (2015) In planta production of flock house virus transencapsidated RNA and Its potential use as a vaccine. *Molecular biotechnology* **57**, 325-336.
Zhu, F-C, Zhang, J, Zhang, X-F, Zhou, C, Wang, Z-Z, Huang, S-J, Wang, H, Yang, C-L, Jiang, H-M, Cai, J-P (2010) Efficacy and safety of a recombinant hepatitis E vaccine in healthy adults: a large-scale, randomised, double-blind placebo-controlled, phase 3 trial. *The Lancet* **376**, 895-902.

Zimran, A, Brill-Almon, E, Chertkoff, R, Petakov, M, Blanco-Favela, F, Muñoz, ET, Solorio-Meza, SE, Amato, D, Duran, G, Giona, F (2011) Pivotal trial with plant-cell–expressed recombinant glucocerebrosidase, taliglucerase alfa, a novel enzyme replacement therapy for Gaucher disease. *Blood* **118**, 5767 - 5773.

Zwart, L, Potgieter, CA, Clift, SJ, van Staden, V (2015) Characterising Non-Structural Protein NS4 of African Horse Sickness Virus. *PLoS One* **10**, e0124281.